ON THE NIP MECHANICS OF ROLLING PROCESSES

# ON THE NIP MECHANICS OF ROLLING PROCESSES S.K. SINHA

#### ABSTRACT

A theory has been proposed to predict the behaviour of a viscoelastic sheet in rolling contact with smooth, rigid cylinders at slow speed.

A contact length is first assumed which is then divided into a number of elements. The force on any element is taken as a line load of unknown magnitude. Influence functions are obtained by first obtaining the elastic solutions and then applying the correspondence principle. Constitutive equations are represented by a generalized mechanical model. Simultaneous equations for the unknown quantities are obtained by matching the normal displacement at the ends of the elements to the geometry of the cylinder. The contact length is later corrected so as to satisfy the total load condition. Solutions for some simple cases have been obtained numerically.

Rolling of an elastic sheet has also been treated. Solutions have been obtained for the extreme cases of "infinite friction" and "no friction".

# QUELQUES ASPECTS DE LA MECANIQUE DU LAMINAGE S.K. SINHA

#### RESUME

Cette thèse élabore une méthode de calcul permettant de prédire le comportement d'une lame viscoélastique subissant un laminage entre des cylindres rigides et lisses a des petits vitesses.

On assume une valeur pour le longeur de contact et on la subdivise ensuite en plusieurs segments. La force, de grandeur inconnue, distribuée sur chaque segment, est appliquée a son centre. On obtient les fonctions d'influence par calcul des solutions du système considéré comme élastique et par application subséquente du principe de correspondance. Les équations des contraintes et de formations sont représentées par un modèle mécanique generalisé. On détermine les paramètres des équations simultanées permetant d'évaluer les inconnues par comparaison des déplacements normaux des extrémités des segments avec la configuration du cylindre. On effectue ensuite une correction de la valeur supposée pour le longeur de contact de facon a satisfaire les conditions de charge totale. Cette thèse comprend aussi le solution numérique de cas simples.

Le problème du laminage d'une lame élastique a également été abordé; on a calculé les deux cas extrêmes supposant d'une part un frottement infine et de l'autre un frottement nul.

# ON THE NIP-MECHANICS OF ROLLING PROCESSES by SHAILENDRA K. SINHA, M.ENG.

A THESIS SUBMITTED TO THE FACULTY OF

GRADUATE STUDIES AND RESEARCH IN PARTIAL FULFILLMENT

OF THE REQUIREMENTS FOR THE DEGREE OF

DOCTOR OF PHILOSOPHY

DEPARTMENT OF MECHANICAL ENGINEERING

McGILL UNIVERSITY

MONTREAL, CANADA MARCH 1972

To

Pramila

· ·

#### ABSTRACT

A theory has been proposed to predict the behaviour of a viscoelastic sheet in rolling contact with smooth, rigid cylinders at slow speed.

A contact length is first assumed which is then divided into a number of elements. The force on any element is taken as a line load of unknown magnitude. Influence functions are obtained by first obtaining the elastic solutions and then applying the correspondence principle. Constitutive equations are represented by a generalized mechanical model. Simultaneous equations for the unknown quantities are obtained by matching the normal displacement at the ends of the elements to the geometry of the cylinder. The contact length is later corrected so as to satisfy the total load condition. Solutions for some simple cases have been obtained numerically.

Rolling of an elastic sheet has also been treated.

Solutions have been obtained for the extreme cases of "infinite friction" and "no friction".

#### **ACKNOWLEDGEMENTS**

The author wishes to express his gratitude and appreciation to Professors D.R. Axelrad, D. Atack, and J.W. Provan for many hours of their valuable discussions in the preparation of this thesis.

Thanks are also due to the Pulp and Paper Research
Institute of Canada for providing financial assistance
to the author and to the National Research Council of
Canada, Grants No.A7280 and A2290, for supporting the project of this thesis.

Finally, the author would like to thank Miss Diane McKeown for her care and patience in typing the text and preparing the drawings of this thesis.

# TABLE OF CONTENTS

			Page
ABSTRACT			i
ACKNOWLEDGEMEN	TS		ii
TABLE OF CONTE	NTS		iii
LIST OF NOTATI	ONS		vi
LIST OF FIGURE	S		xiii
LIST OF TABLES			xviii
CHAPTER I	INTR	ODUCTION	1
·	1.1	Rolling of Two Bodies	3
	1.2	Rolling of a Sheet	6
	1.3	Outline of the Present Investigation	9
CHAPTER II	BASI	C THEORY	14
	2.1	Boundary Conditions	15
	2.2	Representation of the Nip Forces	20
	2.3	Derivation of the Matching Equations	21
	2.4	Determination of the Contact Length	25
	2.5	Determination of the Ratio $m_1:m_2$	26
CHAPTER III	SOME	EQUATIONS OF ELASTICITY	30
CHAPTER IV		ACE DISPLACEMENTS OF AN ELASTIC T DUE TO MOVING LOADS	42
	4.1	Influence Functions for Normal Line Load	42
	4.2	Influence Functions for Shear Line Load	48

		- iv -		
		<u>I</u>	Page	
	4.3	Simplified Forms of the In- fluence Functions	53	
	4.4	Numerical Results	56	
CHAPTER V	SOLUT	TION OF THE ELASTIC PROBLEM	59	
	5.1	The Choice of the Pinned Point (0, 1)	60	
•	5.2	Relations Common to Both Cases	60	
,	5.3	Matching Equations for the Case (A)	62	
	5.4	Matching Equations for the Case (B)	66	
	5.5	Creep Ratio for the Case (A)	67	
	5.6	Creep Ratio for the Case (B)	69	
	5.7	Numerical Results	70	
CHAPTER VI	SURF ELAS	ACE DISPLACEMENTS OF A VISCO- TIC SHEET DUE TO MOVING LOADS	73	
	6.1	Elastic Solution for Fixed Coordinates	74	
	6.2	Material Function	78	
	6.3	Solution for Viscoelastic Sheet	81	
	6.4	Numerical Results	89	
CHAPTER VII	SOLU	JTION OF THE VISCOELASTIC PROBLEM	91	
	7.1	The Choice of the Pinned Point (0, %)	92	
	7.2		93	
	7.3	Coefficient of Rolling Resistance	e 97	
	7.4	Creep Ratio for Complete Slip	99 .	
	7.5	Numerical Results	100	

•			e San
e de la companya de l		- v -	
			Page
	CHAPTER VIII	DISCUSSION AND CONCLUSION	102
		8.1 Elastic Case	102
		8.2 Viscoelastic Case	104
		8.3 Conclusion	105
	APPENDIX I	EVALUATION OF THE INTEGRALS I <sub>1</sub> -I <sub>7</sub> FOR THE ELASTIC CASE	107
		AI.1 The Integral $I_1(\alpha)$	107
		AI.2 The Integral $I_2(\alpha)$	111
		AI.3 The Forms of the Remaining Integrals	112
	APPENDIX II	EVALUATION OF THE INTEGRALS J1-J6 FOR THE VISCOELASTIC CASE	115
		AII.1 Integrals $J_1(\lambda,T)$ to $J_4(\lambda,T)$ for the Case T>0	115
		AII.2 Integrals $J_1(\lambda,T)$ to $J_4(\lambda,T)$ for the Case T<0	120
		AII.3 Integrals $J_5(T)$ and $J_6(T)$ for the Case T>0	121
		AII.4 Integrals $J_5(T)$ and $J_6(T)$ for the Case T<0	124
	APPENDIX III	$\Theta_1$ (t) AND $\Theta_2$ (t) FOR A STANDARD LINEAR SOLID	125
	APPENDIX IV	ROOTS OF SINH(Z)+Z=0	130
	REFERENCES		134

# LIST OF NOTATIONS

В	Thickness of the sheet
D	The operator $\frac{d}{dt}$
$A_0, B_0$ $C_0, D_0$	Some coefficients occurring in equation (3.4)
$A_1, B_1$ $C_1, D_1$	Some coefficients defined by equation (4.3)
$A_2, B_2$ $C_2, D_2$	Some coefficients defined by equation (4.14)
$A_n^{(1)}, B_n^{(1)}$	Constants of residues defined by equation (AI.8)
$A_n^{(K)}, B_n^{(K)}$	Constants of residues defined by equation (AI.13)
$c_L$	An arbitrary constant
C <sub>r</sub>	The ratio of the cylinder diameter to the thickness of the sheet
E	Young's modulus of elasticity
F	Nominal velocity of the cylinder
F <sub>0</sub>	Nominal velocity of the sheet

F <sub>1</sub> ,F <sub>2</sub>	Some functions of $\eta$ defined by equation (4.24)
G	Shear modulus of elastic sheet
G <sub>0</sub>	Instantaneous shear modulus of viscoelastic sheet
G <sub>1</sub> ,G <sub>2</sub>	Spring constants in the mechanical model for shear
G <sup>0</sup>	Fourier transform of $\Phi$
G <sup>(1)</sup> ,G <sup>(2)</sup>	Special forms of G <sup>o</sup>
H(•)	Heavyside's unit step function
H <sub>1</sub>	A function defined by equation (AI.2)
I <sub>1</sub> -I <sub>7</sub>	Some integrals defined by equations (4.9) and (4.20)
J <sub>1</sub> -J <sub>6</sub>	Some integrals defined by equation (6.20)
К	Bulk modulus of elastic sheet
K <sub>0</sub>	Instantaneous bulk modulus of visco- elastic sheet
$K_1, K_2$	Spring constants in the mechanical model for dilatation
L	Length of contact
L <sub>1</sub>	Length of contact on the leading side
$L_2$	Length of contact on the trailing side
М	A point on the surface of the visco- elastic sheet where displacements are to be determined
M <sub>1</sub>	The moment of the forces acting on the leading side
M <sub>2</sub>	The moment of the forces acting on the trailing side

и,и'	Degrees of some polynomials occurring in material function expressions
0	Origin of the X-Y coordinate system
0 1	Origin of the x-y coordinate system
P.L.I.	Pounds per linear inch
P,P'	Some polynomials of D
<sup>P</sup> j	The magnitude of the normal force on the jth element
Q,Q'	Some polynomials of D
٩ <sub>غ</sub>	The magnitude of the shear force on the jth element
R	The radius of the cylinder
$R_n, R_n^{\dagger}$	The nth residue of the function $H_1(\alpha,z)$ in the first and second quadrant respectively
Т	The time required for the load to reach the point ${\tt M}$
W	The total normal load per unit length exerted by the cylinder
X-Y	A coordinate system fixed in space
Y <sub>i</sub>	The distance of the ith matching point
Y i	The distance of the jth load
Z ij	The distance of the ith matching point from the jth load
[A],[A']	Coefficient matrices
[X],[X']	Unknown vectors
[B],[B']	Known vectors
SIGN(·)	Equals 1 if the argument is positive Equals -1 if the argument is negative

	•
	- ix -
	- 1x -
a	The semi-width of each element
Ъ	The semi-thickness of the sheet
a <sub>n</sub> ,b <sub>n</sub>	Some parameters defined by equation (6.10)
$a_n', b_n'$	Special forms of $a_n, b_n$ defined by equation (6.22)
$c$ , $c_1$ , $c_2$ $c^{(1)}$ , $c^{(1)}$ , $c^{(1)}$	Some numerical constants
c <sup>(2)</sup> ,c <sub>1</sub> <sup>(2)</sup> ,c <sub>2</sub> <sup>(2)</sup>	
đ <sub>0</sub>	The depth of indentation
d <sub>1</sub> ,d <sub>2</sub>	The normal displacements of the surface of the sheet at the ends of the nip on the leading and the trailing sides respectively
f	A function of x
fy	The velocity of a point on the surface of the sheet within the nip
f(Y)	A function representing the geometry of the surface of the cylinder
g	A function of y
$g_n, h_n$	Some functions defined by equation (AI.5)
$g_n^{(K)}, h_n^{(K)}$	Some functions defined by equation (6.9)
k.s.i.	Kips per square inch
L	the distance of the pinned point from point 0'
$m_n, K_n$	The real and imaginary parts respectively of the nth root of sinh2z+2z=0 in the first quadrant

m <sub>1</sub> ,m <sub>2</sub>	The number of elements on the leading and trailing sides respectively
n	A dummy index of summation
p	The Laplace transform parameter
$P_{\text{max}}$	The peak pressure in the nip
$q_{max}$	The magnitude of the peak shear in the nip
r	A dummy index of summation
t	A measure of time
t <sub>0</sub>	The time required for the load to arrive at a point right over the pinned point
u,v	Displacements in $x$ and $y$ directions respectively
u;,v;	Normal and shear displacements respectively of the ith matching point
ue(V), ve(V)	The normal and shear displacements respectively of the surface of the elastic (viscoelastic) sheet due to a unit normal line load
ue,ve	The normal and shear displacements respectively of the surface of the elastic sheet due to a unit shear line load
u <sup>n</sup> ,v <sup>n</sup> ij,vij	The normal and shear displacements respectively of the ith matching point due to a unit normal line load on the jth element
us,vs ij,vij	The normal and shear displacements respectively of the ith matching point due to a unit shear line load on the jth element

x-y A coordinate system moving with the load

A complex variable

# Greek Alphabet

α	A dimensionless parameter = y/b
α <sub>ij</sub>	A dimensionless parameter = z <sub>ij</sub> /b
β	The ratio of the width of an element to the thickness of the sheet
Υο, Υο, Υ <sub>r</sub> , Υ <sub>r</sub>	The coefficients of the partial fractions of the material functions
$\gamma_{xy}$	Shear strain in the x-y plane
δ	The eccentricity of the resultant load
δ(•)	The dirac delta function
$\epsilon_{\mathbf{x}}$	Normal strain in the x-direction
εχ	Normal strain in the y-direction
ξ	The Fourier transform parameter
Θ <sub>1</sub> ,Θ <sub>2</sub>	Material functions defined by equation (4.23)
$\lambda_{r}, \lambda_{r}$	The roots of the polynomials occurring in the expressions of the material functions
μ	The coefficient of friction
μ <sub>R</sub>	The coefficient of rolling resistance

en de la companya de la co

		- xii -	
•		- XII -	
-			
	ν	Poisson's ratio	
	g	Normal stress in the x-direction	
	$^{\sigma}$ x	HOT MALE SCIESS III THE X-ALICE LION	
	σ.	Normal stress in the y-direction	
	σу	Normal Stress in the y-direction	
	-	The relevation time of the metapical	
	τ	The relaxation time of the material in both shear and dilatation	
		In both shear and arratation	
	$^{ au}$ xy	Shear stress in the x-y plane	:
	<b>A</b> y		
	V	The creep ratio	
	Χ	The creep racto	
	Χo	The creep ratio for the case of	
		complete slip	
		The energy metic for the energy	
	$\chi_{\infty}$	The creep ratio for the case of no slip	
•		10 011	
	η	A dimensionless parameter = l/b	
		A 3	
	η <sub>j</sub>	A dimensionless parameter = Y <sub>.</sub> /b	
	1 11		
	η',η'	The viscosities of the dashpots in	
		the mechanical models for shear	
		and dilatation respectively	
	Φ	A biharmonic function in rectangular	
	•	coordinates	
	<sub>Φ</sub> (K) <sub>.Ψ</sub> (K)	·	
	$\Phi_{\mathbf{n}}^{K}, \Psi_{\mathbf{n}}^{K}$		
	$\phi_{n}^{(K)}, \psi_{n}^{(K)}$	Some functions defined by equation (6.21)	
	n		
	$\overline{\phi}_{n}^{(K)}, \overline{\psi}_{n}^{(K)}$		
	$^{\phi}$ n $^{,\psi}$ n		
		m, , , , , , , , , , , , , , , , , , ,	
	ω	The angular speed of the cylinder	

## - xiii -

## LIST OF FIGURES

Figure No	<u>•</u>	Page
1	A Sheet Rolling Between a Pair of Rigid Cylinders	136
2	Nip Forces in Rolling Contact	137
3	Physical Behaviour of a Sheet Between Rigid Cylinders	138
· ц	Representation of the Nip Forces	139
5	Consequences of Underestimation or Overestimation in the Value of $\mathtt{m_2}$ on Load Distribution	140
6	Representation of Line Loads (Normal and Shear) Moving on Elastic Sheet	141
7	Normal Displacement of the Surface (X=-b) of an Elastic Sheet Due to Normal Line Load	142
8	Normal Displacement of the Surface (X=-b) of an Elastic Sheet Due to Shear Line Load	143
9	Variation of the Functions $F_1$ and $F_2$ with $\eta$	144
10	Variation of $V^{n'}$ with $\alpha$	145
11	Variation of $V^{s'}$ with $\alpha$	146
12	Shear Displacement of the Surface (X=-b) of an Elastic Sheet Due to Normal Line Load	147
13	Shear Displacement of the Surface (X=-b) of an Elastic Sheet Due to Shear Line Load	148
14	The Geometry of the Nip (Elastic Sheet)	149
15	Possible Range of the Creep Ratio Satisfying Equations (2.2) and (2.4) for No-Slip Condi- (Elastic Case; D=12 in., B=0.005 in.)	g 150 tion
16	Schematic Representation of the Shear Displacements of the Sheet Surface (Elastic)	151

Figure	No.	Page
17	Variation of Peak Pressure with Load and Sheet Thickness for No-Slip Condition (Elastic Case)	152
18	Variation of the Ratio $\frac{L}{B}$ with Load and Sheet Thickness for No-Slip Condition (Elastic Case)	153
19	Variation of the Ratio $\frac{d_0}{B}$ with Load and Sheet Thickness for No-Slip Condition (Elastic Case)	154
20	Variation of Creep Ratio with Load and Sheet Thickness for No-Slip Condition (Elastic Case)	155
21	Variation of Peak Pressure with Load and Sheet Thickness for Complete Slip (Elastic Case)	156
22	Variation of the Ratio $\frac{L}{B}$ with Load and Sheet Thickness for Complete Slip (Elastic Case)	157
23	Variation of the Ratio $\frac{d_0}{B}$ with Load and Sheet Thickness for Complete Slip (Elastic Case)	158
24	Variation of Creep Ratio with Load and Sheet Thickness for Complete Slip (Elastic Case)	159
25	Limiting Values of Contact Length and In- dentation for Different Normal Loads (Elastic Case; B=0.005 in.)	160
26	Limiting Values of Nip Pressure (Elastic Case; B=0.005 in., W=100 P.L.I.)	161
27	Nip Shear for No-Slip Condition and for Different Normal Loads (Elastic Case; B=0.005 in.)	162
28	Surface Displacements of an Elastic Sheet under the Nip (B=1 in., W=100 P.L.I.)	163

Figure	No.	Page
29	Surface Displacements of an Elastic Sheet under the Nip (B=0.005 in., W=100 P.L.I.)	164
3 0	Geometric Representation of a Moving Line Load	165
31	Four Distinct Cases Depending upon the Location of Point M and the Starting Posi- tion of the Starting Position of the Load	166
32	Mechanical Model and Creep Response of a Standard Linear Solid	167
33	Normal Displacement of the Point M on the Surface of a Viscoelastic Sheet Due to Moving Line Load when T>0	168
34	Normal Displacement of the Point M on the Surface of a Viscoelastic Sheet Due to Moving Line Load when T<0	169
35	Shear Displacement of the Point M on the Surface of a Viscoelastic Sheet Due to Moving Line Load when T>0 and t <sub>0</sub> >0	170
36	Shear Displacement of the Point M on the Surface of a Viscoelastic Sheet Due to Moving Line Load when T<0 and $t_0$ <0	171
37	Shear Displacement of the Point M on the Surface of a Viscoelastic Sheet Due to Moving Line Load when T>0 and t <sub>0</sub> >0	172
38	Shear Displacement of the Point M on the Surface of a Viscoelastic Sheet Due to Moving Line Load when T<0 and $t_0$ <0	173
39	The Geometry of the Nip (Viscoelastic Case)	174
40	Force Equilibrium of a Viscoelastic Sheet in Rolling Contact	175
41	Variation of Peak Pressure with Normal Load for Different Values of $F_0\tau$ (B=0.005 in.)	176

Figure N	<u>o.</u>	Page	
42	Variation of the Ratio $\frac{L}{B}$ with Normal Load for Different Values of F0 $\tau$ (B=0.005 in.)	177	
43	Variation of the Ratio $\frac{d_0}{B}$ with Normal Load for Different Values of F <sub>0</sub> $\tau$ (B=0.005 in.)	178	
цц	Variation of Creep Ratio with Normal Load for Different Values of $F_0\tau$ (B=0.005 in.)	179	
45	Variation of Peak Pressure with $F_0\tau$ for Different Normal Loads (B=0.005 in.)	180	
46	Variation of the Ratio $\frac{L}{B}$ with Forfor Different Normal Loads (B=0.005 in.)	181	
47	Variation of the Ratio $\frac{d_0}{B}$ with F <sub>0</sub> tfor Different Normal Loads (B=0.005 in.)	182	
48	Variation of Creep Ratio with $F_0\tau$ for Different Normal Loads (B=0.005 in.)	183	
49	Variation of Nip Pressure with F <sub>0</sub> τ (B=0.005 in., W=100 P.L.I.)	184	
 50	Variation of the Coefficient of Rolling Resistance with $F_0\tau$ for Different Normal Loads (B=0.005 in.)	185	
 51	Variation of the Coefficient of Rolling Resistance with $F_0\tau$ for Different Thicknesses of the Sheet (W=100 P.L.I.)	186	

# - xvii -

Figure	No.	Page
52	Variation of the Normal Displacement of the Sheet Surface within and outside the	187
	Nip with $F_0\tau$ (B=0.005 in., W= 100 P.L.I.)	
53	Variation of the Shear Displacement of the Sheet Surface within and outside the	188
	Nip with F <sub>0</sub> τ(B=0.005 in., W=100 P.L.I.)	
54	Contour C for the Evaluation of Integral	189

# - xviii -

# LIST OF TABLES

Table	•	<u>Page</u>
Ī	A Brief Review of the Literature Involving the Rolling of Two Bodies	190
II	A Brief Review of the Literature Involving the Rolling of a Sheet	191
III	Some Results of Elastic Rolling for No-Slip Condition (B=1 inch)	192
IV	Some Results of Elastic Rolling for No-Slip Condition (B=0.25 inch)	193
V	Some Results of Elastic Rolling for No-Slip Condition (B=0.0625 inch)	194
VI	Some Results of Elastic Rolling for No-Slip Condition (B=0.005 inch)	195
VII	Some Results of Elastic Rolling for Complete Slip (B=1 inch)	196
VIII	Some Results of Elastic Rolling for Complete Slip (B=0.25 inch)	197
IX	Some Results of Elastic Rolling for Complete Slip (B=0.0625 inch)	198
Х	Some Results of Elastic Rolling for Complete Slip (B=0.005 inch)	199
XI	Some Results of Viscoelastic Rolling for Complete Slip (B=1 inch, W=50 P.L.I.)	- 200
XII	Some Results of Viscoelastic Rolling for Complete Slip (B=1 inch, W=100 P.L.I.)	ı- 201
XIII	Some Results of Viscoelastic Rolling for Complete Slip (B=1 inch, W=150 P.L.I.)	n- 202
XIV	Some Results of Viscoelastic Rolling for Corplete Slip (B=1 inch, W=200 P.L.I.)	n- 203
XV	Some Results of Viscoelastic Rolling for Complete Slip (B=0.25 inch, W=50 P.L.I.)	n- 204

Age to the second of the second

Table		Page
XVI	Some Results of Viscoelastic Rolling for Complete Slip (B=0.25 inch, W=100 P.L.I.)	205
XVII	Some Results of Viscoelastic Rolling for Complete Slip (B=0.25 inch, W=150 P.L.I.)	206
XVIII	Some Results of Viscoelastic Rolling for Complete Slip (B=0.25 inch, W=200 P.L.I.)	207
XIX	Some Results of Viscoelastic Rolling for Complete Slip (B=0.0625 inch, W=50 P.L.I.)	208
XX	Some Results of Viscoelastic Rolling for Complete Slip (B=0.0625 inch, W=100 P.L.I.)	209
XXI	Some Results of Viscoelastic Rolling for Complete Slip (B=0.0625 inch, W=150 P.L.I.)	210
XXII	Some Results of Viscoelastic Rolling for Complete Slip (B=0.0625 inch, W=200 P.L.I.)	211
XXIII	Some Results of Viscoelastic Rolling for Complete Slip (B=0.005 inch, W=50 P.L.I.)	212
XXIV	Some Results of Viscoelastic Rolling for Complete Slip (B=0.005 inch, W=100 P.L.I.)	213
XXV	Some Results of Viscoelastic Rolling for Complete Slip (B=0.005 inch, W=150 P.L.I.)	214
XXVI	Some Results of Viscoelastic Rolling for Complete Slip (B=0.005 inch, W=200 P.L.I.)	215

#### CHAPTER I

#### 1. INTRODUCTION

During the rolling process, two bodies are pressed together by some external force and then one body is made to roll on the other. Due to the applied force, the two bodies come closer, within a certain distance (which is commonly known as the amount of relative approach), and make contact over a finite area. The applied force is distributed over this contact area in the form of some unknown distribution.

If the two bodies are identical (in size and in properties), they will deform equally. But if they are not identical, they will deform unequally and the contacting points tend to move relative to each other. This tendency is opposed by the presence of friction and gives rise to shearing forces. If the shearing force at any point in the contact zone is less than the limiting frictional force at that point, then there will be no slip. On the other hand, if the shearing force at any point is equal to the available limiting frictional force, then slip will occur.

Problems involving the rolling of two bodies are mainly concerned with the determination of the area of contact, the

forces on the contacting surface and the amount of relative approach of the two bodies. In this case, neither the boundary nor the conditions on the boundary are known. Hence, in this respect, the problem of rolling of two bodies is radically different from the general stress analysis problems where the boundary as well as the conditions on the boundary are prescribed. The only helpful information is the fact that, in the contact region, the two bodies have a common surface. Outside the contact zone, the external forces are zero. But this information does not help in determining the unknown forces on the contact surface. If the area of contact is small compared to the size of the two bodies, the bodies may be treated as half spaces. In that case, there is one boundary at infinity. The condition that the stresses and displacements must be bounded at infinity becomes helpful information in determining the right stress function or the displacement potential, as the case may be, for the particular problem. If the two bodies are elastic, there is a line of symmetry and therefore the problem becomes less difficult. But if one of the bodies (or both) is viscoelastic then, due to the dissipative nature of viscoelastic materials, there will be no symmetry and the problem becomes more complicated.

As an introduction to the formulation of the problem

treated in this thesis, a brief review of some earlier works, in which at least one of the bodies is a cylinder, is presented in the next two articles.

#### 1.1 Rolling of Two Bodies

Table I gives an outline of the problems involving the rolling of two bodies. Hertz<sup>[1]</sup> solved the problem of contact of two perfectly elastic bodies having smooth surfaces. Carter [2] and Poritsky [3] have treated tractive rolling (where a net tractive force is transmitted from one body to the other). Hertz's analysis ignored the presence of any shear force on the contact surface. This implies complete slip, but in practice, it is impossible to get completely smooth surfaces. Bufler [4] solved the same problem assuming no-slip anywhere (which represents another extreme case). Johnson [5] and later Bentall and Johnson [6] relaxed the assumption of "no-slip anywhere" and allowed for partial slip. Since the regions of adhesion and slip are not known in the beginning, the problem cannot be solved analytically. They used numerical methods and solved the problem by an iteration process.

Note: Numbers in brackets after a name indicate references given at the end of this thesis.

Examples of rolling between elastic-viscoelastic bodies are the rolling of an elastic cylinder (or sphere) over a viscoelastic half space. For further simplicity, the cylinder (or the sphere) is assumed to be rigid as compared to the half space.

Hunter<sup>[7]</sup> and Morland<sup>[8]</sup> have treated the rolling of a rigid cylinder over a viscoelastic half space. They considered slow rolling (neglecting inertial effects), constant velocity, steady conditions with respect to the cylinder position, plane deformation, and smooth surfaces. Hunter<sup>[7]</sup> expressed the surface displacement as an integral of the moving line-load solution. This resulted in a singular integral equation for the pressure distribution. He assumed the material to behave like a standard linear solid in shear and having a fixed Poisson's ratio. resulting integral equation is transformed into a standard logarithmic kernel of a differential operator in terms of the pressure. He obtained a closed form solution for a material characterized by one viscoelastic creep function having a single retardation time. But for materials having more than one characteristic retardation time, including the case of two or more creep functions, the integrals diverge. Morland [8] obtained two pairs of coupled integral equations for the unknown displacements and stresses.

Representing the unknown functions by a series of Bessel's functions, an infinite set of simultaneous algebraic equations were obtained for the coefficients of the Bessel's functions. The truncation of the infinite matrix depended on a small parameter, the loss tangent of the material in the non-diagonal terms. The final solution again was a numerical one.

The rolling of two identical viscoelastic cylinders has also been investigated by Morland  $^{[9]}$ . This problem differs from the previous one in that the cylinders are subjected to the nip forces periodically, varying at a frequency of  $\omega/_{2\pi}$ . He also considered slow rolling at constant speed, smooth surfaces, plane deformation, and steady-state conditions for this problem. He solved Navier's equations by separating the variables and obtained expressions for stresses and displacements in terms of Fourier series of unknown coefficients. The analysis is rigorous and applies to materials having any number of retardation times, including materials having a continuous spectrum of retardation times. Subsequently, this analysis was extended to treat the rolling of dissimilar viscoelastic cylinders  $^{[10]}$ .

#### 1.2 Rolling of a Sheet

The rolling of a sheet is more complex than the rolling of two bodies due to the presence of an additional boundary at the central line of the sheet. Sneddon<sup>[11]</sup> suggested the use of Fourier transforms for the solution of such problems when the boundary forces are prescribed. But for the rolling problems, the boundary forces are not known. Table II gives a brief indication of the work done in this context.

Wang [12] tried to determine the contact forces for an elastic strip pressed between identical cylinders. He assumed smooth surfaces and plane deformation. Following Sneddon's method, he obtained an integral equation for the unknown pressure distribution as follows:

$$\int_{0}^{a} q(\eta) K(y,\eta) d\eta = f(y) \qquad 0 \le y \le a \qquad (1.1)$$

where

q(q) = the unknown pressure distribution in the nip

 $\alpha$  = semi-contact length

$$K(y,q) = \Theta_1 \cdot K_1(y,q) + \Theta_2 \cdot K_2(y,q)$$

$$K_1(y, \eta) = \int_0^\infty \frac{\cos \xi y \cdot \cos \xi \eta}{\xi} d\xi$$

$$K_2(y,\eta) = \int_0^\infty G(b\xi) \cdot \frac{\cos \xi y \cdot \cos \xi \eta}{\xi} d\xi$$

The function  $G(b\xi)$  in the integrand has the form:

$$G(b\xi) = \frac{2 \sinh^2 b\xi}{\sinh 2b\xi + 2b\xi}$$

and the material property is given by:

$$\Theta_i = \frac{4(1-v_i^2)}{n E_i}$$

i = 1, 2

l for cylinder

2 for strip

The function f(y) is a function of the maximum indentation of the strip as well as the geometry of the surface of the cylinder.

In order to simplify the integral equation, Wang approximated the kernel, considering two separate cases, viz.: (a) thick strip, and (b) thin strip. For thin strip, he argues that:

since

$$\mathcal{L}_{\text{im.}} \frac{G(x)}{x} = \frac{1}{2} \quad ,$$

$$\int_{0}^{\infty} \lim_{\beta \to 0} \left[ \frac{G(r\beta)}{r\beta} \right] \cos rt \cdot \cos rt \, dr$$

$$= \frac{1}{2} \int_0^\infty \cos rt \cdot \cos rt \, dr$$

where 
$$\beta = \frac{a}{b} = \frac{\text{semi-strip thickness}}{\text{semi-contact length}}$$

It is true that for a very thin strip, the parameter  $\beta \rightarrow 0$ . But even for very small  $\beta$ , the product of r and  $\beta$  will still not tend to zero since the upper limit of integration is infinite. Thus, the above approximation appears to be invalid. After approximating the kernel, Wang then solved the integral equation by expressing the unknown pressure distribution in the form of Chebyshev's polynomials.

Hence, it appears that Wang's solution is only valid for thick strips.

Bentall and Johnson<sup>[13]</sup> applied Sneddon's method for solving the contact forces produced in the rolling of an elastic strip. Unlike others, they did not ignore the presence of shearing forces. They divided the contact length into a selected number of elements and represented the forces on each element by triangular forces of unknown magnitudes. They presented a set of simultaneous equations for the unknowns by matching the displacement boundary con-

ditions at a number of discrete points. In this work, an assumption was made in the beginning for the conditions of slip or no-slip at different points and these conditions were imposed on the equations. By solving the simultaneous equations, the unknowns were then determined. Whenever necessary, a correction had to be made in the assumptions for slip or 'no-slip'. The final solution of the problem is essentially a numerical one. Details of that treatment are given in reference [14].

Alblas and Kuipers<sup>[15]</sup> have also investigated the rolling of a viscoelastic sheet. They assumed rigid cylinders, smooth surfaces, plane deformation, and incompressible material of the sheet. They obtained a Wiener-Hopf type equation by using Sneddon's method. The solution is approximate and needs a further extension.

#### 1.3 Outline of the Present Investigation

The aim of the present investigation is the determination of the stress and deformation fields in the nip during the rolling of a thin viscoelastic sheet. This problem is of great importance, for example, in the paper industry.

On reviewing the literature, it was realized that

Bentall's approach<sup>[14]</sup>, although it provides a very good insight into the problem of rolling, cannot be extended to the rolling process of a viscoelastic sheet.

For the solution of a viscoelastic problem, it is, in general, necessary to look for an associated elastic problem in order to solve the viscoelastic problem. However, in the present case, there is no associated elastic problem (since the contact loundaries for the elastic and the viscoelastic rolling case are different).

But, a line load (normal or shear) or any precisely defined loading acting on a viscoelastic sheet, has an associated elastic problem. Therefore, the influence functions for a viscoelastic sheet may be obtained from the corresponding elastic solutions by applying the correspondence principle [16], provided it is possible to carry out the required mathematical operations. A technique is proposed in this thesis to determine the necessary viscoelastic influence functions. It is then possible to formulate the complete problem of the rolling of a viscoelastic sheet in a manner similar to that of Bentall. It is apparent that the elastic case must be considered first.

Since the problem formulated here is rather complicated, it is necessary to make some simplifying assumptions. Hence,

the following assumptions are made for the subsequent analysis:

- (i) The cylinders are assumed to be rigid as compared to the sheet. Also, they are supposed to be identical. Thus, the stresses and displacements will be symmetrical with respect to the centre line of the sheet.
- (ii) The sheet is supposed to be sufficiently wide and, therefore, the deformation of the sheet is assumed to take place essentially in the plane perpendicular to the axis of the cylinder.
- (iii) The cylinders are assumed to be rotating slowly, but at constant speed. Therefore, all inertia terms are disregarded.
- (iv) The deformations are assumed to be small so that the solutions can be superposed linearly.
- (v) It is assumed that the material properties of the sheet do not change during its passage through the nip.

Since it is very likely that the coefficient of friction between the contact surfaces varies along the length of contact, therefore, even though the problem is solved for the case of partial slip for some given values of the coefficient of friction, the solutions may be far from the true solutions. In view of this fact, it is decided to solve the two extreme cases of the problem, viz.:

CASE A: we no when there will be complete "no slip" and no bound on the shear forces,

and

<u>CASE B:</u>  $\mu = 0$ , when there will be complete slip and the shear forces will be zero.

The true solution of the problem is considered to lie somewhere within the range of the above limiting solutions. It will be seen later that this range is small, and, therefore, it is possible to make an estimate of the true solution for any particular case.

The present work is divided into eight chapters.

Chapter II contains the basic theory, the specified boundary conditions, and the formulation of the problem. Equations of the theory of elasticity related to the problem are reviewed in Chapter III. The influence functions for elastic sheet are obtained in Chapter IV by using a Fourier transform

technique. The integrals involved in these expressions have been evaluated analytically by using the calculus of residues, as shown in Appendix I. Chapter V deals with the rolling of an elastic sheet. The influence functions for a viscoelastic sheet are obtained in Chapter VI, using the principle of correspondence and the convolution theorem. The integrals occurring in these expressions are evaluated in Appendix II. Chapter VII finally deals with the rolling of a viscoelastic sheet and in Chapter VIII, the discussions of the elastic and the viscoelastic solutions are presented.

#### CHAPTER II

### 2. BASIC THEORY

The rolling of a viscoelastic sheet in contact with two rigid and identical cylinders is indicated in Figure 1. The cylinders are assumed to be rotating at some small speed  $\omega$ . Since the cylinders are identical, there is a line of symmetry with respect to the centre line of the sheet. Therefore, only one half of the sheet needs to be considered in the following analysis.

The nip-conditions are illustrated in an exaggerated form by Figure 2. The cylinder makes contact with the sheet over some unknown length L. The total normal load M, exerted by the cylinder, is distributed over the contact length in some unknown fashion. Because of the dissipative nature of the sheet material, the pressure distribution is skewed towards the leading side and the lengths of contact on the leading and trailing edges are different. Owing to the presence of friction between the contacting surfaces, some shearing forces with an unknown distribution will be generated. Under the applied load, the cylinder will come closer to (or approaches) the sheet by some distance  $d_0$ .

A theory required for the determination of the unknown pressure and shear distributions, the lengths of contact on the leading and the trailing sides of the sheet, as well as the amount of relative approach, will be proposed in the following paragraphs. The co-ordinate system used in the analysis is shown in Figure 2.

#### 2.1 Boundary Conditions

The boundary conditions of the problem are of the mixed type. In other words, some of the conditions are prescribed in terms of forces whilst others are prescribed in terms of displacements. These conditions can be grouped into the following four classes.

#### (i) THE NORMAL FORCE CONDITIONS

The conditions for the normal forces are the following:

$$p(Y) \geqslant 0$$
 within the nip 
$$p(Y) = 0$$
 outside the nip 
$$\int p(Y) dY = W$$

where the integration is carried out over the whole contact area.

The conditions in (2.1) imply that no tensile force is permitted within the nip and that the normal forces must be zero outside the nip.

#### (ii) THE NORMAL DISPLACEMENT CONDITION

Physically, it is required that the two bodies have a common surface within the nip. Since the cylinder is rigid, the surface of the sheet must follow the circular profile of the cylinder within the nip. Assuming small deformation, this condition can be written as:

$$U(Y) = d_o - f(Y) \qquad \text{within the nip}$$

$$= \qquad \text{unknown outside the nip}$$

$$(2.2)$$

where f(Y) represents the geometry of the surface of the cylinder.

#### (iii) THE SHEAR FORCE CONDITIONS

Before analysing the conditions for the shear forces, it is necessary to study how they are generated. If the

sheet is thin, the cylinders have a squeezing action on the sheet. The latter, therefore, tries to move away from the centre. This action is illustrated in Figure 3(a). On the other hand, if the sheet is thick, the latter behaves like a string. In this case, the sheet tries to move in. This action is illustrated in Figure 3(b).

If the contact surfaces are smooth, the sheet can move freely. If not, then the frictional force will oppose the motion of the sheet. This generates the shear forces which act against the direction of movement of the sheet.

The conditions for the shear forces may then be expressed as follows:

FOR CASE A: Q(Y) to be acting either inwards or outwards within the nip

= O outside the nip

FOR CASE B: Q(Y) = O for all Y.

The former condition of Case A implies that there can be only one reversal in the direction of the shear forces and that it reaches zero somewhere in the middle of the contact. Since the tendency of the sheet to move occurs mostly at the ends and least — near the centre, the magnitude of the shear forces should reach maximum value near the end and should decrease monotonically to zero somewhere in the middle. Bufler [4] mentions that for the case of infinite friction, the ratio of the shear force to the normal force rises to infinity at the ends. This suggests that:

#### FOR CASE A:

19(Y)1 P(Y)

should be maximum at the ends and should decrease monotonically to zero somewhere in the middle.

(2.4)

# (iv) THE SHEAR DISPLACEMENT CONDITIONS

When the coefficient of friction is zero, there is no limitation on the movement of the sheet in the Y-direction. The amount of shear displacement will depend upon the normal forces. But when the coefficient of friction is infinite, the sheet is not permitted to move relative to the cylinder. Hence, it is essential that the contact points move at equal speeds. Then, let:

F = Nominal velocity of the cylinder,

F. = Nominal velocity of the sheet,

 $f_{Y}$  = Velocity of any point in the sheet within the nip.

Then, neglecting second order terms, one can write:

$$f_Y = F_0 \left( 1 + \frac{\partial y}{\partial y} \right)$$

Since the cylinder is assumed to be rigid, it is not deformed and the velocity of any point on the cylinder remains the same. Hence, in order that the two points have the same velocity, it is required that:

$$f_Y = F$$

or,

or,

$$\frac{\partial V}{\partial Y} = \frac{F - F_0}{F_0} = \chi \tag{2.5}$$

Since  $\mathbf{X}$  depends upon the nominal velocities of the two bodies, it must remain a constant for all points in the nip. Hence, differentiating a second time with respect to  $\mathbf{Y}$ ,

$$\frac{9\lambda_5}{9_5 h} = 0$$

The conditions for the shear displacements become then, as follows:

$$\frac{CASE A}{3Y^2} = 0 \qquad \text{everywhere within} \\
\text{the nip} \\
\underline{CASE B} : \quad V(Y) = \qquad \text{unprescribed}$$

Equations (2.1) to (2.6) constitute the complete boundary conditions of the present problem. But it will be difficult to satisfy them until the contact lengths (on the leading and the trailing edges) are determined. For this purpose, a semi-inverse method is being proposed here. The solution must be considered as an approximate one, but by making the elements sufficiently small, a high degree of accuracy can be achieved.

## 2.2 Representation of the Nip Forces

Let the contact length be divided into a number of small elements of equal widths such that there are  $m_1$  elements on the leading side and  $m_2$  elements on the trailing side. (The choice and the determination of  $m_1$  and  $m_2$  will be discussed later.) As an approximation, let it be assumed that the total force on any element acts as concentrated forces (one normal and one shear) at the centre point of the element. Let the magnitudes of these concentrated

forces on the  $j^{\dagger h}$  element be  $P_j$  and  $Q_j$  (normal and shear respectively).

Since the thickness of the sheet is very small compared to the radius of the cylinder, the angle of contact will be very small. And with little loss of accuracy, the normal forces may be considered to be acting vertically and the shearing forces as acting horizontally and all moving horizontally with the surface velocity of the cylinder. The problem then reduces to the determination of the contact length  $\bot$ , the amount of relative approach  $d_o$  and of  $P_j$ 's and  $Q_j$ 's such that they satisfy the conditions expressed by equations (2.1) to (2.6) on the whole sheet. A schematic representation of these forces acting on the viscoelastic sheet is indicated in Figure 4.

#### 2.3 Derivation of the Matching Equations

Let the boundary conditions be satisfied at some discrete points called matching points. Then, by choosing a large number of evenly spread matching points, it may be safely assumed that these conditions are satisfied everywhere on the boundary. For convenience, the matching points will be taken as the points midway between the loads together with the end points of contact. Let

- the normal displacement of the surface of the
  sheet at the ith point due to a unit normal
  line load at the jth point;

- Vij = the tangential displacement of the surface of the sheet at the *ith* point due to a unit shear line load at the *jth* point;
- Ui = the total normal displacement of the surface of
   the sheet at the ith point; and
- $\mathcal{V}_i$  = the total tangential displacement of the surface of the sheet at the ith point.

Then, using superposition, the displacements of the *ith* point can be expressed as follows:

$$U_{i} = \sum_{j=1}^{m_{1}+m_{2}} \left\{ u_{ij}^{n}.P_{j} + u_{ij}^{s}.Q_{j} \right\}$$

$$V_{i} = \sum_{j=1}^{m_{1}+m_{2}} \left\{ V_{ij}^{n}.P_{j} + V_{ij}^{s}.Q_{j} \right\}$$
(2.7)

But the displacements of the *ith* point are also governed by relations (2.2) and (2.6). To obtain the second derivatives, it is only necessary to differentiate the influence functions twice (assuming that the superposition also holds for second derivatives). Hence,

$$\left(\frac{\partial^2 v}{\partial Y^2}\right)_i = \sum_{j=1}^{m_1+m_2} \left\{ \left(\frac{\partial^2 v}{\partial Y^2}\right)_{ij} P_{j} + \left(\frac{\partial^2 v}{\partial Y^2}\right)_{ij} Q_{j} \right\}$$
(2.8)

where,

 $\left(\frac{\partial^2 V^n}{\partial Y^2}\right)_{ij}$  = the second derivative obtained at the ith point with respect to Y of the shear displacement due to a unit normal load situated at the jth point.

Using equations (2.2), (2.6), (2.7), and (2.8), a set of matching equations can be derived for the two cases as follows:

#### CASE A:

$$\sum_{j=1}^{M_{L}+M_{2}} \left\{ (u_{ij}^{n} P_{j}^{n} + u_{ij}^{s} Q_{j}) \right\} = d_{o} - f(Y_{i})$$

$$\sum_{j=1}^{M_{L}+M_{2}} \left\{ (\frac{\partial^{2} V^{n}}{\partial Y^{2}})_{ij} P_{j}^{n} + (\frac{\partial^{2} V^{s}}{\partial Y^{2}})_{ij} Q_{j}^{n} \right\} = 0$$
(2.9)

#### CASE B:

$$Q_{j} = 0$$

$$\sum_{j=1}^{m_{1}+m_{2}} (U_{ij}^{n} P_{j}) = d_{o} - f(Y_{i})$$

$$\sum_{j=1}^{m_{1}+m_{2}} (V_{ij}^{n} P_{j}) = \text{unprescribed}$$

$$(2.10)$$

Equations (2.9) and (2.10) give a set of simultaneous equations for the unknown quantities. By choosing a sufficient number of matching points, these equations can be solved for the unknown quantities, provided that the restrictions imposed by equations (2.1), (2.3), and (2.4) are not violated. Unfortunately, these equations cannot be handled further until the lengths of contact on the leading and the trailing edges are known. The latter, however, are related to the unknown forces and, therefore, cannot be determined directly. A semi-inverse method is being proposed here to solve these complexities.

Either  $\mathbf{M_1}$  or  $\mathbf{M_2}$  may be chosen from the consideration of the required accuracy. But their ratio depends upon the speed of rolling, the rate of relaxation of the material and, perhaps, on the geometry and the loading conditions. The determination of this ratio will be discussed in section 2.5 and, for the purpose of the analysis given in section 2.4, it will be assumed that this is known.

# 2.4 Determination of the Contact Length

Let

$$2\alpha$$
 = width of each element  
 $2b$  = thickness of the sheet  
 $\beta = \frac{a}{b}$  (2.11)

Also, let  $\beta_0$  be an assumed value of the parameter  $\beta$ . Then, rearranging equation (2.9), and solving the set of simultaneous equations, it is possible to determine the unknowns corresponding to the above assumed value of  $\beta$ . It is necessary, however, to make proper corrections on this assumption of  $\beta$ .

If  $P_j^{\circ}$ ,  $Q_j^{\circ}$ ,  $L^{\circ}$ ,  $d_o^{\circ}$ , and  $\mathcal{K}^{\circ}$  denote the approximate values as obtained according to the above assumption, and  $P_j^{\circ}$ ,  $Q_j^{\circ}$ , L,  $d_o^{\circ}$ , and  $\mathcal{K}$  denote values corresponding to the correct solutions, then the loads in either case can be written as follows:

$$W^{\circ} = \sum_{j=1}^{m_1+m_2} P_j^{\circ}$$

$$W = \sum_{j=1}^{m_1+m_2} P_j.$$
(2.12)

where  $oldsymbol{\mathcal{W}}$  is the specified normal load per unit length of the cylinder.

It is assumed that the normal load is mainly utilized in producing elastic deformation. The normal load W will then be proportional to the area of deformation of the sheet. But the latter is roughly proportional to  $(L\times d_{\circ})$ . From geometrical considerations, it can be seen that  $L\propto \beta$  and  $d_{\circ} \propto \beta^2$ . Hence, the deformed area within the nip will be proportional to  $\beta^3$ . Thus, a better approximation, in this case, will be by taking the parameter  $\beta$  as follows:

$$\beta_{N} = \beta_{o} \left( \frac{M}{W_{o}} \right)^{1/3} \tag{2.13}$$

With the new value of  $oldsymbol{\beta}$  , the whole process should be repeated until a desired accuracy is obtained.

Having determined a proper value of the parameter  $oldsymbol{eta}$  , the contact length can be obtained easily by using the relation:

$$L = 2(m_1 + m_2) \beta b$$
 (2.14)

# 2.5 Determination of the Ratio m<sub>1</sub>:m<sub>2</sub>

It was mentioned earlier that either  $m_1$  or  $m_2$  may be chosen depending upon the accuracy that is desired. But the ratio of  $m_1$  and  $m_2$  depends upon many parameters and cannot be determined directly. For an elastic sheet there is a

symmetry and therefore  $m_1 = m_2$ . It is only for a visco-elastic sheet that this ratio needs to be determined. A semi-inverse method is being proposed here for this purpose.

A value of  $\mathbf{m_2}$  should be assumed first and then the solutions for the unknowns should be obtained. It should then be checked if the boundary conditions are completely satisfied. It will be shown in the following paragraphs that if the value of  $\mathbf{m_2}$  is underestimated, then the boundary conditions can be completely satisfied. On the other hand, if this value is overestimated, then the normal force condition, as expressed by equation (2.1), will be violated and therefore the boundary conditions in this case cannot be satisfied completely.

Since  $\mathbf{m_2}$  cannot be greater than  $\mathbf{m_1}$ , for the first approximation  $\mathbf{m_2}$  should be given a value equal to that of  $\mathbf{m_1}$ . The solutions should be obtained and the boundary conditions should be checked. If they are completely satisfied, the choice of  $\mathbf{m_2}$  was a right one. If not, then the value of  $\mathbf{m_2}$  should be decreased by one and the process should be repeated until the boundary conditions are completely satisfied. The greatest value of  $\mathbf{m_2}$  which does satisfy the boundary conditions completely, is the right one.

First, consider the case of underestimation and, for

simplicity, assume that the value of  $\mathbf{m_2}$  is underestimated by one. Figure 5(a) represents this situation in an exaggerated form. Curve I represents the deformed shape of the surface of the sheet. The sheet loses contact with the cylinder at the point  ${f D}$  . By underestimating the value of  $\mathbf{m_2}$  , it is implied that there is no force on the last element and that the sheet apparently loses contact with the cylinder at the point  ${f D}^{\prime}$  . As such, the displacement boundary conditions are to be matched only up to the and not up to  ${\bf D}$  . Curve II represents the displacement profile of the surface when the forces on the last element have been removed and when all other forces remain unchanged. It is seen that it is possible to satisfy the displacement conditions up to the point  $\mathbf{D}^{\prime}$  by adjusting the values of the remaining forces, and especially that of  $P_{m_1+m_2-1}$  . This proves that when the value of  $m_2$  is underestimated, the boundary conditions can be completely satisfied.

Now, consider the case of overestimation and, again for simplicity, assume that the value of  $\mathbf{m_2}$  is overestimated by one. Figure 5(b) represents this situation in an exaggerated form. Because of the overestimation in the value of  $\mathbf{m_2}$ , one extra element is introduced in the nip and the displacement boundary conditions are now required to be satisfied up to the point  $\mathbf{p''}$ . Since the displacement at any point is mostly

influenced by the forces closest to that point, it is evident that the normal force on the last element must be tensile. This violates the condition expressed by equation (2.1). This proves that when the value of  $m_2$  is overestimated, the boundary conditions cannot be completely satisfied.

#### CHAPTER III

# 3. SOME EQUATIONS OF ELASTICITY

It is well known that in the absence of body forces, the plane elastostatic problem reduces to the determination of a biharmonic function  $\Phi$  which satisfies the given boundary conditions of the particular problem. In rectangular coordinates, this is expressed by:

$$\nabla^2 \cdot \nabla^2 \cdot \Phi(x,y) = 0 \tag{3.1}$$

where

$$\nabla^2 \equiv \frac{\partial^2}{\partial x^2} + \frac{\partial^2}{\partial y^2}$$

The stresses in the body are related to this function by the following relations:

$$\mathfrak{S}_{x} = \frac{\partial^{2} \Phi}{\partial y^{2}}, \qquad (a)$$

$$\mathfrak{S}_{y} = \frac{\partial^{2} \Phi}{\partial x^{2}}, \qquad (b)$$

$$\mathfrak{T}_{xy} = -\frac{\partial^{2} \Phi}{\partial x \partial y}. \qquad (c)$$

When the boundary conditions are prescribed in terms of "known forces" and when one of the axes extends from  $-\infty$  to  $\infty$ , the Fourier transform makes it very easy to determine the particular biharmonic function. This method is

described below.

Let the **y**-axis extend from  $-\infty$  to  $\infty$ . Then, by taking the Fourier transform of both sides of equation (3.1),

$$\int_{-\infty}^{\infty} \nabla^4 \Phi(x,y) e^{i\xi y} dy = 0$$

or,

$$\left(\frac{d^2}{dx^2} - \xi^2\right)^2 \int_{-\infty}^{\infty} \Phi(x,y) e^{i\xi y} dy = 0$$

which can also be written as:

$$\left(\frac{d^2}{dx^2} - \xi^2\right)^2 G(x,\xi) = 0 \tag{3.3}$$

where

$$G^{\circ}(x,\xi) = \int_{-\infty}^{\infty} \Phi(x,y) e^{i\xi y} dy$$

and where  $\xi$  is the Fourier transform parameter. Equation (3.3) is an ordinary second order differential equation whose general solution is given by:

$$G^{\circ}(x,\xi) = (A_{\circ} + B_{\circ} x \xi) e^{-\xi x} + (C_{\circ} + D_{\circ} x \xi) e^{\xi x}$$

$$Or,$$

$$G^{\circ}(x,\xi) = (A_{\circ} + B_{\circ} x \xi) \cosh x \xi + (C_{\circ} + D_{\circ} x \xi) \sinh x \xi$$
(3.4)

in which  $A_0$ ,  $B_0$ ,  $C_0$  and  $D_0$  are some functions of  $C_0$ . In order to determine these functions, it is necessary to express the given boundary conditions in terms of the function  $G_0$  or its derivatives.

Taking the Fourier transforms of both sides of equation (3.2) yields:

$$\int_{-\infty}^{\infty} \sigma_{x} e^{i\xi^{y}} dy = -\xi^{2} G^{\circ}$$

$$\int_{-\infty}^{\infty} \sigma_{y} e^{i\xi^{y}} dy = \frac{d^{2}G^{\circ}}{dx^{2}}$$

$$\int_{-\infty}^{\infty} T_{xy} e^{i\xi^{y}} dy = i\xi \frac{dG^{\circ}}{dx}$$
(c)

or,

$$G'(x,\xi) = -\frac{1}{\xi^2} \overline{Gx}$$

$$\frac{dG'(x,\xi)}{dx} = -\frac{i}{\xi} \overline{C}xy$$

$$\frac{d^2G'(x,\xi)}{dx^2} = \overline{Gy}$$
(a)
(b)
(3.6)

By substituting the given boundary conditions into equation (3.6), sufficient conditions may be obtained for the function  $G^{\circ}$  or its derivatives to obtain the constants  $A_{\circ}$ ,  $B_{\circ}$ ,  $C_{\circ}$  and  $D_{\circ}$ . Having determined  $G^{\circ}(x,\xi)$ , the stresses and displacements in the body can be established as follows:

Taking the inverse Fourier transforms of equation (3.5) gives:

$$\begin{aligned}
\delta_{X}(x,y) &= -\frac{1}{2\pi} \int_{-\infty}^{\infty} \xi^{2} G(x,\xi) e^{-i\xi y} d\xi & \text{(a)} \\
\delta_{Y}(x,y) &= \frac{1}{2\pi} \int_{-\infty}^{\infty} \frac{d^{2}G(x,\xi)}{dx^{2}} e^{-i\xi y} d\xi & \text{(b)} \\
\mathcal{T}_{XY}(x,y) &= \frac{i}{2\pi} \int_{-\infty}^{\infty} \xi \frac{dG(x,\xi)}{dx} e^{-i\xi y} d\xi & \text{(c)}
\end{aligned}$$

In the case of plane deformation, the strains are given by:

$$\varepsilon_{\chi} = \frac{\partial v}{\partial x} = \frac{1+v}{E} \left[ (1-v) c_{\chi} - v c_{\chi} \right]$$

$$\varepsilon_{\chi} = \frac{\partial v}{\partial x} = \frac{1+v}{E} \left[ (1-v) c_{\chi} - v c_{\chi} \right]$$

in which u, v are the displacement components in the x and y directions, respectively. Substituting for 6x and 6y from equation (3.7a,b) gives:

$$\frac{\partial \mathcal{L}}{\partial x} = -\frac{1+\mathcal{V}}{2\pi\epsilon} \int_{-\infty}^{\infty} \left[ (1-\mathcal{V})\xi^{2}G^{\circ} + \mathcal{V} \frac{d^{2}G^{\circ}}{dx^{2}} \right] e^{-i\xi y} d\xi$$

$$\frac{\partial \mathcal{V}}{\partial y} = \frac{1+\mathcal{V}}{2\pi\epsilon} \int_{-\infty}^{\infty} \left[ (1-\mathcal{V}) \frac{d^{2}G^{\circ}}{dx^{2}} + \mathcal{V}\xi^{2}G^{\circ} \right] e^{-i\xi y} d\xi$$
(3.8)

----

A partial integrating of (3.8a,b) with respect to x and y respectively, yields:

$$U(x,y) = -\frac{1+\nu}{2\pi E} \int_{-\infty}^{\infty} \left[ (1-\nu) \, \xi^2 \int G^0 dx + \nu \, \frac{dG^0}{dx} \right] e^{-i\xi y} d\xi + g(y) \quad (a)$$

$$V(x,y) = \frac{1+\nu}{2\pi E} \, i \int_{-\infty}^{\infty} \left[ (1-\nu) \, \frac{d^2 G^0}{dx^2} + \nu \, \xi^2 G^0 \right] e^{-i\xi y} \, \frac{d\xi}{\xi} + f(x) \quad (b)$$

The functions f(x) and g(y) on the right-hand side of the above relations are interrelated as follows:

$$\delta xy = \frac{\partial U}{\partial y} + \frac{\partial y}{\partial x} = \frac{2(1+y)}{E} Cxy$$

Substituting for U and V from equation (3.9) and for  $\nabla \times y$  from equation (3.7c) and simplifying, yields:

$$\frac{1-v^{2}}{2\pi\epsilon}i\int_{-\infty}^{\infty}\left[\xi^{3}\int G^{3}dx + \frac{1}{\xi}\frac{d^{3}G^{0}}{dx^{3}} - 2\xi\frac{dG^{0}}{dx}\right]e^{-i\xi^{3}}d\xi$$

$$= -\left[\frac{df}{dx} + \frac{d\theta}{dy}\right] \qquad (3.10)$$

Taking any one expression of the forms  $G(x,\xi)$  given in equation (3.4), it is seen that:

$$\xi^{3} \int G^{2} dx + \frac{1}{\xi} \frac{d^{3}G^{2}}{dx^{3}} - 2\xi \frac{dG^{2}}{dx} = 0$$
 (3.11)

From equations (3.10) and (3.11), therefore,

$$\frac{df}{dx} + \frac{dg}{dy} = 0$$

Let

$$\frac{df}{dx} = -C \qquad \text{and} \qquad \frac{dg}{dy} = C$$

in which C is some constant. Then,

$$f(x) = -C x + C_2$$
 (3.12)  
 $g(y) = C y + C_1$ 

Substituting for f(x) and g(y) in equation (3.9), yields:

$$\begin{split} \mathcal{U}(x,y) &= -\frac{1+V}{2\pi E} \int_{-\infty}^{\infty} \left[ (1-V)\xi^{2} \int G^{2}dx + V \frac{dG^{2}}{dx} \right] e^{-i\xi y} d\xi \\ &+ Cy + C1 \\ \mathcal{V}(x,y) &= \frac{1+V}{2\pi E} i \int_{-\infty}^{\infty} \left[ (1-V) \frac{d^{2}G^{2}}{dx^{2}} + V\xi^{2}G^{2} \right] e^{-i\xi y} d\xi \\ &- Cx + C_{2} \end{split}$$

The constants C ,  $C_1$  and  $C_2$  may be determined from the specified constraints on the displacements of the body.

When the external forces are either symmetrical or antisymmetrical with respect to  $\boldsymbol{y}$ , the above equations can be further simplified. There are, therefore, two cases

of particular interest, viz.:

- (i) when  $\Phi(x,y)$  is an even function of y and
- (ii) when  $\Phi(x,y)$  is an odd function of y.

The equations for these cases will be developed subsequently.

# CASE (i): when $\Phi(x,y)$ is an even function of y

It should be noted that if  $\Phi(x,y)$  is an even function of y,  $G_{x} = \frac{\partial^{2} \Phi}{\partial x^{2}} \qquad \text{and} \qquad G_{y} = \frac{\partial^{2} \Phi}{\partial x^{2}}$ 

will be even functions of  $\gamma$ , whilst

$$C^{xh} = -\frac{9x9^{h}}{9\sqrt{\Phi}}$$

will be an odd function of  $\gamma$  . Now,

$$G^{\circ}(x,\xi) = \int_{-\infty}^{\infty} \Phi(x,y) e^{i\xi y} dy = \int_{-\infty}^{\infty} \Phi(x,y) \cos \xi y dy$$
$$= 2 G^{\circ}(x,\xi) \qquad (3.14)$$

where

$$G^{()}(x,\xi) = \int_{0}^{\infty} \Phi(x,y) \cos \xi y \, dy \qquad (3.15)$$

From equations (3.5) and (3.14),

$$\int_{-\infty}^{\infty} G_{x} e^{i\xi y} dy = -2\xi^{2}G^{(i)}$$

$$\int_{-\infty}^{\infty} G_{y} e^{i\xi y} dy = 2\frac{d^{2}G^{(i)}}{dx^{2}}$$

$$\int_{-\infty}^{\infty} T_{xy} e^{i\xi y} dy = 2i\xi \frac{dG^{(i)}}{dx}$$
(3.16)

But

$$\int_{-\infty}^{\infty} 6x e^{i\xi y} dy = 2 \int_{0}^{\infty} 6x \cos \xi y dy$$

$$\int_{-\infty}^{\infty} 6y e^{i\xi y} dy = 2 \int_{0}^{\infty} 6y \cos \xi y dy$$

$$\int_{-\infty}^{\infty} 7xy e^{i\xi y} dy = 2i \int_{0}^{\infty} 7xy \sin \xi y dy$$
(3.17)

From equations (3.16) and (3.17),

$$G^{\omega}(x,\xi) = -\frac{1}{\xi^2} \int_0^{\infty} 6x \cos \xi y \, dy$$

$$\frac{dG^{\omega}(x,\xi)}{dx} = \frac{1}{\xi} \int_0^{\infty} \tau_{xy} \sin \xi y \, dy$$

$$\frac{d^2G^{\omega}(x,\xi)}{dx^2} = \int_0^{\infty} 6y \cos \xi y \, dy$$
(3.18)

Equation (3.18) gives the necessary conditions for the

determination of  $G'(x,\xi)$ . In the case of  $\Phi(x,y)$  being an even function of y,

$$G'(x,\xi)$$
,  $\frac{dG'(x,\xi)}{dx}$  and  $\frac{d^2G'(x,\xi)}{dx^2}$ 

will be even functions of  $\xi$  . Therefore, equations (3.7) and (3.13) become:

$$\mathfrak{G}_{\mathsf{X}}(\mathsf{x},\mathsf{y}) = -\frac{2}{\Pi} \int_{0}^{\infty} \xi^{2} \mathsf{G}^{(1)}(\mathsf{x},\xi) \cos \xi \mathsf{y} \, d\xi$$

$$\mathfrak{G}_{\mathsf{y}}(\mathsf{x},\mathsf{y}) = \frac{2}{\Pi} \int_{0}^{\infty} \frac{\mathsf{d}^{2} \mathsf{G}^{(1)}(\mathsf{x},\xi)}{\mathsf{d}\mathsf{x}^{2}} \cos \xi \mathsf{y} \, d\xi$$

$$\mathfrak{T}_{\mathsf{x}\mathsf{y}}(\mathsf{x},\mathsf{y}) = \frac{2}{\Pi} \int_{0}^{\infty} \xi \, \frac{\mathsf{d} \mathsf{G}^{(1)}(\mathsf{x},\xi)}{\mathsf{d}\mathsf{x}} \sin \xi \mathsf{y} \, d\xi$$
(3.19)

and

$$U(x,y) = -\frac{2(1+v)}{\Pi E} \int_{0}^{\infty} \left[ (1-v) \xi^{2} \int_{0}^{\omega} dx + v \frac{dG^{0}}{dx} \right].$$

$$\cdot \cos \xi y \, d\xi + Cy + C_{1}$$

$$V(x,y) = \frac{2(1+v)}{\Pi E} \int_{0}^{\infty} \left[ (1-v) \frac{d^{2}G^{0}}{dx^{2}} + V\xi^{2}G^{0} \right].$$

$$\cdot \sin \xi y \, \frac{d\xi}{\xi} - cx + C_{2}$$
(3.20)

## CASE (ii): when $\Phi(x,y)$ is an odd function of y

As earlier, when  $\Phi(x,y)$  is an odd function of y, 6x and 6y will be odd functions of y and 7xy will be an even function of y. Therefore, the function 6° will be as follows:

$$G^{(x,\xi)} = \int_{-\infty}^{\infty} \Phi(x,y) e^{i\xi y} dy$$

$$= 2 i G^{(2)}(x,\xi)$$
(3.21)

where,

$$G^{(2)}(x,\xi) = \int_0^\infty \Phi(x,y) \sin \xi y \, dy \tag{3.22}$$

Hence, it follows from equations (3.5) and (3.21) that:

$$\int_{-\infty}^{\infty} 6x e^{i\xi y} dy = -2i \xi^{2} G^{(2)}(x,\xi)$$

$$\int_{-\infty}^{\infty} 6y e^{i\xi y} dy = 2i \frac{d^{2} G^{(2)}(x,\xi)}{dx^{2}}$$

$$\int_{-\infty}^{\infty} 7 x y e^{i\xi y} dy = -2\xi \frac{d G^{(2)}(x,\xi)}{dx}$$
(3.23)

$$\int_{-\infty}^{\infty} 6x e^{i\xi y} dy = 2i \int_{0}^{\infty} 6x \sin \xi y dy$$

$$\int_{-\infty}^{\infty} 6y e^{i\xi y} dy = 2i \int_{0}^{\infty} 6y \sin \xi y dy$$

$$\int_{-\infty}^{\infty} 7xy e^{i\xi y} dy = 2 \int_{0}^{\infty} 7xy \cos \xi y dy$$
(3.24)

and from equations (3.23) and (3.24), therefore,

$$G^{(2)}(x,\xi) = -\frac{1}{\xi^2} \int_0^\infty Gy \sin \xi y \, dy$$

$$\frac{dG^{(2)}(x,\xi)}{dx} = -\frac{1}{\xi} \int_0^\infty Z_{xy} \cos \xi y \, dy$$

$$\frac{d^2G^{(2)}(x,\xi)}{dx^2} = \int_0^\infty Gy \sin \xi y \, dy$$
(3.25)

Equation (3.25) gives thus the necessary conditions for the determination of  $G^{(2)}(x,\xi)$ .

Now, if 
$$\Phi(x,y)$$
 is an odd function of  $y$ ,
$$G^{(x)}(x,\xi), \quad \frac{dG^{(x)}(x,\xi)}{dx} \quad \text{and} \quad \frac{d^2G^{(x)}(x,\xi)}{dx^2}$$

are all odd functions of  $\xi$  . Therefore, equations (3.7) and (3.13) become:

$$\delta x (x,y) = -\frac{2}{\pi} \int_{0}^{\infty} \xi^{2} G^{(2)}(x,\xi) \sin \xi y \, d\xi 
\delta y (x,y) = \frac{2}{\pi} \int_{0}^{\infty} \frac{d^{2} G^{(2)}(x,\xi)}{dx^{2}} \sin \xi y \, d\xi 
Cxy (x,y) = -\frac{2}{\pi} \int_{0}^{\infty} \xi \, \frac{dG^{(2)}(x,\xi)}{dx} \cos \xi y \, d\xi$$
(3.26)

and

$$U(x,y) = -\frac{2(1+v)}{\pi E} \int_{0}^{\infty} \left[ (1-v)\xi^{2} \int_{0}^{(2)} dx + v \frac{dG^{(2)}}{dx} \right].$$

$$\cdot \sin \xi y \ d\xi + cy + 1$$

$$v(x,y) = -\frac{2(1+v)}{\pi E} \int_{0}^{\infty} \left[ (1-v) \frac{d^{2}G^{(2)}}{dx^{2}} + v \xi^{2}G^{(2)} \right].$$

$$\cdot \cos \xi y \frac{d\xi}{\xi} - cx + c_{2}$$
(3.27)

It is seen from the above review of the plane case of elastic deformation that in accordance with specified force boundary conditions, the corresponding stress and deformation fields can be readily determined.

#### CHAPTER IV

# 4. SURFACE DISPLACEMENTS OF AN ELASTIC SHEET DUE TO MOVING LOADS

As pointed out in the introduction to this thesis and in Chapter II, it is necessary, for the formulation of the given elastic problem, to establish expressions for surface displacements. This is done by using the concept of *influence functions*. For this purpose, the loading on the sheet in motion is indicated in Figure 6(a) and (b). The case of the normal loading of the sheet will be considered first and then the effect of shear forces on the moving sheet will be treated.

# 4.1 Influence Functions for Normal Line Load

Figure 6(a) shows an elastic sheet under a pair of concentrated normal line loads of unit magnitude (per unit width of the sheet) representing the pressure of the cylinder over one surface element of the sheet. The sheet is assumed to move with a small velocity  $F_{\bullet}$ , or equivalently, the sheet may be considered as stationary and the line load moving with the same velocity.

Consider now, a coordinate system  $\mathbf{x-y}$  (Figure 6(a)) moving with the load. The boundary conditions can be expressed as:

$$\mathcal{O}_{\mathbf{x}}^{\mathbf{x}}(\pm b, \mathbf{y}) = -\mathbf{1} \delta(\mathbf{y})$$

$$\mathcal{O}_{\mathbf{x}}(\pm b, \mathbf{y}) = 0$$
(4.1)

where  $\delta(y)$  is the Dirac delta function and 1 represents a *unit* step load. It can be seen from relation (4.1) that  $\delta x$  is an even function of y and  $\delta(x,y)$  will also be an even function of y. Therefore, from equations (3.18) and (4.1), it follows that:

$$G^{(1)}(\pm b,\xi) = \frac{1}{\xi^2} \int_0^\infty \delta(y) \cos \xi y \, dy$$

$$= \frac{1}{2\xi^2} \int_{-\infty}^\infty \delta(y) \cos \xi y \, dy = \frac{1}{2\xi^2}$$

$$\frac{dG}{dx}(\pm b,\xi) = \frac{1}{\xi} \int_0^\infty o. \sin \xi y \, dy = 0$$
(4.2)

Taking the following form of the function  $G^{(j)}$ :

$$G^{(i)}(x,\xi) = (A_1 + B_1 x \xi) \cosh x \xi + (C_1 + D_1 x \xi) \sinh x \xi$$

$$\frac{dG^{(i)}}{c'}(x,\xi) = \xi \left[ (A_1 + D_1) \sinh x \xi + (B_1 + C_1) \cosh x \xi + B_1 x \xi \sinh x \xi + D_1 x \xi \cosh x \xi \right]$$

yields, upon substituting the conditions of equation (4.2), the relations:

$$(A_1+B_1b\xi)\cosh b\xi + (C_1+D_1b\xi)\sinh b\xi = \frac{1}{2\xi^2}$$

$$(A_1-B_1b\xi)\cosh b\xi - (C_1-D_1b\xi)\sinh b\xi = \frac{1}{2\xi^2}$$

$$(A_1+D_1)\sinh b\xi + (B_1+C_1)\cosh b\xi$$

$$+B_1b\xi\sinh b\xi + D_1b\xi\cosh b\xi = 0$$

$$(A_1+D_1)\sinh b\xi - (B_1+C_1)\cosh b\xi$$

$$-B_1b\xi\sinh b\xi + D_1b\xi\cosh b\xi = 0$$

By solving these simultaneous equations, the coefficients are obtained as follows:

$$B_{1} = C_{1} = 0$$

$$A_{1} = \frac{\sinh b\xi + b\xi \cosh b\xi}{\xi^{2}(\sinh 2b\xi + 2b\xi)}$$

$$D_{1} = -\frac{\sinh b\xi}{\xi^{2}(\sinh 2b\xi + 2b\xi)}$$
(a)
$$C_{1} = 0$$
(b)
$$C_{2} = 0$$
(c)

Integrating and differentiating  $G^{(i)}(x,\xi)$  with respect to x, substituting into equation (3.20) and simplifying, yields the surface displacements due to the normal loads:

$$U_{e}^{n}(x,y) = -\frac{2(1+V)}{\Pi E} \int_{0}^{\infty} \left[ (A_{1} - D_{1} + 2VD_{1}) \sinh x\xi + D_{1}x\xi \cosh x\xi \right] \cdot \xi \cos \xi y \, d\xi + C^{(i)}y + C^{(i)}_{1}$$

$$V_{e}^{n}(x,y) = \frac{2(1+V)}{\Pi E} \int_{0}^{\infty} \left[ (A_{1} + 2D_{1} - 2VD_{1}) \cosh x\xi + D_{1}x\xi \sinh x\xi \right] \cdot \xi \sin \xi y \, d\xi - C^{(i)}x + C^{(i)}_{2}$$

$$\cdot \xi \sin \xi y \, d\xi - C^{(i)}x + C^{(i)}_{2}$$

where the superscript n refers to normal loading and the subscript e to the elastic case. Due to the symmetry condition along the y axis,

$$U_{0}^{n}(0,y)=0$$

so that

$$C^{(i)} = C_4^{(i)} = 0 (4.5)$$

To find  $C_2^{(\prime)}$ , it is necessary to impose some displacement constraint on the sheet. Thus, assuming that the point ( $O,\ell$ ) is pinned, (see Figure 6(a)) the displacement constraint becomes:

The latter condition gives:

$$C_2^{(1)} = -\frac{2(1+v)}{\Pi E} \int_0^\infty A_1 \xi \sin \xi \xi \, d\xi - \frac{4(1-v^2)}{\Pi E} \int_0^\infty D_1 \xi \sin \xi \xi \, d\xi$$
 (4.6)

It should be noted that by choosing the pinned point  $(0,\ell)$  (see Figure 6(a)) arbitrarily, the coefficient function  $C_2^{(l)}$  will depend on that length  $\ell$ . Substituting conditions (4.5) and (4.6) into relation (4.4) yields the displacements on the surface at the fixed value of  $\mathbf{x} = -\mathbf{b}$ , and in terms of  $C_2^{(l)}(\ell)$  as follows:

$$U_{e}^{n}(-b,y) = \frac{2(1+v)}{\Pi E} \int_{0}^{\infty} \left[ (A_{1}-D_{1}+2vD_{1}) \sinh b\xi + D_{1} b\xi \cosh b\xi \right] \cdot \xi \cosh b\xi$$

$$+ D_{2} b\xi \cosh b\xi \right] \cdot \xi \cosh b\xi$$

$$+ D_{3} b\xi \cosh b\xi$$

$$+ D_{4} b\xi \sinh b\xi \right] \xi \sinh \xi \xi$$

$$+ \frac{2(1+v)}{\Pi E} \int_{0}^{\infty} A_{1}\xi \sinh \xi d\xi - \frac{4(1-v^{2})}{\Pi E} \int_{0}^{\infty} D_{1}\xi \sinh \xi d\xi$$

$$+ \frac{2(1+v)}{\Pi E} \int_{0}^{\infty} A_{1}\xi \sinh \xi d\xi - \frac{4(1-v^{2})}{\Pi E} \int_{0}^{\infty} D_{1}\xi \sinh \xi d\xi$$

Substituting for the coefficients  $A_1(\xi)$  and  $D_1(\xi)$  from equation (4.3b,c) after some simplification, yields:

$$\mathcal{U}_{e}^{n}(\alpha) = \frac{2(1-y^{2})}{\Pi E} I_{1}(\alpha)$$

$$\mathcal{V}_{e}^{n}(\alpha) = -\frac{(1+y)(1-2y)}{\Pi E} I_{2}(\alpha) + \frac{2(1-y^{2})}{\Pi E} I_{3}(\alpha)$$

$$-\frac{1+y}{E} \left[ I_{4}(\gamma) + I_{5}(\gamma) \right] + \frac{2(1-y^{2})}{\Pi E} I_{4}(\gamma)$$
(4.8)

where

$$I_{1}(\alpha) = \int_{0}^{\infty} \frac{2 \sinh^{2}(b\xi) \cos(\alpha b\xi)}{b\xi \left(\sinh(2b\xi) + 2b\xi\right)} d(b\xi)$$

$$I_{2}(\alpha) = \int_{0}^{\infty} \frac{\sin(\alpha b\xi)}{b\xi} d(b\xi)$$

$$I_{3}(\alpha) = \int_{0}^{\infty} \frac{2 b\xi \sin(\alpha b\xi)}{b\xi \left(\sinh(2b\xi) + 2b\xi\right)} d(b\xi)$$

$$I_{4}(\eta) = \int_{0}^{\infty} \frac{2 \sinh(b\xi) \sin(\eta b\xi)}{b\xi \left(\sinh(2b\xi) + 2b\xi\right)} d(b\xi)$$

$$I_{5}(\eta) = \int_{0}^{\infty} \frac{2 \cosh(b\xi) \sin(\eta b\xi)}{\sinh(2b\xi) + 2b\xi} d(b\xi)$$

In which the parameters pprox and  $\gamma$  are given by

$$\alpha = \frac{9}{b}$$

It is to be noted that for the elastic case, the displacements are dependent on instantaneous positions only. Therefore, equation (4.8) has been expressed as functions of  $\varpropto$  and  $\eta$  .

#### 4.2 Influence Functions for Shear Line Load

In addition to the normal line load acting on the surface of the sheet, a shear line load as indicated in Figure 6(b) will also be occurring. The latter is represented by a pair of concentrated shear line loads of unit magnitude (per unit width of the sheet). (Either the shear load is moving and the sheet is stationary, or the load is stationary and the sheet is moving.)

Again, considering a coordinate system **x-y** moving with the load, the boundary conditions become:

$$G_{x}(\pm b, y) = 0$$
 (a)  
 $C_{xy}(b, y) = 1.8(y)$  (b)  
 $C_{xy}(-b, y) = -1.8(y)$  (c) (4.10)

It is seen that  $C_{xy}$  is an even function of y, but an odd function with respect to x. The stress function  $\Phi(x,y)$  for this case will be an odd function of y, and an even function of x (see also equation 3.2c). Hence,

from equations (3.25) and (4.10), the function  $G^{(2)}$  and its derivatives become:

$$G^{(2)}(\pm b, y) = -\frac{1}{\xi^2} \int_0^{\infty} o. \sin \xi y \, dy = 0$$

$$\frac{dG^{(2)}}{dx}(b, y) = -\frac{1}{\xi} \int_0^{\infty} \delta(y) \cos \xi y \, dy$$

$$= -\frac{1}{2\xi} \int_{-\infty}^{\infty} \delta(y) \cos \xi y \, dy = -\frac{1}{2\xi}$$

$$\frac{dG^{(2)}}{dx}(-b, y) = \frac{1}{2\xi}$$
(b)

where, for relation (4.11b), the equations (3.25b) and (4.10b) have been used, whilst equations (3.25b) and (4.10c) were used for relation (4.11c). As before, taking the function  $G^{(2)}$  of the following form:

$$G^{(2)}(x,\xi) = (A_2 + B_2 x \xi) \cosh x \xi + (C_2 + D_2 x \xi) \sinh x \xi$$
(a)
gives
$$\frac{dG^{(2)}}{dx}(x,\xi) = \xi \left[ (A_2 + D_2) \sinh x \xi + (B_2 + C_2) \cosh x \xi + (B_2 x \xi) \sinh x \xi + (B_2 x \xi) \cosh x \xi \right]$$

$$+ B_2 x \xi \sinh x \xi + D_2 x \xi \cosh x \xi \right]$$
(b)

Using the forms of (4.11a-c) and relations (4.12a,b) yields, upon rearranging, the following expressions:

$$\begin{array}{l} (A_2 + B_2 b\xi) \cosh b\xi + (C_2 + D_2 b\xi) \sinh b\xi = 0 \\ (A_2 - B_2 b\xi) \cosh b\xi - (C_2 - D_2 b\xi) \sinh b\xi = 0 \\ (A_2 + D_2) \sinh b\xi + (B_2 + C_2) \cosh b\xi + B_2 b\xi \sinh b\xi \\ + D_2 b\xi \cosh b\xi = -\frac{1}{2\xi^2} \\ (A_2 + D_2) \sinh b\xi - (B_2 + C_2) \cosh b\xi - B_2 b\xi \sinh b\xi \\ + D_2 b\xi \cosh b\xi = -\frac{1}{2\xi^2} \\ \end{array}$$

Upon solving these simultaneous equations, the coefficients will be:

$$B_{2} = C_{2} = 0$$

$$A_{2}(\xi) = \frac{b\xi \sinh b\xi}{\xi^{2}(\sinh 2b\xi + 2b\xi)}$$

$$D_{2}(\xi) = -\frac{\cosh b\xi}{\xi^{2}(\sinh 2b\xi + 2b\xi)}$$
(a)
$$(4.14)$$

Integrating and differentiating  $G^{(2)}(x,\xi)$  with respect to x and substituting in equation (3.27) gives, upon simplifying, the following values of the surface displacements due

to shear:

$$\begin{split} U_{e}^{s}(x,y) &= -\frac{2(1+\nu)}{\pi E} \int_{0}^{\infty} \left[ \left( A_{2} - D_{2} + 2\nu D_{2} \right) \sinh x \xi + D_{2} x \xi \cosh x \xi \right] \\ & \cdot \xi \sin \xi y \ d\xi + C^{(2)} y + C_{1}^{(2)} \\ \mathcal{V}_{e}^{s}(x,y) &= -\frac{2(1+\nu)}{\pi E} \int_{0}^{\infty} \left[ \left( A_{2} + 2D_{2} - 2\nu D_{2} \right) \cosh x \xi + D_{2} x \xi \sinh x \xi \right] \\ & \cdot \xi \cos \xi y \ d\xi - C^{(2)} y + C_{2}^{(2)} \end{split}$$

in which, as before, the superscript s refers now to shear loading. Due to symmetry along the y-axis,

$$U_{0}^{s}(0, y) = 0$$

Hence, the coefficients:

$$C^{(2)} = C_1^{(2)} = 0$$
 (4.16)

In order to determine  $C_2^{(2)}$ , it is again necessary to impose the same displacement constraint on the sheet as before. This implies that

$$U_{e}^{s}(0,\ell) = 0$$
 (a)   
 $V_{e}^{s}(0,\ell) = 0$  (b) (4.17)

Part of

The condition (4.17b) determines the value of  $C_2^{(2)}$  as:

$$C_{2}^{(2)} = \frac{1+V}{\Pi E} \int_{0}^{\infty} \frac{2b\xi \sinh b\xi \cdot \cos \xi \ell}{\xi \left( \sinh 2b\xi + 2b\xi \right)} d\xi$$

$$-\frac{2(1-V^{2})}{\Pi E} \int_{0}^{\infty} \frac{2\cosh b\xi \cos \xi \ell}{\xi \left( \sinh 2b\xi + 2b\xi \right)} d\xi$$
(4.18)

Substituting the value of  $A_2$ ,  $D_2$ ,  $C_1^{(2)}$ ,  $C_1^{(2)}$ , and  $C_2^{(2)}$  from equations (4.14), (4.16), and (4.18) into (4.15) yields, finally, the displacement components as follows:

$$U_{e}^{s}(\alpha) = \frac{(1+\sqrt{3})(1-2\sqrt{3})}{\pi E} I_{2}(\alpha) - \frac{2(1-\sqrt{3})}{\pi E} I_{3}(\alpha) \qquad (a)$$

$$V_{e}^{s}(\alpha, \eta) = \frac{2(1-\sqrt{3})}{\pi E} I_{6}(\alpha, \eta) + \frac{1+\sqrt{3}}{\pi E} I_{7}(\eta) \qquad (b)$$

where, as before, the integrals  $I_6\,,\,I_7\,,$  by using again the parameters  $\alpha,\,\gamma$  , will be as follows:

$$I_{6}(\alpha, \gamma) = \int_{0}^{\infty} \frac{2 \cosh(b\xi) \{\cosh(b\xi) \cos(\alpha b\xi) - \cos(\gamma b\xi)\}}{b\xi \left(\sinh(2b\xi) + 2b\xi\right)} d(b\xi)$$

$$I_{7}(2) = \int_{0}^{\infty} \frac{2 \sinh(b\xi) \cos(\gamma b\xi)}{\sinh(2b\xi) + 2b\xi} d(b\xi)$$
(b)

It should be noted that the above formulations (4.8) and (4.19) contain integrals of a particular form which, for the subsequent analysis, must be evaluated. The evaluation of these integrals is treated in Appendix I.

# 4.3 Simplified Forms of the Influence Functions

Using the relations (AI.9) for  $\mathbf{I_4}$ , (AI.10) for integral  $\mathbf{I_2}$ , and (AI.12) for the integrals  $\mathbf{I_3}$  to  $\mathbf{I_7}$  and substituting them into equations (4.9) and (4.19) yields a simplified form of the influence functions in the following manner:

$$\begin{split} U_{e}^{n}(\alpha) &= \frac{2(1-\nu^{2})}{E} \sum_{n=1}^{\infty} e^{-K_{n}|\alpha|} \left( A_{n}^{(\nu)} \sin m_{n}|\alpha| + B_{n}^{(\nu)} \cos m_{n}|\alpha| \right) \\ \mathcal{V}_{e}^{n}(\alpha,2) &= -\frac{(1+\nu)(1-2\nu)}{2E} \operatorname{SIGN}(\alpha) + \frac{2(1-\nu^{2})}{E} \left[ \frac{1}{4} + \frac{1}{4} + \frac{\sum_{n=1}^{\infty} e^{-K_{n}|\alpha|} \left( A_{n}^{(3)} \sin m_{n}|\alpha| + B_{n}^{(3)} \cos m_{n}|\alpha| \right) \right] }{-\frac{1+\nu}{E} \operatorname{SIGN}(\varrho) \left[ \frac{1}{2} + \sum_{n=1}^{\infty} e^{-K_{n}|\alpha|} \left( A_{n}^{(4)} \sin m_{n}|\alpha| + \frac{1}{2} + \frac{1}{2} \left( A_{n}^{(4)} \sin m_{n}|\alpha| \right) \right] \right] } \\ &+ B_{n}^{(4)} \cos m_{n}|\alpha| \right] + \sum_{n=1}^{\infty} e^{-K_{n}|\alpha|} \left( A_{n}^{(5)} \sin m_{n}|\alpha| + \frac{1}{2} \left( A_{n}^{(4)} \sin m_{n}|\alpha| + \frac{1}{2} \left( A_{n}^{(4)} \sin m_{n}|\alpha| \right) \right] \end{split}$$

$$U_{e}^{s}(\alpha) = \frac{(1+V)(1-2V)}{2E} \operatorname{SIGN}(\alpha) - \frac{2(1-V^{2})}{E} \operatorname{SIGN}(\alpha) \cdot \left[\frac{1}{4} + \frac{S}{2} + \frac{S}{2} e^{-K_{n}|\alpha|} \left(A_{n}^{(3)} \operatorname{sinm_{n}|\alpha|} + B_{n}^{(3)} \cos m_{n}|\alpha|\right)\right]$$

$$V_{e}^{s}(\alpha, \eta) = \frac{2(1-V^{2})}{E} \left[\sum_{n=1}^{\infty} e^{-K_{n}|\alpha|} \left(A_{n}^{(6)} \operatorname{sinm_{n}|\alpha|} + B_{n}^{(6)} \cos m_{n}|\alpha|\right) + \sum_{n=1}^{\infty} e^{-K_{n}|\gamma|} \left(A_{n}^{(7)} \operatorname{sinm_{n}|\gamma|} + B_{n}^{(7)} \cos m_{n}|\gamma|\right) + \frac{1+V}{E} \sum_{n=1}^{\infty} e^{-K_{n}|\gamma|} \left(A_{n}^{(8)} \sin m_{n}|\gamma| + B_{n}^{(8)} \cos m_{n}|\gamma|\right)$$

Introducing now two material functions of the following type:

$$\Theta_{1} = \frac{1}{2G}$$

$$\Theta_{2} = \frac{3}{6K + 2G}$$

$$(4.23)$$

it can be seen that the relations (4.21) and (4.22) containing material parameters in terms of Poisson's ratio  $\nu$  and the modulus of elasticity E can be simplified further. Moreover, a grouping of the terms depending on  $\gamma$  can be done by using the following forms:

$$F_{1}(\eta) = \frac{\theta_{2}}{\theta_{1} + \theta_{2}} \left[ \sum_{\eta=1}^{\infty} e^{-K_{n}|\eta|} \left( A_{n}^{(4)} \sin m_{n}|\eta| + B_{n}^{(4)} \cos m_{n}|\eta| \right) - \sum_{n=1}^{\infty} e^{-K_{n}|\eta|} \left( A_{n}^{(5)} \sin m_{n}|\eta| + B_{n}^{(5)} \cos m_{n}|\eta| \right) \right]$$

$$- \frac{\theta_{1} - \theta_{2}}{4 (\theta_{1} + \theta_{2})}$$

$$F_{2}(\eta) = \sum_{n=1}^{\infty} e^{-K_{n}|\eta|} \left( A_{n}^{(7)} \sin m_{n}|\eta| + B_{n}^{(7)} \cos m_{n}|\eta| \right) + \frac{1}{4} |\eta|$$

$$+ \frac{\theta_{1}}{\theta_{1} + \theta_{2}} \sum_{n=1}^{\infty} e^{-K_{n}|\eta|} \left( A_{n}^{(8)} \sin m_{n}|\eta| + B_{n}^{(8)} \cos m_{n}|\eta| \right)$$

This permits, finally, writing of the displacements for the normal and shear loading in a shorter form as functions of the parameters  $\propto$  and  $\eta$  as follows:

$$\begin{aligned} & \mathcal{U}_{e}^{n}\left(\mathbf{A}\right) = \left(\theta_{1} + \theta_{2}\right) \sum_{n=1}^{\infty} e^{-\mathbf{k}_{n} |\mathbf{A}|} \left(A_{n}^{(1)} \sin m_{n} |\mathbf{A}| + B_{n}^{(1)} \cos m_{n} |\mathbf{A}|\right) & \text{(a)} \\ & \mathcal{U}_{e}^{s}(\mathbf{A}) = -\sin(\mathbf{A}) \cdot \left(\theta_{1} + \theta_{2}\right) \sum_{n=1}^{\infty} e^{-\mathbf{k}_{n} |\mathbf{A}|} \left(A_{n}^{(3)} \sin m_{n} |\mathbf{A}|\right) & \text{(b)} \\ & + \theta_{n}^{(3)} \cos m_{n} |\mathbf{A}|\right) - \frac{1}{4} \sin(\mathbf{A}) \cdot \left(\theta_{1} - \theta_{2}\right) & \text{(4.25)} \end{aligned}$$

$$V_{e}^{5}(\alpha, \eta) = (\theta_{1} + \theta_{2}) \sum_{n=1}^{\infty} e^{-k_{n}|\alpha|} (A_{n}^{(6)} sinm_{n}|\alpha| + B_{n}^{(6)} cos m_{n}|\alpha|)$$

$$-\frac{1}{4} (\theta_{1} + \theta_{2}) |\alpha| + (\theta_{1} + \theta_{2}) F_{2}(\eta) \qquad (d) \qquad (4.25)$$

The constants  $A_n^{(k)}$ ,  $B_n^{(k)}$  with corresponding superscripts are defined in Appendix I.

### 4.4 Numerical Results

Numerical results of the above functions were obtained using an IBM 360/75 computer of McGill University. For this purpose, the elastic properties of the material were assumed to be as follows:

Young's Modulus 
$$E = 1.45 \times 10^5 \text{ p.s.i.}$$
  
Poisson's Ratio  $v = \frac{1}{3}$ 

The above values are regarded as representatives of mechanical properties of a paper web in the idealized case.

The results of the computation are shown in Figures 7 to 13.

It may be noticed that the normal displacements

(Figures 7,8) are independent of  $\eta$ . Whereas, the shear displacements are composed of two terms, one dependent upon  $\alpha$  and another dependent upon  $\eta$  only, according to the dependence of the functions  $F_1$ ,  $F_2$  (equation 4.24). The corresponding graphs of these functions are shown in Figure 9.

Figures 10 and 11 indicate the plots of the & dependent terms occurring in the shear displacement equations due to normal and shear load respectively. Figures 12 and 13 indicate total shear displacements (due to normal and shear load respectively) for some selected values of It should be noted that the basic pattern of the shear displacement is not changed by the parameter  $\eta$  . Its effect is in the shift of the origin only. It may be seen that the normal displacement caused by normal load decays exponentially (Figure 7). However, the normal displacement due to the shear load and the shear displacement due to the normal load reach a certain value at approximately | | = 2.5 and maintains this value for the higher values of < (Figures 8 and 10). It is of interest to note that the shear displacement due to shear load shows a peculiar behaviour (Figure 13). Thus, in the vicinity of the load, the shear displacement decays exponentially, but beyond an approximate value of  $|\alpha|=1$ , it diverges linearly. This appears to be in direct violation

to the equilibrium of the sheet. But this type of behaviour is very common for the idealized concept of concentrated load. It is a general feature of the steady state solutions of two dimensional problems in an unbounded region (see Fung<sup>[17]</sup>, page 264).

#### CHAPTER V

#### 5. SOLUTION OF THE ELASTIC PROBLEM

With the presentation of the elastic influence functions in the foregoing chapters of this thesis and the evaluation of the important integrals given in Appendix I, it is now possible to formulate the required matching equations to satisfy the specified boundary conditions.

Thus, the analysis of the rolling of an elastic sheet can now be completed. For this purpose, one half of an elastic sheet in contact with a rigid cylinder is indicated in Figure 14. As pointed out earlier, in the elastic case the lengths of contact on the leading and the trailing sides are equal. Therefore  $m_1 = m_2 = m_3$ .

To simplify the formulation of the problem, all shear forces will be assumed at first to be acting in the direction of  $\gamma$  only. Their actual direction will be determined subsequently by the sign associated with their magnitudes.

The equations will be derived for a certain assumed value of the parameter  $\beta$  (see equation (2.11)) which will later be corrected according to relation (2.13) to satisfy the total load condition. All distances will be measured from point 0 which lies on the intersection of the central line

of the sheet and the line joining the centres of the cylinders.

# 5.1 The Choice of the Pinned Point (0,1)

In the derivation of the influence functions, it was assumed that a certain point on the central line of the sheet is pinned and, hence, has no displacement. It is now necessary to specify this point.

Within the nip, the central line of the sheet is stretched or compressed, as indicated earlier in Figure 3(a), (b). Because of symmetry with respect to the line joining the centres of the cylinders, it is evident that point O remains undisplaced. Hence, this point is taken as the pinned point for the following analysis.

#### 5.2 Relations Common to Both Cases

Some important relations, common to both these cases, will be derived here. Let

 $Y_i$  = distance of the j<sup>th</sup> load,

 $Y_i$  = distance of the i<sup>th</sup> matching point,

Z; = distance of the i<sup>th</sup> matching point from the j<sup>th</sup>
load,

$$\alpha_{ij} = Z_{ij} / b$$
 $Q_j = Y_j / b$ 

From Figure 14, it may be noticed that:

$$Y_i = 2(i-m-1)a$$
  
 $Y_j = (2j-2m-1)a$ 

and hence

$$Z_{ij} = Y_{i} - Y_{j} = (2i - 2j - 1)\alpha$$

$$d_{ij} = (2i - 2j - 1)\beta \quad i = 1, \dots, 2m + 1$$

$$Q_{j} = (2j - 2m - 1)\beta \quad j = 1, \dots, 2m$$
(5.1)

where the quantity  $\beta$  is defined by equation (2.11).

For an elastic material, the displacement of any point on the surface of the sheet due to a moving load is dependent upon the instantaneous distance of the load from that particular point. Hence, using the definition of the displacements as given in section 2.3 of Chapter II and using equation (4.25):

$$U_{ij}^{n} = U_{e}^{n}(\alpha_{ij})$$

$$V_{ij}^{n} = V_{e}^{n}(\alpha_{ij}, n_{ij})$$

$$U_{ij}^{s} = U_{e}^{s}(\alpha_{ij})$$

$$V_{ij}^{s} = V_{e}^{s}(\alpha_{ij}, n_{ij})$$
(5.2)

Further, by considering the geometry, as shown in Figure 14, the variable distance of a contact point from the point A can be written as:

$$f(Y_i) = \frac{{Y_i}^2}{2R} = \frac{2(i-m-1)^2 a^2}{R}$$

$$= \frac{2(i-m-1)^2 \beta^2 b}{Cr}$$
(5.3)

in which Cr represents

$$\frac{\text{Diameter of the cylinder}}{\text{Thickness of the sheet}} = \frac{2R}{2b} = C_r$$
 (5.4)

#### 5.3 Matching Equations for the Case (A):

The matching equations for the Case (A) can be formulated by using equations (2.9), (5.2) and (5.3). The first part of equation (2.9) has been derived from equation (2.6) which states that

$$\frac{\partial^2 V}{\partial Y^2} = 0$$
 everywhere within the nip.

However, this condition cannot be rigorously satisfied since, in the present analysis, a continuously acting pressure distribution on the sheet during rolling has been replaced by a discrete arrangement of line loads. The difficulty in the analysis arising from this line-load concept can be overcome

by employing a semi-inverse method of analysis as presented below.

For this purpose, integrating both sides of equation (2.5) gives:

$$V(Y) = XY + constant$$
 (5.5)

Due to symmetry with respect to the line joining the centres of the cylinders, the constant in (5.5) will be equal to zero. From equations (2.7), (2.9), (5.2), (5.3), and (5.5), it follows that:

$$\sum_{j=1}^{2m} \left\{ \mathcal{U}_{e}^{n}(\alpha_{ij}) P_{j} + \mathcal{U}_{e}^{s}(\alpha_{ij}) Q_{j} \right\} = d_{o} - \frac{2(i-m-1)^{2} \beta^{2} b}{Cr}$$

$$\sum_{j=1}^{2m} \left\{ \mathcal{V}_{e}^{n}(\alpha_{ij}, \gamma_{i}) P_{j} + \mathcal{V}_{e}^{s}(\alpha_{ij}, \gamma_{i}) Q_{j} \right\} = 2 \mathcal{L}(i-m-1) \beta b$$
(5.6)

By rearrangement of the above relation, the following set of equations is obtained:

$$\frac{1 \cdot \frac{d_{0}}{b} - \frac{1}{b} \sum_{j=1}^{2m} \left\{ U_{e}^{n}(\alpha_{ij}) P_{j} + U_{e}^{s}(\alpha_{ij}) Q_{j} \right\} = \frac{2(i-m-1)^{2} \beta^{2}}{C_{r}}}{C_{r}}$$

$$0 \cdot \frac{d_{0}}{b} - \frac{1}{b} \sum_{j=1}^{2m} \left\{ V_{e}^{n}(\alpha_{ij}, \eta_{j}) P_{j} + V_{e}^{s}(\alpha_{ij}, \eta_{j}) Q_{j} \right\} = 2\chi (m+1-i)\beta$$

$$i = 1, \dots, 2m+1$$
(5.7)

Relation (5.7) represents a set of simultaneous equations in which the total number of unknowns is:

$$\left.\begin{array}{ccc}
 P_j & 2m \\
 Q_j & 2m \\
 d_o & 1 \\
 \chi & 1
 \end{array}\right\} 4m+2$$

and the total number of available equations is seen to be:

Normal displacement equations 
$$2m+1$$
  
Shear displacement equations  $2m+1$   $4m+2$ 

Although the number of unknowns is equal to the number of available equations, it is not possible to solve this set since the resulting coefficient matrix becomes singular. The reason for this occurrence is that one of the equations is, in fact, redundant. This suggests that the parameter  $\chi$  should be determined in some other way. For this purpose, a semi-inverse method is proposed in section 5.5. For the present moment, it will be assumed that the value of  $\chi$  is a known quantity.

In order to make the set of equations balanced, it will be necessary to discard one of the equations since the number of unknowns is reduced by one. It was realized that the shear displacement equation for the point A (Figure 14) was a redundant equation. Hence, this equation will be discarded in the following analysis.

Now, defining a coefficient matrix [A], vectors [X] and [b] as follows:

the following matrix equation for the assumed value of X can be written:

$$[A][X] = [B]$$
(5.9)

The unknown vector  $[\chi]$  can easily be determined by the matrix inversion:

$$[X] = [A]^{-1}[B]$$
(5.10)

The solution obtained by equation (5.10) represents a solution corresponding to the assumed value of  $\beta$ . This value should now be corrected according to equation (2.13) and the process should be repeated until the total load requirement is satisfied.

# 5.4 Matching Equation for the Case (B):

Equations for Case (B) can be obtained from those of Case (A) when all shear forces tend to zero. Defining, for this case, a coefficient matrix [A'], vectors [B'] and [X'] as follows:

$$\begin{bmatrix} A' \end{bmatrix} = \begin{bmatrix} 1 & -u_e^n(\alpha_{ij}) \\ 1 & -u_e^n(\alpha_{ij}) \end{bmatrix} \begin{bmatrix} \chi' \end{bmatrix} = \begin{bmatrix} \frac{d_0}{b} \\ \frac{p_i}{b} \end{bmatrix} \begin{bmatrix} \frac{1}{b} \\$$

the equation for Case (B) may be written in matrix form as:

$$[A'].[X'] = [B]$$
 (5.12)

The unknowns here can be determined from

$$[X'] = [A']^{-1}[B']$$
(5.13)

As in the previous case, the parameter  $\beta$  may be corrected according to equation (2.13) to satisfy the boundary conditions.

#### 5.5 Creep Ratio for the Case (A)

The parameter X introduced earlier has been referred to by some authors (see, for instance, Johnson<sup>[5]</sup>) as the creep ratio. It represents the overall differential velocity between the rotating bodies (see equation (2.5)). It is also a measure of the amount of stretch (or compression) of the sheet surface in the nip. Since, by nature, friction opposes the tendency of relative motion of the contacting bodies, it follows that:

$$|\mathcal{X}_{o}| \geqslant |\mathcal{X}_{o}| \geqslant 0 \tag{5.14}$$

in which the subscripts correspond to the value of the coefficient of friction for each case. It is to be noted that for Case (B) (complete slip), the matching equations are independent of  $\mathbf{Z}$  (see equations (5.11) and (5.12)).  $\mathbf{Z_0}$  can be determined from the knowledge of the actual shear displacement of the sheet surface and by using equation (2.5). Further details are given in the next section.

Equation (5.14) gives a guide line for the value of  $\chi_{\infty}$  when the value of  $\chi_{\infty}$  is known. With this in mind, the proper value of  $\chi_{\infty}$  was determined by trial in the following manner.

As a first approximation,  $\mathcal{K}_{\infty}$  was assumed to be zero. The unknown quantities were then determined by using equation (5.10). Later, it was checked if the conditions of equations (2.1) to (2.3), (specifically that of equation (2.1)) were satisfied. If any of the conditions were violated, then it was evident that the previous value of  $\mathcal{K}_{\infty}$  was not a good approximation and, therefore, some correction was needed. The value of  $\mathcal{K}_{\infty}$  was then altered (increased or decreased by trial) by some small amount within the range of equation (5.14) and the procedure was repeated until all the conditions of equations (2.1) to (2.3) were satisfied.

Realizing that  $\chi$  is a function of  $(m \times \beta)$ , a plot of .  $\chi$  versus  $(m \times \beta)$  was obtained. It was found that for every

-

selected value of  $(\mathbf{m} \times \boldsymbol{\beta})$ , there was a certain range of the value of  $\boldsymbol{\chi}_{\boldsymbol{\omega}}$  which could satisfy the above stated conditions. The upper and lower limits of the possible range of  $\boldsymbol{\chi}_{\boldsymbol{\omega}}$  are shown in Figure 15. The graph represents the case of  $\mathbf{B} = \mathbf{0.005''}$ , only. Other values of  $\boldsymbol{\delta}$  are considered in the discussion on the numerical results (section 5.7). It was further noted that within the range, as the magnitude of  $\boldsymbol{\chi}_{\boldsymbol{\omega}}$  was decreased, the ratio  $\frac{|\boldsymbol{Q}|}{|\boldsymbol{P}|}$  at the edges increased. Hence, in view of relation (2.4), the curve corresponding to the least magnitudes of  $\boldsymbol{\chi}_{\boldsymbol{\omega}}$ , within the permissible range, was accepted as the proper curve of  $\boldsymbol{\chi}_{\boldsymbol{\omega}}$  versus  $(\mathbf{m} \times \boldsymbol{\beta})$ .

#### 5.6 Creep Ratio for the Case (B)

To determine the creep ratio for Case (B), it is only necessary to determine the shear displacements of the end points due to the total nip force. Furthermore, because of symmetry, it is sufficient to consider only one end-point.

The shear displacement of the end point can be written as:

$$V_{(2m+1)} = \sum_{i=1}^{2m} V_{(2m+1),i}^n P_i.$$
 (5.15)

The shear displacement distribution on the surface of the sheet within the nip is schematically illustrated in Figure 16. It can be seen from Figure 16 that the value of the creep ratio  $\mathcal{X}_{o}$  is given by:

$$\chi_{0} = \frac{2}{L} \sum_{j=1}^{2m} v_{(2m+1)j}^{2n} P_{j}.$$
 (5.16)

#### 5.7 Numerical Results

In order to illustrate the foregoing analysis of the rolling of an elastic sheet, numerical solutions for the pressure distribution, the shear distribution, the length of contact, the depth of indentation, the normal displacement at the end of the nip, the creep ratio as well as their corresponding interrelations were obtained for both Cases (A) and (B) with the aid of an IBM 360/75 computer of McGill University. For this purpose, the following geometrical and mechanical properties were considered.

Young's modulus E=1.45×10<sup>5</sup>p.s.i.

Poisson's ratio V=1/3

Radius of the R=6 inches cylinder

Total normal load W=25, 50, 75, 100, 125, 150, 175 and 200 P.L.I.

Thickness of the B=1.0, 0.25, 0.0625, and sheet 0.005 inch

The relevant results for the two cases and for the above variations in normal load and the thickness of the sheet are tabulated in Tables III to X.

From the wide choice of the results, the peak pressure  $p_{max}$ , the ratio of the contact length to the thickness of the sheet  $L_{/B}$ , the ratio of the depth of indentation to the thickness of the sheet  $d_{\circ}/B$  and the creep ratio  $\chi$ , were picked up as the typical results and have been plotted against normal load in Figures 17 to 20 for Case (A), and in Figures 21 to 24 for Case (B).

To illustrate the influence of friction on the contact surfaces, plots of the contact length L and the depth of indentation  $d_0$  for B=0.005 in. have been obtained against normal load for the limiting Cases (A) and (B) as shown in Figure 25. For the same purpose, the distribution of nip pressure for the limiting cases and for B=0.005 in. and W= 100 P.L.I., is shown in Figure 26. The variation in the distribution of nip shear with normal load, for the case of no-slip and for B=0.005 in., is shown in Figure 27. Surface displacements (normal and shear) within and outside the nip

for the two limiting cases are shown in Figure 28 (representing a thick sheet) and Figure 29 (representing a thin sheet). It is considered that the actual results will be within the bounds of these limiting cases.

#### CHAPTER VI

# 6. SURFACE DISPLACEMENTS FOR A VISCOELASTIC SHEET DUE TO MOVING LOADS

In order to obtain a solution of the viscoelastic problem, it is necessary to assess the surface displacements of the viscoelastic sheet caused by moving loads.

The results of the elastic case show that the contribution of the shear forces is rather small. This is evident from Figures 25 and 26 which show that the change in the pressure distribution and the contact length with friction is within about 10% and that in the depth of indentation is within 20%. In view of this, and in order to simplify the presentation, only normal forces are considered in the formulation of the viscoelastic problem.

It should be noted that a line load moving on a viscoelastic sheet and a line load moving on an elastic sheet will have identical boundary conditions. Moreover, with respect to a coordinate system moving with the load, the regions of the boundary over which the stresses and the displacements are prescribed remains the same in both problems. Hence, the solution for the viscoelastic case may be obtained from that of the elastic case by using the principle of correspondence (see, for example, Bland<sup>[16]</sup>).

# 6.1 Elastic Solution for Fixed Coordinates

The influence functions for the elastic case, with respect to a coordinate system that moves with the load, were obtained in Chapter IV. In order to apply the correspondence principle, it is necessary to express these functions with respect to a coordinate system fixed in space (see Lee<sup>[18]</sup>). This will be done in the following paragraphs.

Let x-y be the coordinate system moving with the load and X-Y be the coordinate system fixed in space (see Figure 30). Let the starting position of the loads be (±b, Y<sub>o</sub>) and let it be required to determine the displacements of the surface of the sheet at some arbitrary point M. The two coordinate systems are related as follows:

$$X = X$$

$$y = Y - Y_0 - F_0 t$$

$$\ell = -(Y_0 + F_0 t)$$
(6.1)

where  $\ell$  represents the distance of the pinned point (Figure 30) to the origin of the moving coordinate system, and  $F_o$  is the velocity of the loads. Hence, the parameters  $\alpha$  and  $\gamma$  used in Chapter IV (Section 4.1) become now:

$$\alpha = \frac{Y - Y_o - F_o t}{b}$$

$$\gamma = -\frac{Y_o + F_o t}{b}$$
(6.2)

Suppose that the loads arrive at a point right over the pinned point in a certain time  $\boldsymbol{t_o}$  and that they reach the point  $\boldsymbol{M}$  in some other time  $\boldsymbol{T}$  . Then,

$$T = \frac{Y - Y_o}{F_o}$$

$$t_o = -\frac{Y_o}{F_o}$$
(6.3)

With this definition, the parameters  $\boldsymbol{\alpha}$  and  $\boldsymbol{\eta}$  become:

$$\alpha = \frac{F_{o}(T-t)}{b}$$

$$\gamma = \frac{F_{o}(t_{o}-t)}{b}$$
(6.4)

Introducing now a Heavyside unit step function such that

it can be seen that the forms contained in relations (4.24 and 4.25) of Chapter IV can be expressed as follows:

$$SIGN(\alpha) = H(T-t) - H(t-T)$$

$$SIGN(\eta) = H(t_0-t) - H(t-t_0)$$

$$|\alpha| = \left[H(T-t) - H(t-T)\right] \frac{F_0}{b} (T-t)$$

$$|\eta| = \left[H(t_0-t) - H(t-t_0)\right] \frac{F_0}{b} (t_0-t)$$

$$(6.6)$$

$$\frac{e^{-K_{n}|A|}(A_{n}^{(K)}\sin m_{n}|A| + B_{n}^{(K)}\cos m_{n}|A|})}{= H(T-t)e^{-K_{n}A}(A_{n}^{(K)}\sin m_{n}A + B_{n}^{(K)}\cos m_{n}A)} \\
- H(t-T)e^{-K_{n}A}(A_{n}^{(K)}\sin m_{n}A - B_{n}^{(K)}\cos m_{n}A)} \\
= \frac{e^{-K_{n}|Q|}(A_{n}^{(K)}\sin m_{n}|Q| + B_{n}^{(K)}\cos m_{n}|Q|})}{= H(t_{0}-t)e^{-K_{n}Q}(A_{n}^{(K)}\sin m_{n}Q + B_{n}^{(K)}\cos m_{n}Q)} \\
- H(t-t_{0})e^{-K_{n}Q}(A_{n}^{(K)}\sin m_{n}Q - B_{n}^{(K)}\cos m_{n}Q)}$$
(6.7)

and

$$SIGN(\alpha). e^{-K_{n}|\alpha|} (A_{n}^{(K)} sin m_{n}|\alpha| + B_{n}^{(K)} cosm_{n}|\alpha|)$$

$$= H(T-t)e^{-K_{n}\alpha} (A_{n}^{(K)} sin m_{n}\alpha + B_{n}^{(K)} cosm_{n}\alpha)$$

$$+ H(t-T)e^{-K_{n}\alpha} (A_{n}^{(K)} sin m_{n}\alpha - B_{n}^{(K)} cosm_{n}\alpha)$$

$$SIGN(\eta). e^{-K_{n}|\eta|} (A_{n}^{(K)} sin m_{n}|\eta| + B_{n}^{(K)} cosm_{n}|\eta|)$$

$$= H(t_{0}-t)e^{-K_{n}\eta} (A_{n}^{(K)} sin m_{n}\eta + B_{n}^{(K)} cosm_{n}\eta)$$

$$+ H(t-t_{0})e^{K_{n}\eta} (A_{n}^{(K)} sin m_{n}\eta - B_{n}^{(K)} cosm_{n}\eta)$$

where the coefficients  $A_n^{(\kappa)}$ ,  $B_n^{(\kappa)}$  have the same meaning as in relations (4.24, 4.25) except that they are expressed in a more general way. Defining two generalized functions  $g_n^{(\kappa)}$  and  $h_n^{(\kappa)}$  as:

$$g_{n}^{(k)}(t,T) = H(T-t)e^{-Q_{n}(T-t)} \left\{ A_{n}^{(k)} \sin b_{n}(T-t) + B_{n}^{(k)} \cos b_{n}(T-t) \right\}$$

$$h_{n}^{(k)}(t,T) = H(t-T)e^{Q_{n}(T-t)} \left\{ A_{n}^{(k)} \sin b_{n}(T-t) - B_{n}^{(k)} \cos b_{n}(T-t) \right\}$$
(6.9)

in which

$$a_n = \frac{K_n F_0}{b} \quad ; \quad b_n = \frac{m_n F_0}{b} \tag{6.10}$$

the normal and shear displacements due to the moving line load (described earlier in Chapter IV, equations 4.24, 4.25) can now be expressed by:

$$U_{e}^{n}(t,T) = (\theta_{1} + \theta_{2}) \sum_{n=1}^{\infty} \left[ g_{n}^{(i)}(t,T) - h_{n}^{(i)}(t,T) \right]$$

$$V_{e}^{n}(t,T) = (\theta_{1} + \theta_{2}) \sum_{n=1}^{\infty} \left[ g_{n}^{(3)}(t,T) + h_{n}^{(3)}(t,T) \right]$$

$$+ \frac{1}{4} (\theta_{1} - \theta_{2}) \left[ H(T-t) - H(t-T) \right]$$

$$- \frac{1}{4} (\theta_{1} - \theta_{2}) \left[ H(t_{0} - t) - H(t-t_{0}) \right]$$

$$+ \theta_{2} \sum_{n=1}^{\infty} \left[ g_{n}^{(4)}(t,t_{0}) + h_{n}^{(4)}(t,t_{0}) \right]$$

$$- \theta_{1} \sum_{n=1}^{\infty} \left[ g_{n}^{(5)}(t,t_{0}) + h_{n}^{(5)}(t,t_{0}) \right]$$

#### 6.2 Material Function

The quantities  $\Theta_1$  and  $\Theta_2$  occurring in equation (6.11) are material-dependent functions (see equation (4.23)) which, for a viscoelastic material, will be time-dependent. In order to perform the operations of the correspondence principle on equation (6.11), it is necessary to specify the nature of these functions.

The constitutive equations of a linear viscoelastic material can be written (see Bland  $^{[16]}$  or Fung  $^{[17]}$ ), in general, as:

$$P(D) S_{ij}(t) = Q(D) e_{ij}(t)$$

$$P'(D) G_{kk}(t) = Q'(D) \epsilon_{kk}(t)$$
(6.12)

in which  $S_{ij}(t)$  and  $e_{ij}(t)$  are the deviatoric components of the stress and strain tensors respectively and the indices i,j and k vary from 1 to 3. The quantities  $G_{kk}(t)$  and  $E_{kk}(t)$  are the dilatational components of the stress and strain tensors respectively. P(D), Q(D), P'(D) and Q'(D) are some polynomials of the operator D where  $D \equiv \frac{d}{dt}$ .

Taking the Laplace tranforms of both sides of equation (6.12) and assuming that the material was completely stress-free before t=0,

$$P(\flat) \, \bar{S}_{ij}(\flat) = Q(\flat) \, \bar{e}_{ij}(\flat)$$

$$P'(\flat) \, \bar{\delta}_{kk}(\flat) = Q'(\flat) \, \bar{e}_{kk}(\flat)$$
(6.13)

in which **b** is the Laplace transform parameter and a bar sign over a quantity designates the Laplace transform of that quantity.

The viscoelastic moduli can be obtained from equation (6.13) as follows:

$$\vec{\bar{G}}(P) = \frac{Q(P)}{P(P)}$$

$$\vec{K}(P) = \frac{Q'(P)}{P'(P)}$$
(6.14)

Using equations (4.23) and (6.14) yields:

$$\bar{\theta}_{1}(\flat) = \frac{P(\flat)}{2Q(\flat)}$$

$$\bar{\theta}_{2}(\flat) = \frac{3P(\flat).P'(\flat)}{6P(\flat)Q'(\flat) + 2P'(\flat)Q(\flat)}$$
(6.15)

The right-hand side of equation (6.15) represents the ratios of two polynomials. In each case, the order of the polynomial of the numerator is either smaller by one or equal to the order of the polynomial of the corresponding denominator. Hence, using partial fractions, equation (6.15) may be written as:

$$\bar{\Theta}_{1}(P) = \delta_{0} + \sum_{r=1}^{N} \frac{\delta_{r}}{P + \lambda_{r}}$$

$$\bar{\Theta}_{2}(P) = \delta_{0}' + \sum_{r=1}^{N'} \frac{\delta_{r}'}{P + \lambda_{r}'}$$
(6.16)

where  $\delta_0$ ,  $\delta_0'$ ,  $\delta_r'$  and  $\delta_r'$  are the coefficients of partial fractions and  $\lambda_r$  and  $\lambda_r'$  are the roots of the polynomials of the respective denominators. N and N' represent the degree of the polynomials in the two cases. In general, the roots and the coefficients will be complex.

Inversion of equation (6.16) yields:

$$\theta_{i}(t) = \delta_{o} \delta(t) + \sum_{r=1}^{N} \delta_{r} e^{-\lambda_{r}t}$$

$$\theta_{2}(t) = \delta_{o}^{'} \delta(t) + \sum_{r=1}^{N'} \delta_{r}^{'} e^{-\lambda_{r}^{'}t}$$
(6.17)

It is seen that equation (6.17) represents two material functions in a general form which can be specified by adopting a particular mechanical model for the material properties. The influence functions for a viscoelastic sheet will be formulated in the next section by employing these general forms. Subsequently, for the purpose of illustration of the proposed method, numerical results will be given for an ideal material which behaves as a standard linear solid in both shear and dilatation.

#### 6.3 Solution for the Viscoelastic Sheet

By applying the principle of correspondence and the convolution theorem on equation (6.11), the following expressions for the displacements are obtained:

$$\begin{split} & \mathcal{U}_{V}^{n}(t,T) = \sum_{n=1}^{\infty} \int_{0}^{t} \left[ \Theta_{i}(t-\tau) + \Theta_{2}(t-\tau) \right] \left[ 9_{n}^{(i)}(\tau,T) - h_{n}^{(i)}(\tau,T) \right] d\tau \\ & \mathcal{V}_{V}^{n}(t,T,t_{o}) = \sum_{n=1}^{\infty} \int_{0}^{t} \left[ (\Theta_{i}(t-\tau) - \Theta_{2}(t-\tau)) \right] \left[ 9_{n}^{(3)}(\tau,T) + h_{n}^{(3)}(\tau,T) \right] d\tau \\ & + \frac{1}{4} \int_{0}^{t} \left[ \Theta_{i}(t-\tau) - \Theta_{2}(t-\tau) \right] \left[ H(T-\tau) - H(\tau-T) \right] d\tau \\ & - \frac{1}{4} \int_{0}^{t} \left[ \Theta_{i}(t-\tau) - \Theta_{2}(t-\tau) \right] \left[ H(t_{o}-\tau) - H(\tau-t_{o}) \right] d\tau \\ & + \sum_{n=1}^{\infty} \int_{0}^{t} \Theta_{2}(t-\tau) \left[ 9_{n}^{(4)}(\tau,t_{o}) + h_{n}^{(4)}(\tau,t_{o}) \right] d\tau \\ & - \sum_{n=1}^{\infty} \int_{0}^{t} \Theta_{i}(t-\tau) \left[ 9_{n}^{(5)}(\tau,t_{o}) + h_{n}^{(5)}(\tau,t_{o}) \right] d\tau \end{split}$$

Substituting the expressions of  $\theta_1$  and  $\theta_2$  from equation (6.17) and of  $9_n^{(k)}$  and  $h_n^{(k)}$  from equation (6.9) into equation (6.18) yields:

$$\begin{split} U_{\nu}^{N}(t,T) &= (\, \forall_{o} + \, \forall_{o}^{'} \,) \sum_{n=1}^{\infty} \underbrace{e^{-K_{n}[d_{i}]}}_{n=1} \left( \, A_{n}^{(i)} \sin m_{n}[d_{i}] + B_{n}^{(i)} \cos m_{n}[d_{i}] \right) \\ &+ \sum_{n=1}^{\infty} \sum_{r=1}^{N} \underbrace{v_{i}^{r} \left[ A_{n}^{(i)} \left\{ J_{2} \left( A_{r}, T \right) - J_{3} \left( A_{r}, T \right) \right\} + B_{n}^{(i)} \left\{ J_{2} \left( A_{r}, T \right) + J_{4} \left( A_{r}, T \right) \right\} \right] \\ &+ \sum_{n=1}^{\infty} \sum_{r=1}^{N} \underbrace{v_{i}^{r} \left[ A_{n}^{(i)} \left\{ J_{2} \left( A_{r}^{'}, T \right) - J_{3} \left( A_{r}^{'}, T \right) \right\} + B_{n}^{(i)} \left\{ J_{2} \left( A_{r}^{'}, T \right) + J_{4} \left( A_{r}^{'}, T \right) \right\} \right] \\ &+ \sum_{n=1}^{\infty} \sum_{r=1}^{N} \underbrace{v_{i}^{r} \left[ A_{n}^{(i)} \left\{ J_{2} \left( A_{r}^{'}, T \right) - J_{3} \left( A_{r}^{'}, T \right) \right\} + B_{n}^{(3)} \left\{ J_{2} \left( A_{r}^{'}, T \right) + J_{4} \left( A_{r}^{'}, T \right) \right\} \right] \\ &+ \sum_{n=1}^{\infty} \sum_{r=1}^{N} \underbrace{v_{i}^{r} \left[ A_{n}^{(3)} \left\{ J_{2} \left( A_{r}^{'}, T \right) + J_{3} \left( A_{r}^{'}, T \right) \right\} + B_{n}^{(3)} \left\{ J_{2} \left( A_{r}^{'}, T \right) - J_{4} \left( A_{r}^{'}, T \right) \right\} \right] \\ &+ \sum_{n=1}^{\infty} \sum_{r=1}^{N} \underbrace{v_{i}^{r} \left[ A_{n}^{(3)} \left\{ J_{2} \left( A_{r}^{'}, T \right) + J_{3} \left( A_{r}^{'}, T \right) \right\} + B_{n}^{(3)} \left\{ J_{2} \left( A_{r}^{'}, T \right) - J_{4} \left( A_{r}^{'}, T \right) \right\} \right] \\ &- \sum_{n=1}^{\infty} \sum_{r=1}^{N} \underbrace{v_{i}^{r} \left[ A_{n}^{(3)} \left\{ J_{2} \left( A_{r}^{'}, T \right) + J_{3} \left( A_{r}^{'}, T \right) \right\} + B_{n}^{(3)} \left\{ J_{2} \left( A_{r}^{'}, T \right) - J_{4} \left( A_{r}^{'}, T \right) \right\} \right] \\ &- \sum_{n=1}^{\infty} \sum_{r=1}^{N} \underbrace{v_{i}^{r} \left[ A_{n}^{(3)} \left\{ J_{2} \left( A_{r}^{'}, T \right) + J_{3} \left( A_{r}^{'}, T \right) \right\} + B_{n}^{(3)} \left\{ J_{2} \left( A_{r}^{'}, T \right) - J_{4} \left( A_{r}^{'}, T \right) \right\} \right] \\ &+ \sum_{n=1}^{\infty} \sum_{r=1}^{N} \underbrace{v_{i}^{r} \left[ A_{n}^{(3)} \left\{ J_{2} \left( A_{r}^{'}, T \right) + J_{3} \left( A_{r}^{'}, T \right) \right\} + B_{n}^{(3)} \left\{ J_{2} \left( A_{r}^{'}, T \right) - J_{4} \left( A_{r}^{'}, T \right) \right\} \right] \\ &+ \sum_{n=1}^{\infty} \sum_{r=1}^{N} \underbrace{v_{i}^{r} \left[ A_{n}^{(3)} \left\{ J_{2} \left( A_{r}^{'}, T \right) + J_{3} \left( A_{r}^{'}, T \right) \right\} + B_{n}^{(3)} \left\{ J_{2} \left( A_{r}^{'}, T \right) - J_{4} \left( A_{r}^{'}, T \right) \right\} \right] \\ &+ \sum_{n=1}^{\infty} \sum_{r=1}^{N} \underbrace{v_{i}^{r} \left[ A_{n}^{(3)} \left\{ J_{2} \left( A_{r}^{'}, T \right) + J_{3} \left( A_{r}^{'}, T \right) \right\} + B_{n}^{(3)} \left\{ J_{2} \left( A_{r}^{'}, T \right) - J_{4} \left( A_{r}^{'}, T \right) \right\} \right] \\ &+ \sum_{n=1}^{\infty} \sum_{n$$

(6.19b)

in which  $J_1$  to  $J_6$  are integrals of the following forms:

$$J_{1}(A,T) = \int_{0}^{t} H(T-z)e^{-A(t-z)}e^{-\alpha_{n}(T-z)} \sin b_{n}(T-z) dz$$

$$J_{2}(A,T) = \int_{0}^{t} H(T-z)e^{-A(t-z)}e^{-\alpha_{n}(T-z)} \cos b_{n}(T-z) dz$$

$$J_{3}(A,T) = \int_{0}^{t} H(z-T)e^{-A(t-z)}e^{\alpha_{n}(T-z)} \sin b_{n}(T-z) dz$$

$$J_{4}(A,T) = \int_{0}^{t} H(z-T)e^{-A(t-z)}e^{\alpha_{n}(T-z)} \cos b_{n}(T-z) dz$$

$$J_{5}(T) = \int_{0}^{t} \theta_{1}(t-z) \left[H(T-z) - H(z-T)\right] dz$$

$$J_{6}(T) = \int_{0}^{t} \theta_{2}(t-z) \left[H(T-z) - H(z-T)\right] dz$$

It should be noted that the arguments of these have been denoted for simplicity by  $(\Lambda, T)$ , whereas, in a more detailed form, they should be denoted by  $(\Lambda_r, T)$ ,  $(\Lambda'_r, T)$ ,  $(\Lambda'_r, T_0)$  and  $(\Lambda'_r, t_0)$ . It will be seen subsequently that these forms are only intermediate ones and are not employed in the final representation.

It is of further interest to note that the integrals in equation (6.20) involve the Heavyside's function in their integrands and are, therefore, discrete functions. Since  ${\sf T}$  and  ${\sf t_o}$  are both fixed time values that can be either

positive or negative (depending upon the starting position of the load and the location of the pinned point), the value of the integrals in (6.20) will be affected accordingly. There are four cases to be distinguished as shown in Figure 31. Taking into account these four possibilities, the integrals have been evaluated in Appendix II.

Substituting the values of the different integrals from Appendix II into equation (6.19), four different expressions (for the four distinct cases) for the displacements are obtained which are given below. It has been found to be convenient to introduce the following coefficient functions

$$\Phi_{n}^{(K)}(\lambda,T) = \frac{A_{n}^{(K)}(\lambda+a_{n}') - B_{n}^{(K)}b_{n}'}{(\lambda+a_{n}')^{2} + b_{n}^{2}}$$

$$\Psi_{n}^{(K)}(\lambda,T) = \frac{A_{n}^{(K)}b_{n}' + B_{n}^{(K)}(\lambda+a_{n}')}{(\lambda+a_{n}')^{2} + b_{n}^{2}}$$

$$\Phi_{n}^{(K)}(\lambda) = \frac{A_{n}^{(K)}(\lambda+a_{n}) - B_{n}^{(K)}b_{n}}{(\lambda+a_{n})^{2} + b_{n}^{2}}$$

$$\Phi_{n}^{(K)}(\lambda) = \frac{A_{n}^{(K)}(\lambda-a_{n}) + B_{n}^{(K)}b_{n}}{(\lambda-a_{n})^{2} + b_{n}^{2}}$$

$$\Psi_{n}^{(K)}(\lambda) = \frac{A_{n}^{(K)}b_{n} + B_{n}^{(K)}(\lambda+a_{n})}{(\lambda+a_{n})^{2} + b_{n}^{2}}$$

$$\Psi_{n}^{(K)}(\lambda) = \frac{A_{n}^{(K)}b_{n} + B_{n}^{(K)}(\lambda+a_{n})}{(\lambda+a_{n})^{2} + b_{n}^{2}}$$

$$\Psi_{n}^{(K)}(\lambda) = \frac{A_{n}^{(K)}b_{n} + B_{n}^{(K)}(\lambda-a_{n})}{(\lambda-a_{n})^{2} + b_{n}^{2}}$$

(6.21)

in which again, the arguments  $\lambda$ , T and the superscript ( $\kappa$ ) stand for the general case, and where

$$a'_{n} = SIGN(T-t) a_{n}$$

$$b'_{n} = SIGN(T-t) b_{n}$$

$$a_{n} = \frac{K_{n} F_{o}}{b}$$

$$b_{n} = \frac{m_{n} F_{o}}{b}$$
(6.22)

The symbol SIGN(·) has the same meaning as explained in (AI.11).

#### CASE I: T>0, $t_0>0$

$$\begin{split} U_{v}^{n}(t,T) &= \sum_{n=1}^{\infty} \left[ \left\{ (\delta_{s} + \delta_{o}^{'}) A_{n}^{U} + \sum_{r=1}^{N} \delta_{r}^{r} \Phi_{n}^{U}(A_{r},T) + \sum_{r=1}^{N} \delta_{r}^{'} \Phi_{n}^{U}(A_{r},T) \right\} \sin m_{n} |\alpha| \\ &+ \left\{ (\delta_{s} + \delta_{o}^{'}) \beta_{n}^{U} + \sum_{r=1}^{N} \delta_{r}^{r} \Psi_{n}^{U}(A_{r},T) + \sum_{r=1}^{N} \delta_{r}^{'} \Psi_{n}^{U}(A_{r},T) \right\} \cos m_{n} |\alpha| \right] e^{-K_{n} |\alpha|} \\ &- \sum_{n=1}^{\infty} \left[ \left\{ \sum_{r=1}^{N} \delta_{r}^{r} \Phi_{n}^{U}(A_{r}) e^{-A_{r}^{'}t} + \sum_{r=1}^{N} \delta_{r}^{'} \Phi_{n}^{U}(A_{r}^{'}) e^{-A_{r}^{'}t} \right\} \sin b_{n} T \right. \\ &+ \left\{ \sum_{r=1}^{N} \delta_{r}^{r} \Psi_{n}^{U}(A_{r}) e^{-A_{r}^{'}t} + \sum_{r=1}^{N} \delta_{r}^{'} \Psi_{n}^{U}(A_{r}) e^{-A_{r}^{'}t} \right\} \cos b_{n} T \right] e^{-\alpha_{n} T} \\ &+ H(t-T) \sum_{n=1}^{\infty} \left[ \sum_{r=1}^{N} \delta_{r}^{r} \left\{ \Psi_{n}^{U}(A_{r}) + \overline{\Psi}_{n}^{U}(A_{r}) \right\} e^{-A_{r}^{'}(t-T)} \right. \\ &+ \sum_{r=1}^{N} \delta_{r}^{'} \left\{ \Psi_{n}^{U}(A_{r}) + \overline{\Psi}_{n}^{U}(A_{r}^{'}) \right\} e^{-A_{r}^{'}(t-T)} \right] \tag{6.23} \end{split}$$

#### CASE II: T<0, $t_0>0$

$$\begin{split} U_{v}^{n}(t,T) &= \sum_{n=1}^{\infty} \left[ \left\{ (\aleph_{o} + \aleph_{o}') A_{n}^{(i)} + \sum_{r=1}^{N} \aleph_{r} \bar{\Phi}_{n}^{(i)}(A_{r}) + \sum_{r=1}^{N} \aleph_{r}' \bar{\Phi}_{n}^{(i)}(A_{r}') \right\} \sin m_{n} |a| \\ & \left\{ (\aleph_{o} + \aleph_{o}') B_{n}^{(i)} + \sum_{r=1}^{N} \aleph_{r}' \bar{\Psi}_{n}(A_{r}) + \sum_{r=1}^{N} \aleph_{r}' \bar{\Psi}_{n}(A_{r}') \right\} \cos m_{n} |\alpha| \right] e^{-K_{n} |\alpha|} \\ & + \sum_{n=1}^{\infty} \left[ \left\{ \sum_{r=1}^{N} \aleph_{r} \bar{\Phi}_{n}^{(i)}(A_{r}) e^{-A_{r}t} + \sum_{r=1}^{N} \aleph_{r}' \bar{\Phi}_{n}^{(i)}(A_{r}') e^{-A_{r}'t} \right\} \sin b_{n} T \\ & + \left\{ \sum_{r=1}^{N} \aleph_{r}' \bar{\Psi}_{n}^{(i)}(A_{r}) e^{-A_{r}t} + \sum_{r=1}^{N} \aleph_{r}' \bar{\Psi}_{n}^{(i)}(A_{r}') e^{-A_{r}'t} \right\} \cos b_{n} T \right] e^{a_{n}T} \quad (6.25) \end{split}$$

$$\begin{split} \mathcal{V}_{V}^{n}(t,T,t_{o}) &= \frac{1}{4} \left(\delta_{o}^{'} - \delta_{o}\right) + \frac{1}{4} sign(t_{0}) \cdot \left(\delta_{o}^{'} - \delta_{o}\right) - \frac{1}{4} \sum_{r=1}^{N} \frac{\delta_{r}}{\Lambda_{r}} \left[1 - e^{-A_{r}t}\right] + \frac{1}{4} \sum_{r=1}^{N'} \frac{\delta_{r}'}{A_{r}'} \left[1 - e^{-A_{r}t}\right] \\ &- \frac{1}{4} \sum_{r=1}^{N} \frac{\delta_{r}}{\Lambda_{r}} \left[sign(t_{0}) - e^{-A_{r}t} + 2 H(t - t_{o}) e^{-A_{r}(t - t_{o})}\right] \\ &+ \frac{1}{4} \sum_{r=1}^{N'} \frac{\delta_{r}'}{\Lambda_{r}} \left[sign(t_{0}) - e^{-A_{r}t} + 2 H(t - t_{o}) e^{-A_{r}(t - t_{o})}\right] \\ &- \sum_{n=1}^{N} \left[\left\{(\delta_{o} + \delta_{o}') A_{n}^{(3)} + \sum_{r=1}^{N} \delta_{r}' \bar{\phi}_{n}^{(3)}(A_{r}) + \sum_{r=1}^{N} \delta_{r}' \bar{\phi}_{n}^{(3)}(A_{r}')\right\} sinm_{n}|\alpha| \\ &+ \left\{(\delta_{o} + \delta_{o}') B_{n}^{(3)} + \sum_{r=1}^{N} \delta_{r}' \bar{\psi}_{n}^{(3)}(A_{r}) + \sum_{r=1}^{N} \delta_{r}' \bar{\psi}_{n}^{(3)}(A_{r}')\right\} cosm_{n}|\alpha| \right] e^{-K_{n}|\alpha|} \\ &- \sum_{n=1}^{\infty} \left[\left\{\sum_{r=1}^{N} \delta_{r}\bar{\phi}_{n}^{(3)}(A_{r}) e^{-A_{r}t} + \sum_{r=1}^{N} \delta_{r}' \bar{\phi}_{n}^{(3)}(A_{r}') e^{-A_{r}t}\right\} cosm_{n}|\alpha| \right] e^{-K_{n}|\alpha|} \\ &+ \left\{\sum_{r=1}^{N} \delta_{r}' \bar{\psi}_{n}^{(3)}(A_{r}) e^{-A_{r}t} + \sum_{r=1}^{N} \delta_{r}' \bar{\psi}_{n}^{(3)}(A_{r}') e^{-A_{r}t}\right\} cosm_{n}|\alpha| \right] e^{-K_{n}|\alpha|} \\ &+ \left\{\sum_{n=1}^{N} \sum_{r=1}^{N} v_{n}^{(3)}(A_{r}) e^{-A_{r}t} + \sum_{r=1}^{N} \delta_{r}' \bar{\psi}_{n}^{(3)}(A_{r}') e^{-A_{r}t}\right\} cosm_{n}|\alpha| \right\} \\ &+ \left\{\sum_{n=1}^{N} \sum_{r=1}^{N} v_{n}^{(3)}(A_{r}) e^{-A_{r}t} - \sum_{r=1}^{N} \delta_{r}' \bar{\psi}_{n}^{(3)}(A_{r}') e^{-A_{r}t}\right\} sinm_{n}|\alpha| \right\} \\ &+ \sum_{n=1}^{\infty} \left[\left\{\sum_{r=1}^{N} \sum_{r=1}^{N} v_{n}^{(5)}(A_{r}) e^{-A_{r}t} - \sum_{r=1}^{N} \delta_{r}' \psi_{n}^{(4)}(A_{r}') e^{-A_{r}t}\right\} cosm_{n}|\alpha| \right] e^{-A_{n}t} \\ &- H(t - t_{o}) \sum_{n=1}^{\infty} \left[\sum_{r=1}^{N} \sum_{r=1}^{N} v_{n}^{(5)}(A_{r}) e^{-A_{r}}(A_{r}') e^{-A_{r}t}\right\} cosm_{n}t_{o} \right] e^{-A_{n}t_{o}} \\ &- \sum_{n=1}^{N} \left[\sum_{r=1}^{N} v_{n}^{(5)}(A_{r}) e^{-A_{r}t} - \sum_{r=1}^{N} v_{n}^{(4)}(A_{r}') e^{-A_{r}t}\right\} cosm_{n}t_{o} \right] e^{-A_{n}t_{o}} \\ &- H(t - t_{o}) \sum_{n=1}^{N} \left[\sum_{r=1}^{N} v_{n}^{(5)}(A_{r}) - \bar{\psi}_{n}^{(5)}(A_{r})\right\} e^{-A_{r}t_{o}} - \frac{A_{r}t_{o}^{(5)}(t - t_{o})}{-\sum_{r=1}^{N} v_{n}^{(4)}(A_{r}')} e^{-A_{r}t_{o}}(t - t_{o})} \right]$$

#### CASE III: T>0, $t_0<0$

 $U_v^n(t,T) = \text{same as equation (6.23)}$ 

$$\begin{split} \mathcal{V}_{V}^{N}(t,T,t_{o}) &= \frac{1}{4} \, \text{SIGN} \, (\alpha_{i}) \, \left( \, \delta_{o} - \delta_{o}' \right) \, + \, \frac{1}{4} \, \left( \, \delta_{o} - \delta_{o}' \right) \\ &+ \frac{1}{4} \sum_{r=1}^{N} \frac{\delta_{r}}{A_{r}} \left[ \, \text{SIGN} \, (\alpha_{i}) - e^{-A_{i}t} \, + \, 2 \, \text{H} \, (t-T) \, e^{-A_{i}t} \, (t-T) \, \right] \\ &- \frac{1}{4} \sum_{r=1}^{N} \frac{\delta_{r}}{A_{r}} \left[ \, \text{SIGN} \, (\alpha_{i}) - e^{-A_{i}t} \, + \, 2 \, \text{H} \, (t-T) \, e^{-A_{i}t} \, t \, \right] \\ &+ \frac{1}{4} \sum_{r=1}^{N} \frac{\delta_{r}}{A_{r}} \left[ \, 1 - e^{-A_{i}t} \, \right] \, - \frac{1}{4} \sum_{r=1}^{N} \frac{\delta_{r}}{A_{r}} \left[ \, 1 - e^{-A_{i}t} \, \right] \\ &+ \frac{1}{4} \sum_{r=1}^{N} \frac{\delta_{r}}{A_{r}} \left[ \, 1 - e^{-A_{i}t} \, \right] \, - \frac{1}{4} \sum_{r=1}^{N} \frac{\delta_{r}}{A_{r}} \left[ \, 1 - e^{-A_{i}t} \, \right] \\ &+ \frac{1}{4} \sum_{r=1}^{N} \frac{\delta_{r}}{A_{r}} \left[ \, 1 - e^{-A_{i}t} \, \right] \\ &+ \frac{1}{4} \left( \delta_{o} + \delta_{o}' \right) A_{n}^{(3)} + \sum_{r=1}^{N} \delta_{r}' \, \Phi_{n}^{(3)} (A_{r}, T) + \sum_{r=1}^{N} \delta_{r}' \, \Phi_{n}^{(3)} (A_{r}, T) \right\} \sin m_{n} |\alpha_{i}| \\ &+ \frac{1}{4} \sum_{r=1}^{N} \delta_{r}' \, \Phi_{n}^{(3)} (A_{r}) e^{-A_{i}t} + \sum_{r=1}^{N} \delta_{r}' \, \Phi_{n}^{(3)} (A_{r}, T) + \sum_{r=1}^{N} \delta_{r}' \, \Psi_{n}^{(3)} (A_{r}, T) \right\} \cos m_{n} |\alpha_{i}| \, d^{-K_{n}} |\alpha_{i}| \\ &+ \frac{1}{4} \left\{ \left( \delta_{o} + \delta_{o}' \right) \left( \delta_{n}' \right) e^{-A_{i}'} + \sum_{r=1}^{N} \delta_{r}' \, \Phi_{n}^{(3)} (A_{r}, T) + \sum_{r=1}^{N} \delta_{r}' \, \Psi_{n}^{(3)} (A_{r}, T) \right\} \cos m_{n} |\alpha_{i}| \, d^{-K_{n}} |\alpha_{i}| \\ &+ \frac{1}{4} \left\{ \left( \delta_{o} + \delta_{o}' \right) \left( \delta_{n}' \right) e^{-A_{i}'} + \sum_{r=1}^{N} \delta_{r}' \, \Psi_{n}^{(3)} (A_{r}, T) e^{-A_{i}'} \, d^{-K_{i}} \right\} \cos b_{n} T \, \right] e^{-K_{n} |\alpha_{i}|} \\ &+ \frac{1}{4} \left\{ \sum_{i=1}^{N} \delta_{r}' \, \Phi_{n}^{(3)} (A_{r}) e^{-A_{i}'} + \sum_{i=1}^{N} \delta_{r}' \, \Phi_{n}^{(3)} (A_{r}') e^{-A_{i}'} \, d^{-K_{i}'} \right\} \cos b_{n} T \, \right] e^{-A_{n} T} \\ &+ \frac{1}{4} \left\{ \sum_{i=1}^{N} \delta_{r}' \, \Psi_{n}^{(3)} (A_{r}) e^{-A_{i}'} + \sum_{i=1}^{N} \delta_{r}' \, \Psi_{n}^{(3)} (A_{r}') e^{-A_{i}'} \, d^{-K_{i}'} \right\} \cos b_{n} T \, \right] e^{-A_{n} T} \\ &+ \frac{1}{4} \left\{ \sum_{i=1}^{N} \delta_{r}' \, \Psi_{n}^{(3)} (A_{r}) e^{-A_{i}'} + \sum_{i=1}^{N} \delta_{r}' \, \Psi_{n}^{(3)} (A_{r}) e^{-A_{i}'} \, d^{-K_{i}'} \right\} \cos m_{n} |\alpha_{i}| \, e^{-A_{i}'} \\ &+ \frac{1}{4} \left\{ \sum_{i=1}^{N} \delta_{r}' \, \Psi_{n}^{(3)} (A_{r}) e^{-A_{i}'} - \sum_{i=1}^{N} \delta_{r}' \, \Psi_{n}^{(4)} (A_{$$

#### CASE IV: T<0, to<0

 $U_v^n(t,T)$  = same as equation (6.25)

$$\begin{split} \mathcal{V}_{v}^{N}(t,T,t_{0}) &= -\sum_{n=1}^{\infty} \left[ \left\{ (\aleph_{0} + \aleph_{0}') \, A_{n}^{(3)} + \sum_{r=1}^{N} \mathscr{V}_{r} \, \bar{\phi}_{n}^{(3)}(A_{r}) + \sum_{r=1}^{N'} \mathscr{V}_{r}' \, \bar{\phi}_{n}^{(3)}(A_{r}') \right\} \sin m_{n} |\alpha| \\ &+ \left\{ (\aleph_{0} + \aleph_{0}') \, B_{n}^{(3)} + \sum_{r=1}^{N} \mathscr{V}_{r}' \, \bar{\psi}_{n}^{(3)}(A_{r}) + \sum_{r=1}^{N'} \mathscr{V}_{r}' \, \bar{\psi}_{n}^{(3)}(A_{r}') \right\} \cos m_{n} |\alpha| \right] e^{-K_{n} |\alpha|} \\ &- \sum_{n=1}^{\infty} \left[ \left\{ \sum_{r=1}^{N} \mathscr{V}_{r}' \, \bar{\phi}_{n}^{(3)}(A_{r}) e^{-A_{r}t} + \sum_{r=1}^{N'} \mathscr{V}_{r}' \, \bar{\phi}_{n}^{(3)}(A_{r}') e^{-A_{r}t} \right\} \sin b_{n} T \\ &+ \left\{ \sum_{r=1}^{N} \mathscr{V}_{r}' \, \bar{\psi}_{n}^{(3)}(A_{r}) e^{-A_{r}t} + \sum_{r=1}^{N'} \mathscr{V}_{r}' \, \bar{\psi}_{n}^{(3)}(A_{r}') e^{-A_{r}t} \right\} \cos b_{n} T \right] e^{A_{n}T} \\ &+ \sum_{n=1}^{\infty} \left[ \left\{ \mathscr{V}_{0} \, A_{n}^{(5)} - \mathscr{V}_{0}' \, A_{n}^{(A)} + \sum_{r=1}^{N} \mathscr{V}_{r}' \, \bar{\psi}_{n}^{(3)}(A_{r}') e^{-A_{r}t} \right\} \cos b_{n} T \right] e^{A_{n}T} \\ &+ \left\{ \mathscr{V}_{0} \, B_{n}^{(5)} - \mathscr{V}_{0}' \, B_{n}^{(4)} - \sum_{r=1}^{N} \mathscr{V}_{r}' \, \bar{\psi}_{n}^{(5)}(A_{r}) + \sum_{r=1}^{N'} \mathscr{V}_{r}' \, \bar{\psi}_{n}^{(A)}(A_{r}') \right\} \cos m_{n} |n| \right] e^{-K_{n}|n|} \\ &+ \sum_{n=1}^{\infty} \left[ \left\{ \sum_{r=1}^{N} \mathscr{V}_{r}' \, \bar{\psi}_{n}^{(5)}(A_{r}) e^{-A_{r}t} - \sum_{r=1}^{N'} \mathscr{V}_{r}' \, \bar{\psi}_{n}^{(4)}(A_{r}') e^{-A_{r}t} \right\} \cos b_{n} t_{0} \right] e^{A_{n}t_{0}} \\ &+ \left\{ \sum_{r=1}^{N} \mathscr{V}_{r}' \, \bar{\psi}_{n}^{(5)}(A_{r}) e^{-A_{r}t} - \sum_{r=1}^{N'} \mathscr{V}_{r}' \, \bar{\psi}_{n}^{(4)}(A_{r}') e^{-A_{r}t} \right\} \cos b_{n} t_{0} \right] e^{A_{n}t_{0}} \end{aligned} \tag{6.28}$$

#### 6.4 Numerical Results

As an illustration of the method outlined in the preceding sections, numerical results were obtained for a specific material which behaves as a standard linear solid in both shear and dilatation. The material functions  $\theta_1(t)$  and  $\theta_2(t)$  for such a material will be of the following form (see Appendix III for detail):

$$\theta_{1}(t) = \frac{4}{9\kappa_{o}}\delta(t) + \frac{4}{9\kappa_{o}\tau}e^{-2t/\tau}$$

$$\theta_{2}(t) = \frac{4}{3\kappa_{o}}\delta(t) + \frac{4}{3\kappa_{o}\tau}e^{-t/\tau}$$
(6.29)

where  $K_{\bullet}$  is the instantaneous bulk modulus and  $\boldsymbol{\tau}$  is the relaxation time of the material in both shear and dilatation.

In the derivation of relation (6.29), it is assumed that the ultimate displacement of the solid in shear or dilatation is twice the corresponding instantaneous displacement and that  $G_o = \frac{3}{8} K_o$  where  $G_o$  is the instantaneous shear modulus.

It was found that the results were dependent upon the parameter  $F_{\circ} \tau$  . As such, numerical results were obtained for

B =0.005 in.  

$$K_0 = 1.45 \times 10^5 \text{ p.s.i.}$$
  
 $F_0 \tau = 10^2 \text{ to } 10^{-5} \text{ in.}$ 

and for the four distinct cases as explained earlier. These results for the normal displacements are shown in Figures 33 and 34, and those for the shear displacements are shown in Figures 35 to 38.

#### CHAPTER VII

## 7. SOLUTION OF THE VISCOELASTIC PROBLEM

After the influence functions for a viscoelastic sheet have been determined, it is now possible to formulate the viscoelastic rolling problem.

Although the theory presented in Chapter II is applicable to the rolling process in the presence of friction, it is not possible to satisfy the shear displacement condition (as given by equation (2.6)) in a continuous manner due to the line-load representation of the nip forces. (In such a case, the displacements and their derivatives diverge at the point of application of the load.) This difficulty has already been mentioned in Chapter V, while dealing with the rolling of the elastic sheet. A semi-inverse method was then proposed which proved to be successful in solving for the creep ratio and the elastic problem at large.

In the rolling of a viscoelastic sheet, some additional unknowns appear due to the asymmetry of the problem. The determination of the creep ratio for this case, using the semi-inverse method, becomes much more complicated.

In view of these difficulties, the viscoelastic problem

will be solved for Case B only (i.e., for complete slip).

If the loads were represented by some finite functions (like triangular loads or rectangular loads or parabolic loads, etc.) this difficulty would not have arisen. The motivation for picking up dirac delta functions was that the resulting integrals were obtained in their simplest form and could, therefore, be evaluated analytically. The latter was an essential requirement to apply the mathematical operations of the correspondence principle for obtaining the viscoelastic influence functions.

#### 7.1 The Choice of the Pinned Point (o, 1)

In the case of complete slip, there are no shear forces and the number of unknowns is therefore reduced considerably. Hence, it is not required to satisfy the shear displacement conditions. Further, since the normal displacements are not dependent upon the location of the pinned point, the position of the latter is not important. However, to determine the shear displacement, it is necessary to choose a pinned point. Thus, for convenience, the point lying on the central line of the sheet and on the line joining the centres of the two cylinders will be taken as the pinned point.

# 7.2 Matching Equation for the Case (B)

Since the influence functions, in this case, are dependent on time, it is necessary to specify the duration for which any particular load has been acting. This can be done in the following manner.

Thus, consider some arbitrary point M (Figure 39) situated at  $(-b, Y_M)$  which is not yet deformed but is just on the verge of getting deformed. Also, consider a unit load situated at the fictitious point  $(-b, Y_j^{\circ})$ , at the time t=0, which starts moving with a velocity  $F_0$  towards M. For convenience, it may be assumed that the load stays stationary while the sheet moves towards the load with the velocity of the load.

By using equation (6.23) the normal displacement of M at a certain time t=t; can be written as:

$$U_{iM}^{n} = U_{v}^{n}(t_{i},T_{j})$$
(7.1)

where

$$T_{j} = \frac{Y_{M} - Y_{j}^{\circ}}{F_{\circ}} \tag{7.2}$$

and  $U_{jM}^n$  represents the normal displacement at point M due to a unit normal load which, at the present instant, is situated at the jth point. Therefore, the normal displacement of M at a certain time t=t; due to the combined effect of

all loads will be

$$\sum_{j=1}^{m_1+m_2} P_{j} U_{jM}^n = \sum_{j=1}^{m_1+m_2} P_{j} U_{v}^n (t_i, T_j)$$
 (7.3)

But since point M is moving, it will travel a distance equal to  $F_0 t_i$  in the time  $t_i$  and will be located at the point  $(-b, Y_i)$  where its normal displacement must be equal to  $U_i$  as shown in Figure 39. Therefore,

$$U_{i} = \sum_{j=1}^{m_{1}+m_{2}} P_{j} U_{v}^{n}(t_{i},T_{j})$$
 (7.4)

Further, from the geometry, the normal displacement at  $(-b, Y_i)$  can be written as:

$$U_i = d_0 - \frac{2(m_1 + 1 - i)^2 \beta^2 b}{C_r}$$
 (7.5)

From equations (7.4) and (7.5), it follows that

$$\sum_{i=1}^{m_1+m_2} P_i U_v^n(t_i, T_j) = d_o - \frac{2(m_1+1-i)^2 \beta^2 b}{C_r}$$

Rearranging the above equation gives

$$\frac{d_{o}}{b} - \frac{1}{b} \sum_{j=1}^{m_{1}+m_{2}} P_{j} U_{v}^{n}(t_{i}, T_{j}) = \frac{2(m_{1}+1-i)^{2} \beta^{2}}{Cr}$$

$$(i=1, \dots, m_{1}+m_{2}+1)$$
(7.6)

Defining a coefficient matrix [A], unknown vector [X] and the known vector [B] as:

$$[A] = \begin{bmatrix} 1 & -U_{v}^{n}(t_{i}, T_{i}) & m_{1} + m_{2} + 1 \\ & & & \\ & & & \\ & & & \\ X \} = \begin{cases} \frac{d_{0}}{b} & \frac{P_{i}}{b} \\ & & \\ & & \\ C_{r} & & \\ & & \\ & & & \\$$

equation (7.7) can be written as follows:

$$[A][X] = [B] \tag{7.8}$$

By matrix inversion, the unknown vector [X] can be obtained as:

$$[X] = [A]^{1}[B]$$
 (7.9)

The value of  $oldsymbol{eta}$  should be corrected in a manner similar to that of the elastic case.

However,  $Y_M$  still remains to be fixed. For convenience, let

$$Y_{M} = 2m_{1}a + C_{L}b \tag{7.10}$$

where  $C_L$  is some constant. It is to be noted that no error will be introduced if the arbitrary point M is chosen to be located sufficiently away from the nip. Thus, an overestimation in the value of the constant  $C_L$  is permissible. The value of  $C_L$  was, therefore, chosen in such a way that the point M was located at a distance equal to approximately five times the contact length for the particular case. It was found that a higher value of  $C_L$  did not yield any significant change in the results.

From the geometry of Figure 39, and by using equation (7.2), it follows that

$$Y_{i} = 2(m_{1}+1-i)\beta b$$

$$Y_{j}^{o} = (2m_{1}+1-2j)\beta b$$

$$t_{i} = \left[2(i-1)\beta + C_{L}\right]\frac{b}{F_{0}}$$

$$T_{j} = \left[(2j-1)\beta + C_{L}\right]\frac{b}{F_{0}}$$
(7.11)

Thus, for some selected values of  $C_L$ , the coefficient matrix may be determined corresponding to  $T_i$  and  $t_i$  as given by equation (7.11). The unknowns may then be determined by using equation (7.9).

## 7.3 <u>Coefficient of Rolling Resistance</u>

In the case of elastic rolling, the pressure distribution is symmetric with respect to the line joining the centres of the cylinders. Hence, there is no net torque on the cylinder and, therefore, there is no resistance to rolling.

In the case of viscoelastic rolling, however, the symmetry in the pressure distribution is lost due to the dissipative nature of the sheet material. The forces acting on the trailing side will be smaller in magnitude to those on the leading side. Figure 40 illustrates the force equilibrium diagram of the upper half of the viscoelastic sheet.

Because of the asymmetric distribution of the pressure, there is now a net moment acting on the cylinder which is balanced by exerting some torque in the direction of the rotation of the cylinder. For the rolling to continue, the cylinder must exert this torque. This is equivalent to applying a force in the direction of rolling of the cylinder and, therefore, this force is known as the resistance to rolling and, more commonly, as the friction of rolling. The coefficient of rolling resistance,  $\mu_R$ , is given by the ratio of the rolling resistance to the total normal load, and

it turns out to be

$$\mu_{R} = \frac{\delta}{R} \tag{7.12}$$

where

 $\delta$  = Eccentricity of the resultant load,

R = Radius of the cylinder.

Let

M<sub>1</sub> = Total moment (at the centre of the cylinder)
 of the forces acting on the leading side; and

M<sub>2</sub>= Total moment (at the centre of the cylinder)
 of the forces on the trailing side.

Then,

$$M_{1} = \sum_{j=1}^{m_{1}} P_{j} \cdot Y_{j}^{\circ} = \sum_{j=1}^{m_{2}} P_{j} (2m_{1}+1-2j) \beta. b$$

$$M_{2} = \sum_{j=m_{1}+1}^{m_{1}+m_{2}} P_{j} \cdot Y_{j}^{\circ} = \sum_{j=m_{2}+1}^{m_{2}+m_{2}} P_{j} \cdot (2m_{1}+1-2j) \beta b$$

$$(7.13)$$

The eccentricity of the resultant load will, therefore, be given by

$$S = \frac{M_1 + M_2}{M} \tag{7.14}$$

and thence, the coefficient of rolling resistance will be

$$\mu_{R} = \frac{M_1 + M_2}{M_1 R} \tag{7.15}$$

## 7.4 Creep Ratio for Complete Slip

The creep ratio for the viscoelastic case may be determined in a manner similar to that of the elastic case. However, because of asymmetry, it is necessary to consider the shear displacements due to the normal force at both the end points.

The shear displacements at the end points can be written as:

$$V_{1} = \sum_{j=1}^{m_{1}+m_{2}} V_{1j}^{n} P_{j}.$$

$$V_{(m_{1}+m_{2}+1)} = \sum_{j=1}^{m_{1}+m_{2}} V_{(m_{1}+m_{2}+1),j}^{n} P_{j}.$$
(7.16)

From which the creep ratio can be obtained as

$$\chi_{o} = \frac{\gamma_{(m_1+m_2+1)} - \gamma_1}{1}$$

or,

$$\chi_0 = \frac{y_{(m_1 + m_2 + 1)} - y_1}{2(m_1 + m_2)\beta b}$$
 (7.17)

#### 7.5 Numerical Results

Numerical results for the same variables as those in the elastic case, were obtained for the case of complete slip in the rolling of a viscoelastic sheet with the aid of an IBM 360/75 computer of McGill University. As stated earlier, it was found that the results were dependent upon the parameter  $F_{\bullet} \tau$ . Therefore, for this case, the following geometrical and mechanical properties were considered.

Instantaneous bulk  $K_0=1.45\times10^5 \,\mathrm{p.s.i.}$  modulus

Instantaneous shear  $G_0=3/8$   $K_0$  modulus

The product of relaxation time to speed  $F_0\tau = 10^3$  to  $10^{-5}$  in. rolling

Radius of the R=6 inches cylinder

Total normal load W=50, 100, 150, and 200 P.L.I.

Thickness of the B=1.0, 0.25, 0.0625, sheet and 0.005 in.

The relevant results for the above variations in normal load, sheet thickness, and the ratio of relaxation time to speed of rolling, are tabulated in Tables XI to XXVI.

As a comparison to the elastic case, plots of peak pressure  $p_{\text{max}}$ , the ratio of the contact length to the thickness of the sheet L/B, the ratio of the depth of indentation to the thickness of the sheet  $d_0/B$ , and the creep ratio against normal load and for the above variations in the parameter  $F_0 c$ , were obtained as shown in Figures 41 to 44. To illustrate the influence of the ratio of the relaxation time to the speed of rolling, the same plots were obtained against this ratio and are shown in Figures 45 to 48.

The variations in pressure distribution and in normal and shear displacements of the surface of the sheet with the parameter  $F_0$ T for B=0.005 in. and W=100 P.L.I. are shown in Figures 49, 52 and 53 respectively.

The results show that for very low, or very high values of this ratio, the material shows elastic behaviour. This is in full agreement with the particular model chosen for the purpose of numerical illustration.

The variations in the coefficient of rolling resistance with the parameter  $F_{\circ} \mathcal{T}$  for different loads and for different thicknesses of the sheet are shown in Figures 50 and 51 respectively.

#### CHAPTER VIII

#### 8. DISCUSSION AND CONCLUSION

In order to give an assessment of the proposed theory, a discussion of the results and the conclusion that may be drawn from them, will be presented in the following paragraphs.

#### 8.1 Elastic Case

For the analysis of the results, it is necessary to categorize them into two distinct cases, viz.: (i) the case of thick sheet and, (ii) the case of thin sheet. These cases are identified by the ratio of the contact length to the thickness of the sheet. If this ratio is small compared to unity, it is a case of thick sheet. On the other hand, if this ratio is large compared to unity, it is a case of thin sheet.

Within the nip, a thick sheet has a tendency to move in (or contract, (Fig.28)) whereas, a thin sheet tries to move out (or elongate, (Fig.29)). These tendencies are opposed by the presence of friction on the contact surfaces which generate the shear forces. Consequently, the magnitudes of

the shear forces become larger and larger as the sheet becomes very thick or very thin. For an intermediate case, the shear forces are very small in magnitude. In both cases, the distribution of the shear forces is antisymmetric with zero value at the centre of the nip and at the ends. It has been found that the maximum value of the shear forces occurs at a distance of approximately  $\frac{L}{8}$  from the ends of the nip (Figure 27). For a thin sheet, the shear forces act inwards, whereas for a thick sheet, they act outwards.

The creep ratio is negative for a thick sheet and positive for a thin sheet and increases in magnitude as the normal load is increased. For an intermediate case, this ratio may change sign as the normal load is changed. Further, as the sheet becomes thinner and thinner, the rate of increase of this ratio with normal load decreases (Figure 20). This is due to the fact that although the shear displacements of the end points increase with load, there is a greater increase in the contact length. This situation is not present in the case of complete slip where the sheet is completely free to move.

The results have been found to be quite sensitive to the thickness of the sheet (Figures 17-19 and 21-23).

As the friction on the contact surfaces reduces, the contact length increases and the peak pressure decreases. This results in a *flattening* of the pressure-distribution curve.

#### 8.2 Viscoelastic Case

It has been found that, in the case of a viscoelastic sheet, all formulated functions are dependent upon the parameter  $F_0$  where C is the relaxation time of the sheet material, and  $F_0$  is the overall speed of the sheet. For very small and very large values of this parameter, the sheet shows elastic behaviour. The results for the latter case  $(F_0C = 10^3 \text{ in.})$  are shown by solid line (——) and those for the former  $(F_0C = 10^6 \text{ in.})$  are shown by a solid line and two broken lines (————). It is to be noticed that there is a difference in magnitude of the results for the two extreme cases  $(F_1\text{gures } +5 - +9)$ . This is due to the particular material chosen for the purpose of numerical illustration (see Figure 32 for the model). For a value of  $F_0C$  between  $10^0$  to  $10^{-4}$  in., the material shows a marked viscoelastic effect.

The pressure distribution is symmetric for the extreme values of the parameter  $F_0 \tau$  but leans forward for its intermediate values. This leaning effect first increases, reaches a certain maximum value, and then decreases with the increase in the value of  $F_0 \tau$  (Figure 49). Consequently, the coefficient of rolling resistance first increases, attains a certain maximum value (for  $F_0 \tau \simeq 10^{-1} \cdot 10^{-2}$  in.) and then decreases monotonically (Figures 50 and 51). The point where the cylinder loses contact with the sheet has almost the same behaviour as that

of the pressure distribution or the coefficient of rolling resistance (Figure 52). These observations are in full agreement with previously published reports (see, for example, Hunter<sup>[7]</sup>).

The comments made above regarding the behaviour of thin and thick sheets hold good for viscoelastic sheet as well.

#### 8.3 Conclusion

In conclusion, it may be stated that by the method of influence functions, and by using the proposed semi-inverse methods, the rolling of an elastic sheet has been treated successfully for the extreme cases of no slip and complete slip. This method permits the treatment of the rolling of a viscoelastic sheet which, until now, has not been solved.

It is the author's belief that his contribution to knowledge lies in the following:

- (i) Influence functions for the surface displacements of an elastic sheet, due to normal and shear line loads, have been determined in a closed form using contour integration;
- (ii) For the first time, influence functions for surface displacements of any general viscoelastic sheet, due

to moving loads, have been obtained in a closed form. This is a very valuable tool in the formulation of the viscoelastic rolling problems.

- (iii) The physical behaviour of elastic, as well as viscoelastic sheet in rolling contact with rigid cylinders, has been discussed in great detail and the related boundary conditions of the sheet have been described for the extreme cases of complete slip and no slip. The theory proposed by Bentall<sup>[14]</sup> has been considerably improved and the modified theory is time-saving, more accurate, and applicable to viscoelastic rolling as well.
- (iv) Direct solutions (in contrast to the previous theories which treat the problem for certain assumed ratios of the contact length to the thickness of the sheet) have been obtained for the cases of both elastic and viscoelastic rolling. Thus, given the mechanical properties of the sheet material and the dynamics of loading, this theory can predict the entire state of the nip.

#### APPENDIX I

- AI <u>EVALUATION OF THE INTEGRALS I</u>1-I7 FOR THE ELASTIC CASE
- AI.1 The Integral  $I_1(\alpha)$

Putting  $b\xi = x$ ,  $I_1(x)$  becomes:

$$I_1(\alpha) = \int_0^\infty \frac{2\sinh^2 x \cos \alpha x}{x \left(\sinh 2x + 2x\right)} dx$$

Because of symmetry with respect to  $\alpha$ ,

$$\int_{-\infty}^{\infty} \frac{\sinh^2 x \cos \alpha x}{x \left(\sinh 2x + 2x\right)} dx = \int_{-\infty}^{\infty} \frac{2 \sinh^2 x \cos \alpha x}{x \left(\sinh 2x + 2x\right)} dx = I_1(\alpha)$$

Also, because of antisymmetry with respect to  $\chi$  ,

$$\int_{-\infty}^{\infty} \frac{\sinh^2 x \sin \alpha x}{x (\sinh 2x + 2x)} dx = 0$$

Hence,

$$\int_{-\infty}^{\infty} \frac{\sinh^2 x e^{i\alpha x}}{x \left(\sinh 2x + 2x\right)} dx = I_1(\alpha)$$

or,

$$\int_{-\infty}^{\infty} H_1(\alpha, x) dx = 2I_1(\alpha)$$
 (AI.1)

where,

$$H_1(\alpha, x) = \frac{2\sinh^2 x}{x\left(\sinh 2x + 2x\right)}$$
(AI.2)

Consider the contour integration  $\oint_C H_1(\alpha,z) dz$  along the contour C as shown in Figure 54. It can be seen that for  $\alpha > 0$ ,

$$\lim_{z \to \infty} H_1(\alpha, z) = 0$$

and hence that for  $\ensuremath{\alpha} > 0$  , the integrand will vanish along the semicircular path so that:

$$\oint_{-\infty} H_1(\alpha, z) dz = \int_{-\infty}^{\infty} H_1(\alpha, z) dz = 2I_1(\alpha)$$

However, from the calculus of residues,

$$\oint_C H_1(\alpha,z) dz = 2\pi i \times \text{sum of the residues of } H_1(\alpha,z) \text{ in } C$$

$$+ \pi i \times \text{sum of the residues of } H_1(\alpha,z) \text{ on } C$$

Therefore,

$$I_1(A) = \pi i \times \text{sum of the residues of } H_1(A,Z) \text{ in } C$$

$$+ \frac{\pi}{2} i \times \text{sum of the residues of } H_1(A,Z) \text{ on } C$$
(AI.3)

It is required now to determine the residues of  $H_1(A,Z)$  within and on the contour C .

 $H_1(\alpha,z)$  does not have any pole on contour C. Within the contour, it has single poles at the points where  $\sinh 2z + 2z = 0$ . Let  $z = z_n$  be one of such points in the
first quadrant and let  $R_n$  be the residue of  $H_1(\alpha,z)$ at that point. Then, from the definition of residues,

$$R_n = \dim_{z \to z_n} (z - z_n) H_1(q, z)$$

Substituting for  $H_1(\alpha, \mathbf{Z})$  from equation (AI.2), taking the limit and simplifying gives:

$$R_n = \frac{\tanh^2 z_n e^{idz_n}}{2 z_n}$$

Substituting  $Z_n = m_n + i K_n$  and simplifying yields:

$$R_{n} = \frac{e^{-K_{n}\alpha}}{2(m_{n}^{2} + K_{n}^{2})} \left[ (g_{n}m_{n} + h_{n}K_{n}) \cos m_{n}\alpha - (h_{n}m_{n} - g_{n}K_{n}) \sin m_{n}\alpha \right]$$

$$+ i \frac{e^{-K_{n}\alpha}}{2(m_{n}^{2} + K_{n}^{2})} \left[ (g_{n}m_{n} + h_{n}K_{n}) \sin m_{n}\alpha + (h_{n}m_{n} - g_{n}K_{n}) \cos m_{n}\alpha \right]$$
(AI.4)

where,

$$g_{n} = \frac{(\tanh^{2}m_{n} - \tan^{2}K_{n})(1 - \tanh^{2}m_{n}\tan^{2}K_{n}) + 4\tanh^{2}m_{n}\tan^{2}K_{n}}{(1 + \tanh^{2}m_{n}\tan^{2}K_{n})^{2}}$$

$$h_{n} = \frac{2\tanh m_{n} \tan K_{n}(1 - \tanh^{2}m_{n}\tan^{2}K_{n} - \tanh^{2}m_{n} + \tan^{2}K_{n})}{(1 + \tanh^{2}m_{n} \cdot \tan^{2}K_{n})^{2}}$$
(AI.5)

If  $(m_n+iK_n)$  is a root of  $\sinh 2z+2z=0$ ,  $(-m_n+iK_n)$  is also a root of this equation (see Appendix IV). Let the residue of  $H_1(\alpha,z)$  at the point  $(-m_n+iK_n)$  be  $R'_n$ . Then, by replacing  $m_n$  by  $-m_n$  in equation (AI.4) and noting that  $g_n$  and  $h_n$  are even and odd functions of  $m_n$  respectively, one obtains:

$$R'_{n} = -\frac{e^{-K_{n}\alpha}}{2(m_{n}^{2} + K_{n}^{2})} \left[ (9_{n}m_{n} + h_{n}K_{n}) \cos m_{n}\alpha - (h_{n}m_{n} - 9_{n}K_{n}) \sin m_{n}\alpha \right]$$

$$+ i \frac{e^{-K_{n}\alpha}}{2(m_{n}^{2} + K_{n}^{2})} \left[ (9_{n}m_{n} + h_{n}K_{n}) \sin m_{n}\alpha + (h_{n}m_{n} - 9_{n}K_{n}) \cos m_{n}\alpha \right]$$
(AI.6)

Adding equations (AI.4) and (AI.6),

$$R_n + R'_n = i \frac{e^{-K_n \alpha}}{m_n^2 + K_n^2} \left[ (g_n m_n + h_n K_n) sin m_n \alpha + (h_n m_n - g_n K_n) cos m_n \alpha \right]$$
(AI.7)

From equations (AI.3) and (AI.7),

$$I_{1}(\alpha) = -\Pi \sum_{n=1}^{\infty} \frac{e^{-K_{n}\alpha}}{m_{n}^{2} + K_{n}^{2}} \left[ (g_{n}m_{n} + h_{n}K_{n}) \sin m_{n}\alpha + (h_{n}m_{n} - g_{n}K_{n}) \cos m_{n}\alpha \right]$$

or,

$$I_1(\alpha) = \prod_{n=1}^{\infty} e^{-K_n \alpha} \left( A_n^{(l)} \sin m_n \alpha + B_n^{(l)} \cos m_n \alpha \right)$$

where,

$$A_{n}^{(i)} = -\frac{(9_{n}m_{n} + h_{n} k_{n})}{m_{n}^{2} + k_{n}^{2}}$$

$$B_{n}^{(i)} = \frac{9_{n}k_{n} - h_{n}m_{n}}{m_{n}^{2} + k_{n}^{2}}$$
(AI.8)

in which  $Z_n=M_n+iK_n$  are the roots of  $\sinh 2z+2z=0$  in the first quadrant only and where <>0. By inspection, it can be seen that  $I_1(-<)=I_i(<)$ . Thus, for any value of <0 the integral

$$I_1(\alpha) = \pi \cdot \sum_{n=1}^{\infty} e^{-Kn|\alpha|} \left( A_n^{(l)} \sin m_n |\alpha| + B_n \cos m_n |\alpha| \right)$$
 (AI.9)

## AI.2 The Integral $I_2(\alpha)$

From the properties of sine integrals,

$$I_{2}(\alpha) = \int_{0}^{\infty} \frac{\sin \alpha \, b \xi}{b \xi} \cdot d(b \xi) = \frac{\pi}{2} \quad \text{if} \quad \alpha > 0$$

$$= 0 \quad \text{if} \quad \alpha = 0$$

$$= -\frac{\pi}{2} \quad \text{if} \quad \alpha < 0$$

Then, for any value of  $\alpha$ , this integral can be written as:

$$I_2(a) = SIGN(a) \cdot \frac{\pi}{2} \tag{AI.10}$$

where,

$$SIGN(\alpha) = 1 \quad \text{if} \quad \alpha > 0$$

$$= -1 \quad \text{if} \quad \alpha < 0$$
(AI.11)

## AI.3 The Forms of the Remaining Integrals:

Following the same procedure as used during the evaluation of  $\mathbf{I_1}(\mathbf{d})$  , the remaining integrals of the elastic case can be expressed as follows:

$$\begin{split} I_{3}(\alpha) &= \text{SIGN}(\alpha) \cdot \Pi \cdot \left[ \frac{1}{4} + \sum_{n=1}^{\infty} e^{-K_{n}(\alpha)} \left( A_{n}^{(3)} \sin m_{n} |\alpha| + B_{n}^{(3)} \cos m_{n} |\alpha| \right) \right] \\ I_{4}(\eta) &= \text{SIGN}(\eta) \cdot \Pi \cdot \left[ \frac{1}{4} + \sum_{n=1}^{\infty} e^{-K_{n} |\eta|} \left( A_{n}^{(4)} \sin m_{n} |\eta| + B_{n}^{(4)} \cos m_{n} |\eta| \right) \right] \\ I_{5}(\eta) &= \text{SIGN}(\eta) \cdot \Pi \cdot \left[ \frac{1}{4} + \sum_{n=1}^{\infty} e^{-K_{n} |\eta|} \left( A_{n}^{(5)} \sin m_{n} |\eta| + B_{n}^{(5)} \cos m_{n} |\eta| \right) \right] \\ I_{6}(\alpha, \eta) &= \Pi \cdot \sum_{n=1}^{\infty} e^{-K_{n} |\eta|} \left( A_{n}^{(6)} \sin m_{n} |\alpha| + B_{n}^{(6)} \cos m_{n} |\eta| \right) - \frac{\Pi}{4} \left( |\alpha| - |\eta| \right) \\ &+ \Pi \cdot \sum_{n=1}^{\infty} e^{-K_{n} |\eta|} \left( A_{n}^{(7)} \sin m_{n} |\eta| + B_{n}^{(7)} \cos m_{n} |\eta| \right) \\ I_{7}(\eta) &= \Pi \cdot \sum_{n=1}^{\infty} e^{-K_{n} |\eta|} \left( A_{n}^{(8)} \sin m_{n} |\eta| + B_{n}^{(8)} \cos m_{n} |\eta| \right) \end{split}$$

in which the various coefficients are given by the following relations:

$$A_{n}^{(3)} = \frac{1}{2} \sinh(2m_{n}) \cdot \sin(2k_{n}) / \Delta^{2}$$

$$B_{n}^{(3)} = (\cosh^{2}m_{n} \cos^{2}k_{n} - \sinh^{2}m_{n} \sin^{2}k_{n}) / \Delta^{2}$$

$$A_{n}^{(4)} = (m_{n} h'_{n} + k_{n} g'_{n}) / (m_{n}^{2} + k_{n}^{2})$$

$$B_{n}^{(4)} = (m_{n} g'_{n} - k_{n} h'_{n}) / (m_{n}^{2} + k_{n}^{2})$$

$$A_{n}^{(5)} = \sinh m_{n} \cdot \sin k_{n} / \Delta$$

$$A_{n}^{(5)} = \sinh m_{n} \cdot \sin k_{n} / \Delta$$

$$B_{n}^{(5)} = \cosh m_{n} \cdot \cos k_{n} / \Delta$$

$$A_{n}^{(6)} = -m_{n} / (m_{n}^{2} + k_{n}^{2})$$

$$B_{n}^{(6)} = k_{n} / (m_{n}^{2} + k_{n}^{2})$$

$$A_{n}^{(7)} = (m_{n} g''_{n} - k_{n} h''_{n}) / (m_{n}^{2} + k_{n}^{2})$$

$$B_{n}^{(7)} = -(m_{n} h''_{n} + k_{n} g''_{n}) / (m_{n}^{2} + k_{n}^{2})$$

$$A_{n}^{(8)} = -g'_{n}$$

$$B_{n}^{(8)} = h'_{n}$$

(AI.13)

and

$$g'_{n} = \sinh m_{n} \cdot \cosh \kappa_{n} \left(\cosh^{2}m_{n} + \sin^{2}\kappa_{n}\right) / \Delta^{2}$$

$$h'_{n} = \cosh m_{n} \cdot \sinh \kappa_{n} \left(\sinh^{2}m_{n} - \cos^{2}\kappa_{n}\right) / \Delta^{2}$$

$$g''_{n} = \cosh m_{n} \cdot \cosh \kappa_{n} / \Delta$$

$$h''_{n} = \sinh m_{n} \cdot \sinh \kappa_{n} / \Delta$$

$$\Delta = \cosh^{2}m_{n} \cdot \cos^{2}\kappa_{n} + \sinh^{2}m_{n} \cdot \sin^{2}\kappa_{n}$$
(AI.14)

and  $Z_n = M_n + i \, K_n$  are the roots of sinh2z + 2z = 0 in the first quadrant only.

#### APPENDIX II

# AII. EVALUATION OF THE INTEGRALS J<sub>1</sub>-J<sub>6</sub> FOR THE VISCOELASTIC CASE

## AII. 1 Integrals $J_1(\lambda,T)$ to $J_4(\lambda,T)$ for the Case T>0:

For the evaluation of integrals  $J_1(\lambda, \tau)$  to  $J_4(\lambda, \tau)$  first consider the following integrals:

$$J' = \int_{t_{i}}^{t_{2}} e^{\kappa \tau} \sin \beta (\phi - \tau) d\tau$$

$$J'' = \int_{t_{i}}^{t_{2}} e^{\kappa \tau} \cos \beta (\phi - \tau) d\tau$$
(AII.1)

Integrating by parts gives:

$$J' = \frac{1}{\beta} \left[ e^{Kt_2} \cos \beta (\phi - t_2) - e^{Kt_1} \cos \beta (\phi - t_1) \right] - \frac{K}{\beta} J''$$

$$J'' = \frac{1}{\beta} \left[ e^{\kappa t_2} \sin \beta (\phi - t_i) - e^{\kappa t_i} \sin \beta (\phi - t_i) \right] + \frac{\kappa}{\beta} J''$$

Solving for J' and J'' yields:

$$J' = \frac{k}{\kappa^2 + \beta^2} \left[ e^{kt_2} \sin\beta(\phi - t_2) - e^{kt_1} \sin\beta(\phi - t_1) \right]$$

$$+ \frac{\beta}{\kappa^2 + \beta^2} \left[ e^{kt_2} \cos\beta(\phi - t_2) - e^{kt_1} \cos\beta(\phi - t_1) \right]$$

$$J'' = \frac{k}{\kappa^2 + \beta^2} \left[ e^{kt_2} \cos\beta(\phi - t_2) - e^{kt_1} \cos\beta(\phi - t_1) \right]$$

$$- \frac{\beta}{\kappa^2 + \beta^2} \left[ e^{kt_2} \sin\beta(\phi - t_2) - e^{kt_1} \sin\beta(\phi - t_1) \right]$$

$$- \frac{\beta}{\kappa^2 + \beta^2} \left[ e^{kt_2} \sin\beta(\phi - t_2) - e^{kt_1} \sin\beta(\phi - t_1) \right]$$

Since the integrands of  $J_1(\Lambda,T)$  and  $J_2(\Lambda,T)$  involve Heavyside's function, it is convenient to break the integrals into two parts as follows:

$$J_{1}(\lambda,T) = e^{-\lambda t - a_{n}T} \left[ H(T-t) \int_{0}^{t} e^{(\lambda+a_{n})T} \sinh_{n}(\tau-\tau) d\tau \right]$$

$$+ H(t-T) \int_{0}^{T} e^{(\lambda+a_{n})T} \sinh_{n}(\tau-\tau) d\tau \right]$$

$$J_{2}(\lambda,T) = e^{-\lambda t - a_{n}T} \left[ H(T-t) \int_{0}^{t} e^{(\lambda+a_{n})T} \cosh_{n}(\tau-\tau) d\tau \right]$$

$$+ H(t-T) \int_{0}^{T} e^{(\lambda+a_{n})T} \cosh_{n}(\tau-\tau) d\tau \right]$$

$$+ H(t-T) \int_{0}^{T} e^{(\lambda+a_{n})T} \cosh_{n}(\tau-\tau) d\tau \right]$$

Letting  $k=\lambda+a_n$ ,  $t_1=0$ ,  $t_2=t$ ,  $\beta=b_n$ , and  $\phi=T$  into equation (AII.2) and, after simplifying,

$$\int_{0}^{t} e^{(A+a_{n})T} \sin b_{n}(T-T) dT$$

$$= \frac{e^{(A+a_{n})t} \left\{ (A+a_{n}) \sin b_{n}(T-t) + b_{n} \cos b_{n}(T-t) \right\}}{(A+a_{n})^{2} + b_{n}^{2}}$$

$$- \frac{(A+a_{n}) \sin b_{n}T + b_{n} \cos b_{n}T}{(A+a_{n})^{2} + b_{n}^{2}}$$

$$= \frac{e^{(A+a_{n})T} \cos b_{n}(T-T) dT}{(A+a_{n})^{2} + b_{n}^{2}}$$

$$= \frac{e^{(A+a_{n})t} \left\{ (A+a_{n}) \cos b_{n}(T-t) - b_{n} \sin b_{n}(T-t) \right\}}{(A+a_{n})^{2} + b_{n}^{2}}$$

$$= \frac{(A+a_{n}) \cos b_{n}T - b_{n} \sin b_{n}T}{(A+a_{n})^{2} + b_{n}^{2}}$$

Further, letting t = T in equation (AII.4) gives:

$$\int_{0}^{T} e^{(\lambda+a_{n})T} \sin b_{n}(T-z) dz$$

$$= \frac{b_{n}e^{(\lambda+a_{n})T} - (\lambda+a_{n}) \sin b_{n}T - b_{n} \cos b_{n}T}{(\lambda+a_{n})^{2} + b_{n}^{2}}$$

$$\int_{0}^{T} e^{(\lambda+a_{n})Z} \cos b_{n}(T-z) dz$$

$$= \frac{(\lambda+a_{n})e^{(\lambda+a_{n})T} - (\lambda+a_{n}) \cos b_{n}T + b_{n} \sin b_{n}T}{(\lambda+a_{n})^{2} + b_{n}^{2}}$$
(AII.5)

Using equations (AII.3), (AII.4), and (AII.5) and simplifying, yields:

$$J_{1}(A,T) = H(T-t) \left\{ \frac{(A+a_{n}) \sin b_{n}(T-t) + b_{n} \cos b_{n}(T-t)}{(A+a_{n})^{2} + b_{n}^{2}} \right\} e^{-a_{n}(T-t)}$$

$$+ \frac{H(t-T) b_{n} e^{-A(t-T)}}{(A+a_{n})^{2} + b_{n}^{2}} - \left\{ \frac{(A+a_{n}) \sin b_{n}T + b_{n} \cos b_{n}T}{(A+a_{n})^{2} + b_{n}^{2}} \right\}.$$

$$\cdot e^{-At - a_{n}T}$$

$$\cdot e^{-At - a_{n}T}$$

$$J_{2}(A,T) = H(T-t) \left\{ \frac{(A+a_{n}) \cos b_{n}(T-t) - b_{n} \sin b_{n}(T-t)}{(A+a_{n})^{2} + b_{n}^{2}} \right\}.e^{-a_{n}(T-t)}$$

$$+ \frac{H(t-T)(A+a_{n}) e^{-A(t-T)}}{(A+a_{n})^{2} + b_{n}^{2}}$$

$$- \left\{ \frac{(A+a_{n}) \cos b_{n}T - b_{n} \sin b_{n}T}{(A+a_{n})^{2} + b_{n}^{2}} \right\}.e^{-At - a_{n}T}$$

In a similar manner:

$$J_3(A,T) = e^{-At + a_n T} H(t-T) \int_{T}^{t} e^{(A-a_n)T} \sinh_n(T-T) dT$$

$$J_4(A,T) = e^{-At + a_n T} H(t-T) \int_{T}^{t} e^{(A-a_n)T} \cosh_n(T-T) dT$$

$$(AII.7)$$

Again, letting  $k=\lambda-\alpha_n$ ,  $t_i=T$ ,  $t_2=t$ ,  $\beta=b_n$ , and  $\phi=T$ , in equation (AII.2) gives, upon simplifying:

$$\int_{T}^{t} e^{(\lambda - a_{n})\tau} \sin b_{n} (\tau - \tau) d\tau 
= e^{(\lambda - a_{n})t} \left\{ \frac{(\lambda - a_{n})\sin b_{n} (\tau - t) + b_{n}\cos b_{n}(\tau - t)}{(\lambda - a_{n})^{2} + b_{n}^{2}} \right\} 
- \frac{b_{n}}{(\lambda - a_{n})^{2} + b_{n}^{2}} 
- \frac{b_{n}}{(\lambda - a_{n})^{2} + b_{n}^{2}} 
= e^{(\lambda - a_{n})\tau} \cos b_{n} (\tau - \tau) d\tau 
= e^{(\lambda - a_{n})t} \left\{ \frac{(\lambda - a_{n})\cos b_{n}(\tau - t) - b_{n}\sin b_{n}(\tau - t)}{(\lambda - a_{n})^{2} + b_{n}^{2}} \right\} 
- \frac{(\lambda - a_{n})}{(\lambda - a_{n})^{2} + b_{n}^{2}}$$
(AII.8)

Using equations (AII.7) and (AII.8), the integrals  $J_3$  and  $J_4$  are obtained as follows:

$$J_{3}(\Lambda,T) = H(t-T) \left[ e^{-a_{n}(t-T)} \left\{ \frac{(\Lambda - a_{n}) \sin b_{n}(\tau - t) + b_{n} \cos b_{n}(\tau - t)}{(\Lambda - a_{n})^{2} + b_{n}^{2}} \right\} - \frac{b_{n} e^{-\Lambda(t-T)}}{(\Lambda - a_{n})^{2} + b_{n}^{2}} \right]$$

$$J_{4}(\Lambda,T) = H(t-T) \left[ e^{-a_{n}(t-T)} \left\{ \frac{(\Lambda - a_{n}) \cos b_{n}(\tau - t) - b_{n} \sin b_{n}(\tau - t)}{(\Lambda - a_{n})^{2} + b_{n}^{2}} \right\} - \frac{(\Lambda - a_{n}) e^{-\Lambda(t-T)}}{(\Lambda - a_{n})^{2} + b_{n}^{2}} \right]$$

### AII.2 Integrals $J_1(\lambda,T)$ to $J_4(\lambda,T)$ for the Case T<0

When T<o, the Heavyside function

$$H(\tau-\tau) = 0$$

$$H(\tau-\tau) = 1$$
(AII.10)

for all values of **z** within the limits of integration. Hence,

$$J_{1}(\lambda,T) = 0$$

$$J_{2}(\lambda,T) = 0$$

$$J_{3}(\lambda,T) = e^{-\lambda t + a_{n}T} \int_{0}^{t} e^{(\lambda-a_{n})T} \sinh_{n}(T-t) dt$$

$$J_{4}(\lambda,T) = e^{-\lambda t + a_{n}T} \int_{0}^{t} e^{(\lambda-a_{n})T} \cosh_{n}(T-t) dt$$
(AII.11)

Letting  $k=\lambda-a_n$ ,  $t_{i=0}$ ,  $t_{2}=t$ ,  $\beta=b_n$ , and  $\phi=T$ , in equation (AII.2) yields:

$$\int_{0}^{t} e^{(A-a_{n})\tau} \sin b_{n}(\tau-\tau) d\tau \\
= \frac{e^{(A-a_{n})t} \left\{ (A-a_{n}) \sin b_{n}(\tau-t) + b_{n} \cos b_{n}(\tau-t) \right\}}{(A-a_{n})^{2} + b_{n}^{2}} \\
- \frac{(A-a_{n}) \sin b_{n}\tau + b_{n} \cos b_{n}\tau}{(A-a_{n})^{2} + b_{n}^{2}} \\
\int_{0}^{t} e^{(A-a_{n})\tau} \cos b_{n}(\tau-\tau) d\tau \\
= \frac{e^{(A-a_{n})t} \left\{ (A-a_{n}) \cos b_{n}(\tau-t) - b_{n} \sin b_{n}(\tau-t) \right\}}{(A-a_{n})^{2} + b_{n}^{2}} \\
- \frac{(A-a_{n}) \cos b_{n}\tau - b_{n} \sin b_{n}\tau}{(A-a_{n})^{2} + b_{n}^{2}}$$

Hence, from equations (AII.11) and (AII.12),

$$J_{3}(\Lambda,T) = \frac{(\Lambda - \alpha_{n}) \sin b_{n}(T-t) + b_{n} \cos b_{n}(T-t)}{(\Lambda - \alpha_{n})^{2} + b_{n}^{2}} e^{-\alpha_{n}(t-T)}$$

$$- \frac{(\Lambda - \alpha_{n}) \sin b_{n}T + b_{n} \cos b_{n}T}{(\Lambda - \alpha_{n})^{2} + b_{n}^{2}} e^{-\lambda t + \alpha_{n}T}$$

$$J_{4}(\Lambda,T) = \frac{(\Lambda - \alpha_{n}) \cos b_{n}(T-t) - b_{n} \sin b_{n}(T-t)}{(\Lambda - \alpha_{n})^{2} + b_{n}^{2}} e^{-\lambda t + \alpha_{n}T}$$

$$- \frac{(\Lambda - \alpha_{n}) \cos b_{n}T - b_{n} \sin b_{n}T}{(\Lambda - \alpha_{n})^{2} + b_{n}^{2}} e^{-\lambda t + \alpha_{n}T}$$

$$(AII.13)$$

# AII.3 Integrals $J_5(T)$ and $J_6(T)$ for the Case T>0

Substituting for  $\theta_1$  (t) from equation (6.17) yields:

$$J_{5}(\tau) = \int_{0}^{t} \left[ x_{0} \, \delta(t-\tau) + \sum_{r=1}^{N} x_{r} \, e^{-A_{r}(t-\tau)} \right] \cdot \left[ H(\tau-\tau) - H(\tau-\tau) \right] d\tau$$

$$= X_{0} \left[ H(\tau-t) - H(t-\tau) \right] + \sum_{r=1}^{N} x_{r} \int_{0}^{t} \left[ H(\tau-\tau) - H(\tau-\tau) \right] e^{-A_{r}(t-\tau)} d\tau$$
(AII.14)

But,

$$\int_{0}^{t} H(T-z)e^{-\Lambda_{r}(t-z)} dz$$
=  $H(T-t)\int_{0}^{t} e^{-\Lambda_{r}(t-z)} dz + H(t-T)\int_{0}^{T} e^{-\Lambda_{r}(t-z)} dz$ 
=  $\frac{H(T-t)\{1-e^{-\Lambda_{r}t}\} + H(t-T)\{e^{-\Lambda_{r}(t-T)}-e^{-\Lambda_{r}t}\}}{\Lambda_{r}}$ 
=  $\frac{H(T-t) + H(t-T)e^{-\Lambda_{r}(t-T)} - e^{-\Lambda_{r}t}}{\Lambda_{r}}$ 
(AII.15)

and,

$$\int_{0}^{t} H(z-T) e^{-\Lambda_{r}(t-z)} dz = H(t-T) \int_{T}^{t} e^{-\Lambda_{r}(t-z)} dz$$

$$= \frac{H(t-T) \left\{ 1 - e^{-\Lambda_{r}(t-T)} \right\}}{\Lambda_{r}}$$
(AII.16)

Therefore, from equations (AII.15) and (AII.16), it is seen that:

$$\int_{0}^{t} \left[ H(T-z) - H(z-T) \right] e^{-\lambda_{r}(t-z)} dz$$

$$= \frac{1}{\lambda_{r}} \left[ H(T-t) - H(t-T) + 2H(t-T) e^{-\lambda_{r}(t-T)} - e^{-\lambda_{r}t} \right] \qquad (AII.17)$$

Using equations (AII.14) and (AII.17) yields:

$$J_{5}(T) = \delta_{0} \left[ H(T-t) - H(t-T) \right]$$

$$+ \sum_{r=1}^{N} \frac{\delta_{r}}{\lambda_{r}} \left[ H(T-t) - H(t-T) - e^{-\lambda_{r}t} + 2H(t-T)e^{-\lambda_{r}(t-T)} \right]$$
(AII.18)

In a similar way,

$$J_{6}(\tau) = \delta'_{0} \left[ H(\tau-t) - H(t-\tau) \right]$$

$$+ \sum_{r=1}^{N'} \frac{\delta'_{r}}{\lambda'_{r}} \left[ H(\tau-t) - H(t-\tau) - e^{-\lambda'_{r}t} + 2H(t-\tau)e^{-\lambda'_{r}(t-\tau)} \right] \quad (AII.19)$$

Now, recalling from relation (6.6) that:

$$[H(T-t)-H(t-T)] = SIGN(A)$$

$$J_{5}(\tau) = \delta_{0} \operatorname{SIGN}(\alpha) + \sum_{r=1}^{N} \frac{\delta_{r}}{\lambda_{r}} \left[ \operatorname{SIGN}(\alpha) - e^{-\lambda_{r}t} + 2 \operatorname{H}(t-\tau) \cdot e^{-\lambda_{r}(t-\tau)} \right]$$

$$\cdot e^{-\lambda_{r}(t-\tau)}$$

$$J_{6}(\tau) = \delta_{0}' \operatorname{SIGN}(\alpha) + \sum_{r=1}^{N'} \frac{\delta_{r}'}{\lambda_{r}'} \left[ \operatorname{SIGN}(\alpha) - e^{-\lambda_{r}'t} + 2 \operatorname{H}(t-\tau) \cdot e^{-\lambda_{r}'(t-\tau)} \right]$$

$$\cdot e^{-\lambda_{r}'(t-\tau)}$$

$$\cdot e^{-\lambda_{r}'(t-\tau)}$$

It is to be noted that when  ${\sf T}$  is to be replaced by  ${\sf t_o}$  , the parameter  ${\sf d}$  must be replaced by  ${\sf \gamma}$  .

## AII.4 Integrals $J_5(T)$ and $J_6(T)$ for the Case T<0

Using relation (AII.10), integrals  ${\bf J_5}$  and  ${\bf J_6}$  become:

$$J_{5}(T) = -\int_{0}^{t} \theta_{1}(t-c) dc$$

$$= -\delta_{0} - \sum_{r=1}^{N} \frac{\delta_{r}}{\lambda_{r}} (1-e^{-\lambda_{r}t})$$

$$J_{6}(T) = -\int_{0}^{t} \theta_{2}(t-c) dc$$

$$= -\delta_{0}' - \sum_{r=1}^{N'} \frac{\delta_{r}'}{\lambda_{r}'} (1-e^{-\lambda_{r}'t})$$
(AII.21)

It should be noticed that in this case, the integrals  ${\it J}_{\it 5}$  and  ${\it J}_{\it 6}$  become independent of their argument.

#### APPENDIX III

# AIII. $\Theta_1$ (t) AND $\Theta_2$ (t) FOR A STANDARD LINEAR SOLID

The differential equation for the stress and strain of a standard linear solid is given by (see Figure 32(a)):

$$\begin{bmatrix}
\frac{d}{dt} + \frac{G_1 + G_2}{\eta'}
\end{bmatrix} \delta'(t) = \begin{bmatrix}
G_1 \frac{d}{dt} + \frac{G_1 G_2}{\eta'}
\end{bmatrix} \epsilon(t)$$

$$\begin{bmatrix}
\frac{d}{dt} + \frac{K_1 + K_2}{\eta''}
\end{bmatrix} \delta'(t) = \begin{bmatrix}
K_1 \frac{d}{dt} + \frac{K_1 K_2}{\eta''}
\end{bmatrix} \epsilon(t)$$
(AIII.1)

The time-dependent moduli (in shear and dilatation) of such a material can be written as:

$$G(P) = \frac{G_1(n'P + G_2)}{n'P + G_1 + G_2}$$

$$K(P) = \frac{K_1(n'P + K_2)}{n'P + K_1 + K_2}$$
(AIII.2)

where b is the Laplace transform parameter. t

The material functions  $\theta_1$  and  $\theta_2$  (as given by equation (4.23)), can be expressed in terms of the transform parameter as follows:

$$\theta_1(b) = \frac{1}{2G(b)} = \frac{\gamma'b + G_1 + G_2}{2G_1(\gamma'b + G_2)}$$
(AIII.3)

$$\theta_{2}(p) = \frac{3}{6 K(p) + 2G(p)}$$

$$= \frac{3(\eta''p + K_{1} + K_{2})(\eta'p + G_{1} + G_{2})}{6 K_{1}(\eta''p + K_{2})(\eta'p + G_{2} + G_{2}) + 2G_{1}(\eta'p + G_{2})(\eta''p + K_{1} + K_{2})}$$
(AIII.4)

By using partial fractions, these can be rewritten as:

$$\Theta_{1}(P) = \delta_{0} + \frac{\delta_{1}}{P + \lambda_{1}}$$

$$\Theta_{2}(P) = \delta_{0}' + \frac{\delta_{1}'}{P + \lambda_{1}'} + \frac{\delta_{2}'}{P + \lambda_{2}'}$$
(AIII.5)

in which

$$\delta_0 = \frac{1}{2G_1}$$
;  $\delta_1 = \frac{1}{2D'}$ ;  $\lambda_1 = \frac{G_2}{D'}$  (AIII.6)

and

$$\delta'_{0} = \frac{\alpha}{d}$$

$$\delta'_{1} = \frac{(bd - ae) \lambda'_{1} - cd + af}{(\lambda'_{1} - \lambda'_{2}) d^{2}}$$

$$\delta'_{2} = \frac{(bd - ae) \lambda'_{2} - cd + af}{(\lambda'_{2} - \lambda'_{1}) d^{2}}$$

$$\lambda'_{1} = \frac{e - \sqrt{e^{2} - 4fd}}{2d}$$

$$\lambda'_{2} = \frac{e + \sqrt{e^{2} - 4fd}}{2d}$$
(AIII.7)

where

$$\begin{aligned}
\alpha &= 3 \, \eta' \eta'' \\
b &= 3 \left[ \eta'(\kappa_1 + \kappa_2) + \eta''(G_1 + G_2) \right] \\
c &= 3(\kappa_1 + \kappa_2)(G_1 + G_2) \\
d &= (6 \kappa_1 + 2 G_1) \, \eta' \, \eta'' \\
e &= 6 \kappa_1 \left[ \eta''(G_1 + G_2) + \eta' \kappa_2 \right] + 2 \, G_1 \left[ \eta'(\kappa_1 + \kappa_2) + \eta'' G_2 \right] \\
f &= 6 \kappa_1 \kappa_2 (G_1 + G_2) + 2 \, G_1 G_2 (\kappa_1 + \kappa_2)
\end{aligned}$$
(AIII.8)

Inverting equation (AIII.5), the time-dependent material function will be of the form:

$$\theta_{1}(t) = \zeta_{0} \delta(t) + \zeta_{1} e^{-\lambda_{1}t}$$

$$\theta_{2}(t) = \zeta_{0}' \delta(t) + \zeta_{1}' e^{-\lambda_{1}'t} + \zeta_{2}' e^{-\lambda_{2}'t}$$
(AIII.9)

For a constant load, the equation for the displacement of a standard linear solid can be expressed as:

$$\epsilon(t) = 6_0 \left[ \frac{1}{G_1} + \frac{1}{G_2} (1 - e^{-G_2 t/2'}) \right]$$

Figure 32(b) shows the variation of the displacement with time. For convenience, choosing the utlimate displacements to be twice the instantaneous displacement in shear and

dilatations, respectively, yields:

$$G_1 = G_2 = G_0$$
 $K_1 = K_2 = K_0$ 
(AIII.10)

Similarly, assuming only one relaxation time for the material in shear and dilatation, yields:

$$\frac{\eta'}{G_2} = \frac{\eta''}{K_2} = \zeta \tag{AIII.11}$$

Since for the elastic material the Poisson's ratio  ${\it 9}$  was taken as 1/3, for which the bulk modulus is related to the shear modulus as

$$K = \frac{8}{3} G$$

it may be assumed that

$$K_o = \frac{8}{3} G_o \tag{AIII.12}$$

Thus, substituting (AIII.10-12) into (AIII.8) gives:

Substituting equation (AIII.13) into equation (AIII.6) and (AIII.7) yields:

$$\begin{aligned}
\delta_{0} &= \frac{4}{3\kappa_{0}} ; & \delta_{1}' &= 0 \\
\delta_{1} &= \frac{4}{3\kappa_{0}C} ; & \delta_{2}' &= \frac{4}{9\kappa_{0}C} \\
\lambda_{1} &= \frac{1}{C} ; & \lambda_{1}' &= \frac{1}{C} \\
\delta_{0}' &= \frac{4}{9\kappa_{0}} ; & \lambda_{2}' &= \frac{2}{C}
\end{aligned}$$
(AIII.14)

Taking the above material constants into consideration yields the two material functions  $\theta_1$  ,  $\theta_2$  as follows:

$$\theta_{1}(t) = \frac{4}{3\kappa_{0}\zeta} \left[ \zeta \delta(t) + e^{-t/\zeta} \right]$$

$$\theta_{2}(t) = \frac{4}{9\kappa_{0}\zeta} \left[ \zeta \delta(t) + e^{-2t/\zeta} \right]$$
(AIII.15)

It is to be noted that equation (AIII.15) represents specific functions that are based on the above assumptions. These assumptions were necessary for an illustration of the analytical method presented in this thesis. For an actual material, accurate values of these constants will have to be found experimentally.

#### APPENDIX IV

#### AIV. ROOTS OF SINH(Z)+Z=0

It is realised that the entire analysis of the present problem is dependent upon the roots of the expression sinhz+z=o. For a meaningful convergence of the expressions of the various influence functions, it is essential that these roots be determined in their proper order. It is therefore considered to be necessary to discuss the location and the evaluation of the roots of this equation.

Substituting z=x+iy, the equation sinhz+z=0 becomes:

$$sinh(x+iy) + x+iy = 0$$

which, on expansion, becomes:

Separating real and imaginary parts

Let

$$F(x,y) = sinhx.cosy + x$$

$$G(x,y) = coshx.siny + y$$

(AIV.1)

Then, the roots of  $\sinh z + z = 0$  are the points where F(x,y) and G(x,y) simultaneously become equal to zero. Let  $(\chi_n, y_n)$  be one of the roots. It can be easily verified that the points  $(\pm \chi_n, \pm y_n)$  are also the roots of this equation. Therefore, the roots in the first quadrant only will be discussed here.

Let 
$$(x_0, y_0)$$
 be a point close to  $(x_n, y_n)$  such that 
$$x_n = x_0 + \delta x$$
 
$$y_n = y_0 + \delta y$$
 (AIV.2)

Then, using a Taylor series expansion at the root,

$$F(x_n, y_n) = F^{\circ} + \delta_x F_x^{\circ} + \delta_y F_y^{\circ}$$

$$G(x_n, y_n) = G^{\circ} + \delta_x G_x^{\circ} + \delta_y G_y^{\circ}$$

where,

$$F(x_n, y_n) = G(x_n, y_n) = 0$$

Therefore,

$$\delta x \cdot F_{x}^{2} + \delta y \cdot F_{y}^{3} = -F^{3}$$

$$\delta x \cdot G_{x}^{2} + \delta y \cdot G_{y}^{3} = -G^{3}$$

Solving for  $\delta_{\mathbf{x}}$  and  $\delta_{\mathbf{y}}$  gives:

$$\delta x = \frac{G^{\circ} F_{y}^{\circ} - F^{\circ} G_{y}^{\circ}}{F_{x}^{\circ} \cdot G_{y}^{\circ} - G_{x}^{\circ} \cdot F_{y}^{\circ}}$$

$$\delta y = \frac{F^{\circ} G_{x}^{\circ} - G^{\circ} F_{x}^{\circ}}{F_{x}^{\circ} \cdot G_{y}^{\circ} - G_{x}^{\circ} \cdot F_{y}^{\circ}}$$
(AIV.3)

Thus, if  $(x_0, y_0)$  be a point close to  $(x_n, y_n)$  then  $(x_0 + \delta x, y_0 + \delta y)$  will be a point closer to  $(x_n, y_n)$  and will therefore be a better approximation. Proceeding in this manner, the actual root  $(x_n, y_n)$  can be determined.

Now, it is necessary to make a guess for  $(x_n, y_n)$ . It is noticed that F(x,y) will be zero only when

$$(2n+\frac{1}{2})\Pi \leq Y \leq (2n+\frac{3}{2})\Pi \qquad n=0,1,2,....$$

Similarly, G(x,y) will be zero only when

$$(2n+1)\Pi \leq Y \leq (2n+2)\Pi \qquad n=0,1,2,....$$

Thus, F(x,y) and G(x,y) will be simultaneously zero only if

$$(2n+1)\pi \leq 9 \leq (2n+\frac{3}{2})\pi$$
  $n=0,1,2,.....(AIV.4)$ 

This gives a range of the locations of the roots. However, it is also required to find out if there is more than one root in each cycle.

Let  $(x_n, y_n)$  be a root and let  $(x_0, y_0)$  be a neighbouring point related by equation (AIV.2). Assume that  $(x_0, y_0)$  is also a root.

From the previous argument,  $\delta x$  and  $\delta y$  will be given by equation (AIV.3). Since  $(x_0, y_0)$  is also a root,

$$F^{\circ} = G^{\circ} = 0$$

This gives:

$$\delta x = \delta y = 0$$

This means that  $(x_n, y_n)$  and  $(x_0, y_0)$  are the same points and therefore there is only one root in each cycle.

The locations of the first two roots were guessed by using equation (AIV.4) and putting x=0 and then the actual roots were obtained by extrapolation. y was increased by  $2\pi$  every time and x was given the increment equal to the difference in x between the last two roots.

## REFERENCES

[1]	Hertz, H.	J. of Math., Vol.92, 1881
[2]	Carter, F.W.	ON THE ACTION OF A LOCOMOTIVE DRIVING WHEEL Proc. of the Royal Society Ser. A., Vol.112, p.151, 1926
[3]	Poritsky, H.	STRESSES AND DEFLECTIONS OF CYLINDRICAL BODIES IN CONTACT WITH APPLICATION TO CONTACT OF GEARS AND LOCOMOTIVE WHEELS J. of App. Mech., p.191-201, June 1950
[4]	Bufler, H.	ZUR THEORIE DER ROLLENDEN REIBUNG Ingenieur-Archiv., Vol.29, p.137- 152, 1959
[5]	Johnson, K.L.	TANGENTIAL TRACTIONS AND MICRO- SLIP IN ROLLING CONTACT Rolling Contact Phenomena (Ed. Bidwell, J.B.)
[6]	Johnson, K.L. Bentall, R.H.	SLIP IN THE ROLLING CONTACT OF TWO DISSIMILAR ROLLERS Int. J. of Mech. Sci., Vol.9, p.389-404, 1967
[7]	Hunter, S.C.	THE ROLLING CONTACT OF A RIGID CYLINDER WITH A VISCOELASTIC HALF SPACE J. of App. Mech., p.611-617, 1961
[8]	Morland, L.W.	A PLANE PROBLEM OF ROLLING CON- TACT IN LINEAR VISCOELASTICITY THEORY J. of App. Mech., p.345-352, 1962
[9]	Morland, L.W.	EXACT SOLUTIONS FOR ROLLING CON- TACT BETWEEN VISCOELASTIC CYLINDERS Quart. J. of Mech. & App. Math., Vol.20, p.73-106, 1967

[10]	Morland, L.W.	ROLLING CONTACT BETWEEN DIS- SIMILAR VISCOELASTIC CYLINDERS Quart. of App. Math., Vol.25, p.363-376, 1968
[11]	Sneddon, I.N.	FOURIER TRANSFORMS McGraw-Hill Book Co. Inc., 1951
[12]	Wang, C.F.	ELASTIC CONTACT OF A STRIP PRESSED BETWEEN TWO CYLINDERS J. of App. Mech., Trans. of the ASME, p.279-286, 1968
[13]	Bentall, R.H. Johnson, K.L.	AN ELASTIC STRIP IN PLANE ROLL- ING CONTACT Int. J. of Mech. Sci., Vol.10, p.637-663, 1968
[14]	Bentall, R.H.	A NUMERICAL APPROACH TO PROBLEMS OF ELASTIC STRESSES IN ROLLING CONTACT Ph.D Thesis, Cambridge University 1966
[15]	Alblas, J.B. Kuipers, M.	THE CONTACT PROBLEM OF A RIGID CYLINDER ROLLING ON A THIN VISCOELASTIC LAYER Int. J. of Eng. Sci., Vol.8, p.363-380, 1970
[16]	Bland, D.R.	THE THEORY OF VISCOELASTICITY Pergamon Press, 1960
[17]	Fung, Y.C.	FOUNDATIONS OF SOLID MECHANICS Prentice-Hall, Inc., Englewood Cliffs, New Jersey, 1965
[18]	LEE, E.H.	STRESS ANALYSIS IN VISCOELASTIC BODIES Quart. of App. Math., Vol.13, p.183-190, 1955

F I G U R E S

THE ...

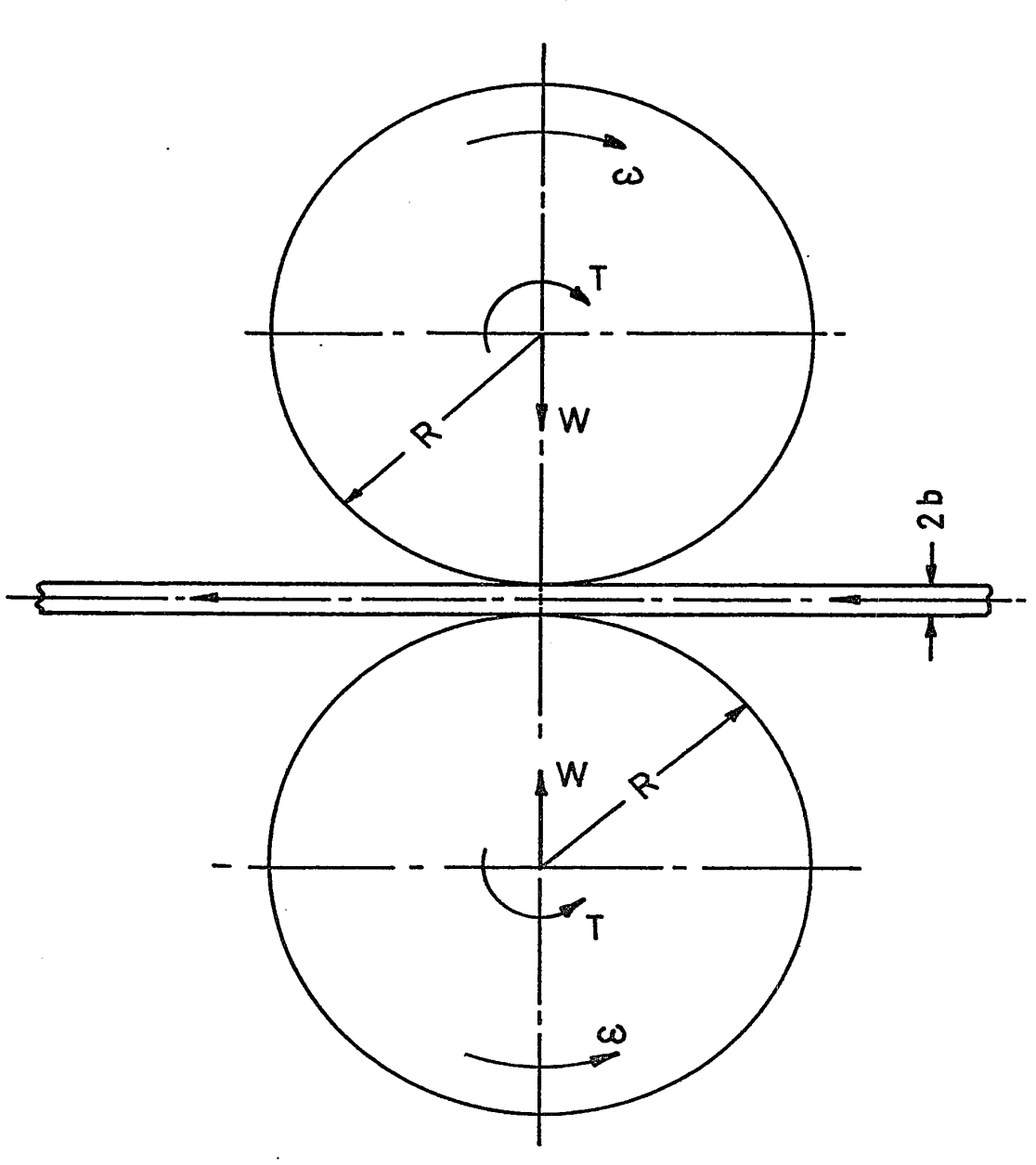


FIGURE 1

A SHEET ROLLING BETWEEN A PAIR OF RIGID CYLINDERS

FIGURE 2

NIP FORCES IN ROLLING CONTACT

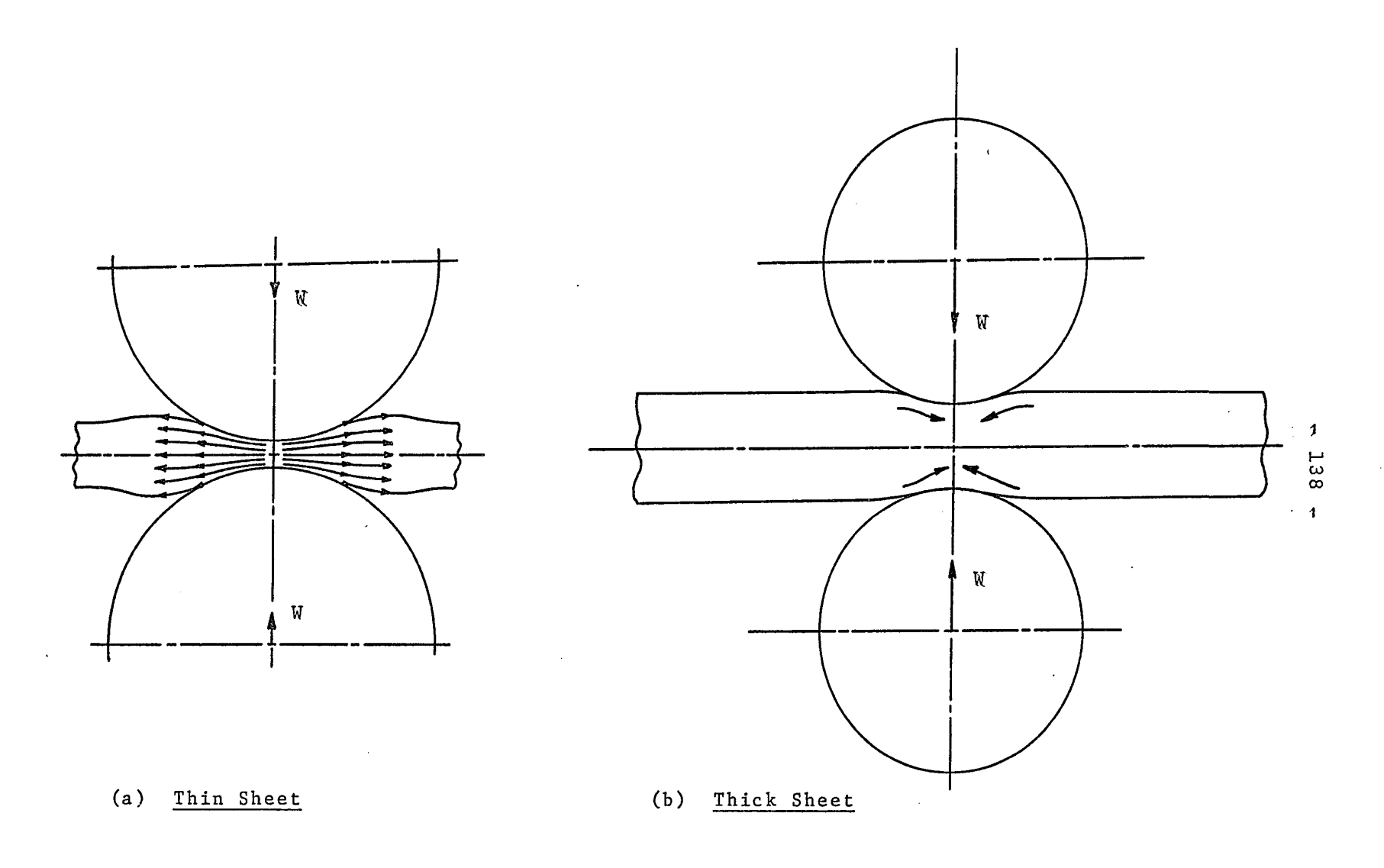


FIGURE 3

PHYSICAL BEHAVIOUR OF A SHEET BETWEEN RIGID CYLINDERS

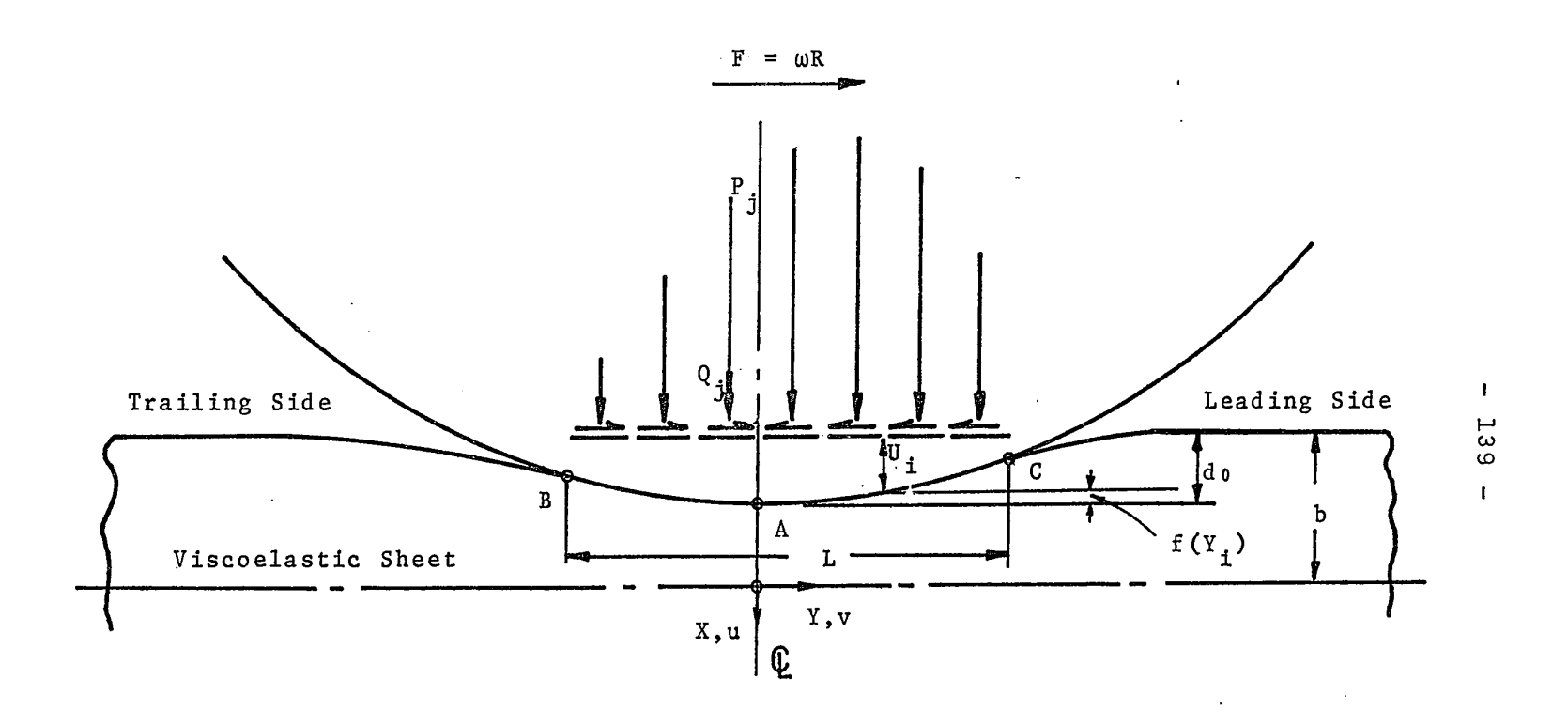
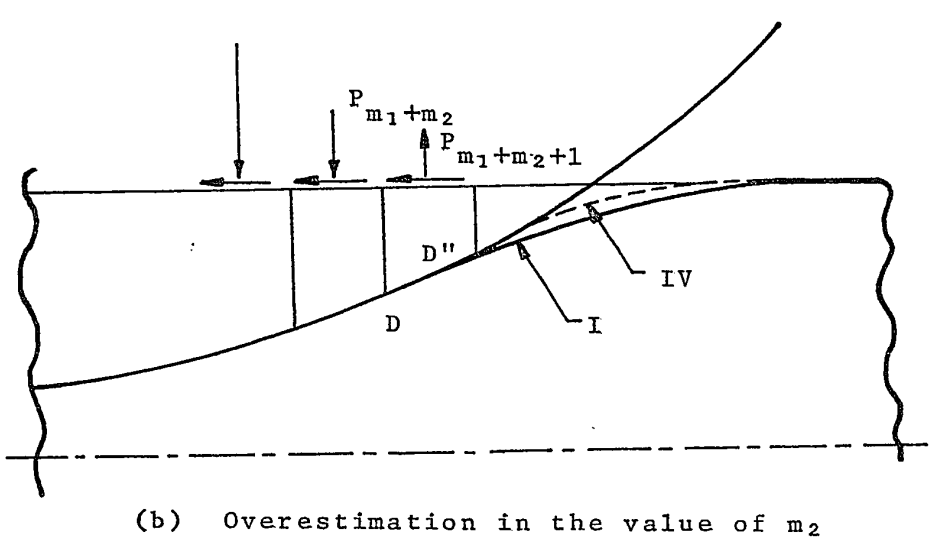


FIGURE 4
REPRESENTATION OF THE NIP FORCES

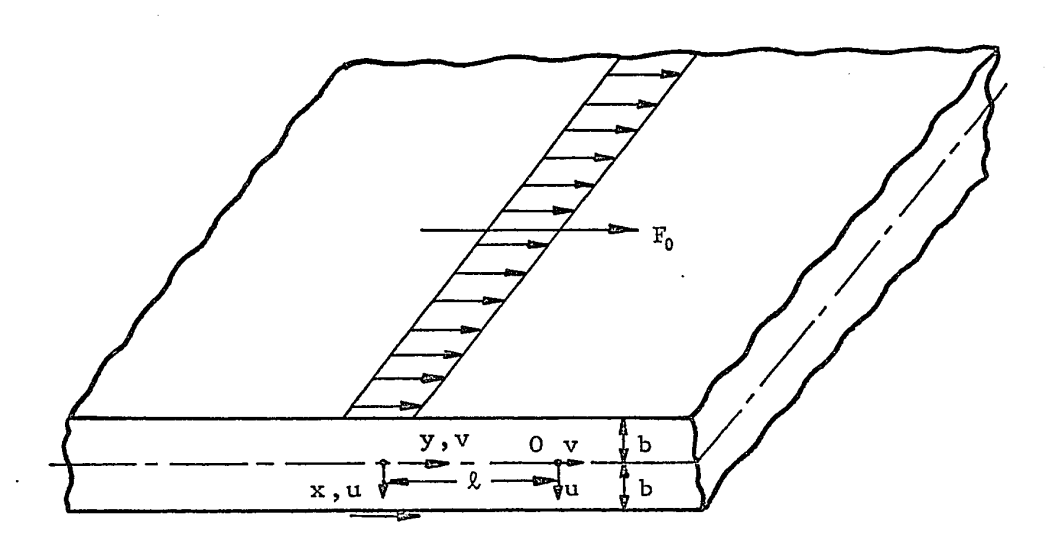
(a) Underestimation in the value of  $m_2$ 



### FIGURE 5

CONSEQUENCES OF UNDERESTIMATION OR OVERESTIMATION IN THE VALUE OF  $m_2$  ON LOAD DISTRIBUTION

(a) Normal line load moving on elastic sheet



- (b) Shear line load moving on elastic sheet
- x-y coordinate system moving with the load
- $F_0$  velocity of the load
- O pinned point

#### FIGURE 6

REPRESENTATION OF LINE LOADS (NORMAL & SHEAR)
MOVING ON ELASTIC SHEET

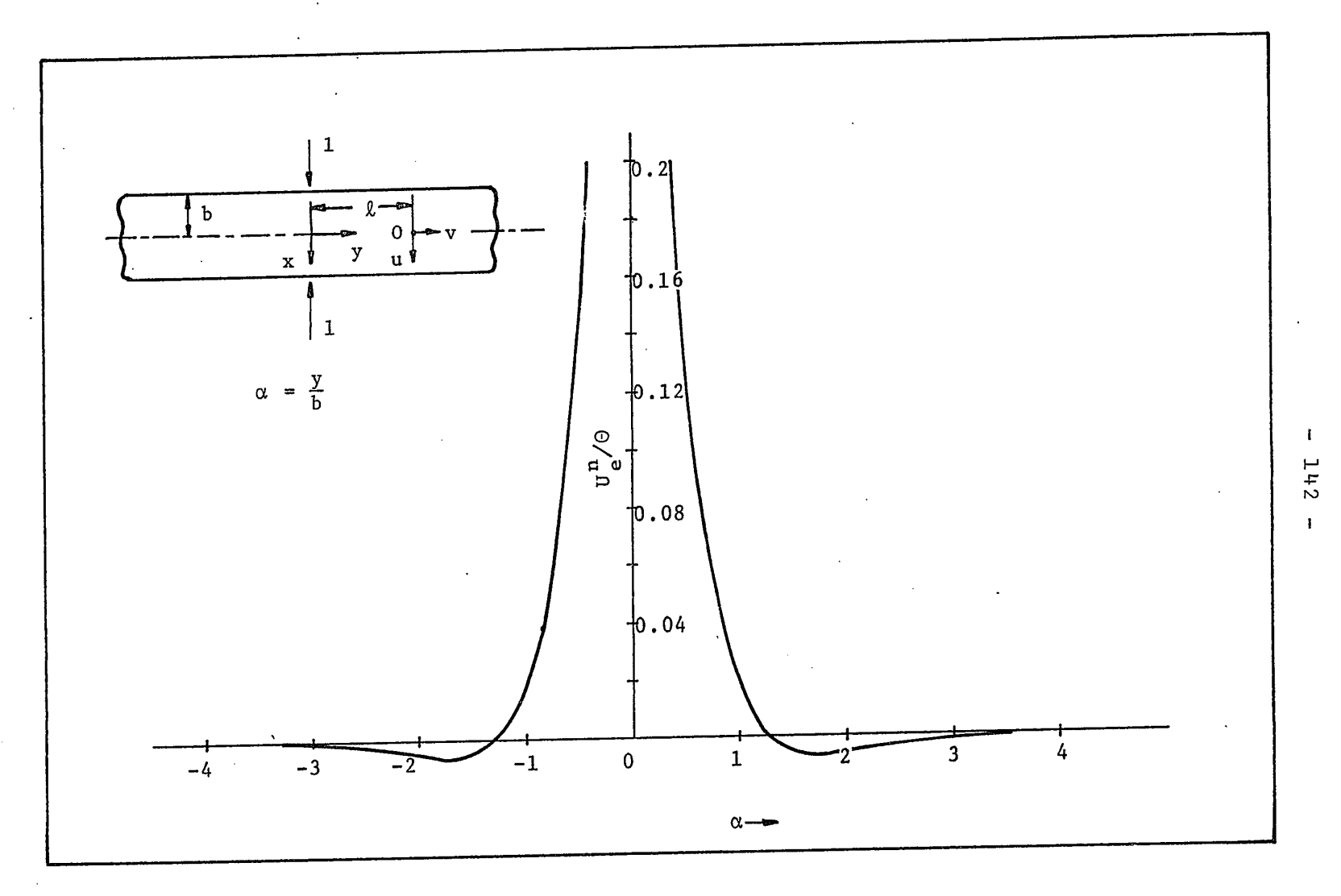
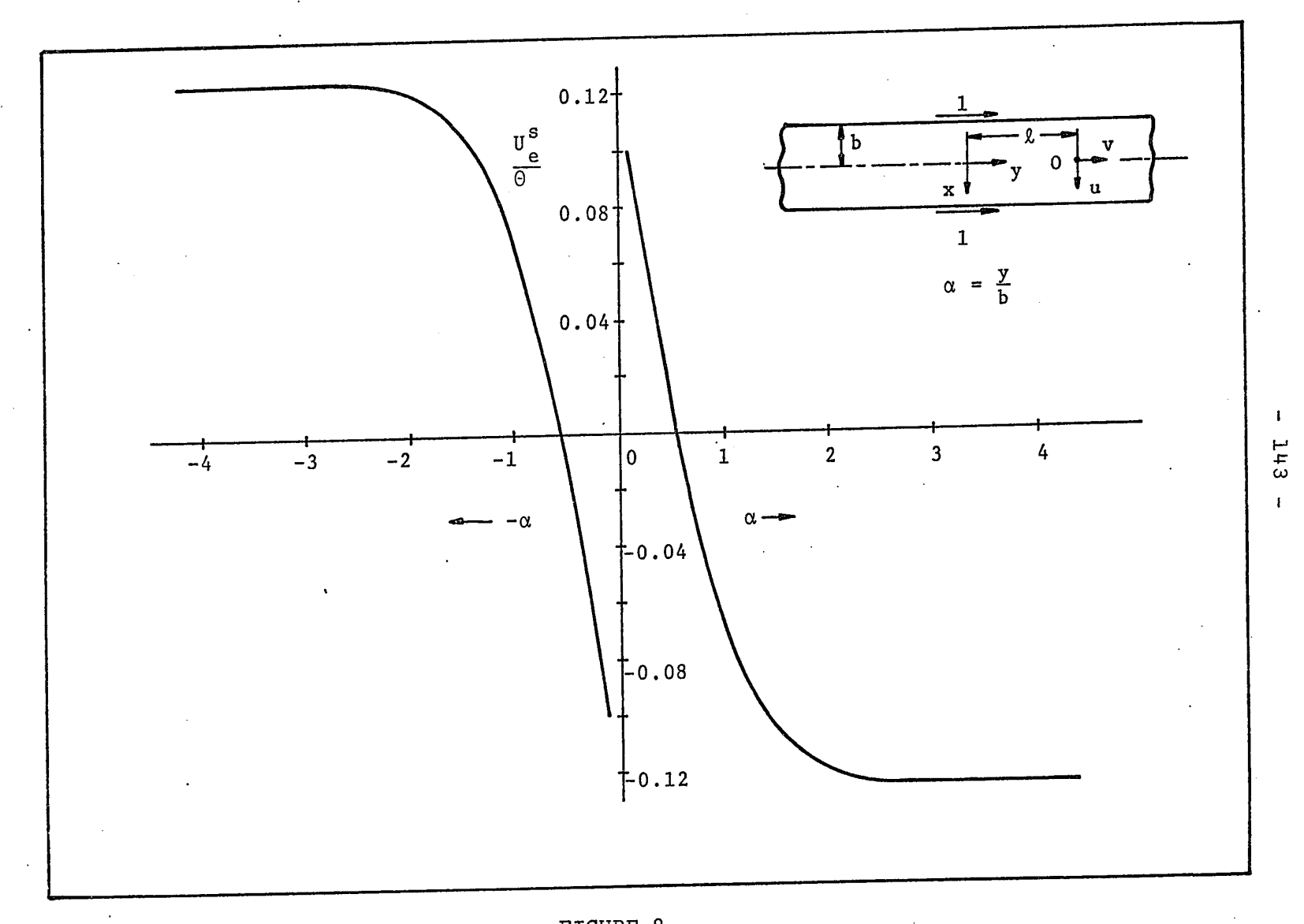
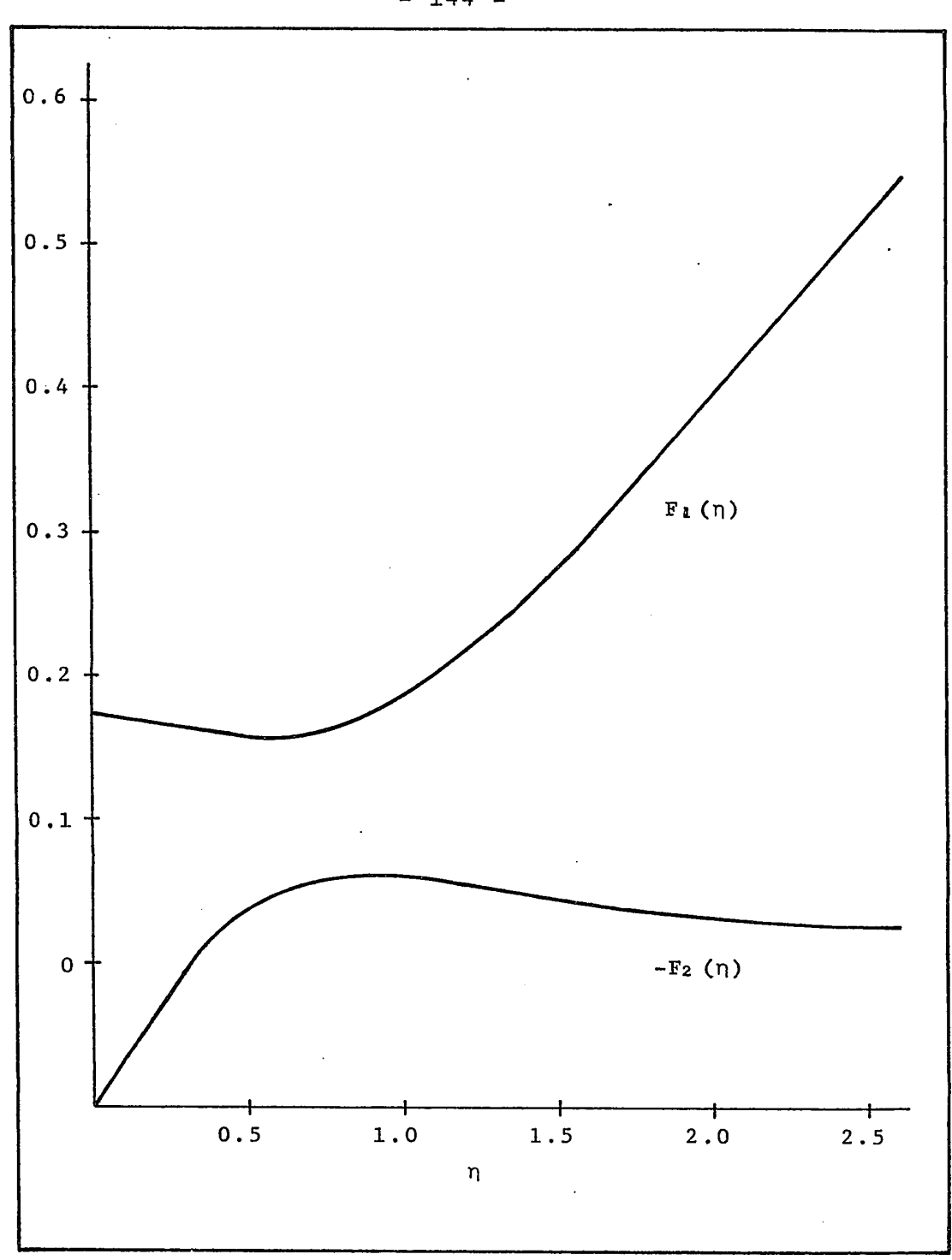


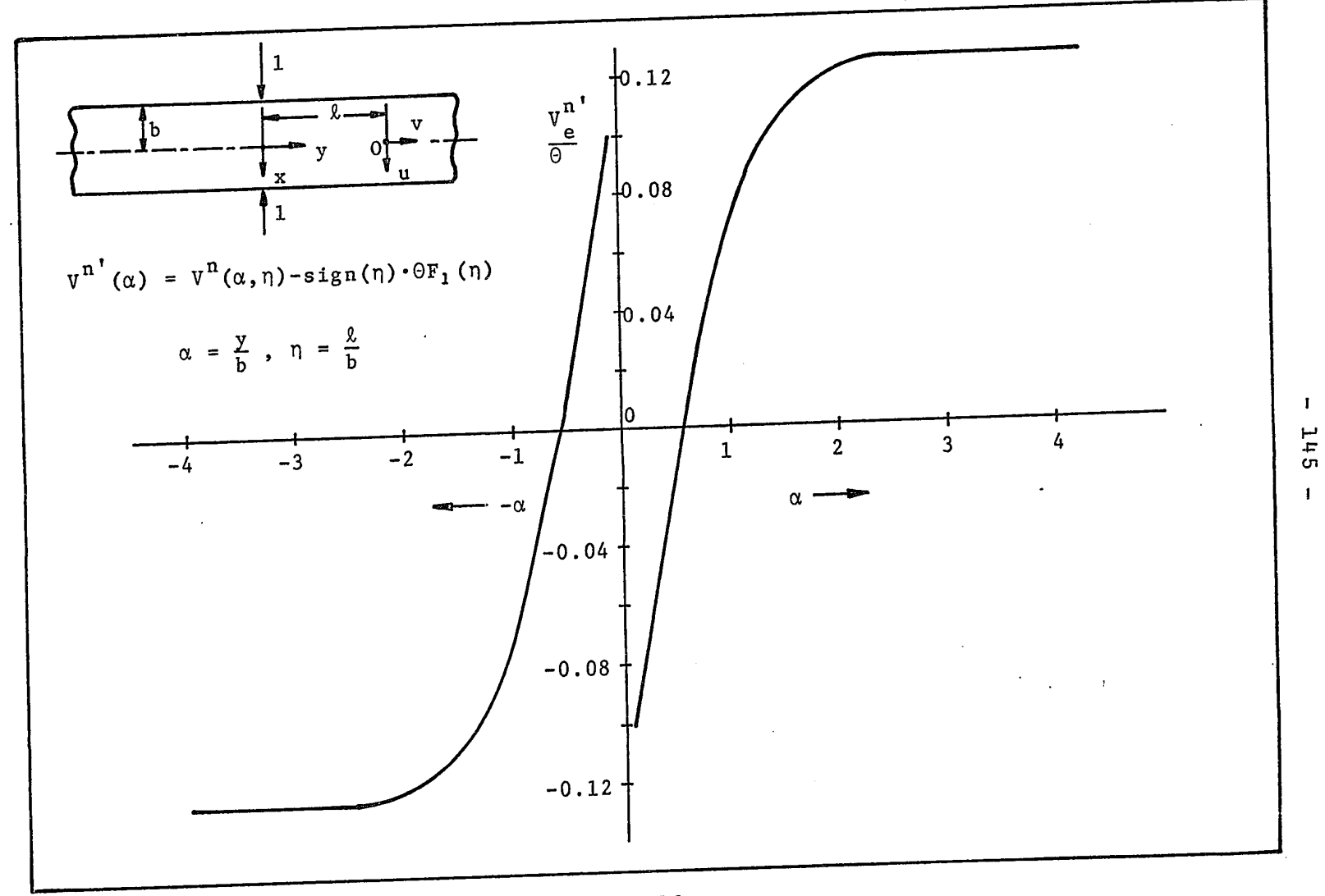
FIGURE 7

NORMAL DISPLACEMENT OF THE SURFACE (x=-b) OF AN ELASTIC SHEET DUE TO NORMAL LINE LOAD

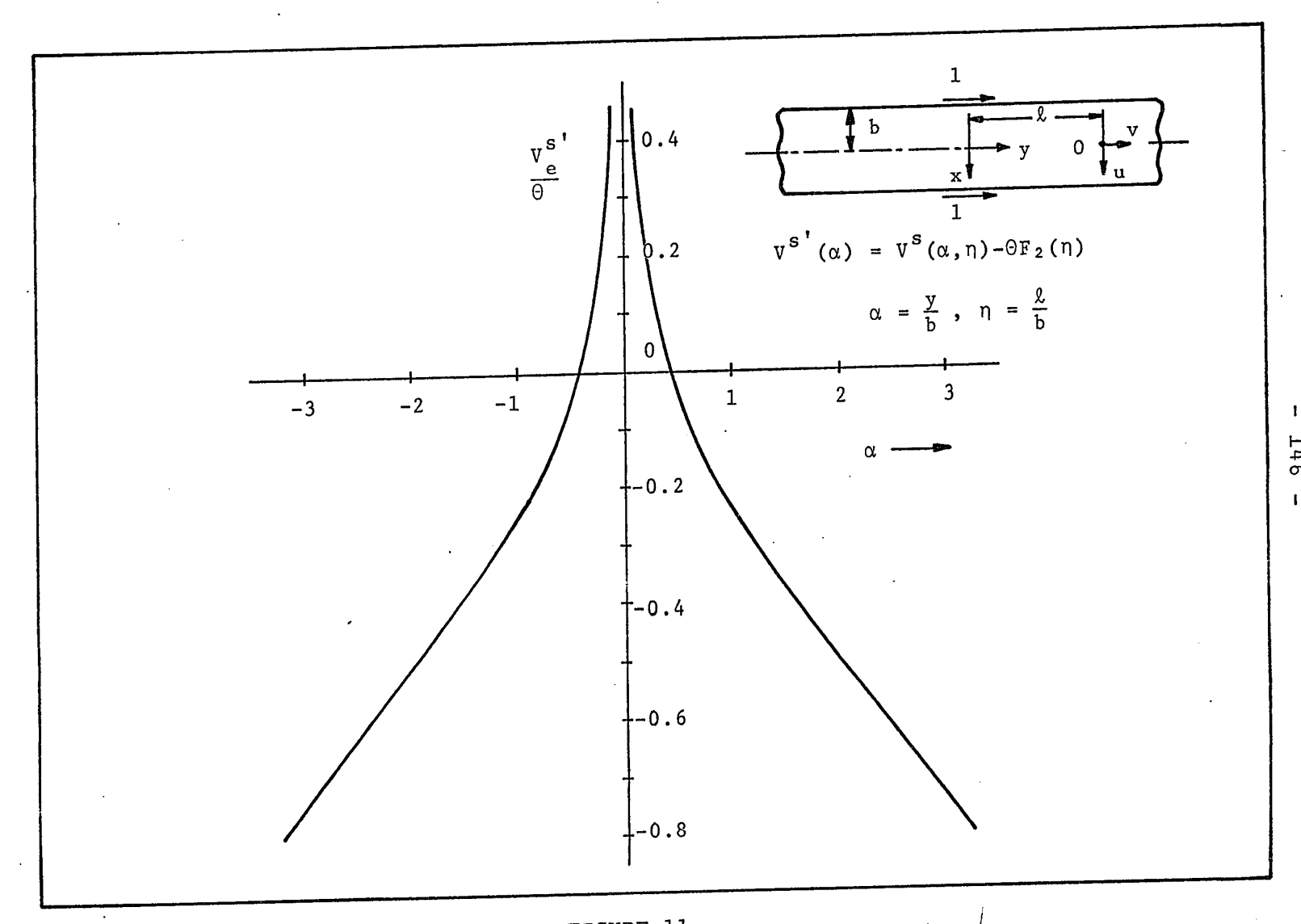


 $\frac{\text{FIGURE 8}}{\text{NORMAL DISPLACEMENT OF THE SURFACE (x=-b) OF AN ELASTIC SHEET DUE TO SHEAR LINE LOAD}}$ 





 $\frac{\text{FIGURE 10}}{\text{VARIATION OF V}^{\text{n'}}} \text{ WITH } \alpha$ 



 $\frac{\text{FIGURE 11}}{\text{VARIATION OF V}^{\text{S}'}} \text{ WITH } \alpha$ 

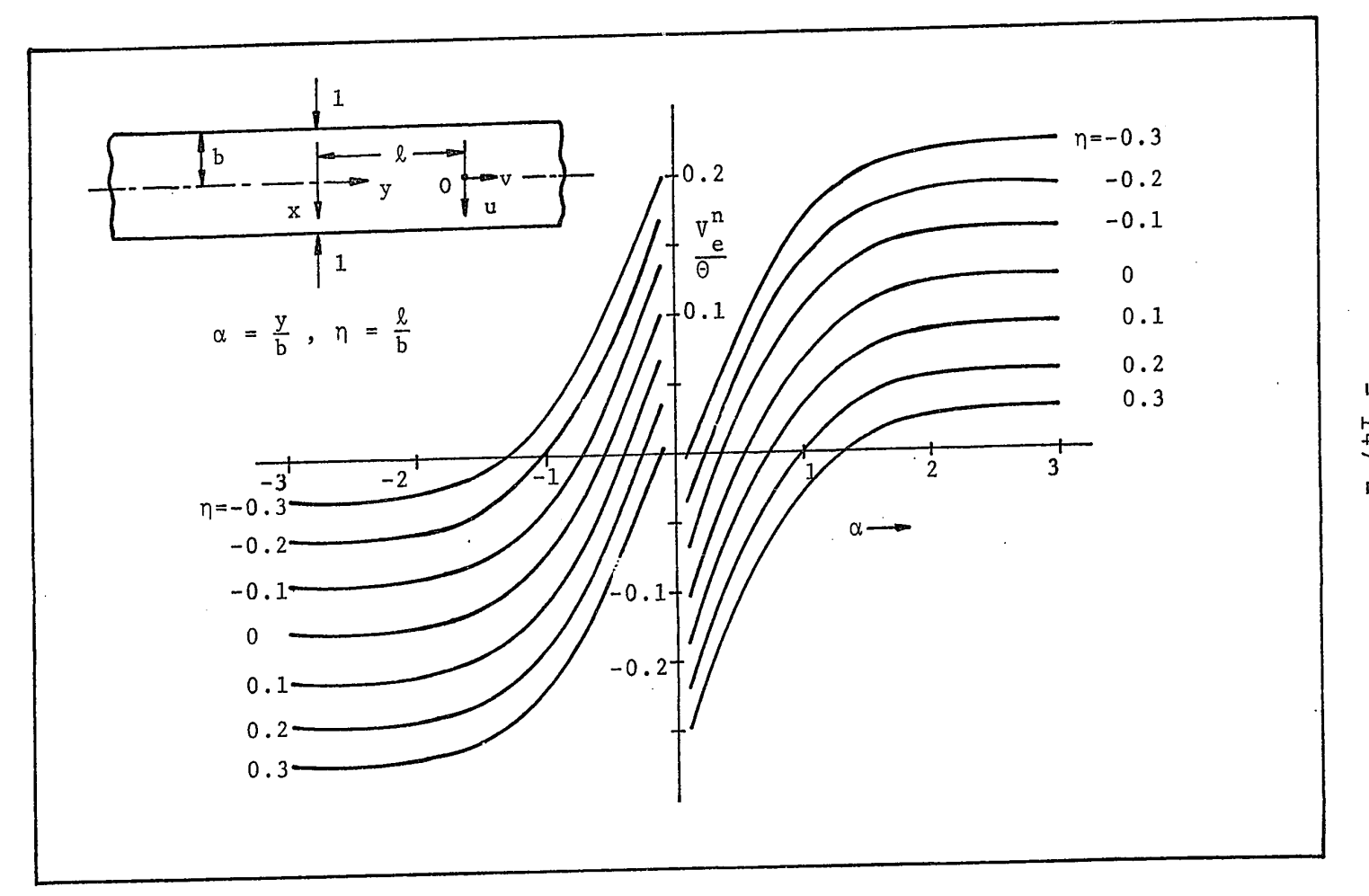


FIGURE 12

SHEAR DISPLACEMENT OF THE SURFACE (x=-b) OF AN ELASTIC SHEET DUE TO NORMAL LINE LOAD

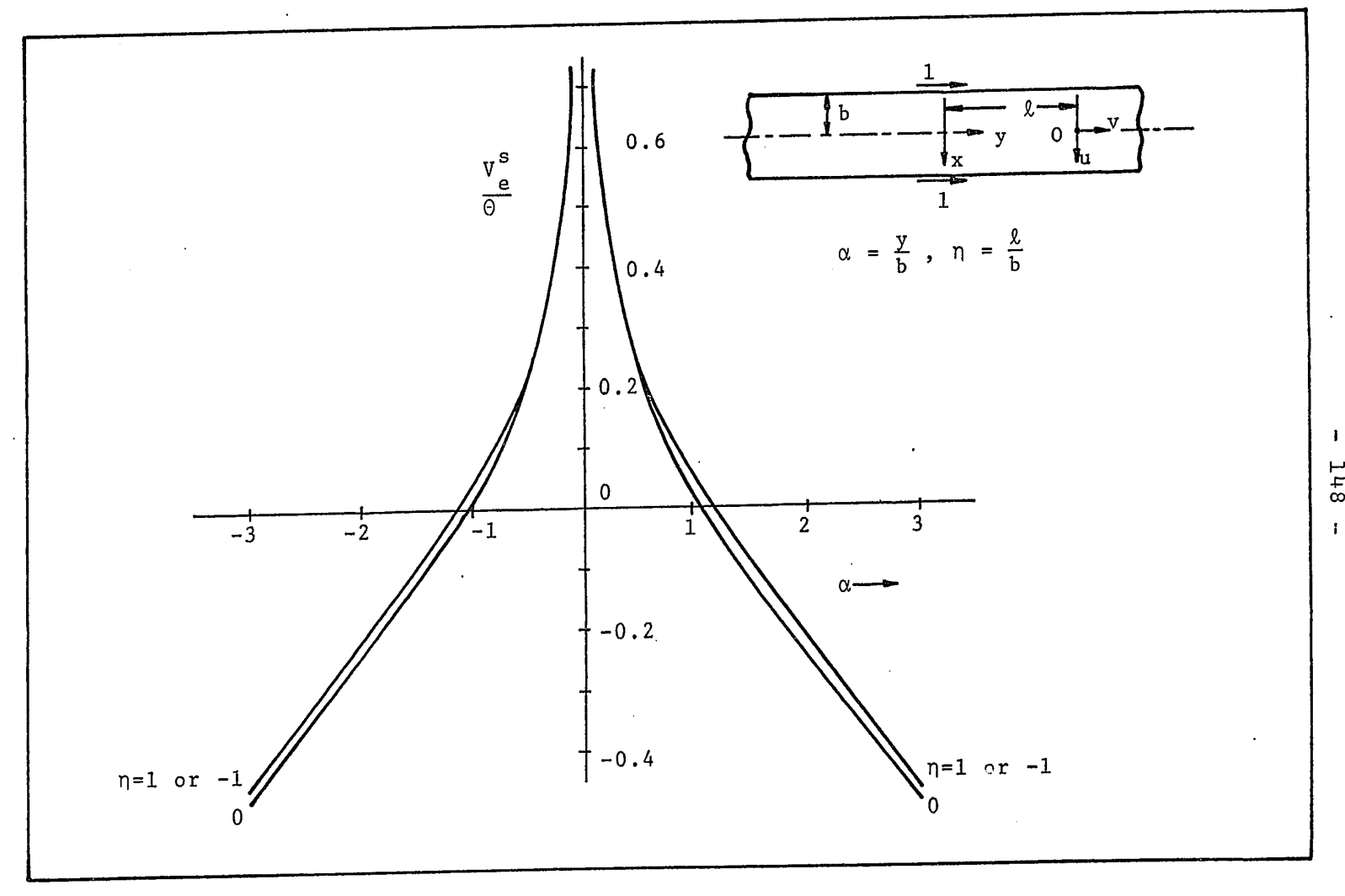


FIGURE 13

SHEAR DISPLACEMENT OF THE SURFACE (x=-b) OF AN ELASTIC SHEET DUE TO SHEAR LINE LOAD

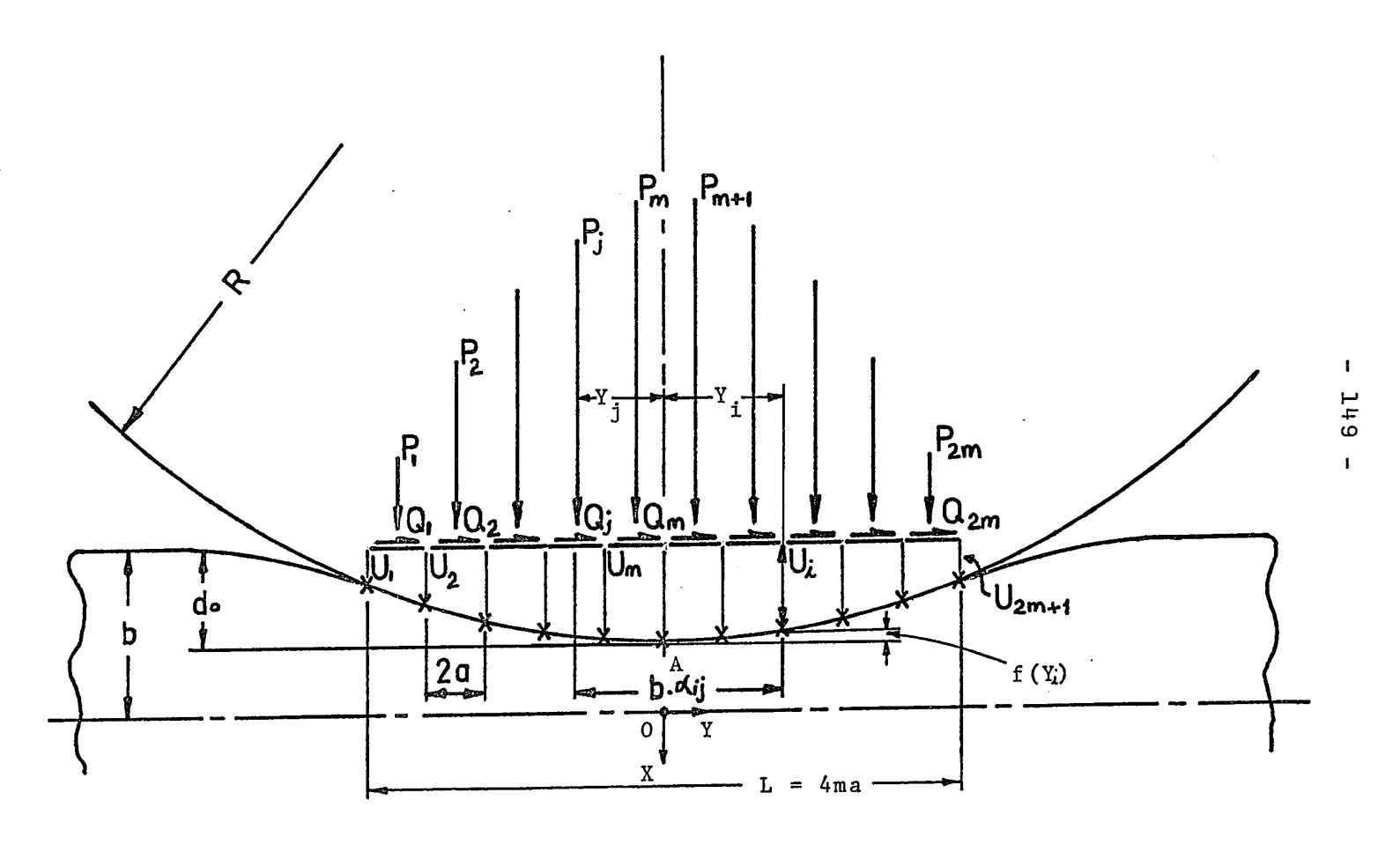


FIGURE 14

THE GEOMETRY OF THE NIP (ELASTIC SHEET)

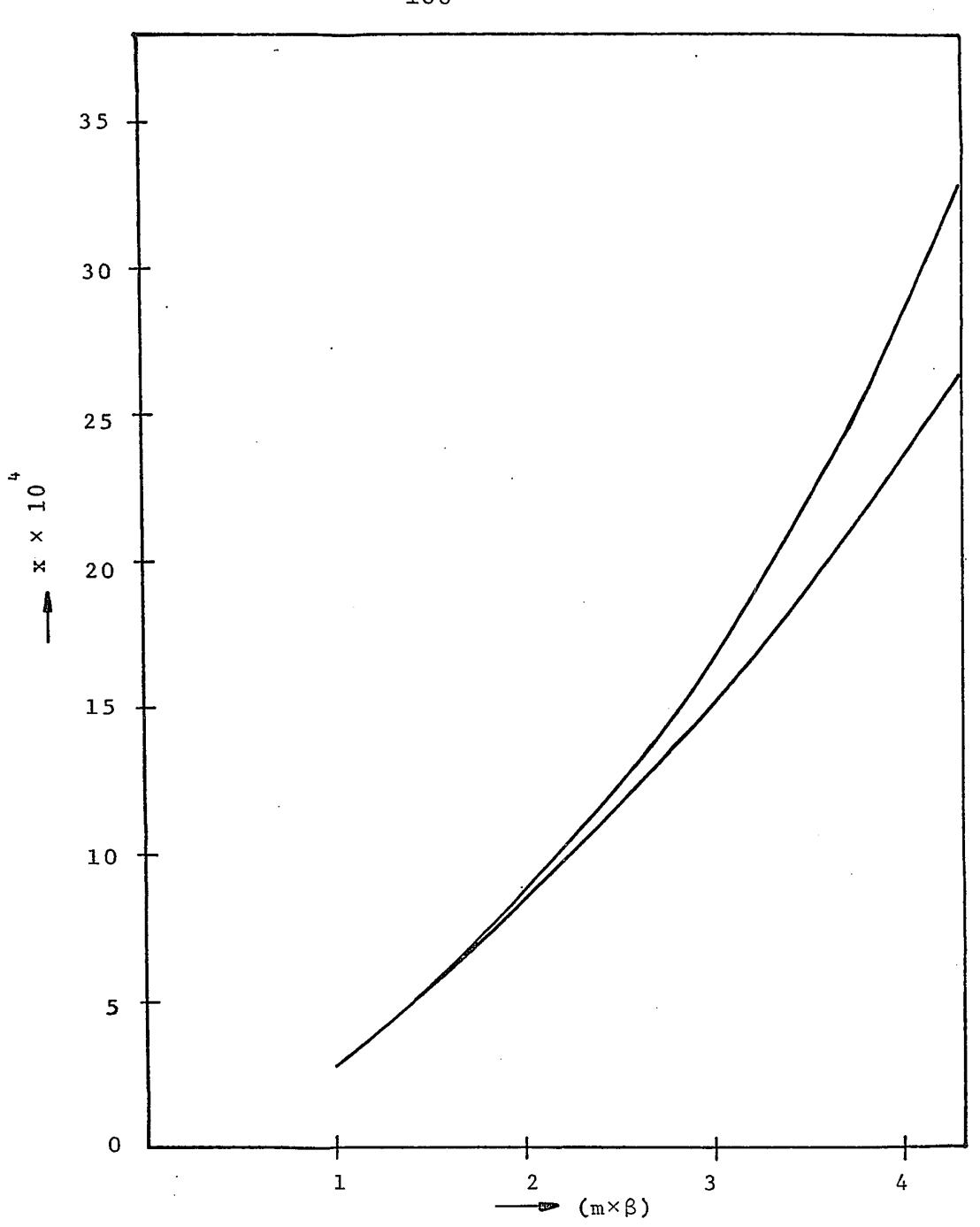


FIGURE 15

POSSIBLE RANGE OF THE CREEP RATIO SATISFYING EQUATIONS (2.2) AND (2.4) FOR NO-SLIP CONDITION (Elastic case; D-12in., B=0.005 in.)

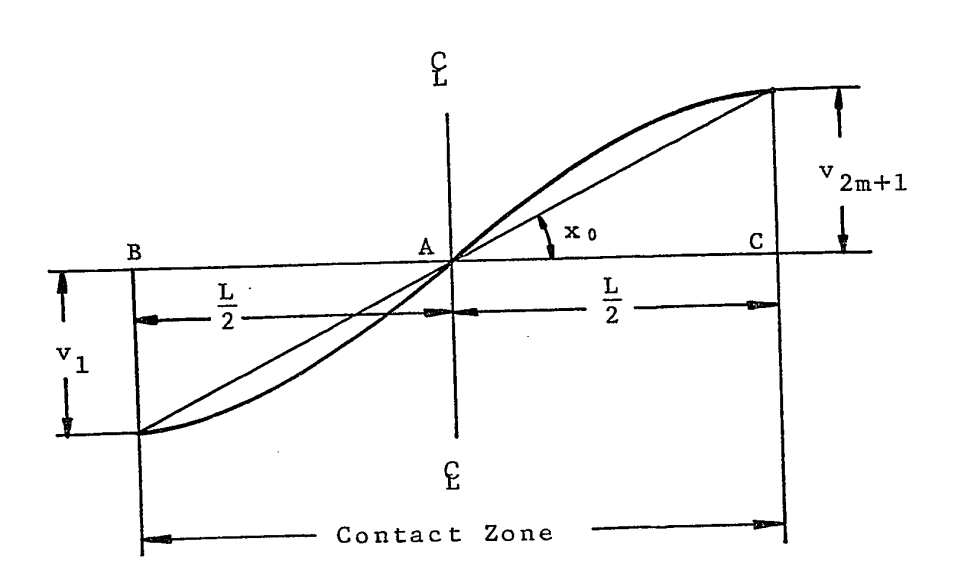


FIGURE 16

SCHEMATIC REPRESENTATION OF THE SHEAR DISPLACEMENTS OF THE SHEET SURFACE (ELASTIC) WITHIN THE CONTACT ZONE

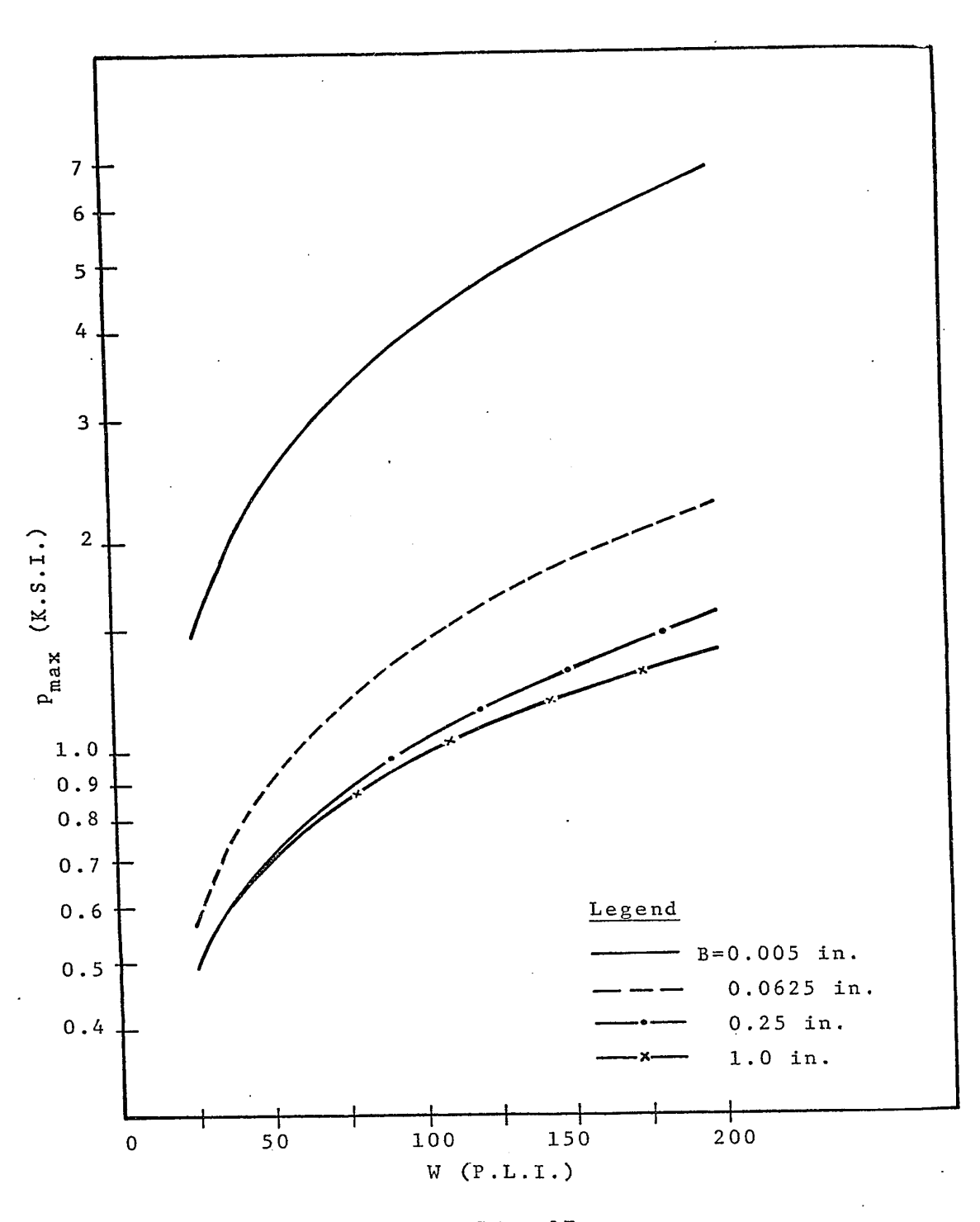
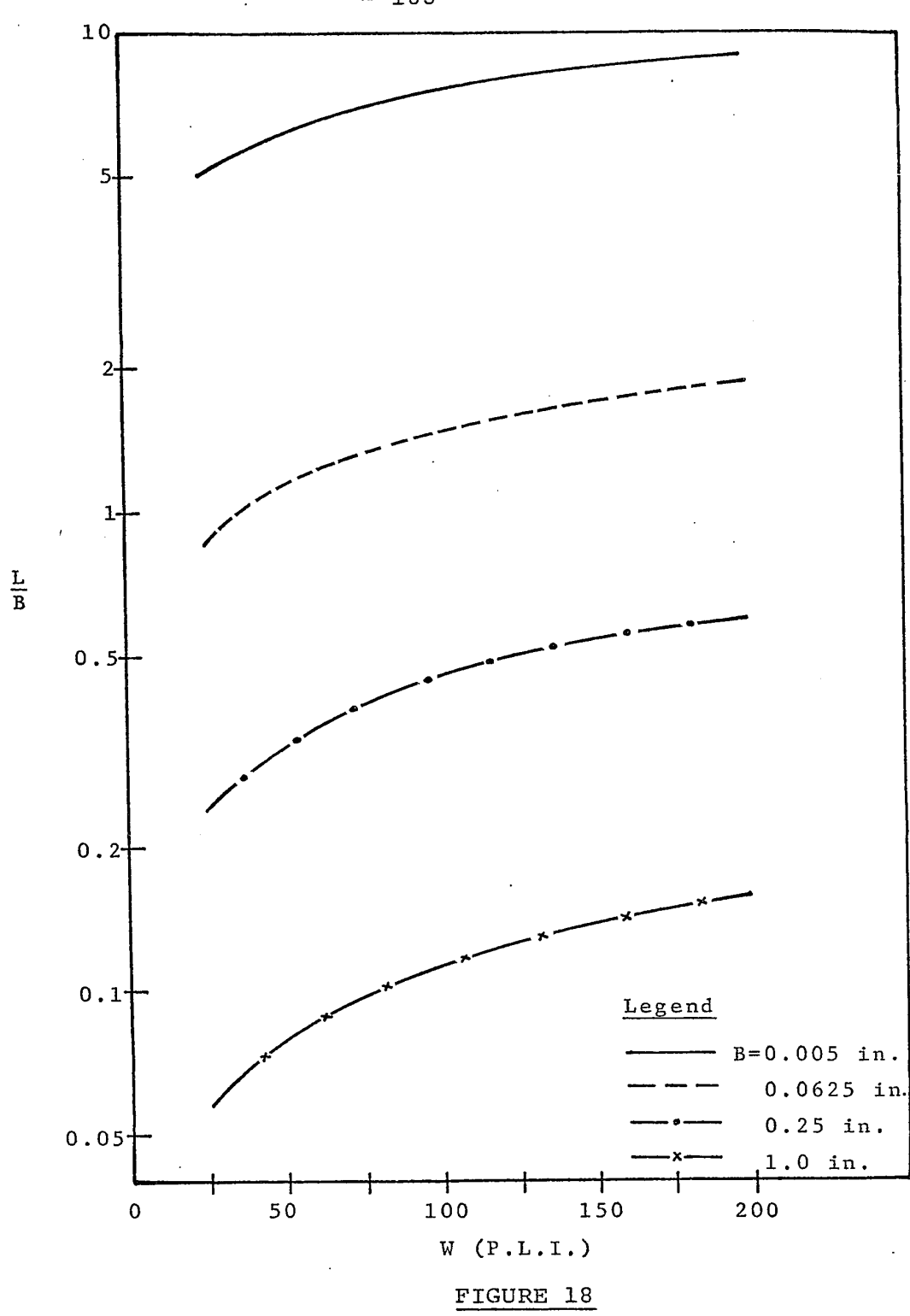


FIGURE 17

VARIATION OF PEAK PRESSURE WITH LOAD AND SHEET THICKNESS FOR NO-SLIP CONDITION (ELASTIC CASE)



VARIATION OF THE RATIO  $\frac{L}{B}$  WITH LOAD AND SHEET THICKNESS FOR NO-SLIP CONDITION (ELASTIC CASE)

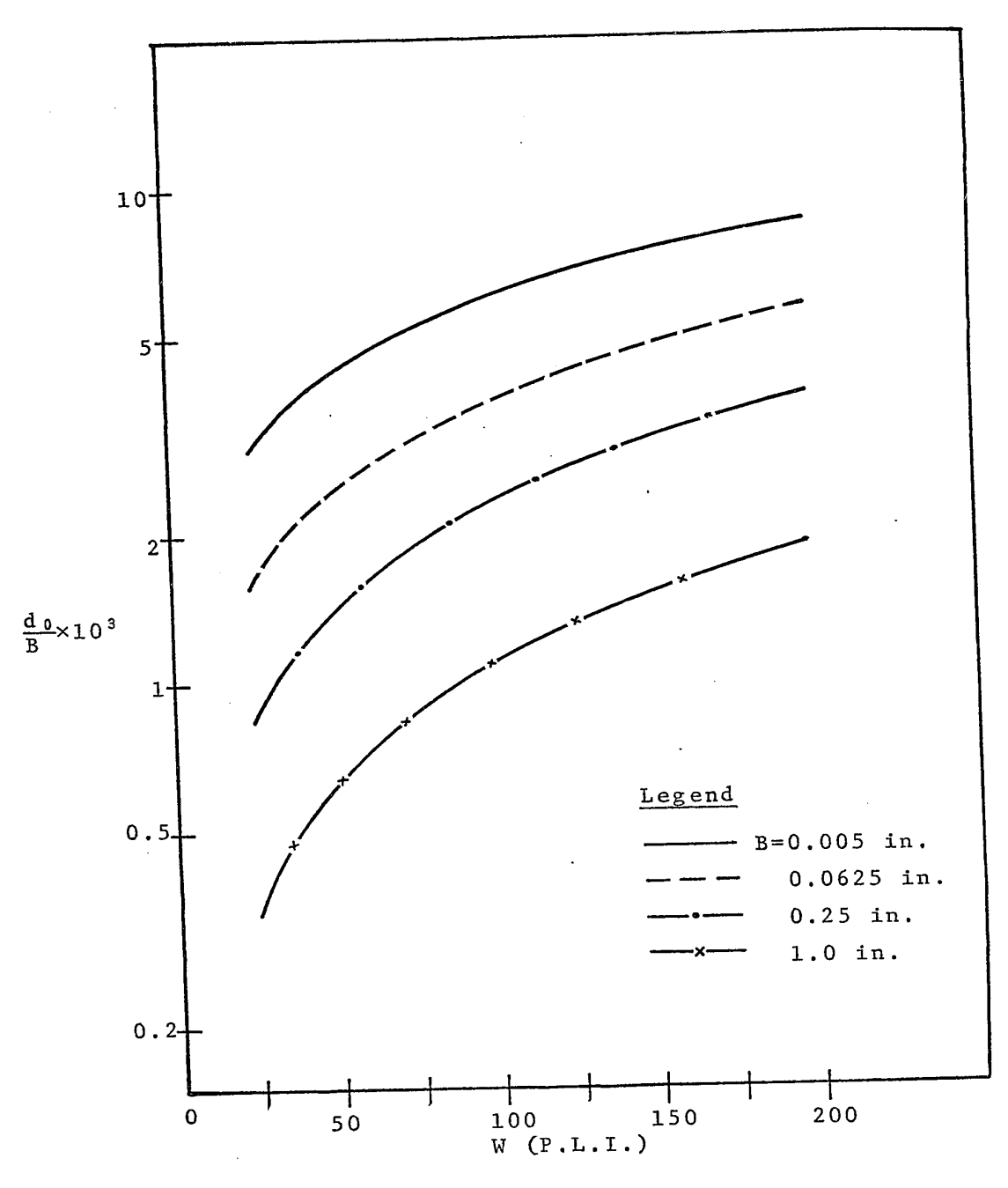


FIGURE 19

VARIATION OF THE RATIO  $\frac{d_0}{B}$  WITH LOAD AND SHEET THICKNESS FOR NO-SLIP CONDITION (ELASTIC CASE)

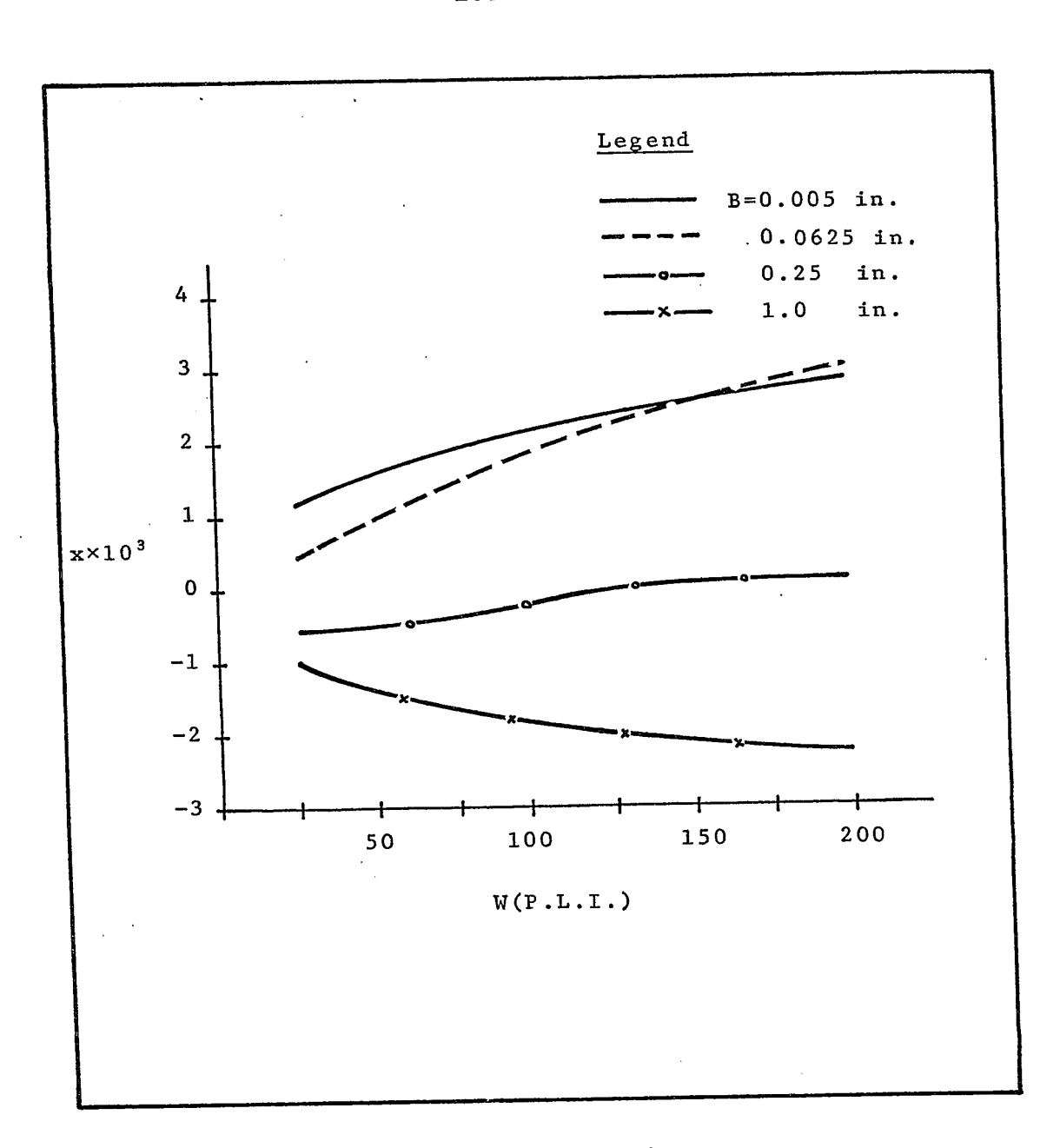


FIGURE 20

VARIATION OF CREEP RATIO WITH LOAD AND SHEET THICKNESS FOR NO-SLIP CONDITION (ELASTIC CASE)

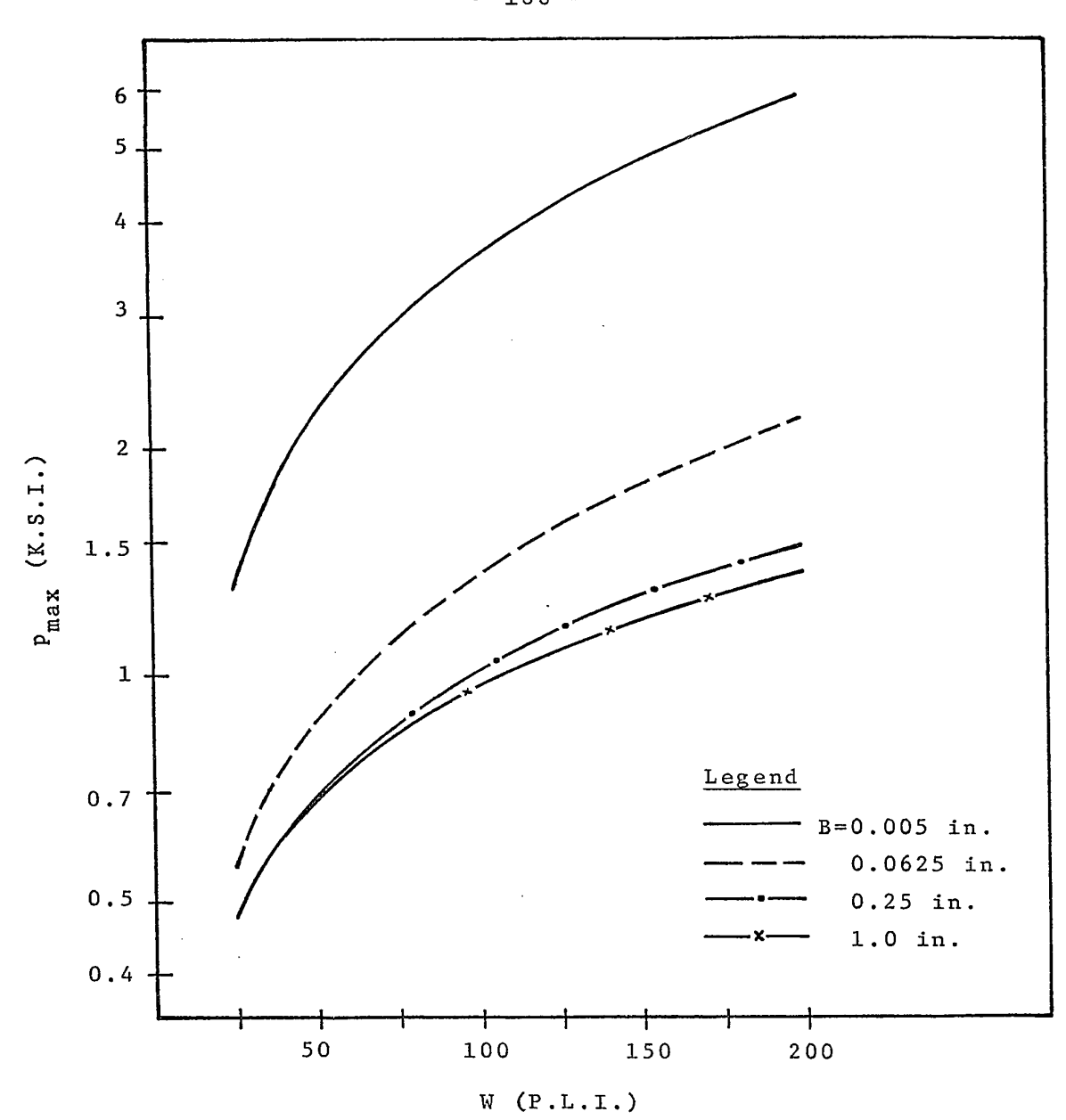
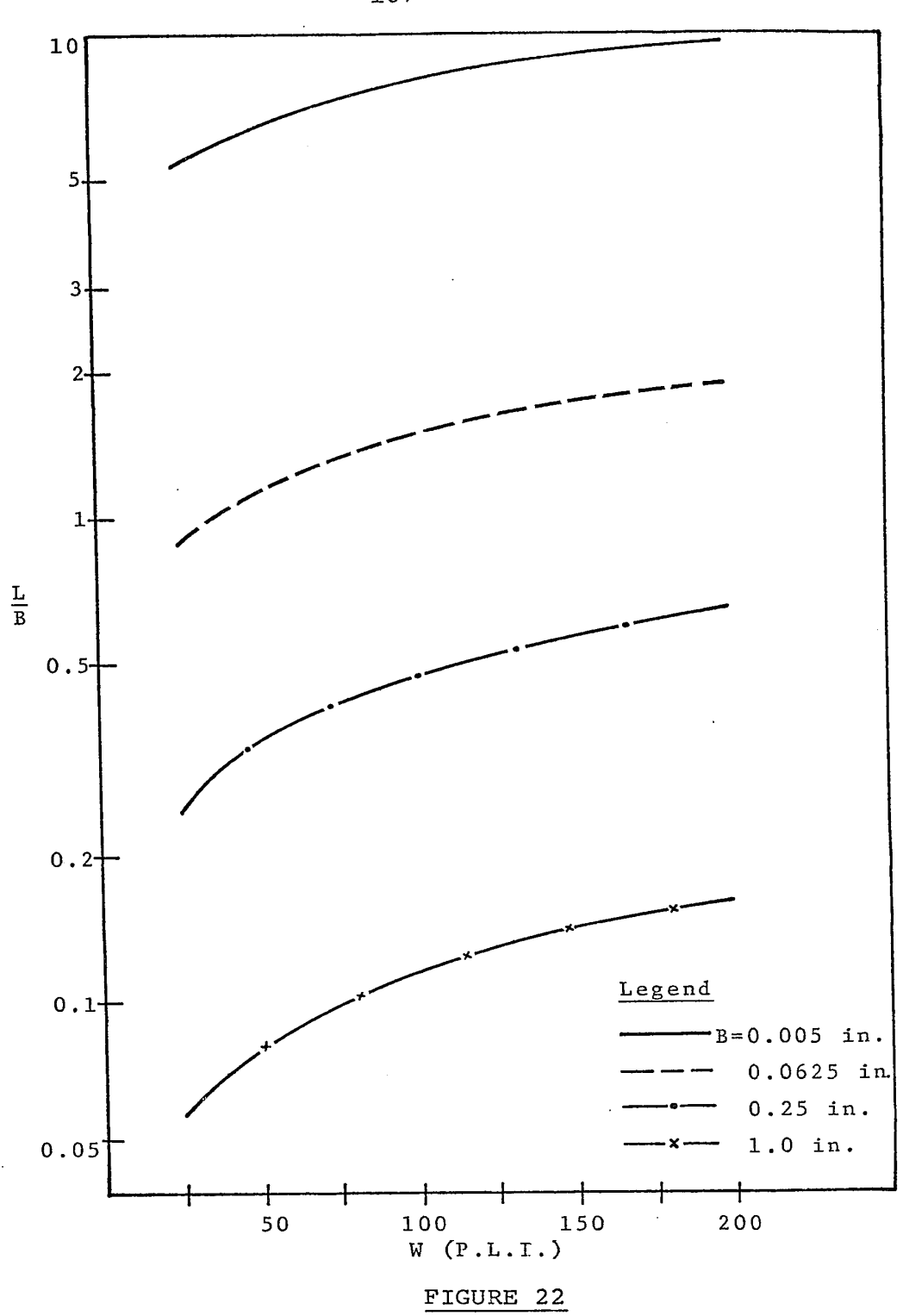
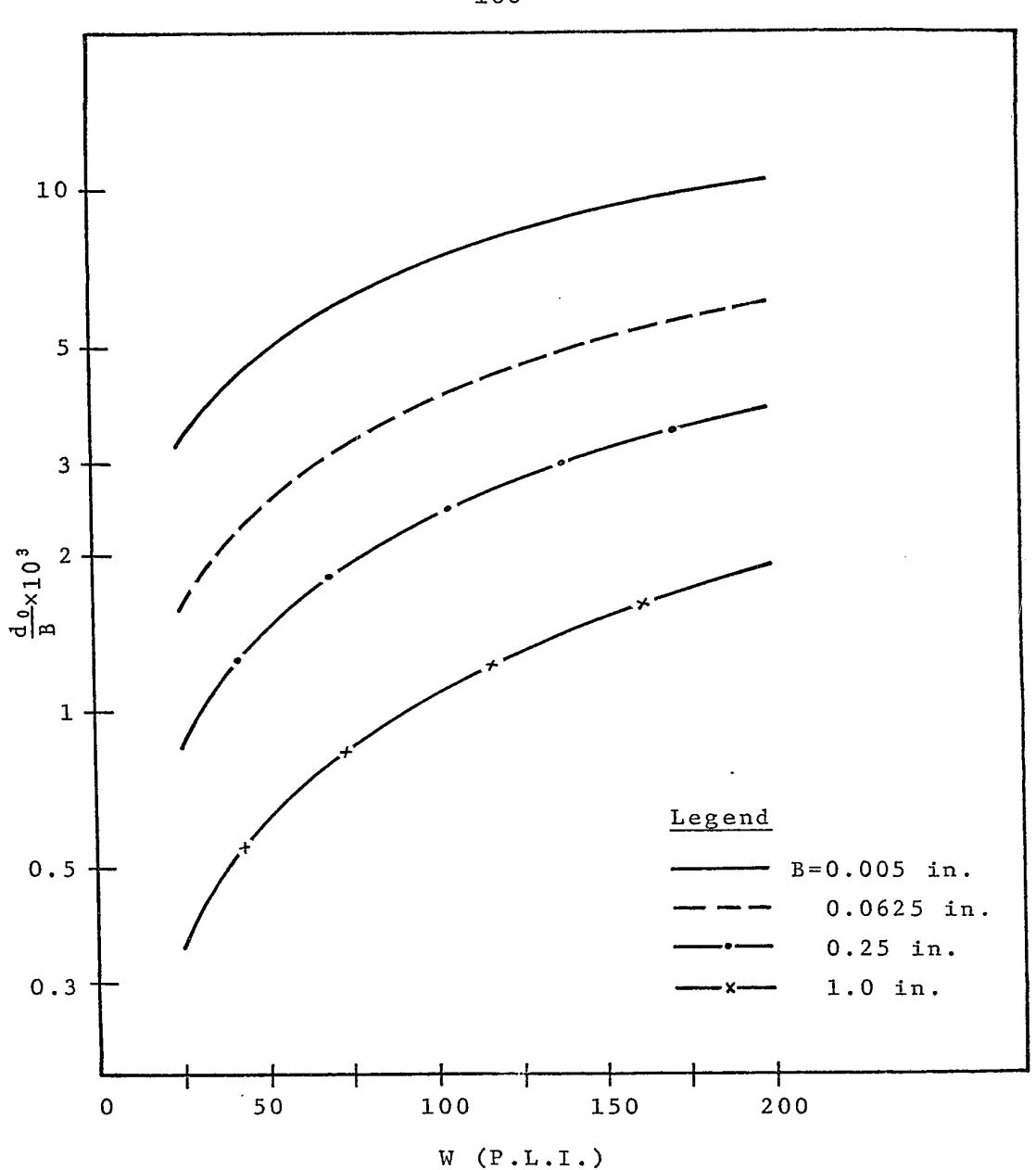


FIGURE 21

VARIATION OF PEAK PRESSURE WITH LOAD AND SHEET THICKNESS FOR COMPLETE SLIP (ELASTIC CASE)



VARIATION OF THE RATIO  $\frac{L}{B}$  WITH LOAD AND SHEET THICKNESS FOR COMPLETE SLIP (ELASTIC CASE)



 $\frac{\text{FIGURE 23}}{\text{VARIATION OF }\frac{\text{d 0}}{\text{B}}} \text{ WITH LOAD AND SHEET THICKNESS}$  FOR COMPLETE SLIP (ELASTIC CASE)

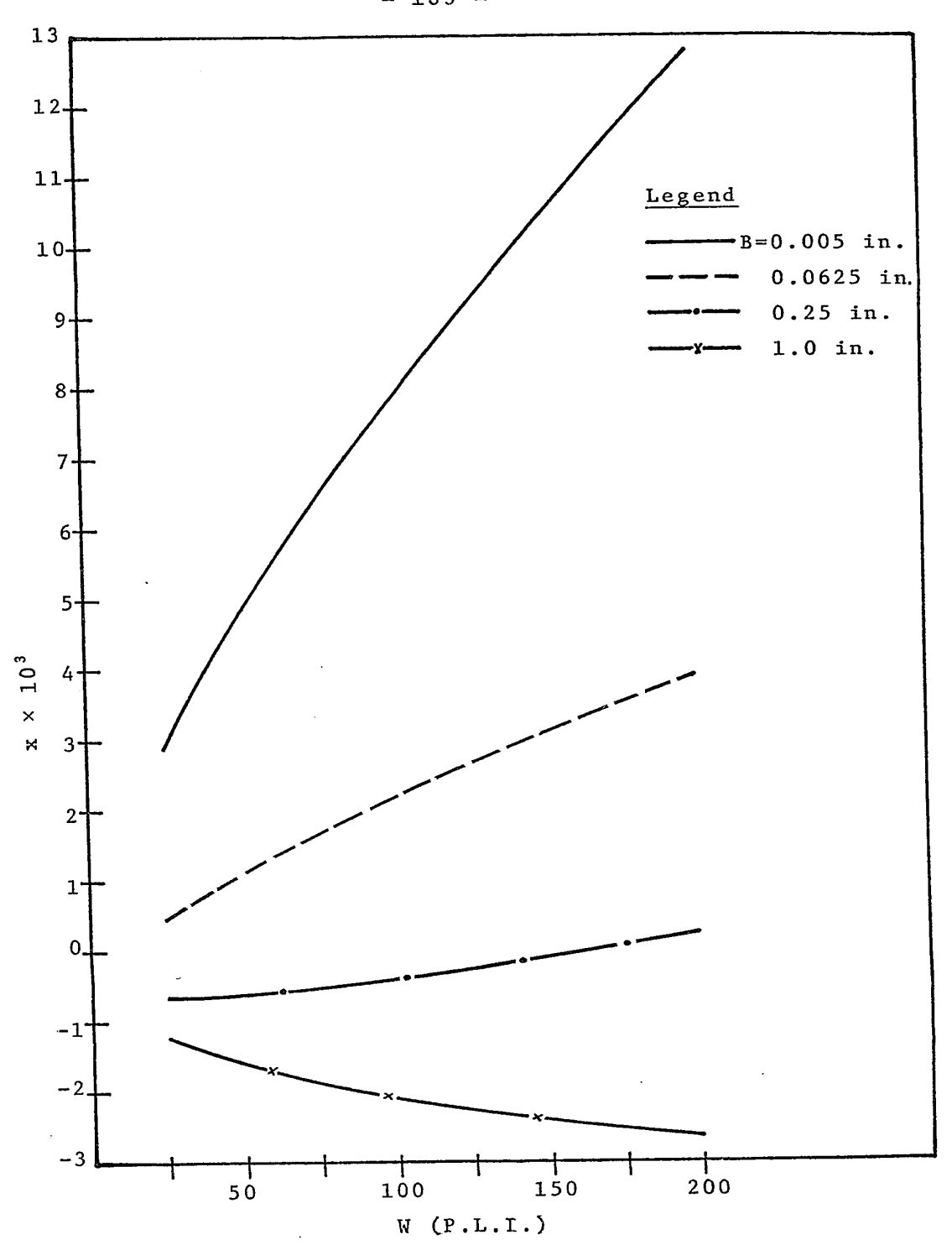


FIGURE 24

VARIATION OF CREEP RATIO WITH LOAD AND SHEET

THICKNESS FOR COMPLETE SLIP (ELASTIC CASE)

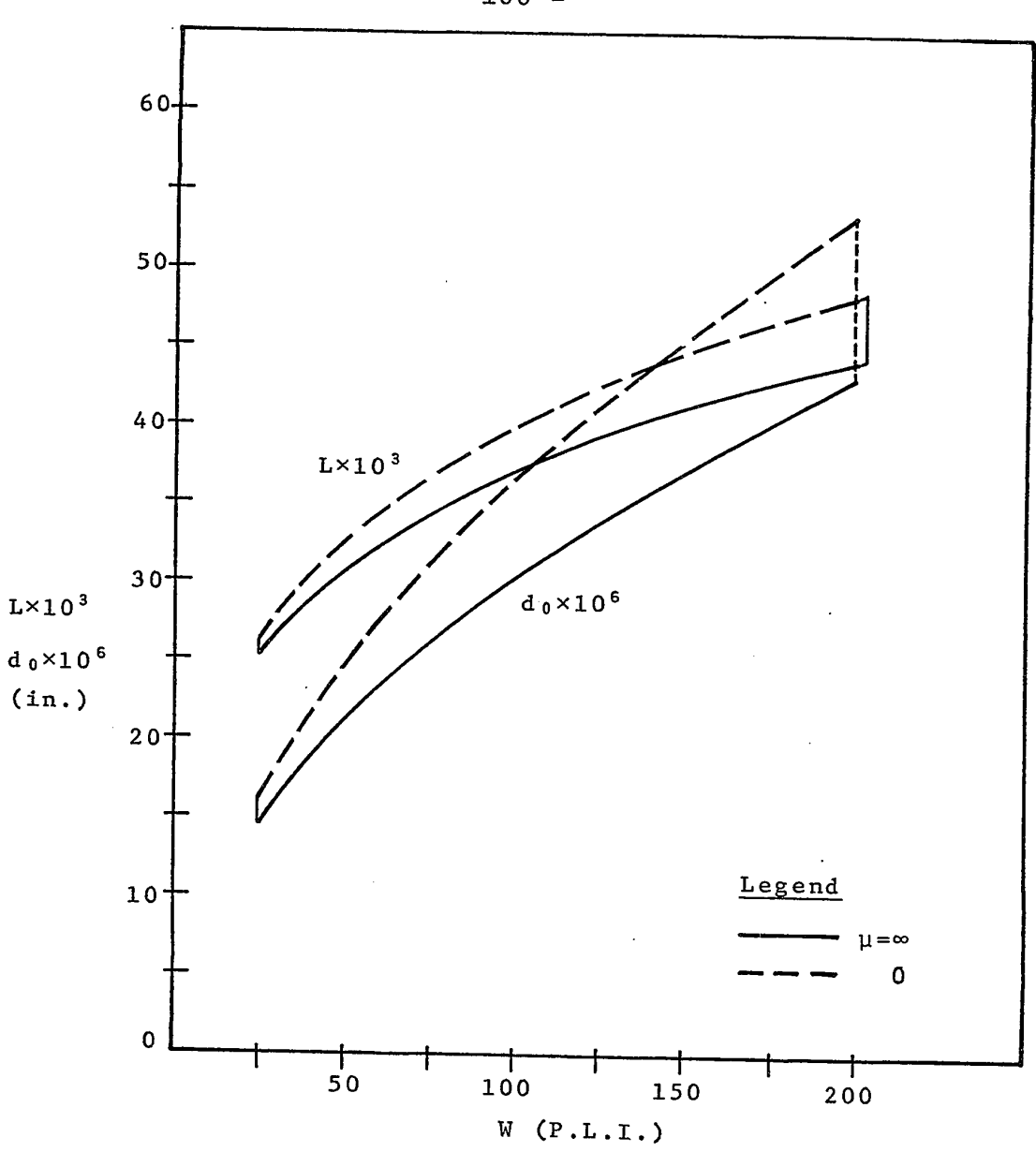
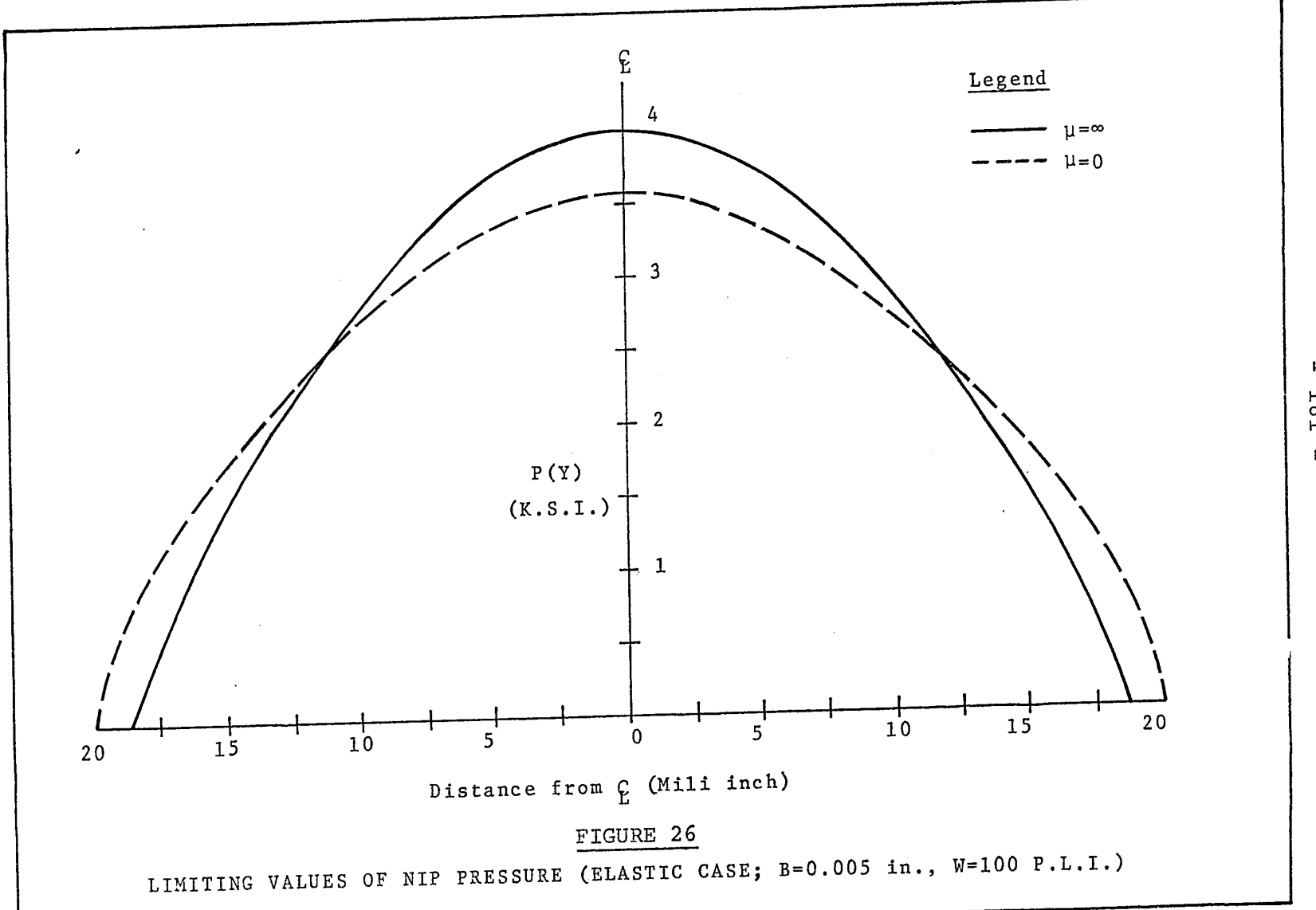
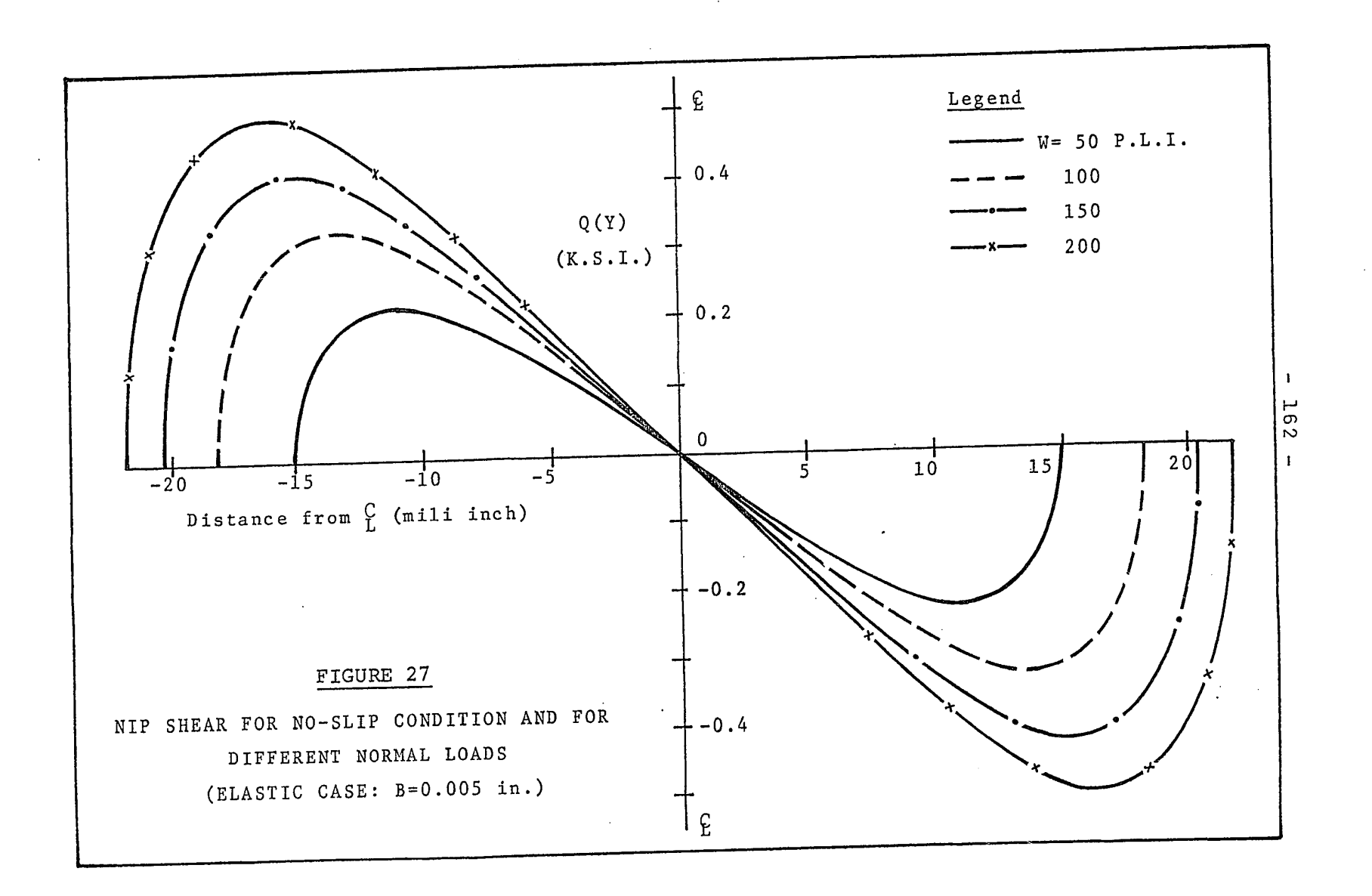
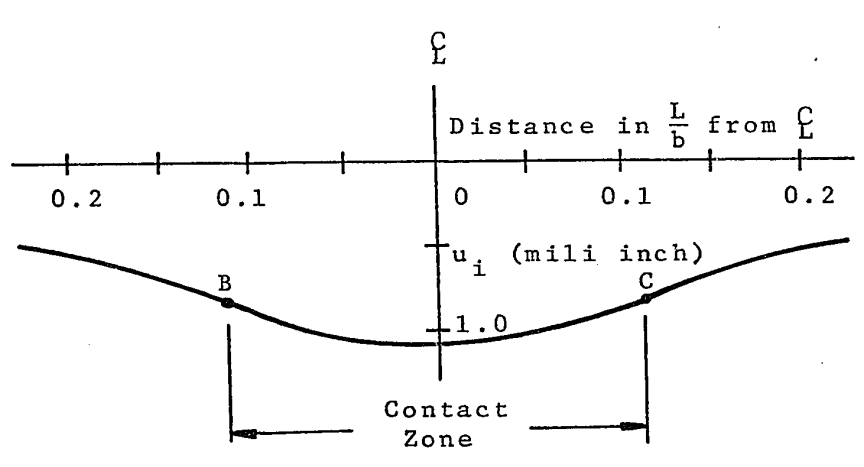


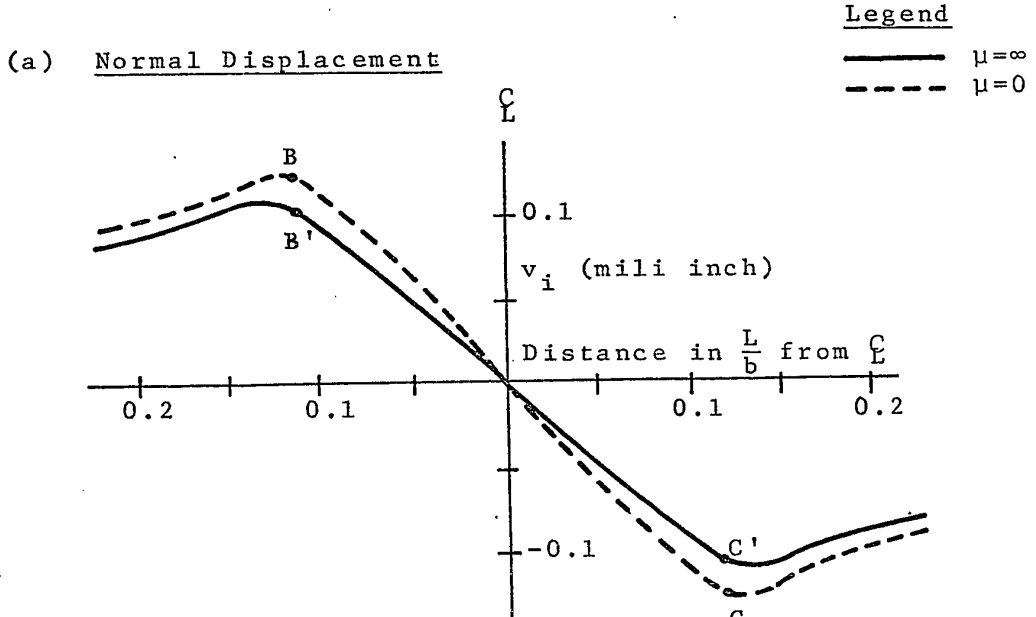
FIGURE 25

LIMITING VALUES OF CONTACT LENGTH AND INDENTATION FOR DIFFERENT NORMAL LOADS (ELASTIC CASE: B=0.005 in.)





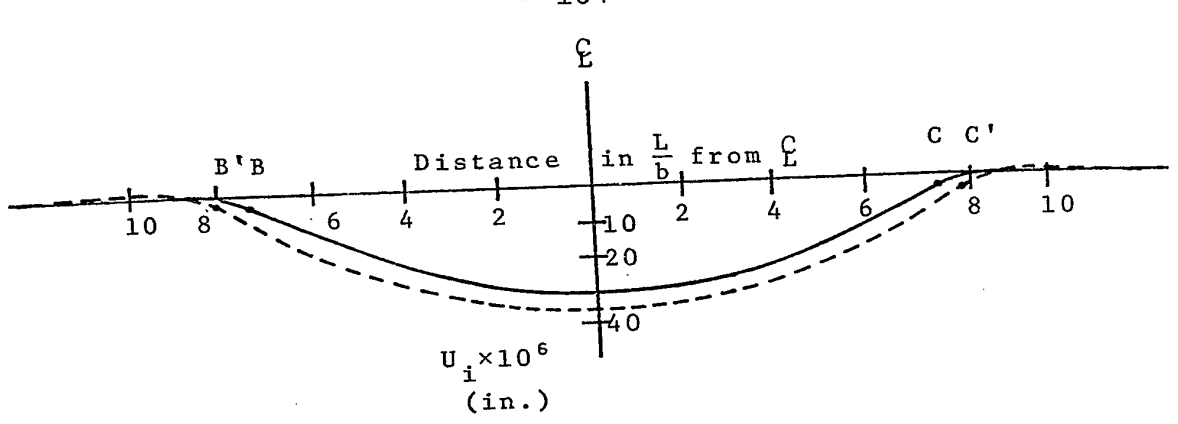




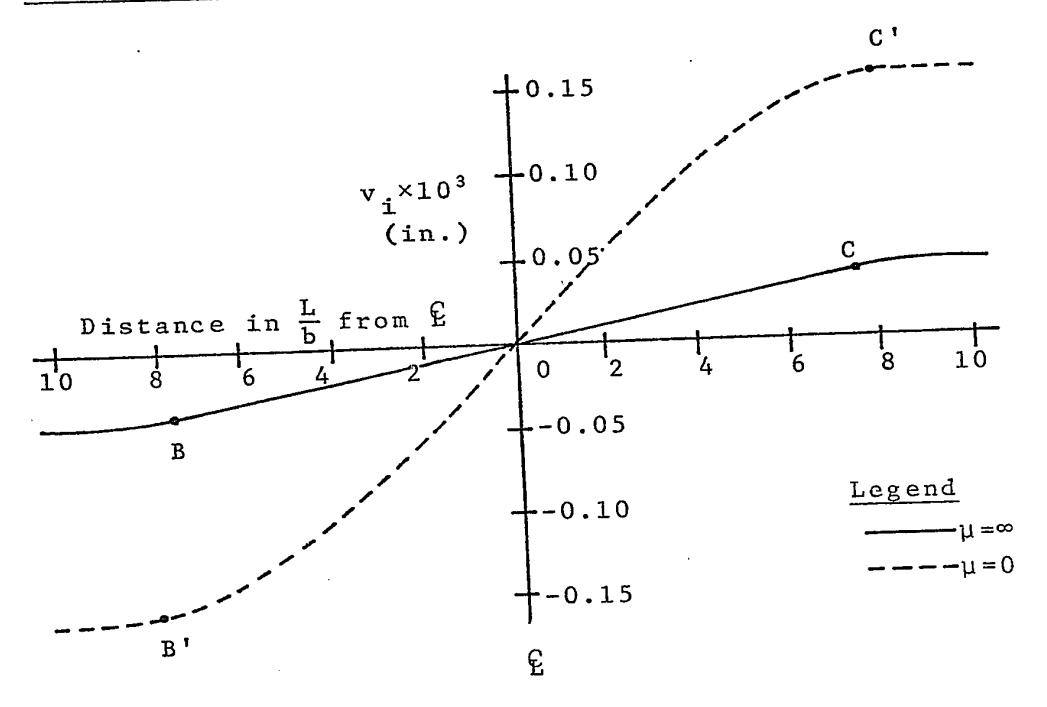
#### (b) Shear Displacement

#### FIGURE 28

SURFACE DISPLACEMENTS OF AN ELASTIC SHEET UNDER THE NIP  $(B = 1 \ \text{in.,} \ W = 100 \ \text{P.L.I.})$ 



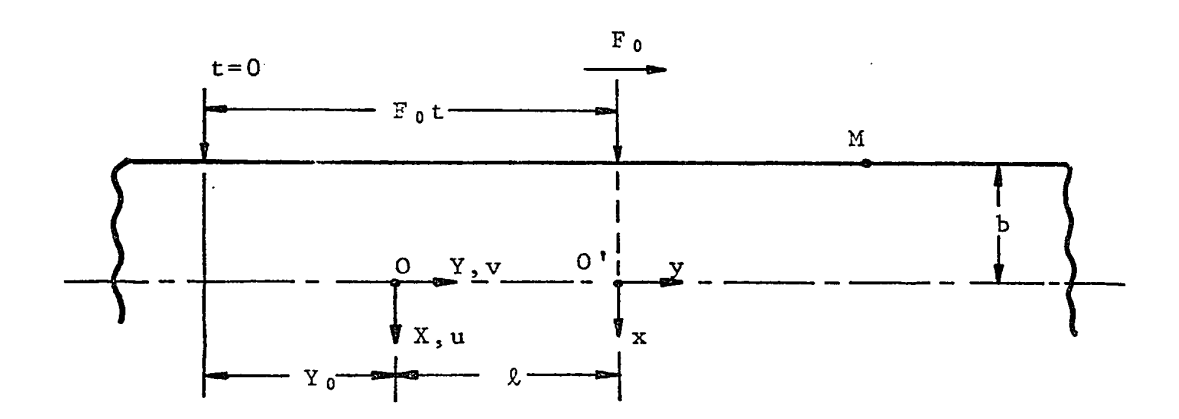
# (a) Normal Displacement



## (b) Shear Displacement

#### FIGURE 29

SURFACE DISPLACEMENTS OF AN ELASTIC SHEET UNDER THE NIP (B = 0.005 in., W = 100 P.L.I.)



x-y coordinate system moving with the load

X-Y coordinate system fixed in space

 $F_0$  velocity of the load

O pinned point

M some arbitrary point

#### FIGURE 30

GEOMETRIC REPRESENTATION OF A MOVING LINE LOAD

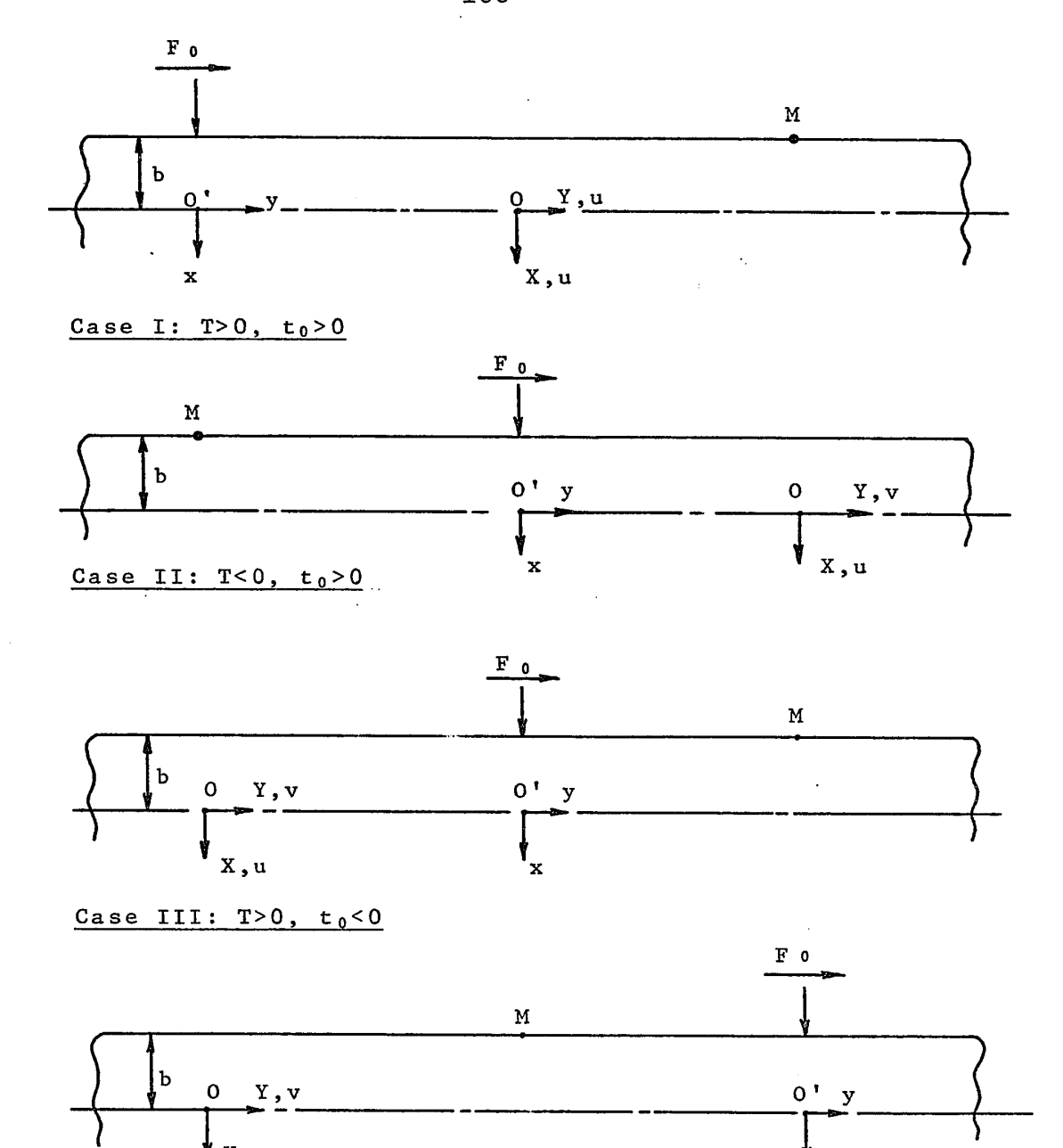
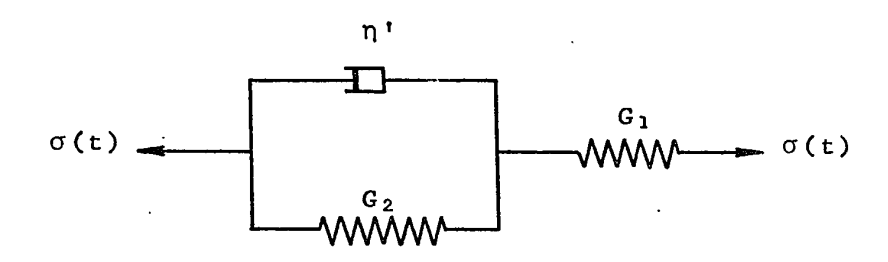


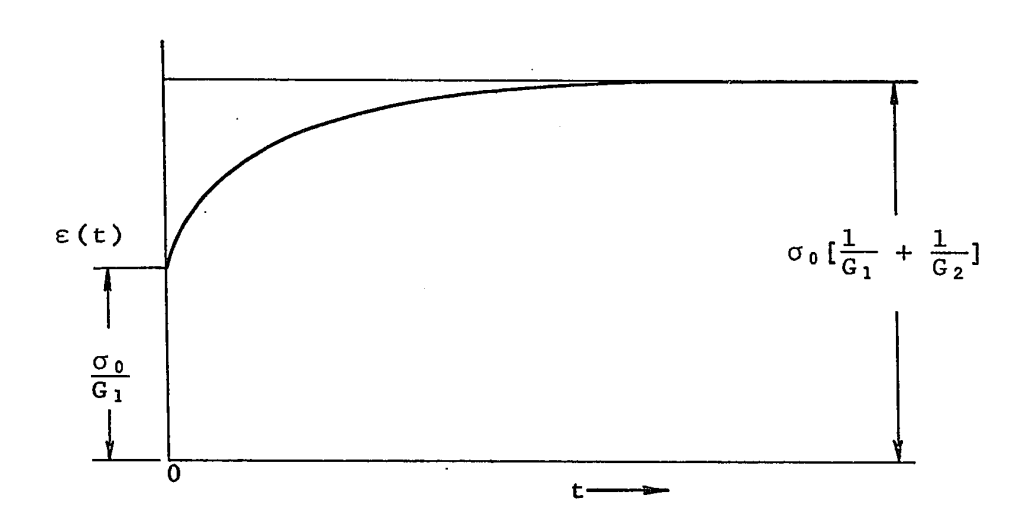
#### FIGURE 31

Case IV: T<0,  $t_0<0$ 

FOUR DISTINCT CASES DEPENDING UPON THE LOCATION OF POINT M
AND THE STARTING POSITION OF THE LOAD



## (a) Mechanical Model of a Standard Linear Solid



### (b) Creep Response of a Standard Linear Solid

### FIGURE 32

MECHANICAL MODEL AND CREEP RESPONSE OF A STANDARD LINEAR SOLID

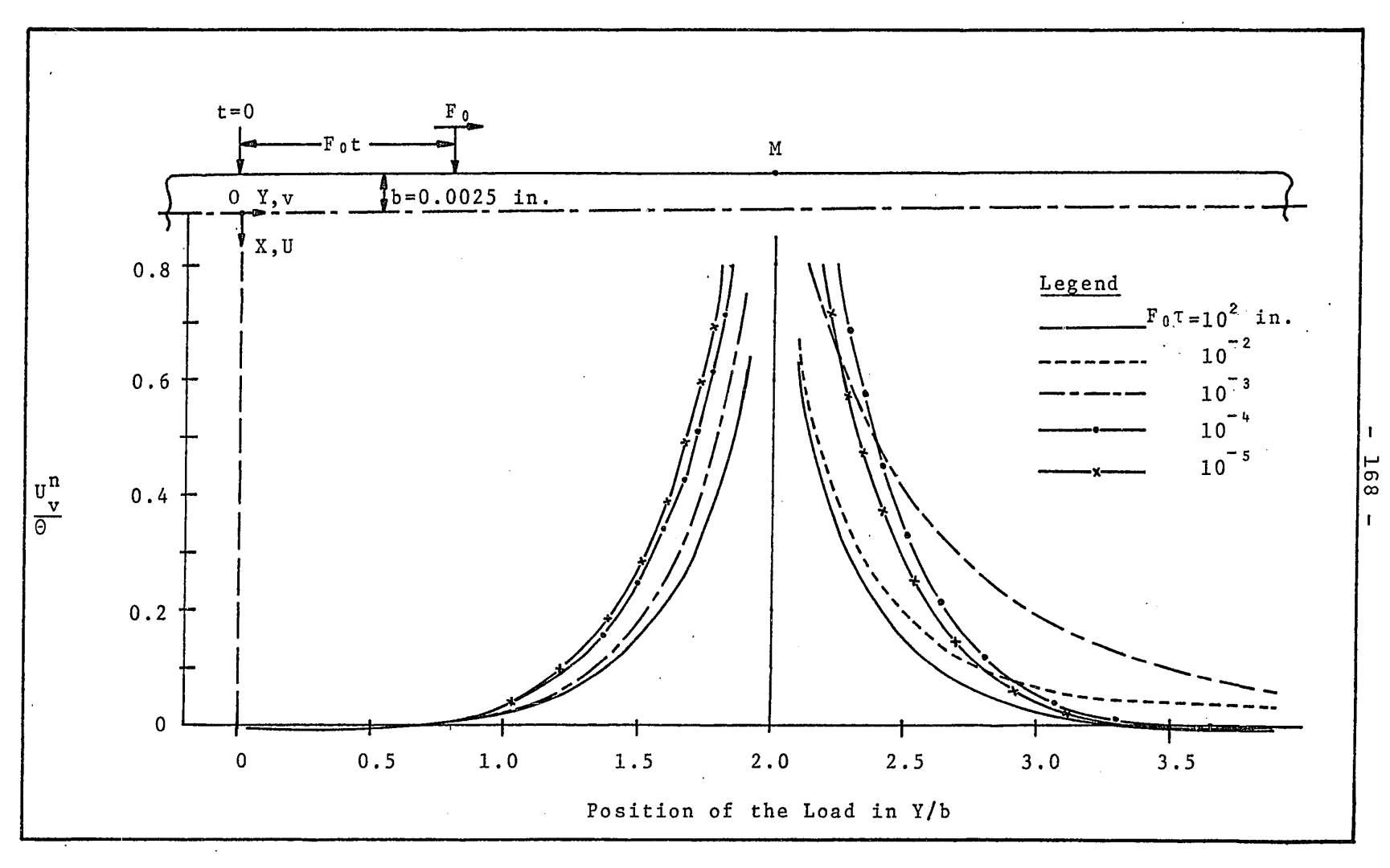
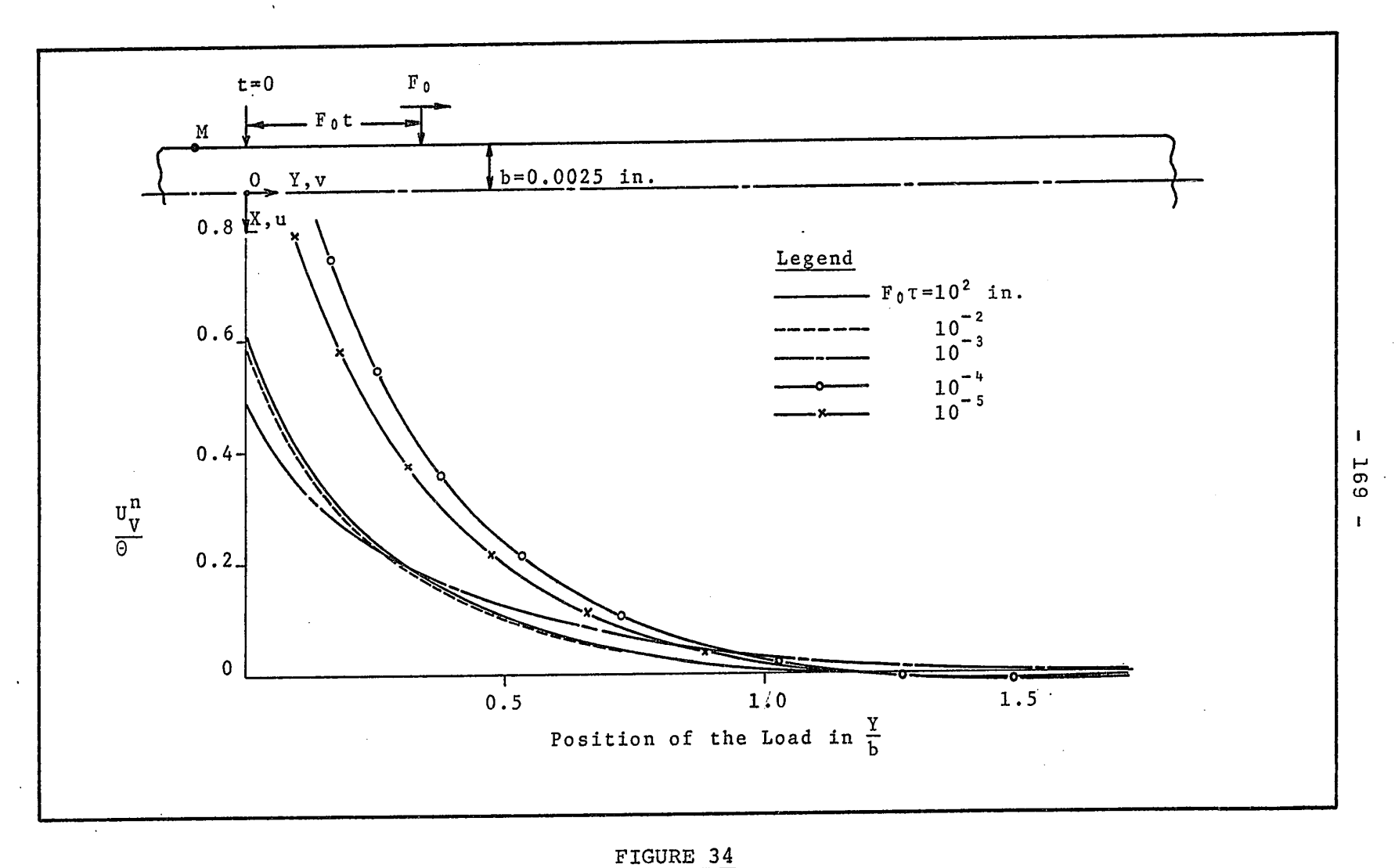


FIGURE 33

NORMAL DISPLACEMENT OF THE POINT M ON THE SURFACE OF A VISCOELASTIC SHEET

DUE TO MOVING LINE LOAD WHEN T>0



NORMAL DISPLACEMENT OF THE POINT M ON THE SURFACE OF A VISCOELASTIC SHEET

DUE TO MOVING LINE LOAD WHEN T<0

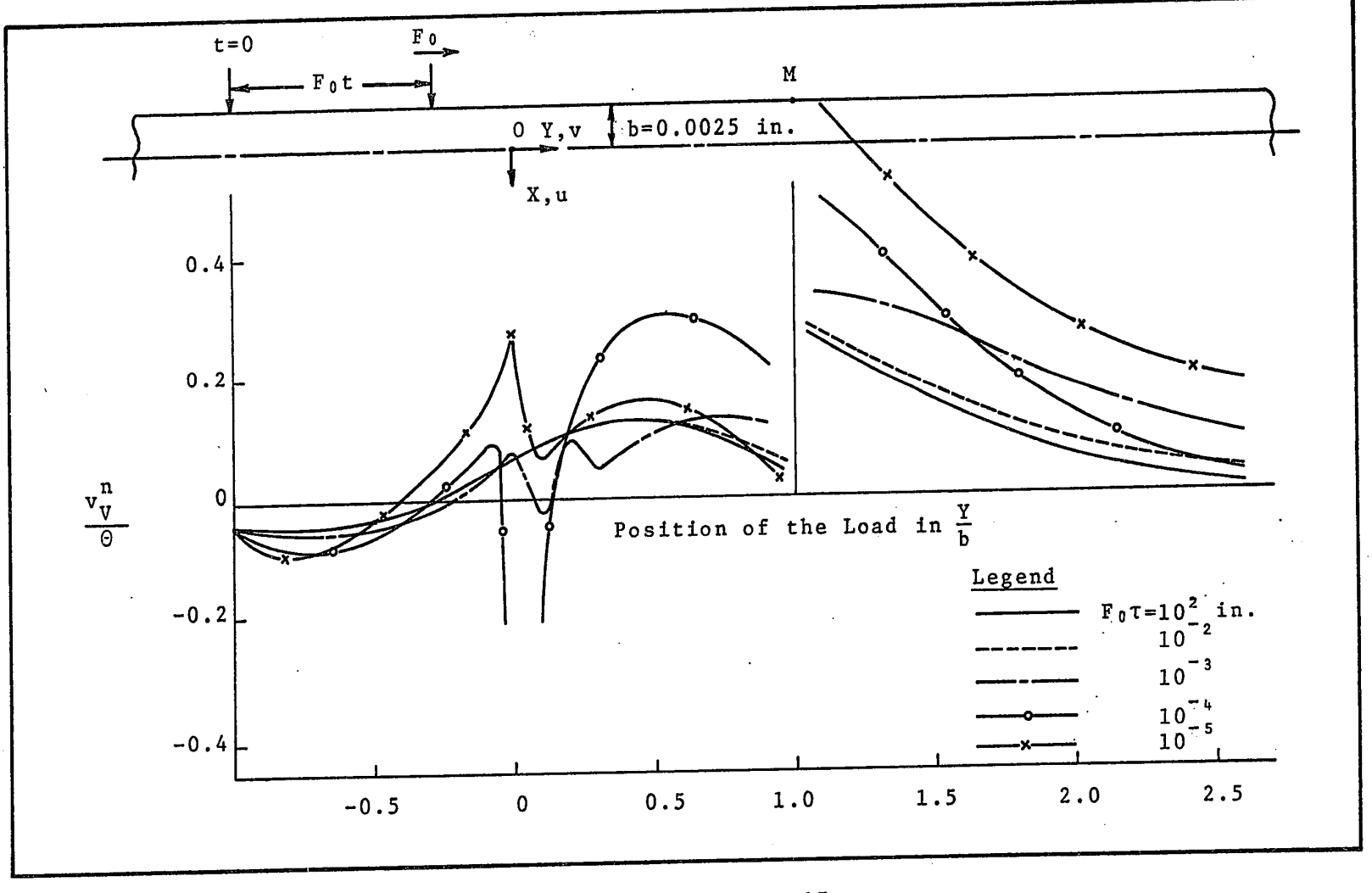
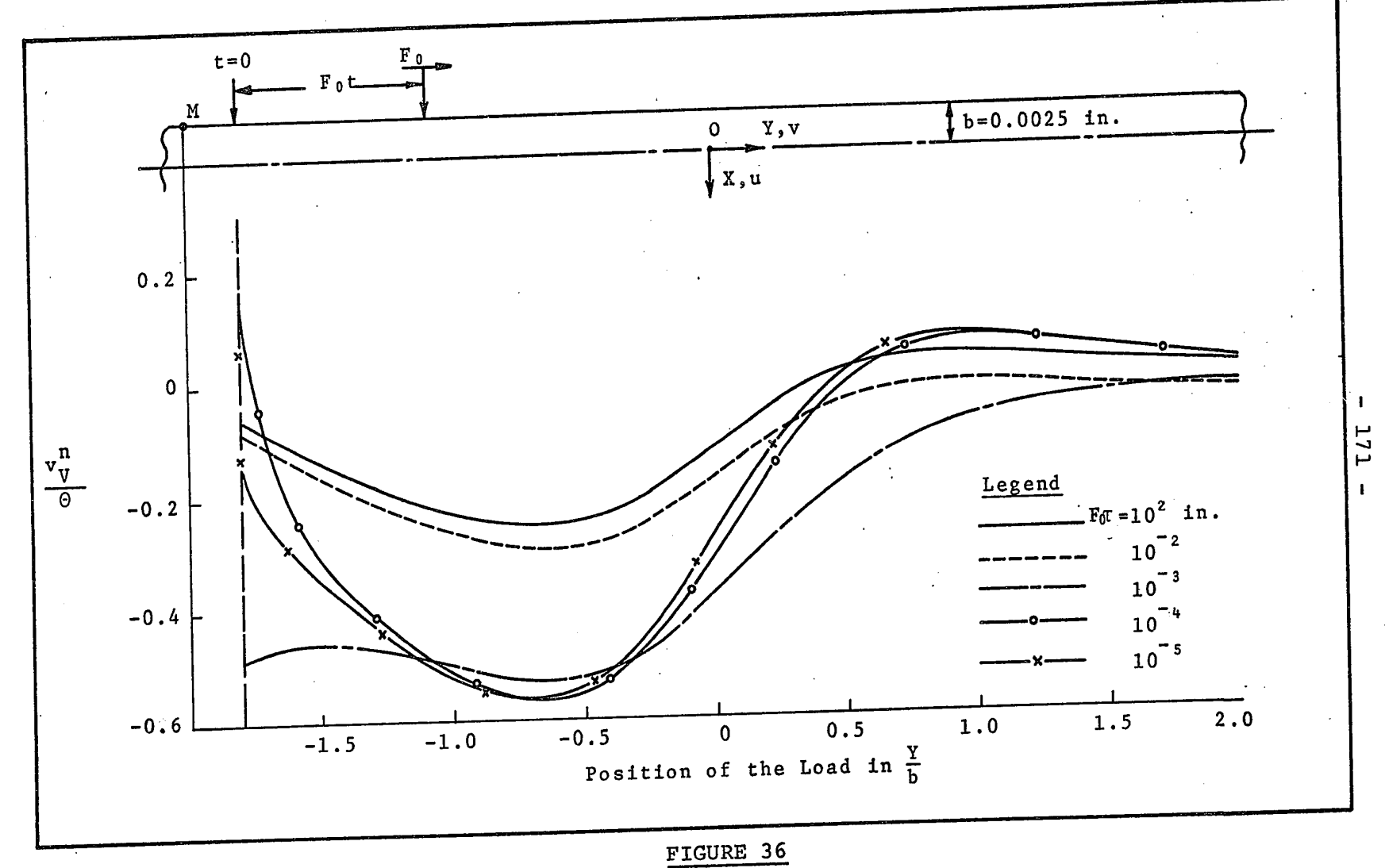
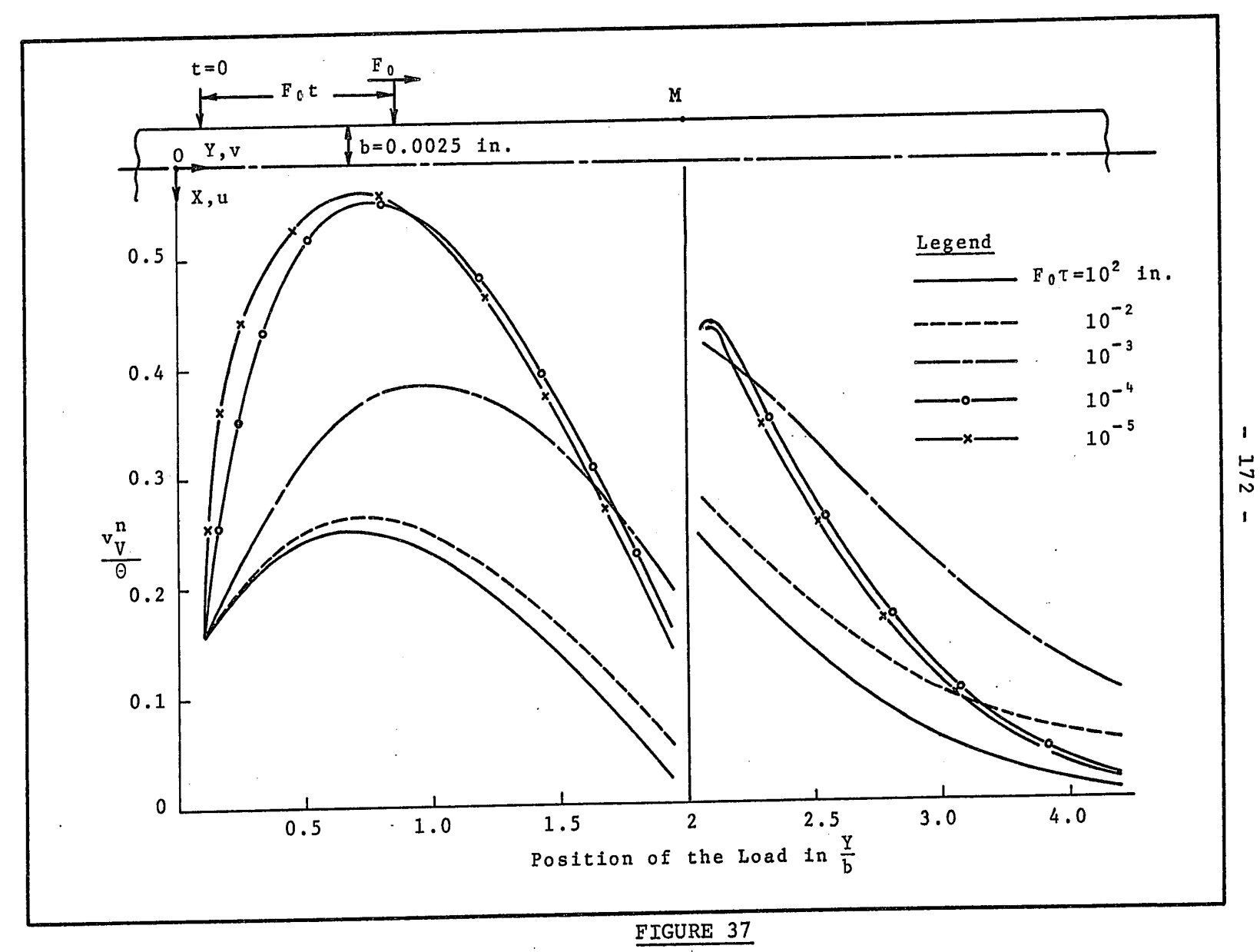


FIGURE 35

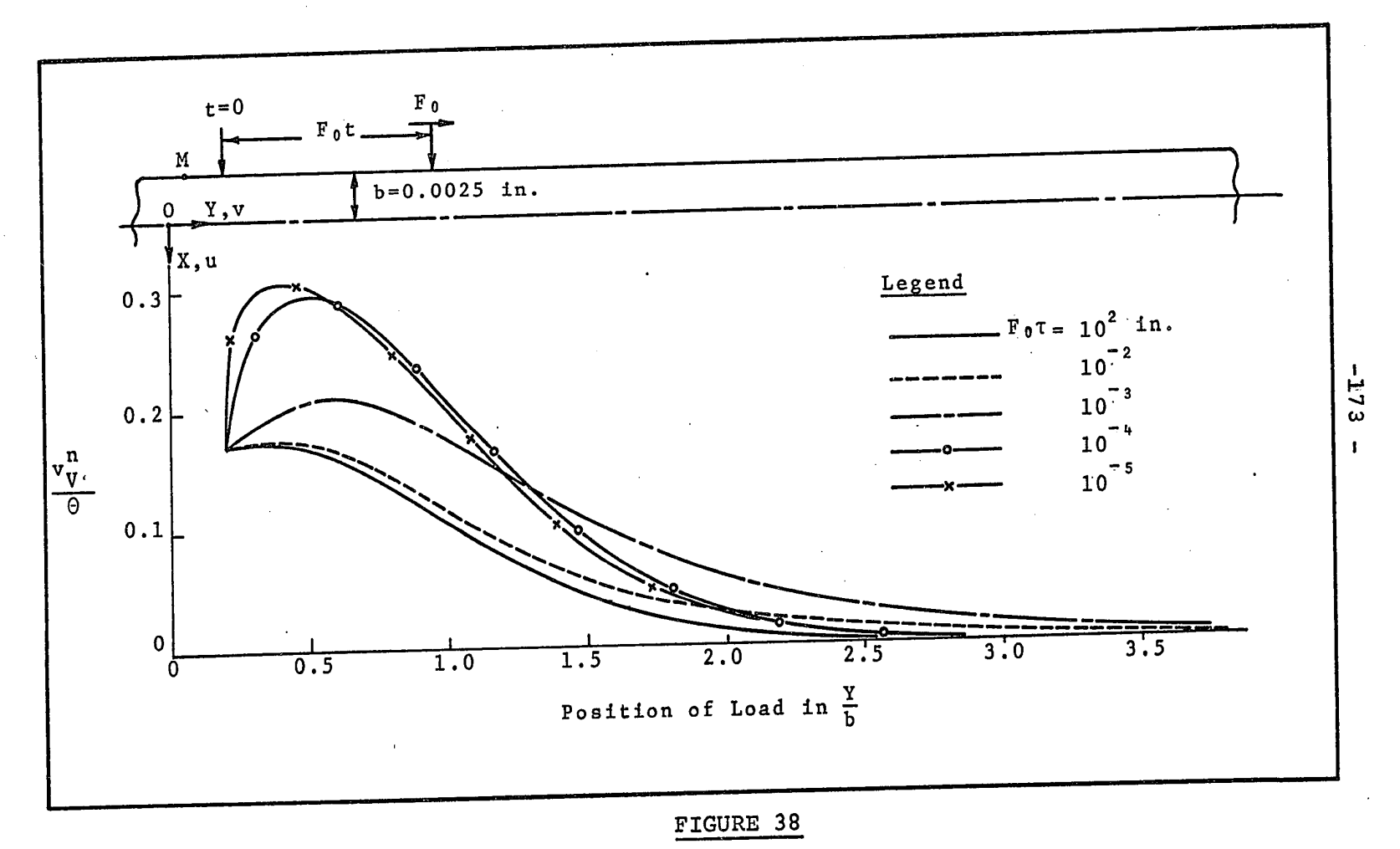
SHEAR DISPLACEMENT OF THE POINT M ON THE SURFACE OF A VISCOELASTIC SHEET DUE TO MOVING LINE LOAD WHEN T>0 AND  $t_0\!>\!0$ 



SHEAR DISPLACEMENT OF THE POINT M ON THE SURFACE OF A VISCOELASTIC SHEET DUE TO MOVING LINE LOAD WHEN T<0 AND  $t_0\!<\!0$ 



SHEAR DISPLACEMENT OF THE POINT M ON THE SURFACE OF A VISCOELASTIC SHEET DUE TO MOVING LINE LOAD WHEN T>0 AND  $t_0\!>\!0$ 



SHEAR DISPLACEMENT OF THE POINT M ON THE SURFACE OF A VISCOELASTIC SHEET DUE TO MOVING LINE LOAD WHEN T<0 AND  $t_0 < 0$ 

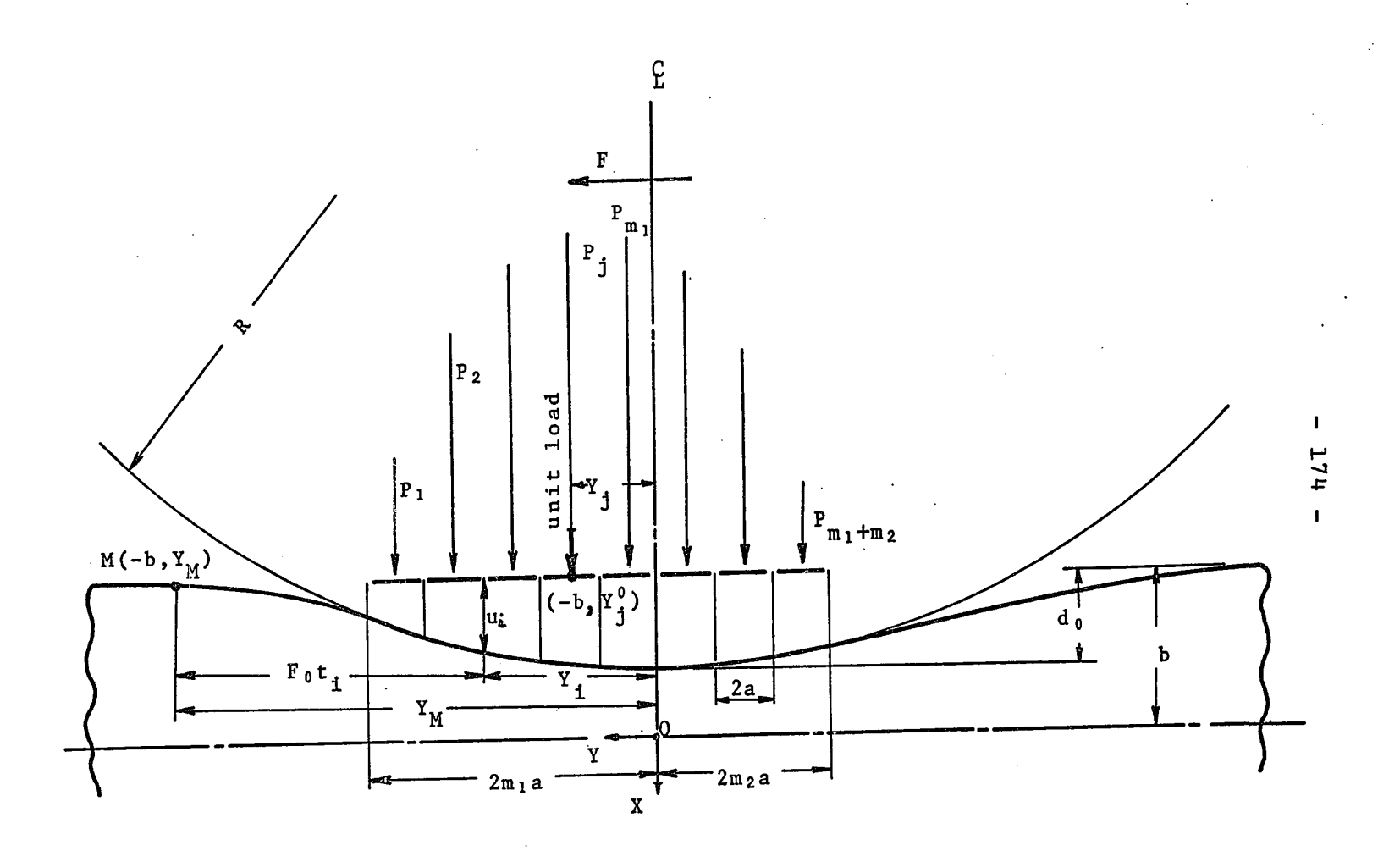


FIGURE 39

THE GEOMETRY OF THE NIP (VISCOELASTIC SHEET)

FIGURE 40

FORCE EQUILIBRIUM OF A VISCOELASTIC SHEET IN ROLLING CONTACT

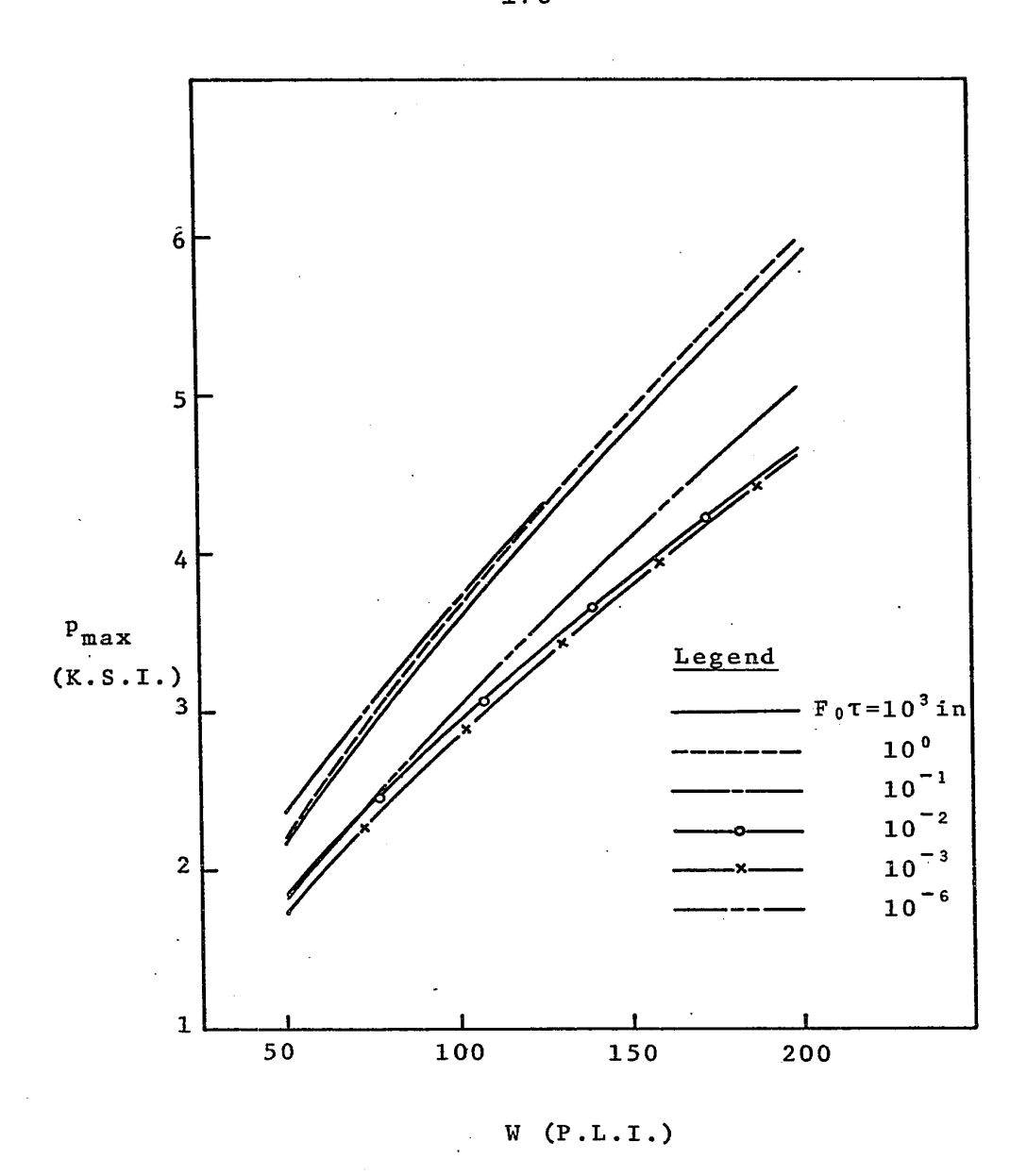
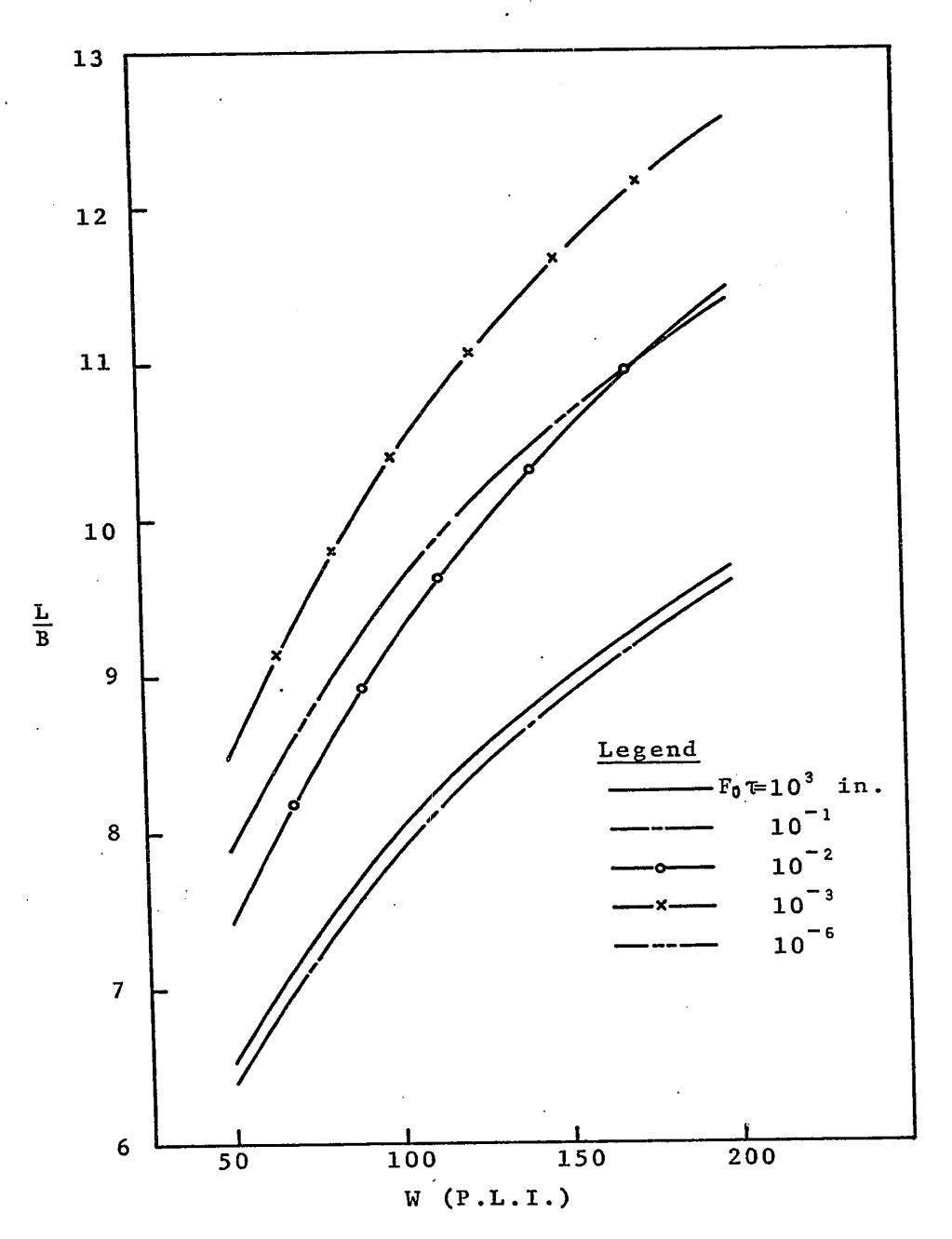
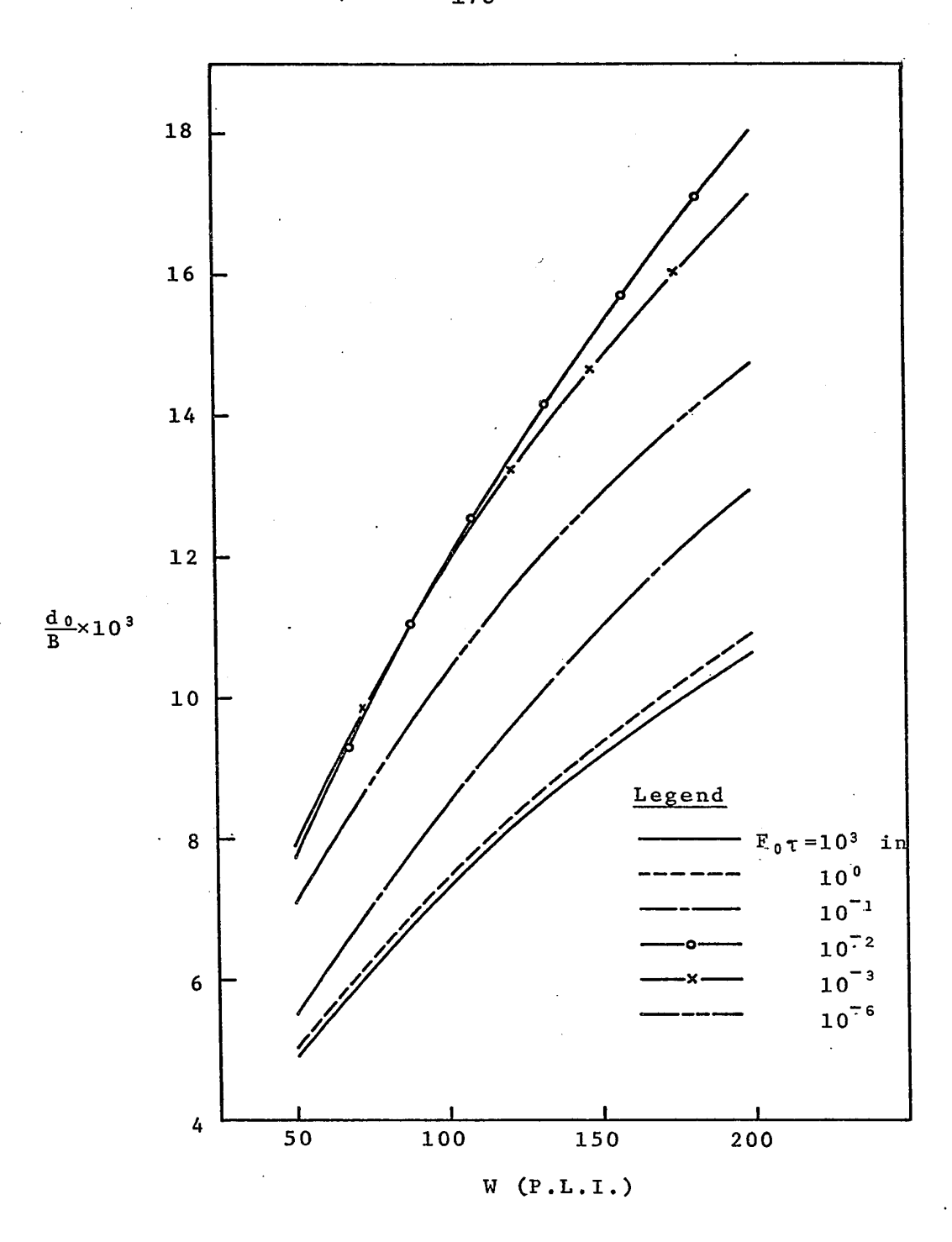


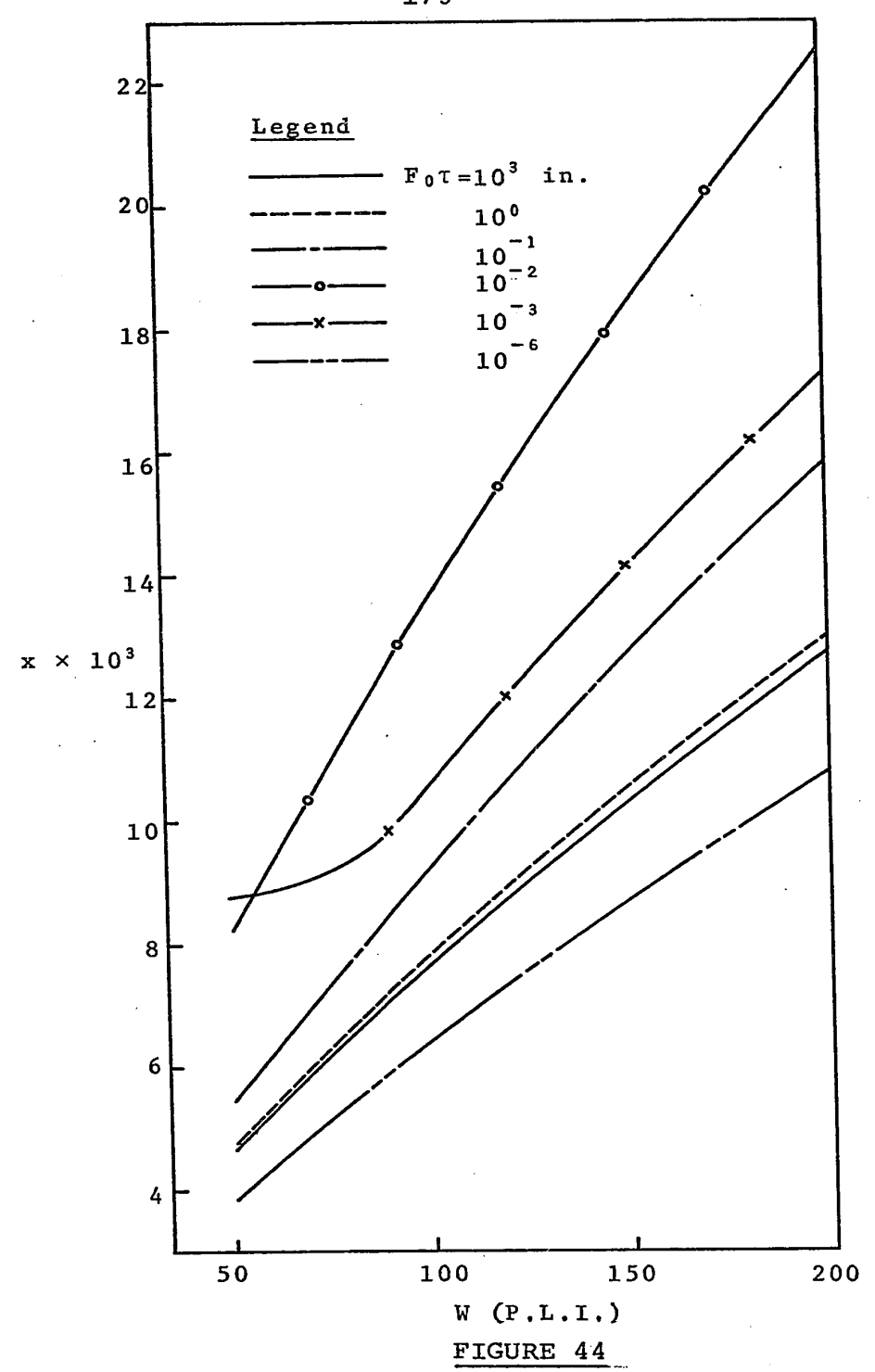
FIGURE 41  $VARIATION \ OF \ PEAK \ PRESSURE \ WITH \ NORMAL \ LOAD$  FOR DIFFERENT VALUES OF F0T(B=0.005 in.)



VARIATION OF THE RATIO  $\frac{L}{B}$  WITH NORMAL LOAD FOR DIFFERENT VALUES OF F0T (B=0.005 in.)



VARIATION OF THE RATIO  $\frac{d\,0}{B}$  WITH NORMAL LOAD FOR DIFFERENT VALUES OF F<sub>0</sub> $\tau$  (B=0.005 in.)



VARIATION OF CREEP RATIO WITH NORMAL LOAD FOR DIFFERENT VALUES OF For (B=0.005 in.)

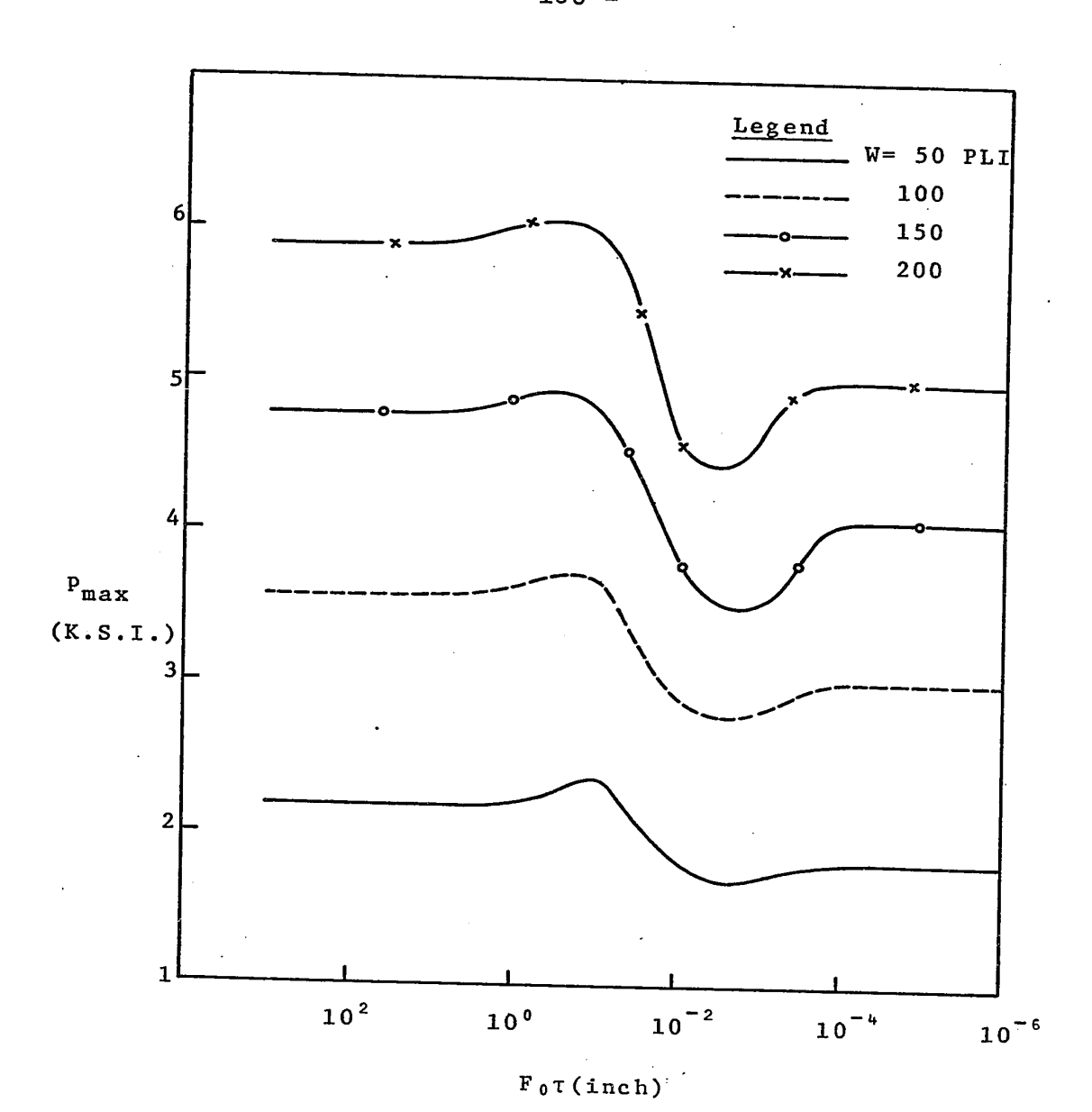
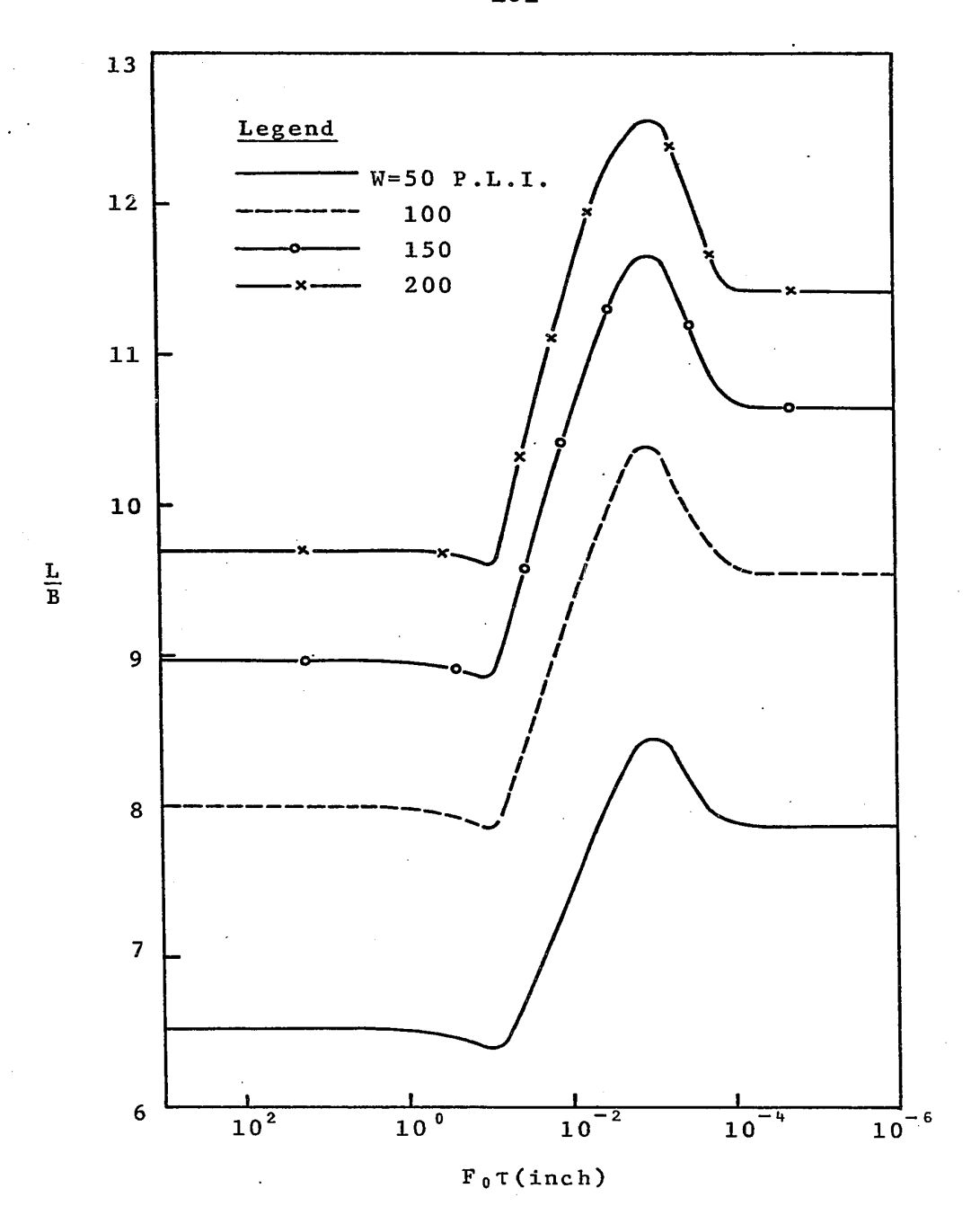
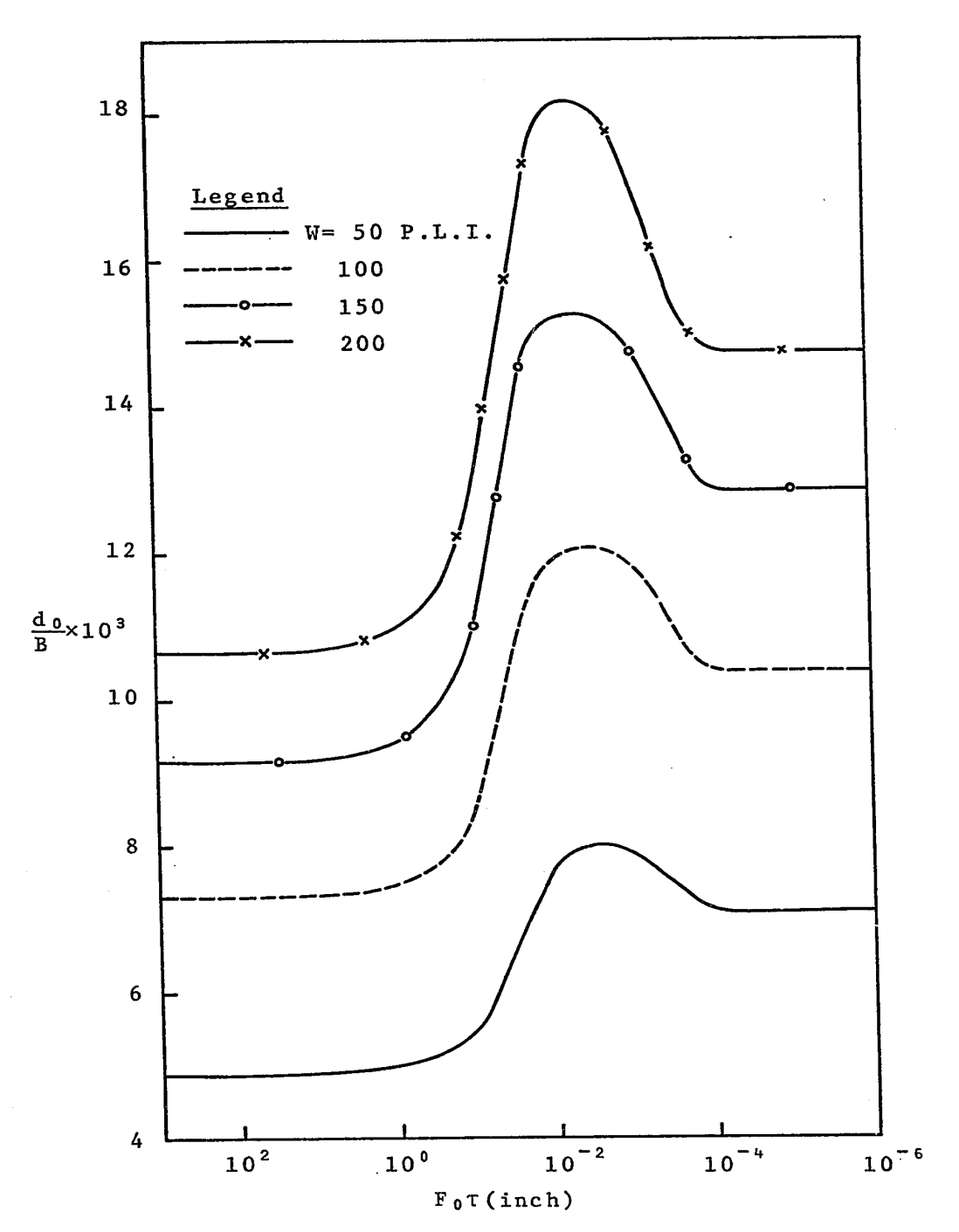


FIGURE 45

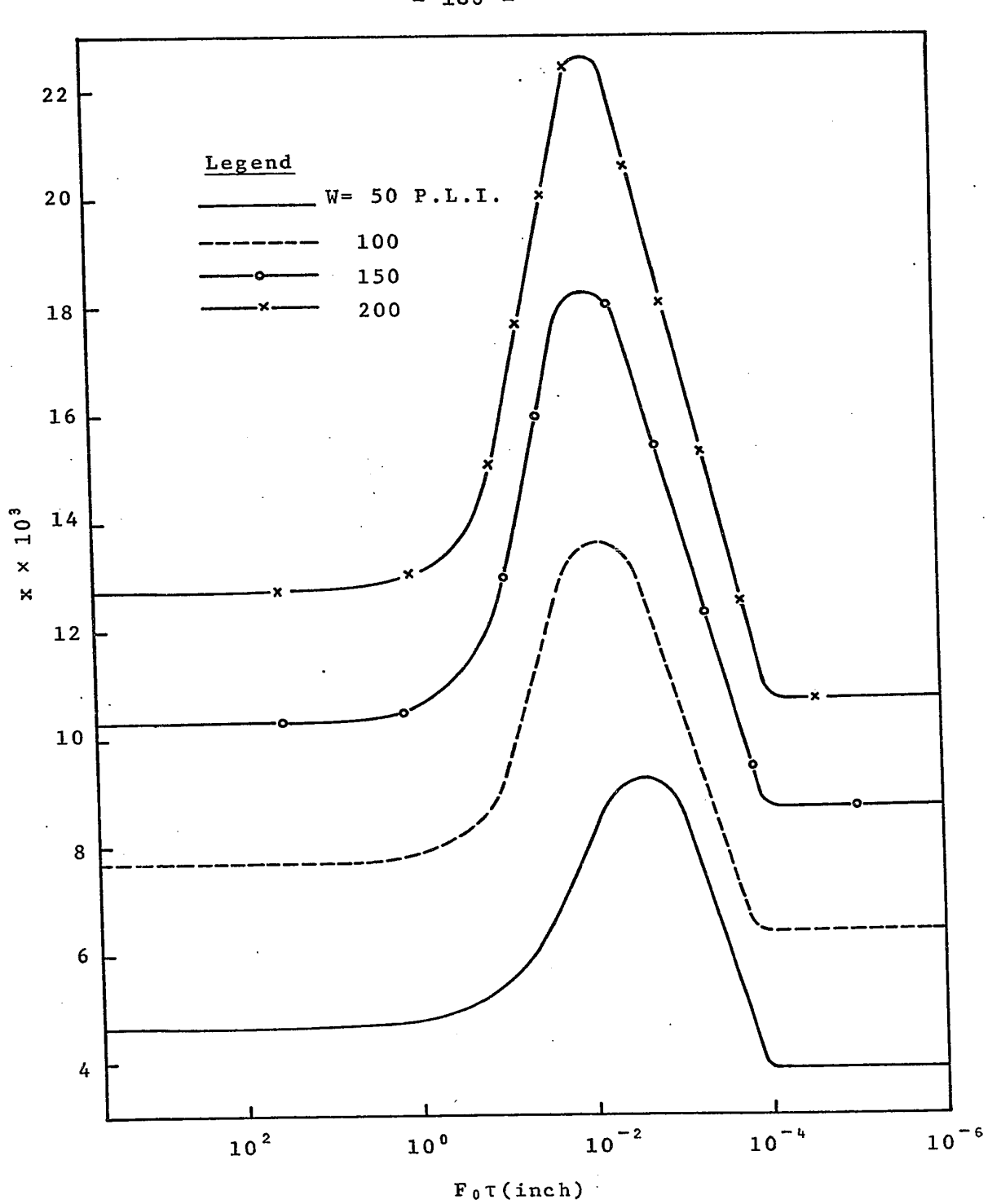
VARIATION OF PEAK PRESSURE WITH FOTFOR DIFFERENT NORMAL LOADS (B=0.005 in.)



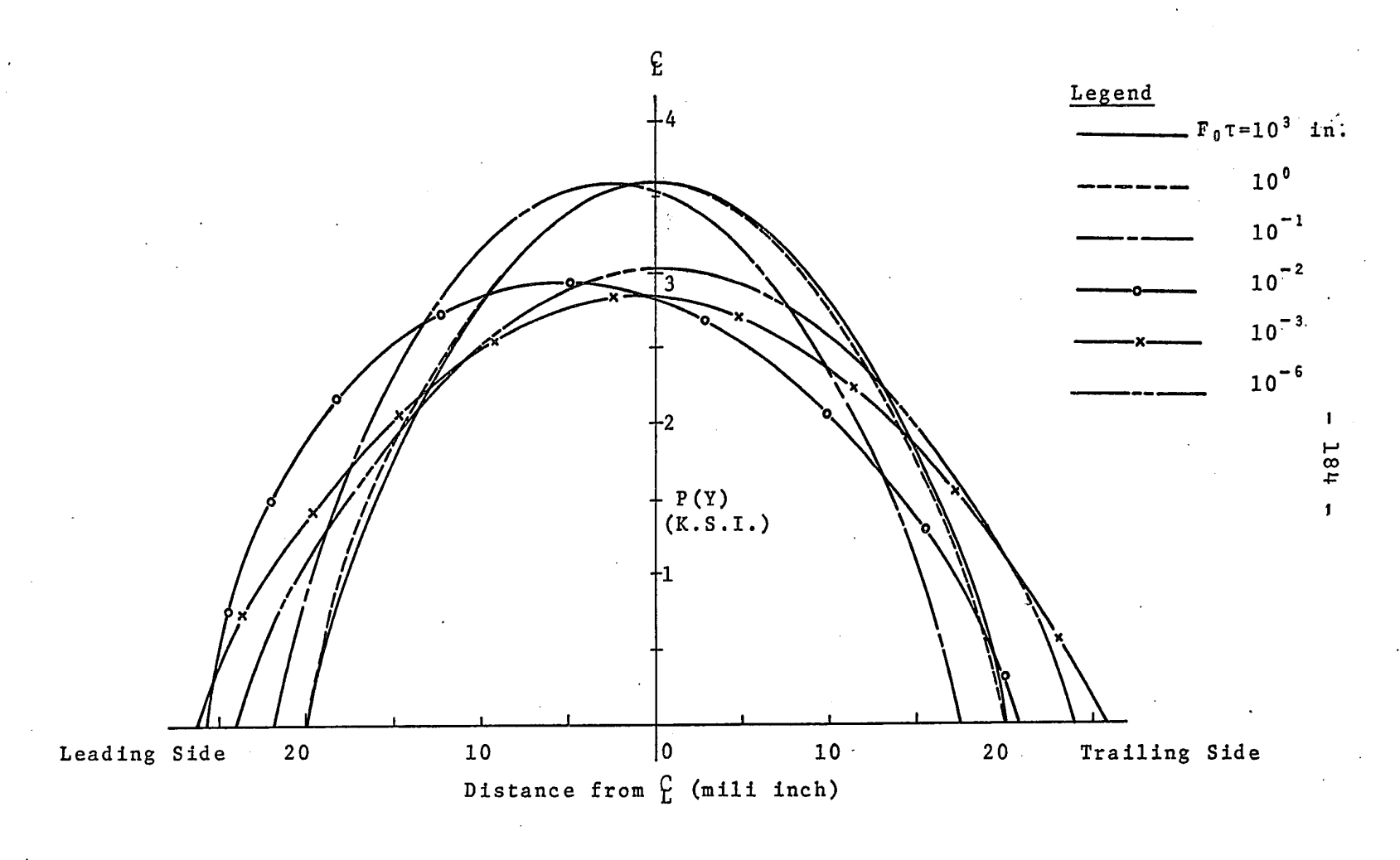
 $\frac{FIGURE~46}{VARIATION~OF~THE~RATIO~\frac{L}{B}~WITH~F_0\tau FOR}$  DIFFERENT NORMAL LOADS (B=0.005 in.)

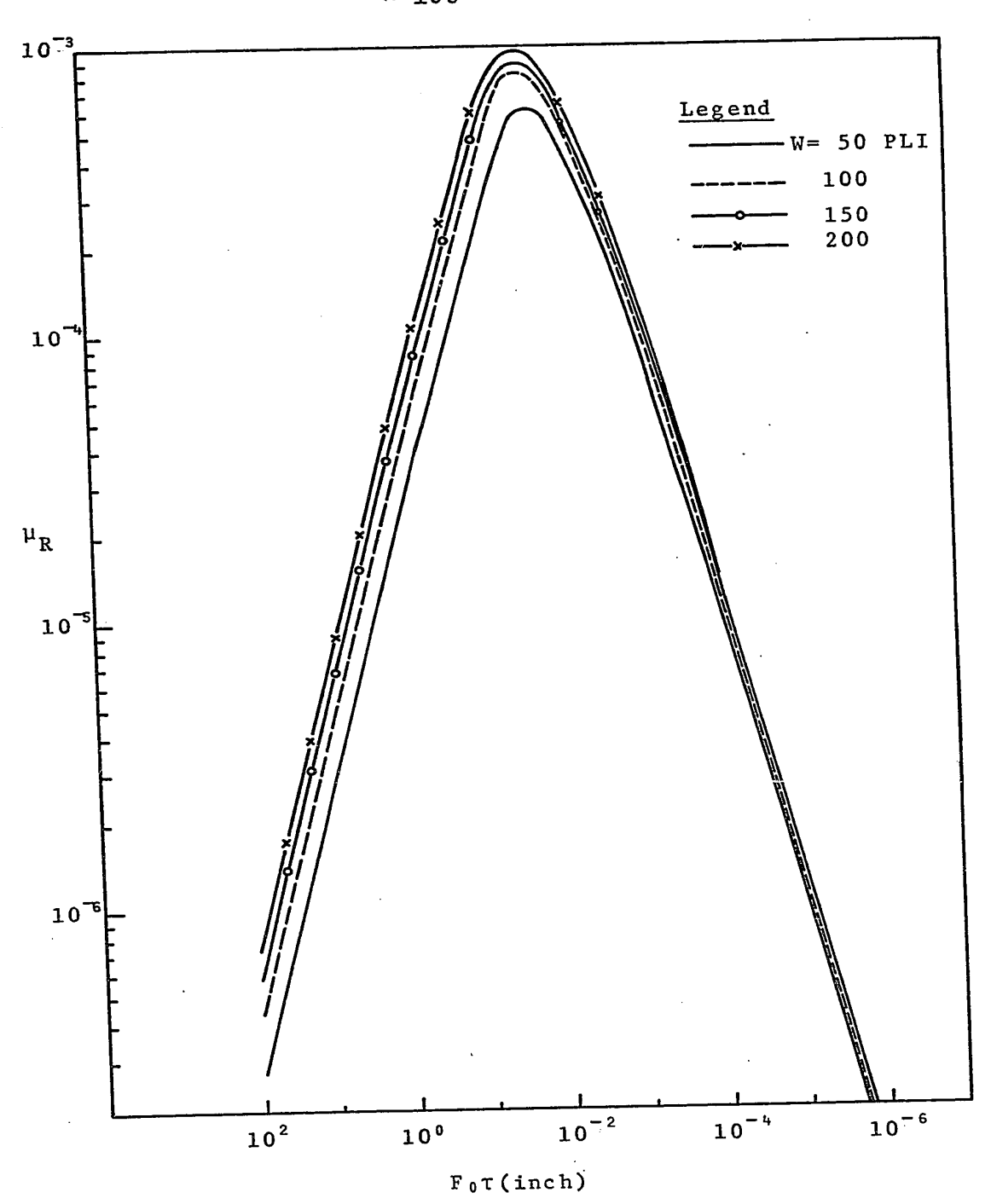


VARIATION OF THE RATIO  $\frac{d_0}{B}$  WITH Fotfor DIFFERENT NORMAL LOADS (B=0.005 in.)



 $\frac{\text{FIGURE 48}}{\text{VARIATION OF CREEP RATIO WITH F0TFOR DIFFERENT NORMAL LOADS}}$  (B=0.005 in.)





 $\frac{\text{FIGURE 50}}{\text{VARIATION OF THE COEFFICIENT OF ROLLING RESISTANCE WITH}}$   $\text{F_0TFOR DIFFERENT NORMAL LOADS (B=0.005 in.)}$ 

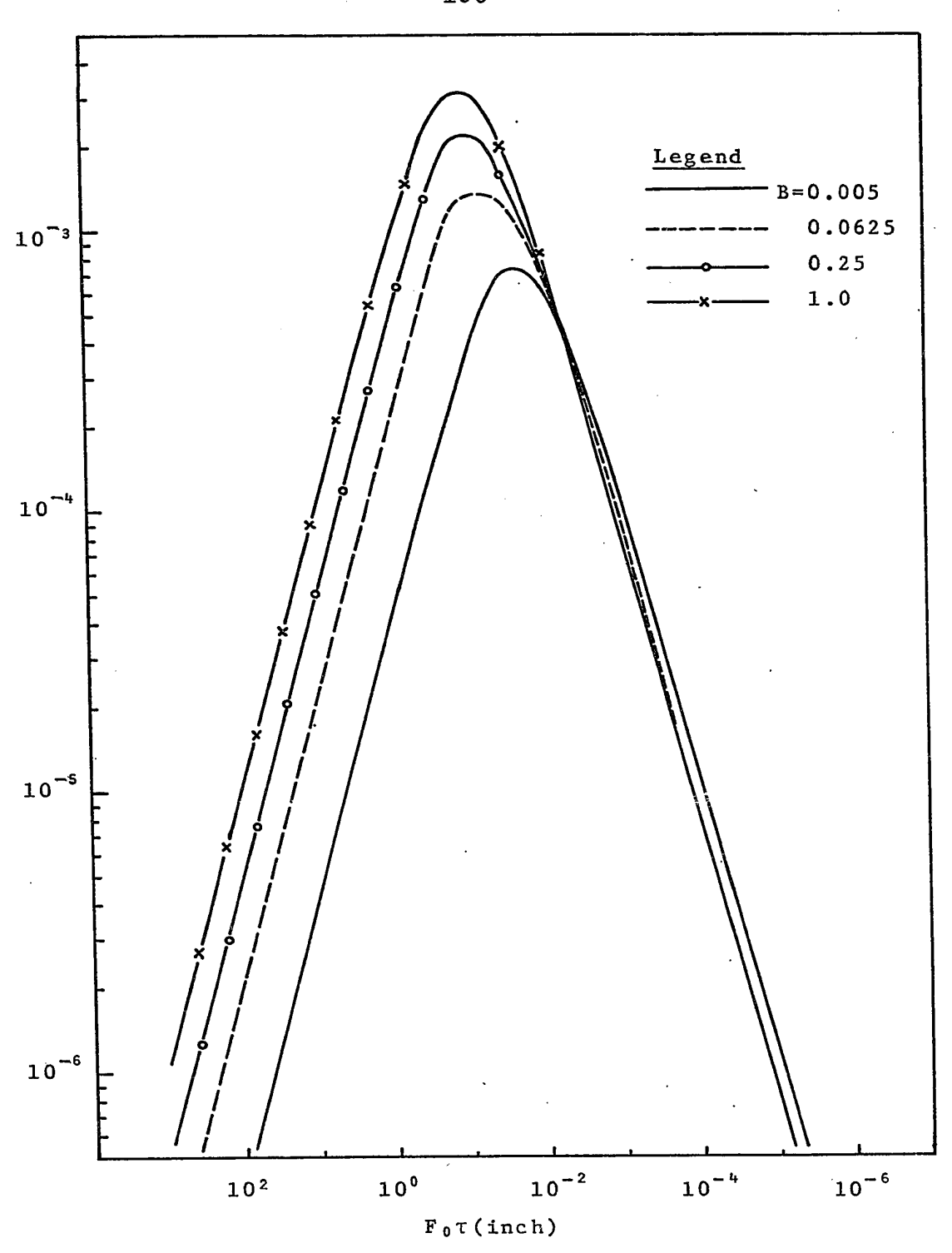


FIGURE 51

VARIATION OF THE COEFFICIENT OF ROLLING RESISTANCE WITH F $_0$ TFOR DIFFERENT THICKNESSES OF THE SHEET (W=100 P.L.T.)

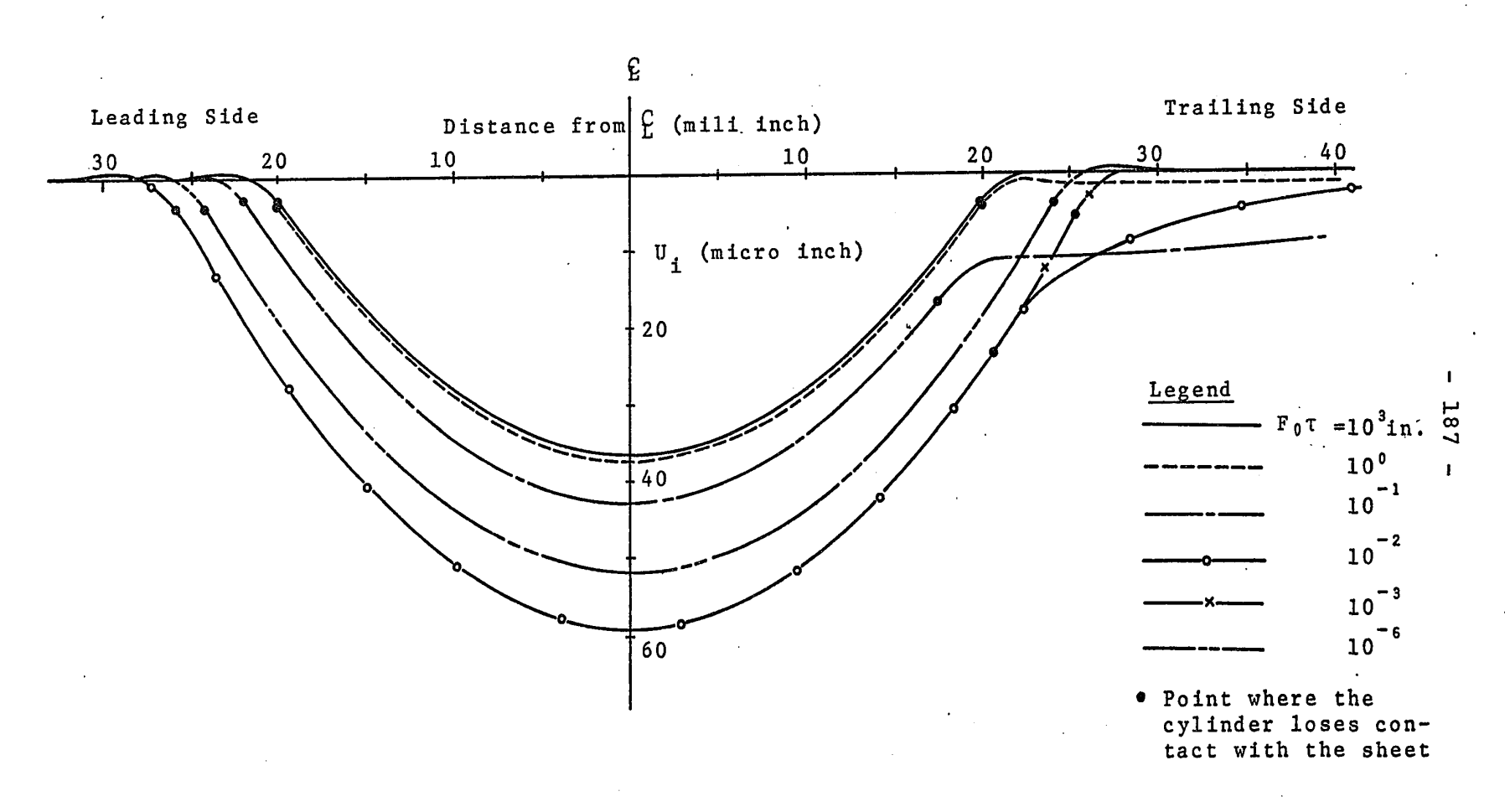
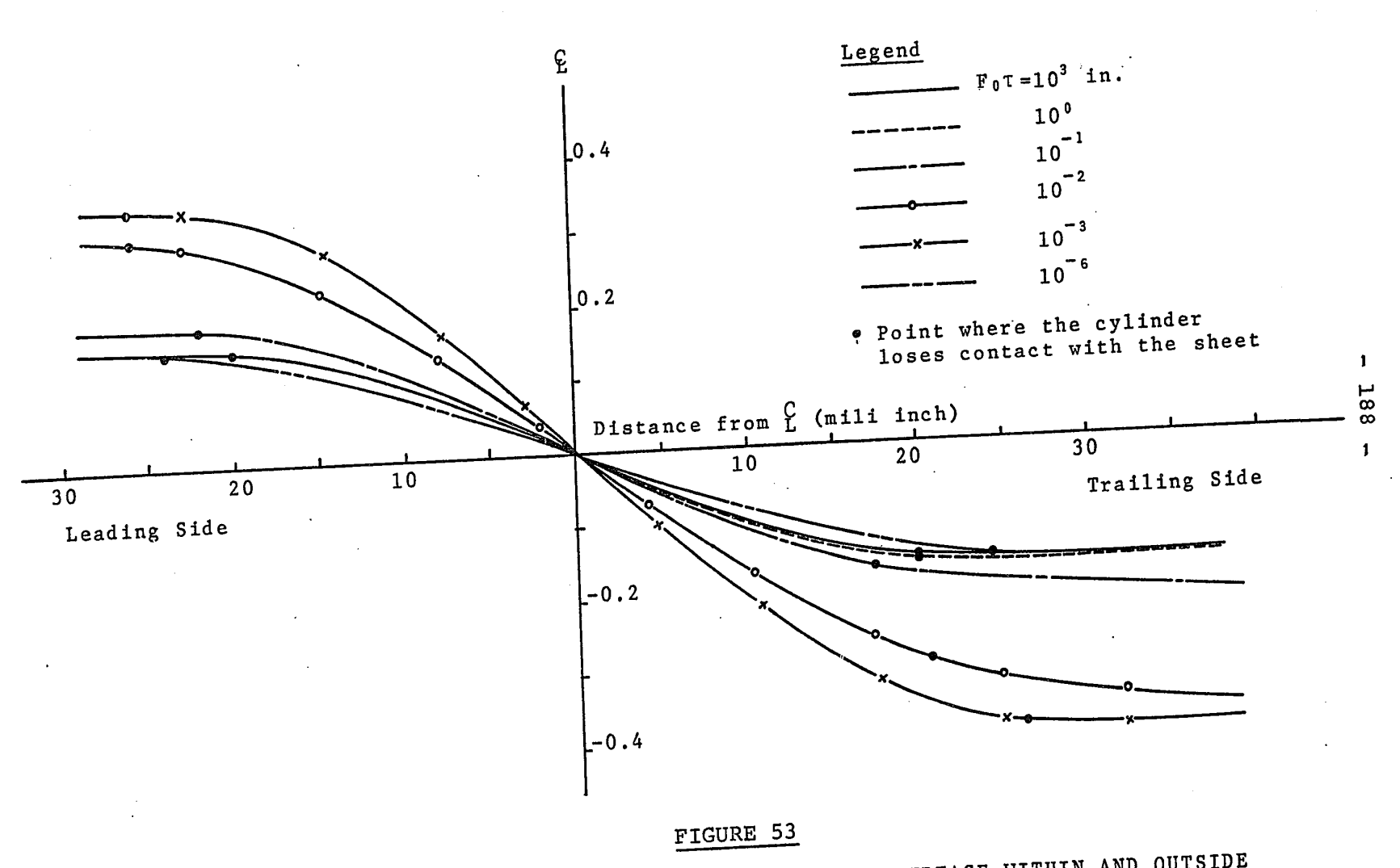
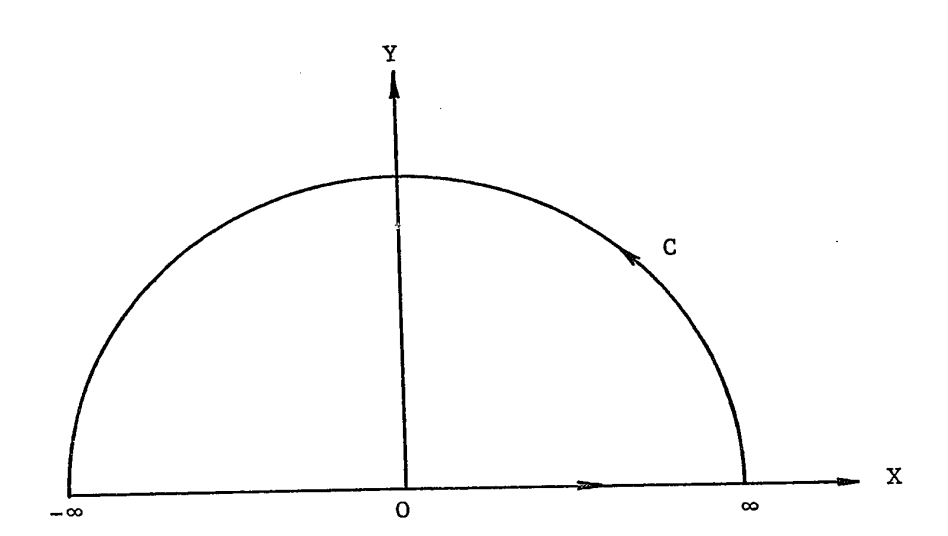


FIGURE 52

VARIATION OF THE NORMAL DISPLACEMENT OF THE SHEET SURFACE WITHIN AND OUTSIDE THE NIP WITH  $F_0\tau(B=0.005~in.,~W=100~P.L.I.)$ 



VARIATION OF THE SHEAR DISPLACEMENT OF THE SHEET SURFACE WITHIN AND OUTSIDE THE NIP WITH  $F_0\tau(B=0.005\ in.,\ W=100\ P.L.I.)$ 



 $\frac{\text{FIGURE 54}}{\text{CONTOUR C FOR THE EVALUATION OF INTEGRAL I}_{1}(\alpha)$ 

TABLES

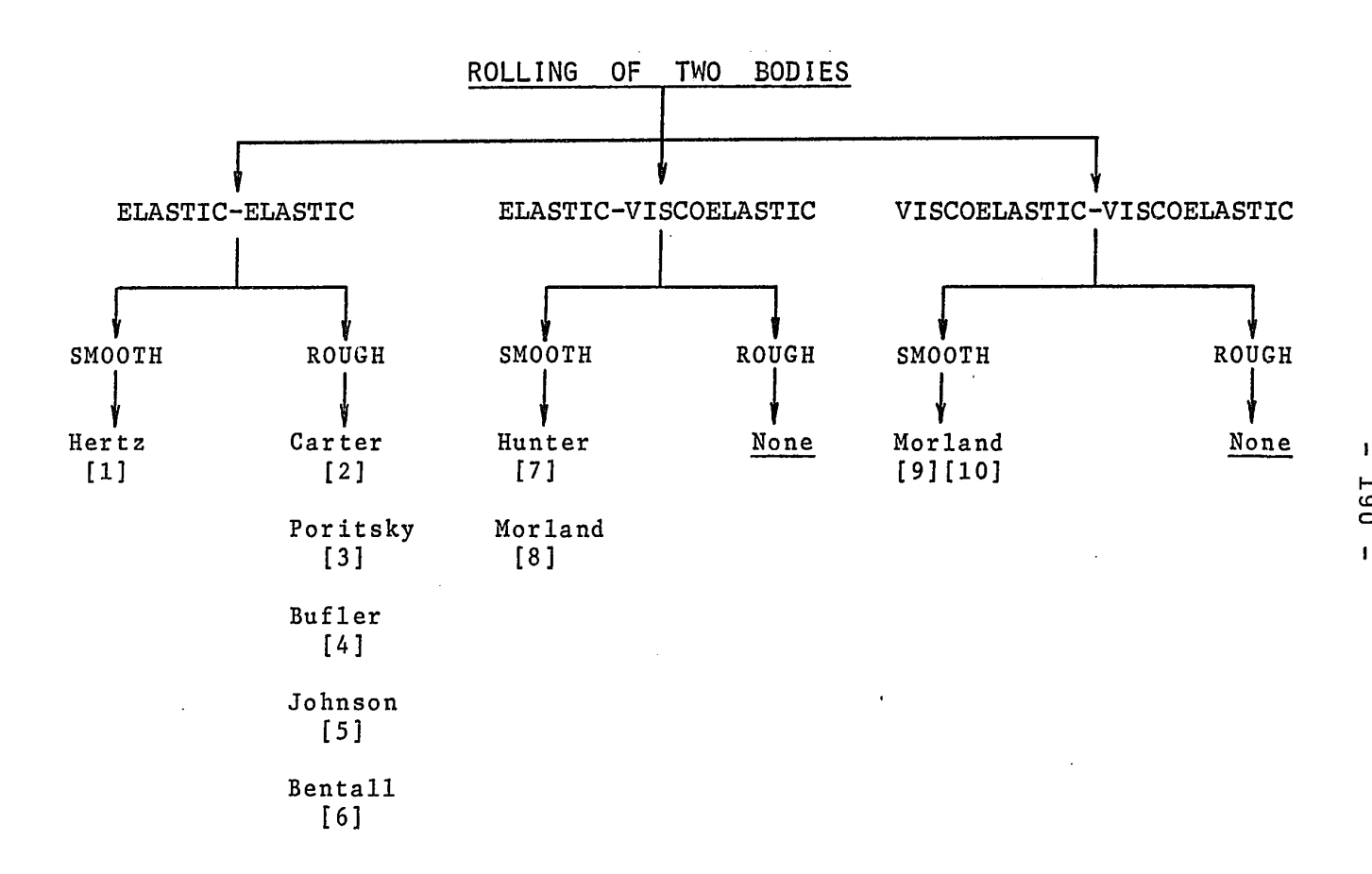


TABLE I

A BRIEF REVIEW OF THE LITERATURE INVOLVING THE ROLLING OF TWO BODIES

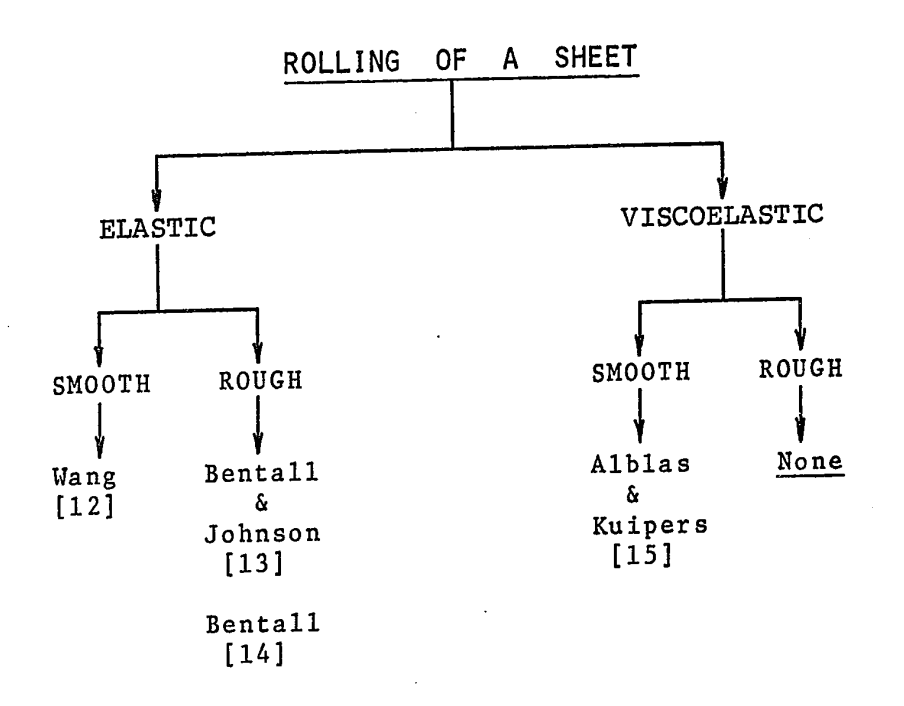


TABLE II

A BRIEF REVIEW OF THE LITERATURE INVOLVING THE ROLLING OF A SHEET

						,				~ ~	ĺ
M	L×10 <sup>3</sup>	do×10 <sup>6</sup>	d <sub>1</sub> ×10 <sup>6</sup> inch	x×10 <sup>4</sup>	p <sub>max</sub> psi	d <sub>1</sub> /B×1000	L/B	d <sub>o</sub> /B×100	d <sub>1</sub> /d <sub>o</sub>	≃ q <sub>max</sub> psi	
PLI	inch	inch	THCH			0.27382	0.05696	0.03414	0.80201	39.924	
25	56.9616	341.415	273.818	-10.613	488.802	0.47852	0.08048	0.06134	0.78005	56.183	
50	80.4768	613.446	478.519	-14.132	692.287	0.47832	0.09837	0.08597	0.76550	69.730	
75	98.3676	859.651	658.064	-16.501	844.185	0.82161	0.11335	0.10893	0.75426	81.730	,
100	113.352	1089.29	821.608	-18.280	979.664	·	0.12649	0.13069	0.74493	92.648	_ ا
125	126.492	1306.86	973.526	-19.686	1095.74	0.97353	0.1383	0.15144	0.73689	102.684	92
150	138.297	1514.42	1115.96	-20.827	1200.74	1.11596	0.14908	0.17133	0.72977	111.936	1
175	149.076	1713.289	1250.30	-21.767	1297.25	1.2503	0.15910	0.19058	0.72329	120.522	
200	150 10	1905.813	1378.45	÷22.554	1387.61	1.3784	0.13910		<u> </u>	1	_

# TABLE III

SOME RESULTS OF ELASTIC ROLLING FOR NO-SLIP CONDITION (B= 1 inch)

										1
W	L×10 <sup>3</sup>	d <sub>o</sub> ×10 <sup>6</sup> inch	d <sub>1</sub> ×10 <sup>6</sup> inch	x×10 <sup>4</sup>	p <sub>max</sub> psi	d <sub>1</sub> /B×1000	L/B	d <sub>o</sub> /B×100	d <sub>1</sub> /d <sub>o</sub>	≃ <sup>q</sup> max isg
<u> </u>		000 07	135.777	-5.41	490.38	0.54311	0.23563	0.08323	0.65255	46.217
25	58.908	208.07		-4.813	704.22	0.84611	0.32792	0.14062	0.60171	63.469
50	81.98	351.544	211.528	) " " "		1.0769	0.39614	0.18943	0.56852	74.809
75	99.036	473.563	269.228	-3.521	875.331	1	0.45185	0.23291	0.54344	83.414
100	112.963	582.278	316.433	-1.930	1023.74	1.2657		0.27299	0.52571	84.954
125	124.648	682.476	358.785	-0.5070	1163.27	1.4351	0.49859		1	i l
i	134.123	774.970	400.200	0.2751	1301.606	1.6008	0.53649	0.30999	0.51641	73.626
150		1	440.823	0.7164	1438.297	1.7633	0.56881	0.34485 .	0.51133	55.029
175	142.204	862.112	}		1572.63	1.9224	0.59695	0.37784	0.50878	31.673
200	149.238	944.591	480.590	0.9314	12/2.03	1.7224		<u> </u>	<u> </u>	<u> </u>

### TABLE IV

SOME RESULTS OF ELASTIC ROLLING FOR NO-SLIP CONDITION (B=0.25 inch)

W	L×10 <sup>3</sup> inch	d <sub>o</sub> ×10 <sup>6</sup> inch	d <sub>1</sub> ×10 <sup>6</sup> inch	x×10 <sup>4</sup>	p <sub>max</sub> psi	d <sub>1</sub> /B×1000	L/B	d <sub>o</sub> /B×100	d <sub>1</sub> /d <sub>o</sub>	≃ ɑmax psi
25	53.8016	96.8023	36.498	4.278	577.358	0.58397	0.86083	0.15488	0.37704	*
50	70.4337	152.541	49.189	9.987	885.508	0.78702	1.12694	0.24407	0.32246	*
75	81.8464	197.584	58.025	14.756	1149.199	0.9284	1.30954	0.31613	0.29367	34.148
100	90.7925	236.848	65.113	18.98	1389.173	1.0418	1.45268	0.37896	0.27491	55.651
125	98.4228	271.294	69.480	21.782	1625.531	1.11169	1.57477	0.43407	0.25611	85.388
150	104.845	303.481	74.472	25.121	1839.299	1.19156	1.67751	0.48557	0.24539	107.628
i75	110.536	333.255	78.709	28.081	2045.275	1.25935	1.76858	0.53321	0.23618	130.433
200	115.664	361.096	82.383	30.747	2244.799	1.31814	1.85063	0.57775		153.413

<sup>\*</sup> Very close to zero

#### TABLE V

SOME RESULTS OF ELASTIC ROLLING FOR NO-SLIP CONDITION (B=0.0625 inch)

	•								T			
	W	L×10 <sup>3</sup>	d <sub>o</sub> ×10 <sup>6</sup>	d <sub>1</sub> ×10 <sup>6</sup> inch	x×10 <sup>5</sup>	p <sub>max</sub> psi	d <sub>1</sub> /B×1000	L/B	d <sub>o</sub> /B×100	d <sub>1</sub> /d <sub>o</sub>	≃ <sup>q</sup> max psi	
						3.453	0.2440	5.0314	0.2881	0.0847	143	
	25	25.18	14.41	1.2201	119.32	1451	Į.	6.1438	0.4228	0.0701	222	
- {	50	30.72	21.14	1.4826	159.22	2409	0.2965		0.5253	0.0635	284	
Ì	75	34.36	26.27	1.6678	188.60	3246	0.3336	6.8724	l .	0.0595	338	
	100	37.13	30.53	1.8159	213.03	4017	0.3632	7.4252	0.6106		385	'
1			34.22	1.9405	234.32	4744	0.3881	7.8728	0.6844	0.0567		195
	125	39.36	1	2.0495	253.66	5447	0.4099	8.2542	0.7507	0.0546	429	5
	150	41.27	37.53	1		6122	0.4291	8.5828	0.8102	0.0530	470	'
İ	175	42.91	40.51	2.1454	271.13	}		8.8686	0.8639	0.0516	509	
l	200	44.34	43.20	2.2299	287.32	6788	0.4460	0.000		L		1

SOME RESULTS OF ELASTIC ROLLING FOR NO-SLIP CONDITION (B=0.005 inch)

W	L×10 <sup>3</sup> inch	d <sub>o</sub> ×10 <sup>6</sup> inch	d <sub>1</sub> ×10 <sup>6</sup> inch	x×10 <sup>4</sup>	p <sub>max</sub> psi	d <sub>1</sub> /B×1000	L/B	d <sub>o</sub> /B×100	d <sub>1</sub> /d <sub>o</sub>
25	57.9	342	272.11	-12.112	479	0.2721	0.0579	0.0342	0.7958
50	81.8	614.4	475.04	-16.261	679	0.4750	0.0818	0.0614	0.7733
75	100	861.2	652.63	-19.108	832	0.6526	0.1000	0.0861	0.7579
100	115.4	1091	813.42	-21.279	962	0.8134	0.1154	0.1091	0.7458
125	128.8	1308	962.51	-23.031	1077	0.9625	0.1288	0.1308	0.7357
150	140.9	1515	1101.4	-24.476	1181	1.1014	0.1409	0.1515	0.7269
175	152.0	1715	1233.1	-25.703	1277	1.2331	0.1520	0.1715	0.7191
200	162.3	1907	1358.3	-26.754	1367	1.3583	0.1624	0.1907	0.7121

TABLE VII

SOME RESULTS OF ELASTIC ROLLING FOR COMPLETE SLIP (B=1 inch)

W PL:	1	d <sub>o</sub> ×10 <sup>6</sup> inch	d <sub>1</sub> ×10 <sup>6</sup> inch	x×10 <sup>4</sup>	p <sub>max</sub> psi	d <sub>1</sub> /B×1000	L/B	d <sub>o</sub> /B×100	d <sub>1</sub> /d <sub>o</sub>	
25	62.5	211.4	130.13	-6.658	478	0.5205	0.2498	0.0846	0.6156	
50		357.9	200.72	-6.508	687	0.8029	0.3474	0.1431	0.5609	
7:		482.6	253.68	-5.494	855	1.0147	0.4193	0.1930	0.5257	ĺ
100		594.1	296.85	-4.126	1002	1.1874	0.4777	0.2376	0.4998	
125		696.5	333.85	-2.576	1136	1.3354	0.5277	0.2786	0.4794	
150		791.8	366.36	-0.933	1200	1.4654	0.5716	0.3167	0.4627	
179		881.5	395.50	0.7592	1377	1.5820	0.6109	0.3526	0.4487	
200	ļ	966.8	422.17	2.486	1489	1.6887	0.6468	0.3868	0.4366	

### TABLE VIII

SOME RESULTS OF ELASTIC ROLLING FOR COMPLETE SLIP (B=0.25 inch)

W IX10 <sup>3</sup> inch         d <sub>0</sub> ×10 <sup>6</sup> inch         d <sub>1</sub> ×10 <sup>6</sup> inch         x×10 <sup>4</sup> psi         pmax psi         d <sub>1</sub> /B×1000         L/B         d <sub>0</sub> /B×100         d <sub>1</sub> /d <sub>0</sub> 25         55.4         98.6         34.62         4.3         560         0.5539         0.8869         0.1578         0.3510           50         72.7         156.8         46.63         10.59         870         0.7461         1.1635         0.2509         0.2974           75         84.7         204.8         55.29         16.19         1134         0.8846         1.3554         0.3277         0.2700           100         94.2         247.1         62.35         21.31         1373         0.9976         1.5069         0.3954         0.2523           125         102.1         285.7         68.42         26.08         1594         1.0947         1.6339         0.4571         0.2394           150         109         321.4         73.81         30.59         1802         1.1809         1.7443         0.5143         0.2296           175         115.2         345.9         78.68         34.87         2000         1.2589         1.8424         0.5679         0.2217           175											
25         55.4         98.6         34.62         4.3         560         0.5539         0.8809         0.2509         0.2974           50         72.7         156.8         46.63         10.59         870         0.7461         1.1635         0.2509         0.2700           75         84.7         204.8         55.29         16.19         1134         0.8846         1.3554         0.3277         0.2700           100         94.2         247.1         62.35         21.31         1373         0.9976         1.5069         0.3954         0.2523           125         102.1         285.7         68.42         26.08         1594         1.0947         1.6339         0.4571         0.2394           150         109         321.4         73.81         30.59         1802         1.1809         1.7443         0.5143         0.2296           175         115.2         345.9         78.68         34.87         2000         1.2589         1.8424         0.6188         0.2151	į		· · · · · · · · · · · · · · · · · · ·		x×10 <sup>4</sup>		d <sub>1</sub> /B×1000	L/B	d <sub>o</sub> /B×100	d <sub>1</sub> /d <sub>o</sub>	
200   120.7   386.7   83.17   38.98   2109   2.5500	50 75 100 125 150 175	72.7 84.7 94.2 102.1 109 115.2	156.8 204.8 247.1 285.7 321.4	46.63 55.29 62.35 68.42 73.81	10.59 16.19 21.31 26.08 30.59	870 1134 1373 1594 1802	0.7461 0.8846 0.9976 1.0947 1.1809	1.1635 1.3554 1.5069 1.6339 1.7443	0.2509 0.3277 0.3954 0.4571 0.5143 0.5679	0.2974 0.2700 0.2523 0.2394 0.2296 0.2217	1

SOME RESULTS OF ELASTIC ROLLING FOR COMPLETE SLIP (B=0.0625 inch)

W	L×10 <sup>3</sup> inch	do×10 <sup>6</sup> inch	d <sub>1</sub> ×10 <sup>6</sup> inch	x×10 <sup>4</sup>	p <sub>max</sub> psi	d <sub>1</sub> /B×1000	L/B	d <sub>o</sub> /B×100	<sup>d</sup> 1∕d₀
25 50 75 100 125 150 175 200	26.4 32.6 36.8 40 42.7 44.9 46.8 48.6	16.3 24.6 31.1 36.6 41.5 45.8 49.8 53.5	1.77 2.38 2.83 3.22 3.56 3.87 4.15 4.41	28.48 46.75 62.56 77.03 90.66 103.59 116.03 127.93	1339 2179 2906 3571 4197 4791 5362 5908	0.3539 0.4758 0.5676 0.6447 0.7127 0.7741 0.8307 0.8829	5.2778 6.5286 7.3635 8.0042 8.5302 8.9762 9.3658	0.3255 0.4917 0.6216 0.7318 0.8292 0.9167 0.9968	0.1087 0.0968 0.0913 0.0881 0.0859 0.0844 0.0833

TABLE X

SOME RESULTS OF ELASTIC ROLLING FOR COMPLETE SLIP (B=0.005 inch)

For Lix103	L <sub>2</sub> ×10 <sup>3</sup> inch	L×10 <sup>3</sup>	d <sub>o</sub> ×10 <sup>6</sup> inch	d <sub>1</sub> ×10 <sup>6</sup> inch	d <sub>2</sub> ×10 <sup>6</sup> inch	L B	$\frac{d_0}{B} \times 10^2$	$\frac{d_1}{B} \times 10^2$	$\frac{d_2}{B} \times 10^2$	$\frac{d_1}{d_0}\kappa lo^2$	$\frac{d_2}{d_0} x i^{0}$	max psi	x×10 <sup>3</sup>	μ <sub>R</sub> ×10 <sup>6</sup>
• •	•	32.110	618.814	478.354	478.354	0.082	0.062	0.048	0.048	77.302	77.302	681	-1.632	0.60
103 41.055			619,531	479.070	479.070	0.082	0.062	0.048	0.048	77,328	77.328	683	-1:631	.6.08
10 <sup>2</sup> 41.055		82.110			485.995	0.082	0.063	0.049	0.049	77.582	77.582	694	-1.624	60.04
101 41.051	41.051		626.424	485.995			0.069							527.81
10° ·41.336	41.330	82.672	690,630	548.241	548.241	0.083	•			-				2224.08
10-1 52,436	26.218	78.654	949.125	720.000	891.845	n•079								
10-2 60,545	60.546	121.091	1050.325	744.844	744.844	c.121								795.91
10-3 56.197				778.217	778.217	0.112	0.104	0.078				•		83.67
10-4 56.086				779.131	779.131	0,112	0.104	0.078	0.078	74.825	74.825	500	-3.328	8.33
				779.141	779,141	4.112	0.104	0.078	0.078	74.826	74.826	499	-3.328	0.83
10 <sup>-5</sup> 56.085				779.141	779.141	0.112	0.104	0.078	0.078	74.826	74.826	499	-3,328	0.03

# TABLE XI

SOME RESULTS OF VISCOELASTIC ROLLING FOR COMPLETE SLIP (B=1 inch, W=50 P.L.I.)

F <sub>0</sub> τ inch	L <sub>1</sub> ×10 <sup>3</sup> inch	L <sub>2</sub> ×10 <sup>3</sup> inch	L×10 <sup>3</sup> inch	d <sub>0</sub> ×10 <sup>6</sup> inch	d <sub>1</sub> ×10 <sup>6</sup> inch	d <sub>2</sub> ×10 <sup>6</sup> inch	L B	$\frac{d_0}{B} \times 10^2$	$\frac{d_1}{B}x10^2$	$\frac{d_2}{B} \times 10^2$	$\frac{d_1}{d_0} \times 10^2$	d2 x102	P <sub>max</sub> psi	x×10 <sup>3</sup>	μ <sub>R</sub> ×10 <sup>6</sup>
103	57.800	57.600	115.600	1094.579	816,175	816.175	0.116	0.109	0.082	0.082	74.555	74.565	964	-2,131	1.07
10²	57,800	57,300	115.600	1096.004	817,600	817.600	0.116	0.110	0.082	0.082	74.599	74.598	966	-2,130	10.76
101	57,778	57.778	115.555	1109.185	830.998	830.998			0.083			•			
10°	59,489	58.489	116.978	1238.694	953.615	953.615	0.117	0.124	0.095	0.095	76.986	76.986	1149	-2.040	919.08
10-1	77,492	38.701	116.104			1597.854									3245.21
						1238.132									839.83
						1302.236									83.58
						1300.175									8.34
						1300.203									0.83
						1300.203									0.08

## TABLE XII

SOME RESULTS OF VISCOELASTIC ROLLING FOR COMPLETE SLIP (B=1 inch, W=100 P.L.I.)

F <sub>0</sub> τ	$L_1 \times 10^3$ $L_2 \times 10^3$ inch inch	3 L×10 <sup>3</sup> inch	d <sub>0</sub> ×10 <sup>6</sup> inch	d <sub>1</sub> ×10 <sup>6</sup> inch	d <sub>2</sub> ×10 <sup>6</sup> inch	L B	$\frac{d_0}{B}$ x10 <sup>2</sup>	$\frac{d_1}{B}$ x10 <sup>2</sup>	$\frac{d_2}{B} \times 10^2$	$\frac{d_1}{d_0} \times 10^{-1}$	2 <u>d<sub>2</sub> xi0 psi</u>	x×10 <sup>3</sup>	μ <sub>R</sub> ×10 <sup>6</sup>
10³	70,253 70.2	8 140.517	1508.258	1096.905	1095.905	0.141	0.151	0.110	0.110	72.727	72.727 117	3 -2,443	1.48
10²	70.253 70.2	8 140.517	1510.376	1099.021	1099.021	0.141	0.151	0.110	0.110	72.765	72.765 118	-2,441	14.82
101	70.263 70.26	3 140.526	1531.071	1119.667	1117.667	0.141	0.153	0.112	0.112	73+130	73.130.120	-2.421	145.74
100	71.270 71.27	0 142.539	1718,100	1294.829	1294.829	0.143	0.172	0.129	0.129	75.364	75.364 142	2 -2,297	1250.15
10-1	95,985 47,99	2 143.977	2393.749	1625.993	2201.810	0.144	0.239	0.163	0.220	67.927	91.982 1166	-2,155	3933.22
10-2	100.961 100.96	1 201.922	2510.341	1660.911	1660.911	n.202	0.251	0.166	0.166	66.163	66.163 94	-4.691	860.35
10-3	95,717 95.71	7 191.435	2484.986	1721.500	1721.500	0.191	0.248	0.172	0.172	69.276	69.276 878	-5.080	83.62
10-4	95.644 95.64	4 191.288	2484.469	1722.155	1722-155	0.191	0.248	0.172	0.172	69.317	69.317 86	-5.085	8.35
10-5	95.643 95.64	3 191.287	2484.467	1722.163	1722.163	0.191	0.248	0.172	0.172	69.317	69.317 866	-5.085	0.84
10-6	95,643 95,64	3 191.287	2484.467	1722.163	1722.163	0.191	0.245	0.172	0.172	69.317	69.317 866	-5.085	0.08

# TABLE XIII

SOME RESULTS OF VISCOELASTIC ROLLING FOR COMPLETE SLIP (B=1 inch, W=150 P.L.I.)

$F_0\tau$ inch	L <sub>1</sub> ×10 <sup>3</sup> inch	L <sub>2</sub> ×10 <sup>3</sup> inch	L×10 <sup>3</sup> inch	d <sub>0</sub> ×10 <sup>6</sup> inch	d <sub>1</sub> ×10 <sup>6</sup> inch	d <sub>2</sub> ×10 <sup>6</sup> inch	<u>L</u> B	$\frac{d_0}{B} \times 10^2$	$\frac{d_1}{B} \times 10^2$	$\frac{d_2}{B} \times 10^{-2}$	$\frac{d_1}{d_0} \times 10^2$	$\frac{d_2}{d_0}$ x10 $\frac{d^2}{d_0}$ psi	x×10 <sup>3</sup>	μ <sub>R</sub> ×10 <sup>6</sup>
10³	80,643	80.843	161.685	1894.959	1350.332	1350.332	0.162	0.189	0.135	0.135	71.259	71.259 1362	-2.569	1.85
10²	80,843	3C,843	161.655	1897.777	1353.147	1353.147	0.162	0.190	0.135	0.135	71.302	71,302 1365	-2,566	18.61
101	80.852	80.852	161.704	1925,361	1380.608	1360.608	0.162	0.193	0.138	0.138	71.706	71.706 1400	-2.639	182.87
10°	82,268	22.268	164.537	2173,061	1609.053	1609.053	0.165	0.217	0.161	0.161	74.045	74.045 1660	-2,467	1556.70
10-1	111,987	55,993	167,980	3028.062	1982.979	2766.791	0.168	. 0.303	0.193	0.277	65.487	91.372 1347	-2.184	4479.99
10-2	115,142	115,142	230.285	3132.806	2027.993	2027.993	0.230	0.313	0.203	0.203	64.734	64.734 1095	-5,228	870.94
10-3	109,932	109.932	219.865	3101.397	2094.302	2094.302	0.220	0.310	0.209	0.209	67.528	67,528 1015	-5,606	83.69
10-4	109.867	109.867	219.734	3100.822	2094.928	2094.928	0.220	0.310	0.209	0.209	67.560	67.560 1004	-5.610	8.36
10-5	109.866	109.866	219.733	3100.819	2094.936	2094.936	0.220	0.310	0.509	0.209	67.561	67.561 1003	-5.510	0.84
10-6	109.866	109,866	219.733	3100.819	2094.937	2094.937	0.220	0.310	0.209	0.209	67.561	67.561 1003	-5.610	80.0

# TABLE XIV

SOME RESULTS OF VISCOELASTIC ROLLING FOR COMPLETE SLIP (B=1 inch, W=200 P.L.I.)

F <sub>0</sub> τ inch	L <sub>1</sub> ×10 <sup>3</sup>	L <sub>2</sub> ×10 <sup>3</sup> inch	L×10 <sup>3</sup> inch	d <sub>0</sub> ×10 <sup>6</sup> .	d <sub>1</sub> ×10 <sup>6</sup> inch	d <sub>2</sub> ×10 <sup>6</sup> inch	L B	$\frac{d_0}{B}$ x10 <sup>2</sup>	$\frac{d_1}{B} \times 10^2$	$\frac{d_2}{B} \times 10^2$	$\frac{d_1}{d_0} \times 10^2$	$\frac{d_2}{d_0} x i 0^2$	P <sub>max</sub> psi	*×10 <sup>3</sup>	$\mu_R$ ×10 <sup>6</sup>
10³	43.518		87.036	359.107	201.289	201.287	0.348	0.144	0.081	0.081	56.053	56.053	689	-0.650	0.33
10 <sup>2</sup>		43.518	87.036	359.286	201.467	201.467	0.348	0.144	0.081	0.081	56.074	56.074	690	0.649	3.28
10 <sup>1</sup>	43.522		87.044	361.095	203.250	203.250	0.348	0.144	0.081	0.081	56.297	56.287	701.	-0.542	32.69
100	43,578		87.355	378.512	219.534	219.534	0.349	0.151	0.088	0.088	57,999	57.999	797	-0.577	306.89
10	·	43.731	98.395	490.535	241.526	331.169	0.394	0.196	0.097	0.132	49.237	67.512	797	-0.219	1650.66
10			121.171	575.042	269.160	269.160	0.485	0.230	0.108	0.108	46.807	46.807	521	-1,436	702.36
10			117.207	568,843	282.646	282.646	0.469	0.228	0.113	0.113	49.688	49.688	527	-1:609	80.79
10			116.167	568,269	287.125	287.125	0.465	0.227	0.115	0.115	50.526	50.526	518	-1.642	7.93
			116.156	568.266	287.179	287.179	0.465	0.227	0.115	0.115	50.536	50.535	517	-1,642	0.79
10 <sup>-5</sup>	•		116.156	568.266	287.180	267.180	0.465	0.227		0.115	50.536	50.536	516	-1.642	0.08
TA															

# TABLE XV

SOME RESULTS OF VISCOELASTIC ROLLING FOR COMPLETE SLIP (B=0.25 inch, W=50 P.L.I.)

F <sub>0</sub> τ inch	L <sub>1</sub> ×10 <sup>3</sup> inch	L <sub>2</sub> ×10 <sup>3</sup> inch	L×10 <sup>3</sup> inch	d <sub>0</sub> ×10 <sup>6</sup> inch	d <sub>1</sub> ×10 <sup>6</sup> inch	d <sub>2</sub> ×10 <sup>6</sup> inch	<u>L</u> B	do x102	$\frac{d_1}{B} \times 10^2$	$\frac{d_2}{B} \times 10^2$	$\frac{d_1}{d_0} \times 10^2$	$\frac{d_2}{d_0}$ x10 <sup>2</sup> $p_{max}$	x×10 <sup>3</sup>	$\mu_R^{\times}10^6$
10³	59.750	59.750	119.500	594.618	297.113	297.113	0.478	0.238	0.119	0.119	49.967	49,967 1003	-0.412	0.54
10²	59,753		119.500	594.973	297.468	297,468	<b>0.47€</b>	0.238	0.119	0.119	49.997	49.997 1005	-0,410	5.39
10¹	59.875	59.875	119.750	600.471	301.719	301.719	0.479	0.240	0.121	0.121	50.247	50.247 1025	-0.393	53.73
10°	60.197	60,197	120.394	634.939	332.968	332,968	0.482	0.254	0.133	0.133	52.441	52.441 1185	-0.260	498.01
10-1			135.000	828.816	360.066	528,816	0.540	0.332	0.144	0.212	43.443	63.804 1027	0.425	2249.45
10-2			164.250	936.759	374.715	374.715	0.657	c.375	0.150	0.150	40.001	40.001 765	-1,334	731.04
10-3			157.500	919.197	402+400	402.400	n.630	0,368	0.161	0.161	43.777	43.777 775	-1.574	80.75
10-4			157.500	926.399	409.603	409,603	0.630	0.371	0.164	0.164	44.214	44.214 768	~ļ.597	7.99
			157.500	926.479	409.692	409.682	0.630	0.371	0.164	0.164	44.219	44.219 766	-1.597	0.80
			157.500	926.480	409.693	409.683	0.630	0.371	0.164	0.164	44.219	44.219 766	-1.597	80.0

TABLE XVI

SOME RESULTS OF VISCOELASTIC ROLLING FOR COMPLETE SLIP (B=0.25 inch, W=100 P.L.I.)

									•					
F <sub>0</sub> τ inch	L <sub>1</sub> ×10 <sup>3</sup> inch	L <sub>2</sub> ×10 <sup>3</sup> inch	L×10 <sup>3</sup>	d <sub>0</sub> ×10 <sup>6</sup> inch	d <sub>1</sub> ×10 <sup>6</sup> inch	d <sub>2</sub> ×10 <sup>6</sup> inch	$\frac{L}{B}$	$\frac{d_0}{B}$ $\times 10^2$	$\frac{d_1}{B} \times 10^2$	$\frac{d_2}{B} \times 10^2$	$\frac{d_1}{d_0} \times 10^2$	$\frac{d_2}{d_0}$ xlo $\frac{2}{2}$ $\frac{p}{max}$	××10 <sup>3</sup>	μ <sub>R</sub> ×10 <sup>6</sup>
			142.377	787.195	364.866	364.866	0.570	0.315	0.146	0.146	46.351	46.351 1254	-0.101	0.71
			142.377	787.713	365.394	365,394	0.570	0.315	0.146	0.146	46.337	46.387 1257	-0.099	7.11
			143.132	800.135	373.029	373.029	0.573	0.320	0.149	0.149	46.621	46.621 1291	-0,065	71.17
			144.141	851.200	418.353	418.353	0.577	0.340	0.167	0.167	49.149	49.149 1503	0.137	653.66
				1117.152	445.844	687.515	r.646	0.447	0.178	0.275	39,909	61.542 1219	1,138	2529.43
				1237.657	448.291	448.291	n.779	0.495	0.179	0.179	35.221	36.221 970	~1:115	748.51
				1218.118	490.403	490.408	<b>1.748</b>	0.487	0.196	.0.196	40.259	40.259 988	-1.393	80.99
					495.133	495.133	0.745	0.487	0.198	0.198	40.685	40.685 972	-1.415	8.04
				1216.980	495.185	495.185	0.745	0.487	0.193	0.198	40.690	40.690 970	-1.416	0.80
				1216,969		495.185		0.487				40.690 970	100	0.08
10	93.067	93.067	136.133	1216.969	495.185	4254703	··• ( 172	C 9 1001				•	•	-

# TABLE XVII

SOME RESULTS OF VISCOELASTIC ROLLING FOR COMPLETE SLIP (B=0.25inch, W=150 P.L.I.)

F <sub>0</sub> τ inch	L <sub>1</sub> ×10 <sup>3</sup> L <sub>2</sub> inch i	×10 <sup>3</sup> L>	10 <sup>3</sup> đ <sub>0</sub> ,	(10 <sup>6</sup> d <sub>1</sub> × nch in	10 <sup>6</sup> d <sub>2</sub> ×1 ch inc	$0^6$ $\frac{L}{B}$	$\frac{d_0}{B} \times 10^2$	$\frac{d_1}{B} \times 10^2$	$\frac{d_2}{B} \times 10^2$	$\frac{d_1}{d_0} \times 10^2$	$\frac{d_2}{d_0} \times 10^2$	р <sub>таж</sub> psi	**10 <sup>3</sup>	μ <sub>R</sub> ×10 <sup>6</sup>
10³	80.735 80	.736 161	473 964	.77í 421	.574 421.	574 0.646	0.386	0.169	0.169	43.697	43,697	1486	0.244	. 0.86
10²	80.736 80	.736 161	473 965	.479 422	.281 422.	281 0.646	0.386	0.169	0.169	43.738	43.738	1489	. 0.247	8.69
101	80,743 80	,743 161	487 972	,534 429	.241 429.	241 0.646	0.389	j n.172	0.172	44,136	44.136	1521	0.275	86.22
10°	81.368 81	.368 162	737 1039	.387 487	.653 487.	653 0.651	0.416	0.195	0.195	46.917	46,917	1780	0.543	786.18
10-1	101.715 81	.372 183.	697 1376	985 514	.323 825.	202 0,732	0.551	0.206	0.330	37.338	59.928	1391	1.861	2909.82
10-2	109,469 109	,469 218	937 1505	958 507	.341 507.	341 0.876	0.602	0.203	0.203	33.689	33,689	1156	-0,861	761.92
10-3	105.010 105	.010 210.	n20 1479	411 560	.487 56c.	467 ^.840	0.592	0.224	0.224	37,886	37,886	1176	-1,166	81.28
10-4	104,669 104	.669 209.	337 1478	238 565	.276 565.	276 0.837	0.591	0.226	0.226	38.240	38,240	1159	-1.186	8.09
10-5	104;665 104	.665 209	330 1478	223 565	.326 565.	326 n.837	0.591	0.226	0.226	38,244	38.244	1157	-1.186	0.81
10-6	104.065 164	.665 209	330 1478	224 565	.327 565.	327 r.837	0.591	0.226	0.226	38.244	38.244	1157	-1.186	C.08

## TABLE XVIII

SOME RESULTS OF VISCOELASTIC ROLLING FOR COMPLETE SLIP (B=0.25 inch, W=200 P.L.I.)

· F <sub>0</sub> τ inch	L <sub>1</sub> ×10 <sup>3</sup> inch	L <sub>2</sub> ×10 <sup>3</sup> inch	L×10 <sup>3</sup> inch	d <sub>o</sub> ×10 <sup>6</sup> inch	d <sub>1</sub> ×10 <sup>6</sup> inch	d <sub>2</sub> ×10 <sup>6</sup> inch	<u>L</u> B	$\frac{d_0}{B} \times 10^2$	$\frac{d_1}{B}$ x10 <sup>2</sup>	$\frac{d_2}{B}$ x 10 <sup>2</sup>	$\frac{d_1}{d_0} \times 10^2$	$\frac{d_2}{d_0} \times 10^{2} p_m$	ax si	*×10 <sup>3</sup>	μ <sub>R</sub> ×10 <sup>6</sup>
10³	35.312	35.312	70.625	153.593	49.679	49.679	1.130	0.246	0.079	0.079	32.344	32.344	184	1.049	0.14
10²	35.312	35.312	70.625	153.638	49.723	49.723	1.130	0.246	0.080	0.080	32.364	32.364 8	185 .	1.050	1.40
10¹	35.312	35.312	70.625	154.081	50.167	50.167	1.130	0.247	0.080	0.080	32,559	32,559 8	191	1.057	13.97
10°	35.275	35.275	70.550	157.813	54.120	54.120	1.129	0.253	0.087	0.087	34.294	34.294 9	45	1,120	134.01
10-1	40,294	32,235	72.529	190.954	55.653	104.361	1.160	0.306	0.039	0.167	29.145	54.653 8	177	1,672	901.74
10-2	46.543	46.543	93.087	237.334	56.811	56.811	1.489	0.380.	0.091	0.091	23.937	23.937 7	2.2	2.636	686.82
10-3	45.131	45.131	90.263	230.975	61.239	61.239	1.444	0.370	0.098	0.098	26.513	26.513 7	22	0.481	87.55
10-4	44.483	44.463	88.966	229.873	64.978	64.978	1.423	0.368	0.104	0.104	28.267	28.267 7	17	0.447	8.40
10-5	44,475	44.475	88.951	229.869	65.031	65.031	1.423	0.368	0.104	0.104	28.290	28.290 7	14	0.447	0.84
10-6	44,475	44,475	88.951	229.869	65.032	65.032	1.423	0.368	0.104	0.104	28.291	28.291 7	13	0.447	0.08

### TABLE XIX

SOME RESULTS OF VISCOELASTIC ROLLING FOR COMPLETE SLIP (B=0.0625 inch, W=50 P.L.I.)

·Foτ		L <sub>2</sub> ×10 <sup>3</sup> inch	L×10 <sup>3</sup> inch	d <sub>o</sub> ×10 <sup>6</sup> inch	d <sub>1</sub> ×10 <sup>6</sup> inch	d <sub>2</sub> ×10 <sup>6</sup> inch	L B	$\frac{d_0}{B}x10^2$	$\frac{d_1}{B} \times 10^2$	$\frac{d_2}{B}$ x 10 <sup>2</sup>	$\frac{d_1}{d_0} \times 10^2$	$\frac{d_2}{d_0} x lo^2 P_{\text{max}}$	x×10 <sup>3</sup>	μ <sub>R</sub> ×10 <sup>6</sup>
inch	inch 45,497	45,497	90.994	239.319	66.821	56.821	1.456	0.383	0.107	0.107	27.921	27.921 1395	2,133	0.22
103	-	45.497	90.994	239.407	66.909	66.909	1.456	0.383	9.107	0.107	27.948	27,948 1396	2.135	2.23
10 <sup>2</sup>			91.025	240.433	67.817	67.817	1.456	0.385	0.109	0.109	28+206	28.206 1498	ݕ151	22.23
101	45.512			249.080	75.796	75.796	1.459	0.399	0.121	0.121	30.430	30,430 1510	2.292	212.32
100		45,671	91.201 95.187	306.985	73.945	157.839	1.523	0.491	0.118	0.253	24.087	51.416 1397	3.331	1205.73
10-1	52,882		-	371.080	73.026	73.026	1.914	0.594	0.117	0.117	19.679	19.679 1135	4,648	734.59
_			119.610	•	83.392	83.392	1.840			0.133	23.235	23.235 1160 .	1,335	89.73
10-3			115.000	358.913		87.354	1.818	0.570				24.523 1144	1.302	8.66
10-4			113.600	356.207	87.354	87.419	1.818	0.570				24.537 1141	1.302	0.87
10-5			113.600	356.272	87.419		1.818	0.570	0.140			24.537 1141	1.302	0.09
10-6	156,800	56,600	113.600	356.273	87.420	87.420	Tearc	1192711	0 # 1 4 0					

TABLE XX

SOME RESULTS OF VISCOELASTIC ROLLING FOR COMPLETE SLIP (B=0.0625 inch, W=100 P.L.I.)

F <sub>0</sub> τ inch	L <sub>1</sub> ×10 <sup>3</sup> inch	L <sub>2</sub> ×10 <sup>3</sup> inch	L×10 <sup>3</sup> inch	d <sub>0</sub> ×10 <sup>6</sup> inch	d <sub>1</sub> ×10 <sup>6</sup> inch	d₂×10 <sup>6</sup> inch	<u>L</u> .	$\frac{d_0}{B} \times 10^2$	$\frac{d_1}{B} \times 10^2$	$\frac{d_2}{B} \times 10^2$	$\frac{d_1}{d_0} \times 10^2$	$\frac{d_2}{d_0}$ $\times 10^2$ $psi$	x×10 <sup>3</sup>	μ <sub>R</sub> ×10 <sup>6</sup>
10³	52.500	52.500	105.000	309.081	79.393	79.393	1.680	0.495	0.127	0.127	25.687	25.687 1833	3,080	0.29
10 <sup>2</sup>	52,500	52.500	105.000	309,213	79.526	79.526	1.680	0.495	0.127	0.127	25.719	25,719 1835	3.082	2.93
10¹	52,500	52,500	105.000	310,527	80.840	80.840	1.680	0.497	0.129	0.129	26.033	26.033 1851	3,104	29.21
10°			105.000	321.913	92.226	92.226	1.680	0.515	0.148	0.148	28.649	28.649 1992	3.292	276.04
10-1	61.553	49.482	111.335	406.972	88.156	202.930	1.781	0.651	0+141	0.325	21.661	49.863 1835	4.847	1576.21
_			138.224	482.747	84.703	84.706	2.212	0.772	0.136	0.136	17.547	17.547 1493	6.822	766.45
_			131.506	459.725	99.435	99.435	2.104	0.736	0.159	0.159	21.629	21.629 1526	2.073	91.33
_			130.346	457,695	103.733	103.733	2.086	0.732	0.166	0.166	22.664	22.564 1509	2.051	8,86
_			130.334	457,679	103.785	103.785	2.085	0.732	U.166	0.166	22.676	22.676 1506	2.051	0.99
						103.785	2.085	0.732	0.166	0.166	22.676	22.675 1505	2:051	0.09

TABLE XXI

SOME RESULTS OF VISCOELASTIC ROLLING FOR COMPLETE SLIP (B=0.0625 inch, W=150 P.L.I.)

$F_0\tau$ inch	L <sub>1</sub> ×10 <sup>3</sup> L <sub>2</sub> ×10 <sup>3</sup> inch inch	L×10 <sup>3</sup>	d <sub>o</sub> ×10 <sup>6</sup> inch	d <sub>1</sub> ×10 <sup>6</sup>	d <sub>2</sub> ×10 <sup>6</sup> inch	L B	₫ <sub>0</sub> x10 <sup>2</sup>	$\frac{d_1}{B}$ × 10 <sup>2</sup>	$\frac{d_2}{B} \times 10^2$	$\frac{d_1}{d_0} \times 10^2$	$\frac{d_2}{d_0}$ $x^{10}$ $psi$	x×10 <sup>3</sup>	μ <sub>R</sub> ×10 <sup>6</sup>
10³	58,125 58,125		371.51n	89.967	89.967	1.860	0.594	0.144	0.144	24.217	24,217 2240	3.965	0.35
10²	58,125 58,125	116.250	371.688	90.145	90.145	1.860	0.595	0.144	0.144	24.253	24.253 2242	3,968	3.59
10¹	58.156 58.156	116.312	373.812	91.966	91.906	1.861	0.598	0.147	0.147	24.602	24.602 2265	4:001	35.71
10°	58.190 58.190	116.380	389,243	107.076	107.076	1.862	0.623	0.171	0.171	27.508	27.508 2434	4.256	335.89
10-1	69.017 55.214	124.230	497.197	100.252	243.152	1.988	0.796	0.160	0.389	20+163	48.905 2226	6.267	1814.79
10-2	76.339 76.339	152.678	579,644	94.010	94.010	2.443	0.927	0.150	0.150	16.219	15.219 1814	8,473	791.44
10-3	72,296 72,296	144.591	548,409	112.854	112.854	2.313	0.877	0.181	0,181	20.578	20,579 1861	2.759	92.76
10-4	71.875 71.875	143.750	548.046	117.545	117.545	2.300	0.877	0.188	0.188	21.448	21.448 1848	2.756	9.03
10-5	71.875 71.875	143.750	548.110	117.609	117,609	2.300	0.877	0.188	0.188	21.457	21.457 1844	2.756	0.90
10-6	71.875 71.875	143.750	548.111	117.610	117.610	2.300	0.877	0.183	0.188	21.457	21.457 1848	2.756	0.09

### TABLE XXII

SOME RESULTS OF VISCOELASTIC ROLLING FOR COMPLETE SLIP (B=0.0625 inch, W=200 P.L.I.)

F <sub>0</sub> τ inch	L <sub>1</sub> ×10 <sup>3</sup> inch	L <sub>2</sub> ×10 <sup>3</sup> inch	L×10 <sup>3</sup> inch	d <sub>o</sub> ×10 <sup>6</sup> inch	d <sub>1</sub> ×10 <sup>6</sup> inch	d <sub>2</sub> ×10 <sup>6</sup> inch	$\frac{L}{B}$	$\frac{d_0}{B}x10^2$	$\frac{d_1}{B}$ x 10 <sup>2</sup>	$\frac{d_2}{B} \times 10^2$	$\frac{d_1}{d_0}$ x10 <sup>2</sup>	$\frac{d_2}{d_0} \times 10^2 $ psi	x×10 <sup>3</sup>	μ <sub>R</sub> ×10 <sup>6</sup>
. 10³	16.313	16.313	32.627	24,555	2.378	2.378	6.525	0.491	0.048	0.048	7.693	9.683 2177	4.670	0.03
10²	16,313	16.313	32.627	24.559	2.381	2.381	6.525	0.491	0.048	0.048	9.696	9.696 2177	4.671	0.27
10¹	16,313	16.313	32.627	24.594	2.416	2.415	6,525	0.492	0.048	0.048	9.825	9.825 2180	4.678	2.74
10°	16,313	15.313	32.627	24.933	2.756	2.756	6.525	0.499	0.055	0.055	11.053	11.053 2214	4.745	27.07
10-1	17.800	14.240	32.040	27.604	1.201	10.706	6.403	0.552	0.024	0.214	4.350	38.784 2376	5.459	236.44
10-2	20.622	16.498	37.119	38.455	3.015	15.774	7.424	0.769	0.060	0.315	7.843	41.020.1847	8.148	518.78
10-3	21.100	21.100	42.200	39,330	2.238	2.238	R.440	0.787	0.045	0.045	5+690	5.690 1721	8,729	99.90
10-4	19.778	19,778	39.557	35.576	2.978	2.973	7,911	0.712	0.060	1.060	8 • 369	8.369 1830	3.841	11.18
10-5	19.685	19,685	39.371	35.433	3.140	3.140	7.874	0.709	0.063	0.063	8.861	P.861 1829	3.852	1.09
10-6	19.684	19.684	39.368	35.431	3.142	3.142	7.874	0.709	0.063	0.063	8.869	8.869 1828	3,852	0.11

# TABLE XXIII

SOME RESULTS OF VISCOELASTIC ROLLING FOR COMPLETE SLIP (B=0.005 inch, W=50 P.L.I.)

F <sub>0</sub> τ inch	L <sub>1</sub> ×10 <sup>3</sup> inch	L <sub>2</sub> ×10 <sup>3</sup> inch	L×10 <sup>3</sup> inch	d <sub>o</sub> ×10 <sup>6</sup> · inch	d <sub>1</sub> ×10 <sup>6</sup> inch	d <sub>2</sub> ×10 <sup>6</sup> inch	$\frac{L}{B}$	$\frac{d_0}{B} \times 10^2$	$\frac{d_1}{B} \times 10^2$	$\frac{d_2}{B}$ x10 <sup>2</sup>	$\frac{d_1}{d_0}$ x 10 <sup>2</sup>	$\frac{d_2}{d_0} x^{10} p_{\text{max}}$	x×103	μ <sub>R</sub> ×10 <sup>6</sup>
103	20.000	20,000	40.000	36,555	3.221	3.221	8.000	0.731	0.064	0.064	8.813	8.813 3566	7.693	0.04
10²	20.000	20,000	40.606	36.562	3.228	3.228	8,000	0.731	0.065	0.065	8.830	8.830 3567	7.695	C.44
101	20,000	20,000	40.000	36.632	3.299	3.299	8.000	0.733	0,066	0.066	9.005	9.005 3574	7.709	4.49
10°	20,001	20.001	40.003	37,308	3.970	3.970	8.001	0.746	0.079	0.079	10.641	10.641 3638	7,843	44,19
10-1	21,860	17,488	39.348	42.421	2.599	16.935	7.870	0.848	0.052	0.339	6.127	39.922 3704	9.247	370.08
10-2	25,760	20,608	46.368	59.400	4.102	24.009	9.274	1.188	0.082	0.480	6.905	40.419 2924	13,578	629.28
10-3	26,000	26.000	52.000	59.244	2.911	2.911	10.400	1.185	0.058	0.058	4.914	4.914 2836	10.587	116.01
10-4	23,969	23.969	47.938	51.959	4.084	4.084	9.588	1.039	0.082	0.082	7.859	7.859 3017	6,398	12.53
10-5	23,905	23.905	47.810	51.919	4.298	4.298	9.562	1.038	0.086	0.086	8.279	8.279 3025	6.437	1.23
10-6	23,905	23.905	47.810	51.922	4.302	4.302	9.562	1,038	0.086	0.086	8 • 285	8.285 3024	6,438	0.12

TABLE XXIV

SOME RESULTS OF VISCOELASTIC ROLLING FOR COMPLETE SLIP (B=0.005 inch, W=100 P.L.I.)

F <sub>0</sub> τ inch	L <sub>1</sub> ×10 <sup>3</sup> inch	L <sub>2</sub> ×10 <sup>3</sup> inch	L×10 <sup>3</sup> inch	d <sub>0</sub> ×10 <sup>6</sup> inch	d <sub>1</sub> ×10 <sup>6</sup> inch	d <sub>2</sub> ×10 <sup>6</sup> inch	L B	$\frac{d_0}{B}x10^2$	$\frac{d_1}{B}$ xlo <sup>2</sup>	$\frac{d_2}{B} \times 10^2$	$\frac{d_1}{d_0} \times 10^2$	$\frac{d_2}{d_0} \times 10^2 \frac{p_{\text{max}}}{psi}$	ж×10 <sup>3</sup>	μ <sub>R</sub> ×10 <sup>6</sup>
10³	22.415	22.415	44.831	45.734	3.855	3.865	8.966	0.915	0.077	0.077	8.450	8.450 4777	10.329	0.06
10 <sup>2</sup>	22,410	22.416	44.831	45.747	3,875	3,875	8,966	0.915	0.078	0.078	8 • 471	8.471 4778	10.331	0.60
101	22,416	22.416	44.931	45.852	3.980	3.980	8,966	0.917	0.080	0.080	A.681	8.681 4798	10+352	6.01
100		22.425	44.850	- 46,888	4.981	4.981	8.970	0.938	9.100	0.100	10.624	10.624 4887	10.558	59.10
10-1	24.645		44.361	54.678	4.063	22.285	8.872	1.094	0.081	0.446	7,431	40.756 4839	12:734	486.05
	29,219		52.594	76.012	4.867	30.479	10.519	1.520	0.097	0.610	6 • 403	40.098 3837	18.269	701.60
20	29,135		58.273	74.123	3.378	3.379	11.655	1.482	0.068	0.068	4.558	4.558 3793	14.167.	128.93
10	.26.718		53.435	64.430	4.944	4.944	10.687	1.289	0.099	0.099	7.674	7.674 4085	8:702	13.63
	26,619		53.239	64.238	5.188	5.168	10.648	1.285	0.104	0.104	8.076	8.076 4080	8.723	1.34
	•	26.618	53.737	64.237	5.191	5.191	10.647	1.285	0.104	0.104	8.082	a.082 4079	8.723	0.13

## TABLE XXV

SOME RESULTS OF VISCOELASTIC ROLLING FOR COMPLETE SLIP (B=0.005 inch, W=150 P.L.I.)

F <sub>0</sub> τ inch	L <sub>1</sub> ×10 <sup>3</sup> inch	L <sub>2</sub> ×10 <sup>3</sup> inch	L×10 <sup>3</sup> inch	d <sub>0</sub> ×10 <sup>6</sup> inch	d <sub>1</sub> ×10 <sup>6</sup> inch	d <sub>2</sub> ×10 <sup>6</sup> inch	L B	$\frac{d_0}{B}$ x10 <sup>2</sup>	$\frac{d_1}{B} \times 10^2$	$\frac{d_2}{B} \times 10^2$	$\frac{d_1}{d_0}$ x 10 <sup>2</sup>	$\frac{d_2}{d_0}$ xl $0^2$ max psi	x×10 <sup>3</sup>	μ <sub>R</sub> ×10 <sup>6</sup>
103	24.235	24.235	48.469	53.343	4.405	4.405	9,694	1.067	0.088	0.088	8.257	8.257 5884	12.741	0.07
10²	24,235	24.235	48.469	53,362	4.419	4.419	9.694	1.067	0.088	680.0	8.281	8.281 5886	12.744	0.73
101	24.235	24.235	48.469	53.502	.4.559	4.559	9.694	1.070	0.091	0.091	8.521	8.521 5900	12,772	7.41
10°	24.235	24.235	48.469	54.818	5.875	5.875	9.694	1.096	0.117	0.117	10.717	10.717 6023	13,026	. 72.58
10-1	25,706	21.365	48.071	64.847	5.412	26,809	9.614	1.297	0.108	0.536	8+346	41.341 5987	15.854	586.87
10-2	31,913	25.531	57.444	90.317	5,444	35.999	11.489	1.806	0.109	0.720	6.028	39.858 4671	22.574	757.91
10.	31.393	31.393	62.787	85.854	3.725	3.725	12.557	1.717	0.074	0.074	4.330	4.339 4631	17.301	139.72
10-4	28,652	28.652	57.305	74.035	5.622	5.622	11.451	1.481	0.112	0.112	7.594	7.594 5017	10.715	14.53
10-5	28,550	28.550	57.100	73.825	5.399	5.899	11.420	1.476	0.118	0.118	7.991	7,991 5010	10.738	1.43
10-6	28,549	28.549	57.098	73.823	5.903	5.903	11.420	1.476	0.118	0.118	7.996	7.996 5008	10.738	0.14

#### TABLE XXVI

SOME RESULTS OF VISCOELASTIC ROLLING FOR COMPLETE SLIP (B=0.005 inch, W=200 P.L.I.)